UNIVERSITY OF SOUTHAMPTON

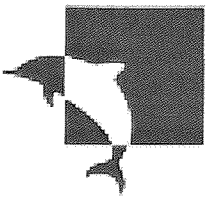

University of Southampton

Synthesis and Coordination Chemistry of Acyclic and Macrocyclic Tellurium-Containing Ligands

by

Matthew James Hesford

A Thesis Submitted for the Degree of Doctor of Philosophy

Department of Chemistry

December 2003

UNIVERSITY OF SOUTHAMPTON

ABSTRACT

FACULTY OF SCIENCE

CHEMISTRY

Doctor of Philosophy

"Synthesis and Coordination Chemistry of Acyclic and Macrocyclic Tellurium-Containing Ligands"

by Matthew James Hesford

The preparation of a series of recently reported and new tellurium-containing ligands are described, along with detailed investigations into their coordination chemistry with a variety of low to medium oxidation state transition metals. These species have been characterised by microanalysis, IR and multinuclear NMR (^{1}H, ^{13}C-{^{1}H}, ^{31}P-{^{1}H}, ^{55}Mn, ^{63}Cu, ^{77}Se-{^{1}H}, ^{125}Te-{^{1}H} and ^{195}Pt) spectroscopy (where appropriate), mass spectrometry and UV-visible spectroscopy (where appropriate) along with the X-ray crystal structures of a number of examples.

The syntheses of the recently reported mixed donor thio-telluroether macrocycles [11]- and [12]aneS_2Te are investigated in detail with increased yields and the identification of possible ditelluride by-products. The synthesis of [9]aneS_2Te is reported in detail, with the identification of several reaction by-products including 1-thia-4-telluracyclohexane. The complexes $[Mn(CO)_3([n]aneS_2Te)][CF_3SO_3]$, $[Rh(cp^*)([n]aneS_2Te)][PF_6]_2$ and $[MCl_2([n]aneS_2Te)]$ (M = Pd and Pt; n = 9, 11 and 12) are described, along with Ag(I) and Cu(I) complexes and the preparation of a number of Te(IV) derivatives. The bonding characteristics of the mixed donor ligands are compared with the open-chain analogue $MeS(CH_2)_3Te(CH_2)_3SMe$ and other relevant systems. The crystal structures of [11]- and [12]aneS_2Te are reported.

The syntheses of two new mixed donor oxa-tellura macrocycles [9]aneO_2Te and [18]aneO_4Te_2 are described in detail and compared with the selenium analogues [9]aneO_2Se and [18]aneO_4Se_2. Several Te(IV) derivatives of the new compounds have been prepared including [9]aneO_2TeMeI and [18]ane$O_4Te_2Me_2I_2$ in order to fully characterise the ligands. The Pt(II) and Pd(II) complexes $[MX_2([18]aneO_4Te_2)]$ (M = Pd or Pt; X = Cl or Br) and $[MCl_2([9]aneO_2Te)]$ (M = Pd and Pt) have been prepared and are compared with the new complex $[PtCl_2([18]aneO_4Se_2)]$. The crystal structures of $[MCl_2([18]aneO_4Te_2)]$ (M = Pd and Pt) confirm the identity of the large ring macrocycle, and the structure of $[PtCl_2([18]aneO_4Se_2)]$ is reported for comparison purposes. A number of Ag(I) and Cu(I) complexes of [18]aneO_4Te_2 are also detailed.

A series of transition metal complexes of the recently reported open-chain ligand $MeS(CH_2)_3Te(CH_2)_3SMe$ (L^3) are described, including $[Mn(CO)_3(L^3)][CF_3SO_3]$, $[Rh(cp^*)(L^3)][PF_6]_2$, $[MCl(L^3)][PF_6]$ (M = Pd and Pt), $[Cu(L^3)][BF_4]$ and $[Ag(L^3)][CF_3SO_3]$ and the complexes are compared with those of [9]-, [11]- and [12]aneS_2Te. The crystal structures of $[Rh(cp^*)(L^3)][PF_6]_2$ and $[PtCl(L^3)][PF_6]$ are described in detail and compared with relevant literature examples.

The synthesis of the new xylyl-based telluroethers *m*- and *p*-$C_6H_4(CH_2TeMe)_2$ are detailed and compared with *o*-$C_6H_4(CH_2TeMe)_2$, and their Te(IV) methiodide and diiodide derivatives and Cu(I) complexes are reported. The structures of *m*- and *p*-$C_6H_4(CH_2TeI_2Me)_2$ are described in detail, and attempts to prepare the first tellurium-containing cyclophane compounds 2,11-ditellura[3.3]orthocyclophane and 2,11-ditellura[3.3]metacyclophane are reported.

Contents

Page

Chapter 1 1

1.0 Introduction 2
1.1 The synthesis of organo-tellurium compounds 3
1.2 Telluroether and related Group 16 ligand complexes 6
1.3 Complexes of the tripodal ligands $MeC(CH_2EMe)_3$ (E = S, Se or Te) 11
1.4 Metal-ligand bonding 13
1.5 The stereochemistry of the M-E bond (E = S, Se, Te) and pyramidal inversion 15
1.6 Macrocyclic ligands and synthesis 18
1.7 The macrocyclic effect 22
1.8 Characterisation techniques 25
1.8.1 Mass spectrometry 25
1.8.2 NMR spectroscopy 28
1.9 Aims of this study 30
1.10 References 31

Chapter 2 36

2.0 Introduction 37
2.1 Results and discussion 51
2.2 Ligand syntheses 51
2.2.1 Synthesis of [11]- and [12]-aneS_2Te and their crystal structures 51
2.2.2 Synthesis of [9]aneS_2Te 59
2.3 Organo-derivatives of [9]-, [11]- and [12]-aneS_2Te and C_4H_8STe 63
2.4 Transition metal complexes 68
2.4.1 $[Mn(CO)_3([n]aneS_2Te)][CF_3SO_3]$ (n = 9, 11 and 12) 68
2.4.2 $[Mo(CO)_4([n]aneS_2Te)]$ (n = 11 or 12) 71

2.4.3 [MCl_2([n]aneS_2Te)] (M = Pd or Pt; n = 11 or 12) 72
2.4.4 [Rh(cp^*)([n]aneS_2Te)][PF_6]$_2$ (n = 9, 11 or 12) 73
2.4.5 [Ag([n]aneS_2Te][X] (n = 9 or 11, X = CF_3SO_3; n = 12,
X = CF_3SO_3 or BF_4 76
2.4.6 [Cu([n]aneS_2Te)][BF_4], n = 11 or 12 77
2.5 Conclusions 78
2.6 Experimental 81
2.7 References 94

Chapter 3 98

3.0 Introduction 99
3.1 Results and discussion 106
3.2 [9]aneO_2Te/[18]aneO_4Te_2 106
3.2 Organo-derivatives 111
3.3 [9]aneO_2Se/[18]aneO_4Se_2 113
3.4 [MX_2([18]aneO_4Te_2)] (M = Pd or Pt; X = Cl or Br) 115
3.5 [MCl_2([9]aneO_2Te)$_2$] (M = Pd or Pt) 119
3.6 [$PtCl_2$([18]aneO_4Se_2)] 122
3.7 Crystal structures of *cis*-[MCl_2([18]aneO_4Te_2)] (M = Pd and Pt)
and *cis*-[$PtCl_2$([18]aneO_4Se_2)] 122
3.8 [$RhCl_2$([18]aneO_4Te_2)$_2$]Cl and [$RhCl_2$([18]aneO_4Te_2)$_2$][PF_6] 127
3.9 [Cu([18]aneO_4Te_2)$_2$][BF_4] and [Ag([18]aneO_4Te_2)$_2$][BF_4] 128
3.10 Conclusions 130
3.11 Experimental 132
3.12 References 141

Chapter 4 143

4.0 Introduction - open-chain tridentate Group 16 ligands 144
4.1 Results and discussion 150
4.2 Synthesis of $MeS(CH_2)_3Te(CH_2)_3SMe$ 150

4.3 *Fac*-[$Mn(CO)_3(MeS(CH_2)_3Te(CH_2)_3SMe)][CF_3SO_3]$ 151
4.4 [$MCl(MeS(CH_2)_3Te(CH_2)_3SMe)][PF_6]$; M = Pd or Pt 154
4.5 [$Rh(cp^*)(MeS(CH_2)_3Te(CH_2)_3SMe)][PF_6]_2$ 160
4.6 [$M(MeS(CH_2)_3Te(CH_2)_3SMe)]^+$; M = Cu, Ag 164
4.7 Conclusions 166
4.8 Experimental 168
4.9 References 173

Chapter 5 175

5.0 Introduction 176
5.1 Results and discussion 182
5.1.1 Ligand synthesis 182
5.2 Organo-derivatives 184
5.3 Crystal structures of *m*- and *p*-$C_6H_4(CH_2TeI_2Me)_2$ 187
5.4 $[Cu(MeCN)_4][BF_4]$ + 2 L-L (L-L = *m*- or *p*-$C_6H_4(CH_2TeMe)_2$ 193
5.5 Attempted preparation of 2,11-ditellura[3.3]orthocyclophane 195
5.6 Attempted preparation of 2,11-ditellura[3.3]metacyclophane 200
5.7 Attempted preparation of *o*-$C_6H_4(CH_2TeMe)_2$ *via* a Grignard intermediate 204
5.8 Conclusions 207
5.9 Experimental 210
5.10 References 218
5.11 Appendix 220

List of Figures

Page

Figure 1.0 - Crystal structure of $[Ag\{MeTe(CH_2)_3TeMe\}_2]^+$ 7

Figure 1.1 - Crystal structure of $[SnCl_4\{o\text{-}C_6H_4(TeMe)_2\}]$ 8

Figure 1.2 - Crystal structure of $[BiBr_3(PhTeMe)]$ 9

Figure 1.3 - Crystal structure of *trans*-$[OsCl_2\{PhTe(CH_2)_3TePh\}_2]$ 10

Figure 1.4 - Crystal structure of $[Mn(CO)_3\{MeC(CH_2TeMe)_3\}]^+$ 12

Figure 1.5 - Crystal structure of $[Rh(COD)\{MeC(CH_2TeMe)_3\}]^+$ 12

Figure 1.6 - The stereochemistry of a group 16 ligand coordinated to a metal (M) centre (E = S, Se or Te) 15

Figure 1.7 - The different invertomers possible for a tridentate chalcogen ligand-metal complex 16

Figure 1.8 - Pyramidal inversion via a planar intermediate 16

Figure 1.9 - The synthesis of $[9]aneS_3$ 21

Figure 1.10 - Crystal structure of $[Ag([11]aneS_2Te)][BF_4]$ 21

Figure 1.11 - Cu(II) complexes of 'tet-a' (i) and '2.3.2-tet' (ii) 22

Figure 1.12 - Born-Haber cycle for a typical complexation reaction 23

Figure 1.13 - Isotope patterns for 1 (i), 2 (ii) and 3 (iii) Te atoms 27

Figure 2.0 - Telluracyclopentane (i) and telluracyclohexane (ii) 37

Figure 2.1 - Crystal structure of telluracyclohexanediiodide 38

Figure 2.2 - 1,4-oxatellurane (i) and 1-thia-4-telluracyclohexane (ii) 39

Figure 2.3 - Crystal structure of *trans*-$[PtCl_2(1,4\text{-oxatellurane})_2]$ 39

Figure 2.4 - 1,3-dihydrobenzo[*c*]tellurophene 40

Figure 2.5 - Crystal structure of $[Mo(CO)_4(1,3\text{-dihydrobenzo}[c]\text{tellurophene})_2]$ 41

Figure 2.6 - 3,4-quinoxalino-1-telluracyclopentane 41

Figure 2.7 - Crystal structure of 3,4-quinoxalino-1-telluracyclopentane 42

Figure 2.8 - Benzoisotellurazole 42

Figure 2.9 - Synthesis of 2,7-dihydro-1 H-dibenzo[*c,e*]tellurepin 42

Figure 2.10 - Tellurophene (i) and dibenzotellurophene (ii) 43
Figure 2.11 - 3,5-naptho-1-telluracyclohexane (i) and
1,2,4,5-bis(diiodotelluracyclopentano)benzene (ii) 44
Figure 2.12 - Telluranthrene (i), telluraxanthene (ii) and phenoxatellurine (iii) 45
Figure 2.13 - Synthesis of 1,5-ditelluracyclooctane 45
Figure 2.14 - The Synthesis of [12]aneTe_3 46
Figure 2.15 - Crystal structure of [12]aneTe_3Cl_6 46
Figure 2.16 - The first Te-containing Schiff base macrocycle 47
Figure 2.17 - Synthesis of the new Te-containing Schiff base macrocycle 48
Figure 2.18 - Tellura-crown macrocycles 48
Figure 2.19 - 1,13-ditellura-24-crown-8 49
Figure 2.20 - Synthesis of [11]- and [12]-aneS_2Te 51
Figure 2.21 - ^{125}Te-{^{1}H} NMR spectrum of [12]aneS_2Te in CH_2Cl_2 53
Figure 2.22 - Proposed structure of the ditelluride [12]aneS_2Te_2 54
Figure 2.23 - EIMS of the ditelluride from the [12]aneS_2Te preparation 54
Figure 2.24 - Crystal structure of [11]aneS_2Te 55
Figure 2.25 - Crystal Structure of [12]aneS_2Te 57
Figure 2.26 - [12]aneS_3 57
Figure 2.27 - Synthesis of [9]aneS_2Te 59
Figure 2.28 - Crystal Structure of 1-thia-4-telluracyclohexane 63
Figure 2.29 - ^{13}C-{^{1}H} NMR Spectrum of [11]aneS_2TeMeI in d_6-dmso 64
Figure 2.30 - ^{125}Te-{^{1}H} NMR Spectrum of [12]aneS_2TeMeI in d_6-dmso 65
Figure 2.31 - Crystal Structure of [12]aneS_2TeI_2 66
Figure 2.32 - IR Spectrum (CsI disk, CO Region) of
[$Mn(CO)_3$([11]aneS_2Te)][CF_3SO_3] 69
Figure 2.33 - ^{55}Mn NMR spectrum of [$Mn(CO)_3$([11]aneS_2Te)][CF_3SO_3]
in d_6-Me_2CO 70
Figure 2.34 - ^{125}Te-{^{1}H} NMR spectrum of [Rh(cp^*)([11]aneS_2Te)][PF_6]$_2$
in d_6-Me_2CO 75
Figure 2.35 - Expected structure of [Rh(cp^*)([9]aneS_2Te)][PF_6]$_2$ 75

Figure 3.0 - [18]aneO$_4$S$_2$ 100
Figure 3.1 - Crystal structure of [PdCl$_2$([18]aneO$_4$S$_2$)] 101
Figure 3.2 -1,4-dithia-15-crown-5, 1-thia-9-crown-3 and 1,4-dithia-9-crown-3 101
Figure 3.3 - Synthesis of 10-tellurabenzo-15-crown-5 102
Figure 3.4 - Tellura-crown ether compounds 103
Figure 3.5 - Tellura-crown macrocycles 104
Figure 3.6 - [18]aneO$_4$Te$_2$ 106
Figure 3.7 - [9]aneO$_2$Te 107
Figure 3.8 - EI Mass Spectra of [18]aneO$_4$Te$_2$ (i) and [9]aneO$_2$Te (ii) 108
Figure 3.9 - ^{13}C-{^{1}H} NMR spectrum of [18]aneO$_4$Te$_2$ in CDCl$_3$ 109
Figure 3.10 - ^{125}Te-{^{1}H} NMR spectrum of [18]aneO$_4$Te$_2$Cl$_4$ in CH$_2$Cl$_2$-CDCl$_3$ 113
Figure 3.11 - ^{125}Te-{^{1}H} NMR spectrum of [PtCl$_2$([9]aneO$_2$Te)$_2$] in CH$_2$Cl$_2$-CDCl$_3$ 120
Figure 3.12 - ^{195}Pt NMR spectrum of [PtCl$_2$([9]aneO$_2$Te)$_2$] in CH$_2$Cl$_2$-CDCl$_3$ 121
Figure 3.13 - Crystal structure of [PdCl$_2$([18]aneO$_4$Te$_2$)] 124
Figure 3.14 - Crystal structure of [PtCl$_2$([18]aneO$_4$Te$_2$)] 125
Figure 3.15 - Crystal structure of [PtCl$_2$([18]aneO$_4$Se$_2$)] 126

Figure 4.0 - Crystal structure of [PtCl(^{i}PrS(CH$_2$)$_2$S(CH$_2$)$_2$S^{i}Pr)]$^+$ 145
Figure 4.1 - The possible invertomers for the [PtCl(RS(CH$_2$)$_2$S(CH$_2$)$_2$SR)]$^+$ cations 145
Figure 4.2 - Synthesis of MeSe(CH$_2$)$_3$Se(CH$_2$)$_3$SeMe 146
Figure 4.3 - Synthesis of RTe(CH$_2$)$_3$Te(CH$_2$)$_3$TeR (R = Me or Ph) 147
Figure 4.4 - Crystal structure of [Rh(cp*){PhTe(CH$_2$)$_3$Te(CH$_2$)$_3$TePh}][PF$_6$]$_2$ 147
Figure 4.5 - The possible invertomers for a *fac*-coordinated tridentate group 16 ligand complex 148
Figure 4.6 - Synthesis of MeS(CH$_2$)$_3$Te(CH$_2$)$_3$SMe 150
Figure 4.7 - Electrospray mass spectrum of *fac*-[Mn(CO)$_3$(MeS(CH$_2$)$_3$Te(CH$_2$)$_3$SMe)]$^+$ (MeCN) 153
Figure 4.8 - Electrospray mass spectrum of [PtCl(MeS(CH$_2$)$_3$Te(CH$_2$)$_3$SMe)]$^+$ (MeCN) 155
Figure 4.9 - The invertomers possible for [PtCl{MeS(CH$_2$)$_3$Te(CH$_2$)$_3$SMe}]$^+$ 156

Figure 4.10 - Crystal Structure of $[PtCl(MeS(CH_2)_3Te(CH_2)_3SMe)]^+$ 158

Figure 4.11 - ^{125}Te-{^1H} NMR Spectrum of $[Rh(cp^*)(MeS(CH_2)_3Te(CH_2)_3SMe)]^{2+}$ in d_6-Me_2CO 162

Figure 4.12 - Crystal Structure of $[Rh(cp^*)(MeS(CH_2)_3Te(CH_2)_3SMe)][PF_6]_2$ 163

Figure 5.0 - Synthesis of *o*-$C_6H_4(CH_2TeMe)_2$ 176

Figure 5.1 - Crystal structure of *o*-$C_6H_4(CH_2TeMe_2I)_2$ 177

Figure 5.2 - The NMR distinguishable isomers possible for *fac*-$[Mn(CO)_3Cl\{o\text{-}C_6H_4(CH_2TeMe)_2\}]$ 178

Figure 5.3 - Crystal structure of $[Mn(CO)_3Cl\{meso\text{-}2\text{-}o\text{-}C_6H_4(CH_2TeMe)_2\}]$ 179

Figure 5.4 - Crystal structure of $[W(CO)_4\{o\text{-}C_6H_4(CH_2TeMe)_2\}]$ 179

Figure 5.5 - 2,11-ditellura[3.3]orthocyclophane (i) and 2,11-ditellura[3.3]metacyclophane (ii) 181

Figure 5.6 - Crystal structures of 2,11-dithia[3.3]orthocyclophane (i) and 2,11-diselena[3.3]orthocyclophane (ii) 181

Figure 5.7 - *m*-$C_6H_4(CH_2TeMe)_2$ and *p*-$C_6H_4(CH_2TeMe)_2$ 182

Figure 5.8 - *o*-, *m*- and *p*-$C_6H_4(CH_2TeI_2Me)_2$ ((i), (ii) and (iii) respectively) 185

Figure 5.9 - ^{125}Te-{^1H} NMR spectrum of *p*-$C_6H_4(CH_2TeI_2Me)_2$ (thf/$CDCl_3$) 186

Figure 5.10 - Crystal structure of *m*-$C_6H_4(CH_2TeI_2Me)_2$ 188

Figure 5.11 - Crystal structure of *p*-$C_6H_4(CH_2TeI_2Me)_2$ 190

Figure 5.12 - The environment about Te(IV) in *p*-$C_6H_4(CH_2TeI_2Me)_2$ 191

Figure 5.13 - Crystal structure of $PhTeI_2(CH_2)_3TeI_2Ph$ 193

Figure 5.14 - ^{125}Te-{^1H} NMR spectrum of "$[Cu\{p\text{-}C_6H_4(CH_2TeMe)_2\}][BF_4]$"in MeCN-$CDCl_3$ 195

Figure 5.15 - 2,11-ditellura[3.3]orthocyclophane (i) and 1,3-dihydrobenzo[*c*]tellurophene (ii) 196

Figure 5.16 - 1-methyl-1-iodo-3,4-benzo-1-telluracyclopentane 197

Figure 5.17 - Crystal structure of 1,1-diiodo-3,4-benzo-1-telluracyclopentane 200

Figure 5.18 - The meta analogue of 1,3-dihydrobenzo[*c*]tellurophene 200

Figure 5.19 - 2,11-ditellura[3.3]metacyclophane 201

Figure 5.20 - Possible [3+3] cyclisation product from the reaction of Na_2Te

with α-α'-dibromo-*m*-xylene 203
Figure 5.21 - The *in-situ* 'TeMgCl' reagent 204
Figure 5.22 - Possible synthetic route to 2,11-ditellura[3.3]orthocyclophane 204
Figure 5.23 - Synthesis of *p*-$C_6H_4(TeMe)_2$ 205

List of Tables

Page

Table 1.0 - Tellurium isotopes: relative abundance and nuclear spin values 26

Table 2.0 - ^{1}H, ^{13}C-{^{1}H} and ^{125}Te-{^{1}H} NMR data for [11]- and [12]aneS_2Te ($CDCl_3$) 52

Table 2.1 - Selected bond lengths (Å), angles (°) and torsion angles (°) for [11]aneS_2Te 56

Table 2.2 - Selected bond lengths (Å), angles (°) and torsion angles (°) for [12]aneS_2Te 58

Table 2.3 - ^{1}H, ^{13}C-{^{1}H} and ^{125}Te-{^{1}H} NMR data for 1-thia-4-telluracyclohexane 61

Table 2.4 - Selected bond lengths (Å), angles (°) and torsion angles (°) for [12]aneS_2TeI_2 67

Table 2.5 - ν(CO)/cm^{-1} for $[Mn(CO)_3([n]aneS_2Te)][CF_3SO_3]$ 69

Table 2.6 - Crystallographic parameters 80

Table 3.0 - ^{1}H, ^{13}C-{^{1}H} and ^{125}Te-{^{1}H} NMR data for [9]aneO_2Te and [18]aneO_4Te_2 110

Table 3.1 - Selected bond lengths (Å) and angles (°) for *cis*-$[PdCl_2([18]aneO_4Te_2)]$ 124

Table 3.2 - Selected bond lengths (Å) and angles (°) for *cis*-$[PtCl_2([18]aneO_4Te_2)]$ 125

Table 3.3 - Selected bond lengths (Å) and angles (°) for *cis*-$[PtCl_2([18]aneO_4Se_2)]$ 126

Table 3.4 - Crystallographic parameters 131

Table 4.0 - Selected bond lengths (Å) and angles (°) for $[PtCl(MeS(CH_2)_3Te(CH_2)_3SMe)][PF_6]$ 159

Table 4.1 - Selected bond lengths (Å) and angles (°) for $[Rh(cp^*)(MeS(CH_2)_3Te(CH_2)_3SMe)]^{2+}$ 164

Table 4.2 - Crystallographic parameters 167

Table 5.0 - ^{1}H, ^{13}C-{^{1}H} and ^{125}Te-{^{1}H} NMR data for *o*-, *m*- and *p*-$C_6H_4(CH_2TeMe)_2$ (*o*, *m* and *p* respectively) 183

Table 5.1 - Selected bond lengths (Å) and angles (°) for *m*-$C_6H_4(CH_2TeI_2Me)_2$ 189

Table 5.2 - Selected bond lengths (Å) and angles (°) for *p*-$C_6H_4(CH_2TeI_2Me)_2$ 191

Table 5.3 - Unit cell data for $C_8H_8TeI_2$ 199

Acknowledgements

I would firstly like to thank my supervisors Professor Bill Levason and Dr. Gill Reid for their support, help and enthusiasm during the course of this research and for their advice in other non-chemistry related areas.

I would also like to thank Nick Hill and Melissa Matthews, who collected most of the crystallographic data presented in this thesis, together with some help from Rina Patel and Lorna Nichols. Special mention must also be given to Drs. Gill Reid and Mike Webster who helped in the solving of any crystallographic problems.

Thanks are also due to Dr. John Langley and Miss Julie Hernimann for running EI mass spectra and their general help in the field of mass spectrometry.

I would also like to thank my friends in the Inorganic Section of the Chemistry Department, in particular those that I have made over the course of my research in lab 30 : 2005 (Melissa Matthews, Rina Patel, Mike Brown and Raju Ratnani).

Finally I would like to thank the EPSRC for their financial support over the past three years and my family and friends outside the Chemistry Deparment.

Abbreviations

Techniques

EDX	Energy Dispersive X-ray
ESMS	Electrospray Mass Spectrum
EIMS	Electron Impact Mass Spectrum
FAB	Fast Atom Bombardment
IR	Infra Red
NMR	Nuclear Magnetic Resonance
MS	Mass Spectrometry
UV	Ultra Violet
Vis	Visible

Solvents

dmf	Dimethyl formamide
dmso	Dimethyl sulfoxide
Et_2O	Diethyl ether
EtOH	Ethanol
Me_2CO	Acetone
MeCN/NCMe	Acetonitrile
thf	Tetrahydrofuran

Ligands and complexes

M	Metal
L	Ligand
L-L	Bidentate ligand
X	Halide (Cl, Br or I)
E	Chalcogen atom
[9]aneS_3	1,4,7-trithiacyclononane
[9]aneS_2Te	1,4-dithia-7-telluracyclononane
[11]aneS_2Te	1,4-dithia-8-telluracycloundecane
[12]aneS_2Te	1,5-dithia-9-telluracyclododecane
[9]aneO_2Te	1-tellura-4,7-dioxacyclononane
[9]aneO_2Se	1-selena-4,7-dioxacyclononane
[18]aneO_4Te_2	1,10-ditellura-4,7,13,16-tetraoxacyclooctadecane
[18]aneO_4Se_2	1,10-diselena-4,7,13,16-tetraoxacyclooctadecane

General

acac	Acetylacetonate
Bpt.	Boiling point

br	Broad
cp^*	1,2,3,4,5-pentamethylcyclopentadienyl
Cod	Cycloocta-1,5-diene
δ	Chemical shift
d	Doublet
Et	Ethyl
$\{^1H\}$	Broadband proton decoupled spectrum
^iPr	Isopropyl
m	Medium
m-	*Meta*
m/z	Mass to charge ratio
Me	Methyl
Mpt.	Melting point
nbd	Norbornadiene
o-	*Ortho*
p-	*Para*
Ph	Phenyl
ppm	Parts per million
q	Quartet
R	Alkyl or aryl substituent
R.T.	Room temperature
s	Strong/singlet
t	Triplet
vs	Very strong
w	Weak

Chapter 1:

Introduction

1.0 Introduction

Tellurium was first isolated in 1782 by an Austrian chemist, F. J. Müller von Reichenstein, who first referred to it as *metallum problematicium* since it had none of the expected properties of antimony. It was not until sixteen years later that H. M. Klaproth established unequivocally that the substance had unique properties and was an element in its own right, naming it "Tellurium" which is derived from the Latin word *tellus* meaning "earth".[1] The first organic derivatives of tellurium were reported by Wöhler as early as 1840,[2] but until relatively recently little work had been undertaken on the synthesis and coordination chemistry of telluroethers (R_2Te) despite the large amount of literature associated with the organic and coordination chemistry of thioether compounds. A review article from 1965[3] listed fewer than 30 references to metal complexes of selenium and tellurium-containing ligands, whilst a more recent summary from 1981 was still dominated by thioethers.[4] By 1993, however, a review devoted to the synthesis and coordination chemistry of Se- and Te-containing ligands was published,[5] and another by Singh and Sharma in 2000 on various aspects of telluroether chemistry.[6] Another comprehensive review on the chemistry of selenoethers and telluroethers was published in 2002,[7] which reflects the recent surge of interest in these heavier group 16 elements and their coordination chemistry.

There are a number of reasons for the late development of telluroether chemistry. One reason was the scarcity of elemental tellurium, which made it expensive and difficult to obtain. Also, a lack of interest in such compounds as SeR_2 and TeR_2 (R = *e.g.* Me, Ph) prevailed due to the belief that they are weak donors except to soft metal centres and that they had very similar properties to their thioether analogues. Other contributing factors were their malodorous and toxic nature, together with the difficulties involved in incorporating tellurium within an organic framework. Both selenium- and tellurium-containing compounds should be treated as toxic, since the elements are absorbed by the kidneys, spleen and liver, producing side effects such as headaches and nausea even in very low concentrations. Selenium, however, does play an essential (but still poorly understood) role in the human dietary system.

The recent surge of interest in selenium and tellurium chemistry has followed the development of selenoether ligand chemistry over the past 30 years or so, with tellurium chemistry only very recently beginning to emerge as an area of significant growth and interest. The development of selenium and tellurium chemistry has been facilitated greatly by modern FT NMR techniques. These allow the study of ^{77}Se- and ^{125}Te-containing species in solution, and are therefore excellent spectroscopic probes with which to follow ligand synthesis and metal complexation reactions. Detailed spectroscopic studies have revealed the superior ligating properties of the heavier group 16 elements to low valent transition metal centres compared to their thioether analogues.[8] ^{77}Se is the only selenium isotope with $I > 0$, which means that it alone may be studied by NMR, but tellurium has two major isotopes with $I = ½$. In the latter case, ^{125}Te is much more abundant (7.07%) than ^{123}Te (0.89%) which makes it the nucleus of choice for Te NMR studies. In contrast, sulfur possesses only an insensitive, low abundance quadrupolar nucleus (^{33}S).

In addition to their academic interest, selenium- and tellurium-containing compounds have potential applications in various important and diverse fields, for example in metal ion recognition and detection,[9,10] photography,[11] new conducting materials,[12] and as carrier ligands for radionuclides used in medical imaging and treatment.[13] The investigation into the catalytic applications of $[Rh(PPh_3)_2([9]aneS_3)][PF_6]$[14] and the activity of the $PtCl_2(SePh_2)_2/SnCl_2$ system for the homogenous hydrogenation of non-aromatic alkenes[15] suggest that other selenoether and telluroether compounds may also have potential catalytic applications.

1.1 The synthesis of organo-tellurium compounds

Organo-tellurium compounds are markedly more air sensitive than their selenium analogues, and this combined with the weakness of tellurium-carbon bonds often results in the elimination of the carbon backbone, and ditelluride formation during the ligand synthesis and subsequent complexation reactions. Monodentate telluroethers remain the major class of the fairly limited number of tellurium ligands known.[16,17] In recent years there have been increasing numbers of studies into organo-tellurium chemistry, the

results of which have revealed tellurium to have a rich and diverse chemistry that differs significantly from those of the well studied lighter chalcogenides.[8]

There are many methods available for the incorporation of tellurium into organic molecules, although many are not suitable for the chemistry discussed in this thesis since Te(II) is often oxidised to form Te(IV). The methods used to prepare thioether and selenoether compounds are not always transferable into telluroether chemistry, and an example of this is provided by the reduction of RSeCN to RSe^- which is a common route for the preparation of multidentate and macrocyclic selenoether ligands. The analogous tellurocyanates (RTeCN) however, are very unstable, being both photochemically and thermally sensitive. Even when the desired tellurium-containing compounds have been prepared, difficulties may arise when trying to employ them in further reaction chemistry, since reaction at tellurium often occurs at the expense of the desired reaction. In addition, the purification of tellurium-containing compounds may be difficult if distillation or recrystallisation are not possible; in these cases flash column chromatography on silica is a common method, although considerable care must be employed in order to minimise their exposure to air. Once purified, the compounds are typically (very) air sensitive (especially in solution) depositing elemental tellurium upon exposure, although the use of Schlenk techniques and degassed solvents overcome these problems. Telluroether compounds may be stored for reasonably long periods of time with no apparent decomposition under an atmosphere of dinitrogen at -18°C. There are several ways in which Te(II) may be incorporated into organic fragments or frameworks, with the most useful methods being outlined below. Firstly, tellurium can be incorporated into a carbon-group 1 or 2 metal bond:[18-20]

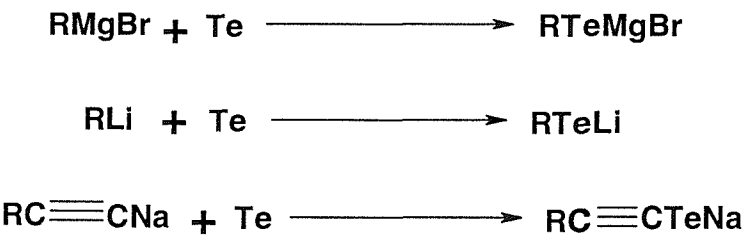

(R = alkyl and/or aryl group)

The above reactions provide unstable intermediates that are both air and moisture sensitive and are usually prepared and used *in situ*. Treatment of these with the appropriate haloalkanes gives the required telluroether compounds:

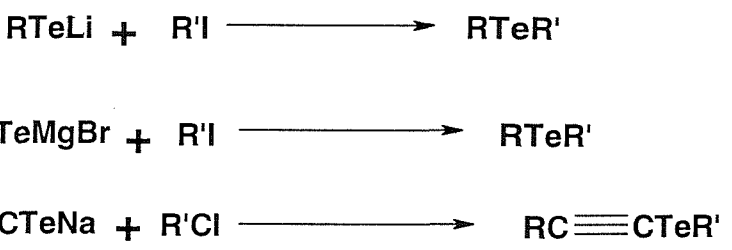

The alkylation of alkali metal tellurides with organic halides, RX, provides an additional route to telluroether compounds. (The alkali metal telluride reagents may be prepared in aqueous,[21] liquid NH_3[22] and dmf[23] media) *e.g.*:

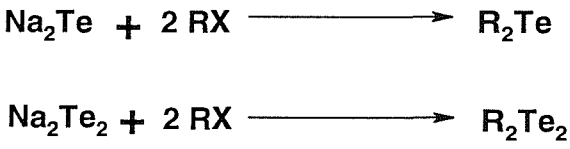

Ditelluroalkanes, $RTe(CH_2)_nTeR$, (R = Me, Ph, 4-$EtOC_6H_4$) proved difficult to obtain, and are only known for n = 1, 3, 6 and 10.[24] They were eventually synthesised by the addition of $X(CH_2)_nX$ (X = Br, I) to frozen (-196°C) solutions of RTeLi in thf and subsequent thawing.[24] A peculiarity of telluroether chemistry is that when n = 2, RTeTeR species are formed, eliminating $CH_2{=}CH_2$ in the process. This is in contrast to the reactions of RS^-[25] or RSe^-[26] with α-ω-dihaloalkanes which produce the corresponding dithio- or diselenoether compounds where n = 2 cleanly and in good yield. The failures to produce $RTeCH_2CH_2TeR$ or indeed *cis*-RTeCH=CHTeR (R = Me or Ph)[27,28] are unfortunate since these two-carbon backboned ligands would form the most favourable ring size (*i.e.* five) upon chelation to a metal centre. The C_2-bridged *o*-phenylenebis(telluroether) compounds *o*-$C_6H_4(TeR)_2$ (R = Me, Ph) have been obtained,

however, *via* the reaction of RTeLi with *o*-$C_6H_4Br_2$.[28] For n = 4 and 5, the corresponding heterocyclic rings are formed:[28]

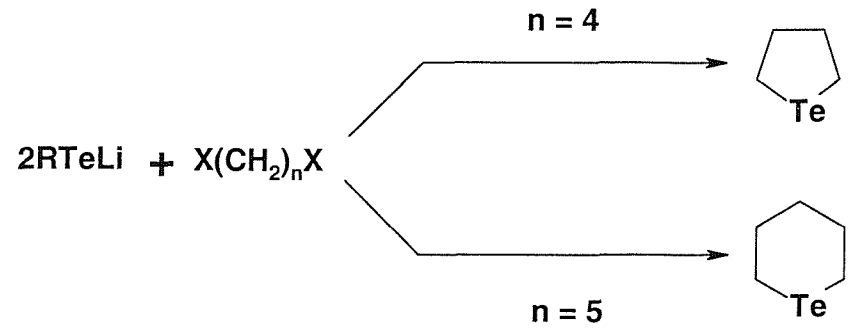

Few examples of poly-telluroethers have been reported, but $MeC(CH_2TeMe)_3$,[24] $MeC(CH_2TePh)_3$[29] and $C(CH_2TeR)_4$ (R = Ph,[29] 4-$EtOC_6H_4$[30]) have been prepared *via* the reactions of RTeLi (R = Me, Ph or 4-$EtOC_6H_4$) with $MeC(CH_2Br)_3$ or $C(CH_2Br)_4$ respectively. (Detailed descriptions of the synthesis and reaction chemistry of various mono-, bi- and multi-dentate telluroether ligands are given in Chapters 2, 3, 4 and 5).

1.2 Telluroether and related Group 16 ligand complexes

The first coordination complex with a tellurium-containing ligand was reported by Fritzman in 1915, *cis*-$[Pt\{Te(CH_2Ph)_2\}_2Cl_2]$.[31] It has only been during the last 20 years, however, that a significant amount of spectral data have been accumulated, but the data on tellurium compounds are still much less comprehensive than for thio- and selenoethers or for group 15 donor ligands.

Low oxidation state complexes mainly involve substituted carbonyl complexes; for example the photolysis of $[Et_4N][V(CO)_6]$ with $TePh_2$ in THF produces $[Et_4N][V(CO)_5(TePh_2)]$.[32,33] Other complexes include niobium,[34] chromium,[35] molybdenum,[36] tungsten,[37] manganese,[38] rhenium,[39] iron[40] and cobalt[41] carbonyl species. Medium oxidation state complexes include several Pd(II) and Pt(II) complexes of the type $[ML_2X_2]$ where X = halide and L = telluroether.[42]

Thorough studies into the coordination chemistry of ditelluroether ligands have been undertaken,[24] although few complexes of the methylene backbone ligands $RTeCH_2TeR$ (R = Me, Ph) have been reported. Amongst them are the Cu(I) and Ag(I) complexes $[M_n(MeTeCH_2TeMe)_{2n}][BF_4]_n$,[43] where M = Cu or Ag, and the complexes

$[MLCl_2]_n$, where M = Pd or Pt and L = $MeTeCH_2TeMe$ or $PhTeCH_2TeMe$.[44] Here, the short methylene backbones of the ligands disfavour chelation to single metal centres due to ring strain, thereby promoting monodentate or bridging modes.[44] The analogous selenoether ligand $MeSeCH_2SeMe$, however, when reacted with half an equivalent of $AgBF_4$ or $[Cu(MeCN)_4][PF_6]$ in dichloromethane forms highly unusual three-dimensional network structures.[43] These structures have been found to incorporate channels which can serve as hosts for PF_6^- or BF_4^- anions. The related bidentate telluroether $MeTe(CH_2)_3TeMe$ forms a light sensitive Ag(I) complex $[Ag\{MeTe(CH_2)_3TeMe\}_2]^+$ in which the $AgTe_4^+$ units are connected through ditelluroether bridges to form an infinite coordination polymer[45] (Figure 1.0).

Figure 1.0 - Crystal structure of $[Ag\{MeTe(CH_2)_3TeMe\}_2]^+$[45]

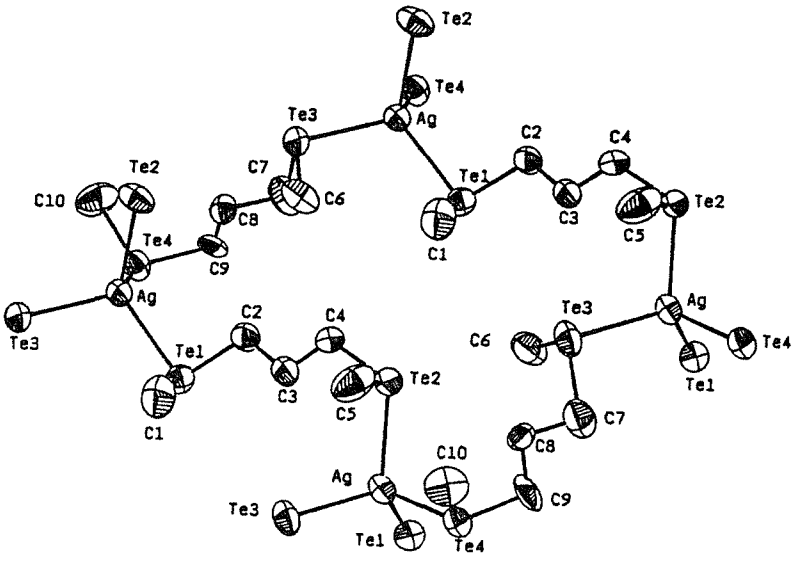

The preference for ligand bridging over chelation in the methylene backbone ligands arises as a result of the highly strained 4-membered chelate ring that would be formed upon bidentate coordination of the ligand to the metal. Examples of chelating diselenoether complexes are $[SnCl_4(MeECH_2EMe)]$, where E = S or Se, which are generated by the reaction of the ligand with $SnCl_4$ in anhydrous dichloromethane.[46] A crystal structure of the dithioether complex shows a mononuclear Sn(IV) species involving a highly distorted octahedral S_2Cl_4 donor set, with the dithioether coordinated

in a bidentate fashion. This produces a highly strained 4-membered chelate ring. The methyl groups of the ligand adopt the DL configuration, being directed to opposite sides of the SnS_2Cl_2 plane. The analogous diselenoether complex has a very similar structure, but in which the methyl groups adopt a *meso* arrangement. The coordination chemistry of telluroethers with the p-block elements is limited, although the Southampton laboratory has recently reported complexes with tin, antimony and bismuth. The complexes $[SnX_4L_2]$ (X = Cl or Br, L = Me_2Te) and $[SnX_4(L\text{-}L)]$ (L-L = $MeTe(CH_2)_3TeMe$, $PhTe(CH_2)_3TePh$ or *o*-$C_6H_4(TeMe)_2$) have all been prepared from the reaction of the appropriate ligand with $SnCl_4$ in anhydrous CH_2Cl_2.[47] The complexes are all very moisture sensitive and slowly decompose over a period of weeks even in a dry-box. The crystal structures of $[SnX_4\{o\text{-}C_6H_4(TeMe)_2\}]$ (X = Cl (Figure 1.1) or Br) show discrete tin(IV) species involving a chelating *o*-$C_6H_4(TeMe)_2$ ligand, giving a distorted octahedral molecule. In both cases, the ditelluroether ligand adopts a *meso* arrangement, with both methyl substituents directed to the same side of the SnX_2Te_2 plane.[47]

Figure 1.1 - Crystal structure of $[SnCl_4\{o\text{-}C_6H_4(TeMe)_2\}]$[47]

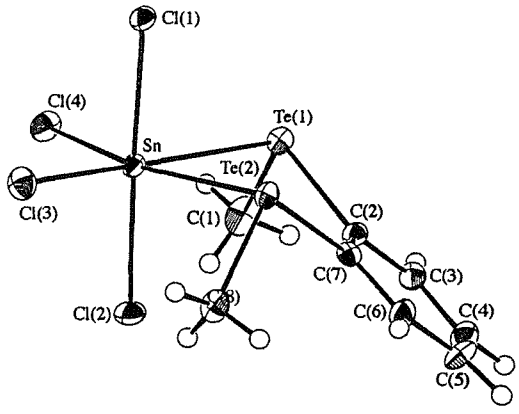

The reaction of $MeTe(CH_2)_3TeMe$ with MX_3 (M = Sb or Bi; X = Cl, Br or I) in anhydrous MeCN solution (or thf for X = I) form the analytically pure compounds $[SbX_3\{MeTe(CH_2)_3TeMe\}]$ (X = Br or I) and $[BiCl_3\{MeTe(CH_2)_3TeMe\}]$, with $[BiBr_3(PhTeMe)]$ also being formed from the reaction of PhTeMe with $BiBr_3$ in MeCN solution.[48] These complexes were the first examples of antimony and bismuth telluroether species, and, other than the tellurolate compounds $[M\{TeSi(SeMe_3)_3\}_3]$ (M =

Sb or Bi) synthesised by Arnold and co-workers,[49] they are the only known complexes involving Sb-Te or Bi-Te bonds. The crystal structure of $[BiBr_3(PhTeMe)]$ revealed a planar asymmetric $Br_2Bi(\mu\text{-}Br)_2BiBr_2$ dimer unit with one PhTeMe ligand coordinated apically to each Bi and occupying mutually *anti* positions. Additional long contacts (3.16 Å) between Br(3) and Br(3b) *via* the open Bi vertex link adjacent units and give a step-like arrangement of infinite chain $Bi_2Br_6(PhTeMe)_2$ dimers (Figure 1.2).

Figure 1.2 - Crystal structure of $[BiBr_3(PhTeMe)]$[48]

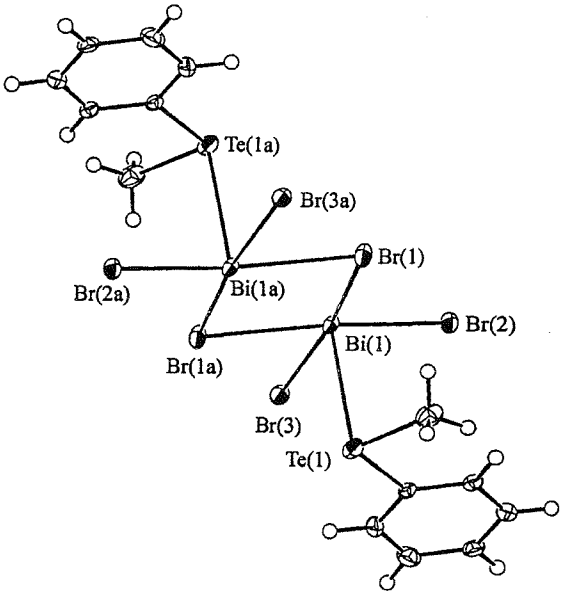

The complexes $[MCl_2(L_2)]$ (L_2 = $PhSCH_2SPh$, $MeSCH_2SMe$, $PhSeCH_2SePh$ or $MeSeCH_2SeMe$, M = Pd or Pt; L_2 = $PhTeCH_2TePh$ or $MeTeCH_2TeMe$, M = Pd) are known, with the ditelluroether ligand forming polymeric chelate complexes of the type $[M(L_2)_2Cl_2]_n$.[44]

The largest collection of ditelluroether metal complexes in the literature involve $RTe(CH_2)_3TeR$ and *o*-$C_6H_4(TeR)_2$ (R = Me, Ph), with the latter forming 5-membered chelate rings in many complexes. Although the Co(III) complexes $[CoX_2\{o\text{-}C_6H_4(TeMe)_2\}_2][BPh_4]$ (X = Br, I)[50] have been prepared, attempts to form Ni(II) and Co(II) complexes with the ligand have failed.[51] The largest number of complexes with the ligand involve Pd(II) and Pt(II). The first of these to be prepared was $[M\{RTe(CH_2)_3TeR\}X_2]$ (R = Me, Ph; X = Cl, Br, I),[52] with the X-ray structure of *meso*-

$[Pd\{PhTe(CH_2)_3TePh\}Br_2]$ being the first reported structure of a ditelluroether ligand complex. Studies into the coordination chemistry of bidentate telluroethers with large chelate rings (p-$EtO(C_6H_4)Te(CH_2)_nTe(C_6H_4)OEt$-$p$) (n = 6, 7, 8, 9, 10) with Pd(II) and Pt(II) halides have also been undertaken.[53] Bis(ditelluroether) complexes of Pd(II)/Pt(II), $[M(L\text{-}L)_2]^{2+}$ have also been prepared *via* the reaction of $[M(NCMe)_2Cl_2]$ (M = Pd/Pt) with two equivalents of L-L (L-L = $RTe(CH_2)_3TeR$ (R = Me or Ph) or o-$C_6H_4(TeMe)_2$) and $TlPF_6$ in acetonitrile.[54] The complexes *fac*-$[Mn(CO)_3(L\text{-}L)X]$ have been generated in moderate yield *via* the reaction of $[Mn(CO)_3X]$ (X = Cl, Br or I) with L-L (L-L = $RTe(CH_2)_3TeR$ (where R = Me or Ph) or o-$C_6H_4(TeMe)_2$) in chloroform.[8] The rhenium analogues (apart from the $PhTe(CH_2)_3TePh$ complex) have also been prepared similarly from $[Re(CO)_3X]$.[8] There are many other examples of transition metal telluroether complexes, including complexes with osmium, for example $[OsCl_2(L\text{-}L)_2]$ (L-L = o-$C_6H_4(TeMe)_2$, $RTe(CH_2)_3TeR$ (R = Me or Ph)) which were prepared from *trans*-$[OsCl_2(dmso)_4]$ and the ditelluroethers in ethanol. The crystal structure of *trans*-$[OsCl_2\{PhTe(CH_2)_3TePh\}_2]$ (Figure 1.3) shows a *trans pseudo*-octahedral molecule with the osmium(II) on an inversion centre and with both ditelluroether ligands adopting the *meso* form.[55] The structure is very similar to the previously reported *trans*-$[RuCl_2\{PhTe(CH_2)_3TePh\}_2]$.[54]

Figure 1.3 - Crystal structure of trans-$[OsCl_2\{PhTe(CH_2)_3TePh\}_2]$[55]

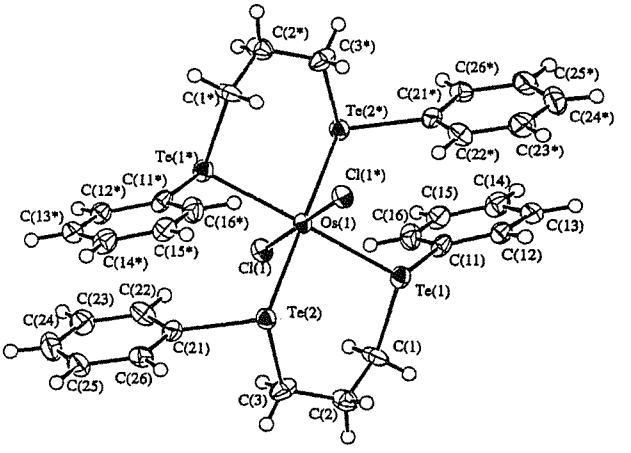

There are relatively few complexes of multidentate cyclic and acyclic telluroether ligands, purely because of the lack of ligands in the first instance. Three such ligands are $MeC(CH_2TeR)_3$ (R = Me[24] or Ph[29]) and $C(CH_2TePh)_4$,[24] upon which complexation studies have only very recently been reported.[56] Studies into the recently synthesised ligand $RTe(CH_2)_3Te(CH_2)_3TeR$ (where R = Me or Ph) have been undertaken, and a variety of low- to medium-valent transition metal complexes have been synthesised[57] (Chapter 4).

1.3 Complexes of the tripodal ligands $MeC(CH_2EMe)_3$ (E = S, Se or Te)

The group 15 tridentate ligand $MeC(CH_2PPh_2)_3$ (triphos) has been well studied as a result of the combination of the catalytic properties of phosphine ligands with the stereochemical constraints imparted on the metal centre by the tripodal ligand.[58] Bianchini and co-workers have studied such complexes with the platinum group metals and have successfully mimicked the hydrodesulfurisation (HDS) process with Ru(II) and Ir(II).[59,60]

Group 16 tripodal ligands had received little attention until a relatively recent study,[56] although many derivatives of the thioether tripod have been synthesised. Only two selenoether and telluroether tripods have been prepared: $MeC(CH_2ER)_3$ (E = Se or Te; R = Me, Ph),[26] and a number of complexes have been prepared. These include *fac*-$[Mn(CO)_3\{MeC(CH_2EMe)_3\}]^+$ (E = S, Se or Te), $[Mn(CO)_3\{MeC(CH_2TePh)_3\}]^{+}$[29] and $[M\{MeC(CH_2SeMe)_3\}_2][PF_6]_2$ (M = Pd or Pt).[56] The crystal structure of *fac*-$[Mn(CO)_3\{MeC(CH_2TeMe)_3\}][CF_3SO_3]$ (Figure 1.4) showed the central Mn(I) centre coordinated to three mutually *fac* carbonyl ligands and all three Te donors from the tritelluroether ligand.[29]

Reaction of $[M(COD)Cl]_2$ (M = Rh or Ir) with two equivalents of $MeC(CH_2ER)_3$ ((L_3), where E = Se, R = Me; E = Te, R = Me or Ph) and NH_4PF_6 in dichloromethane formed the complexes $[M(COD)(L_3)][PF_6]$.[61]

Figure 1.4 - Crystal structure of $[Mn(CO)_3\{MeC(CH_2TeMe)_3\}]^{+}$[29]

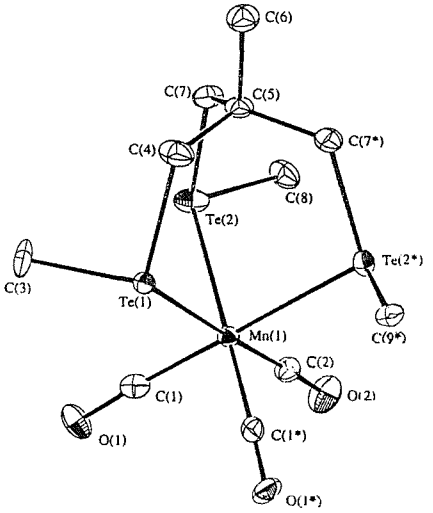

The crystal structure of $[Rh(COD)(L_3)][PF_6]$ where $L_3 = MeC(CH_2TeMe)_3$ showed the Rh(I) centre coordinated to COD and all three donors of the facially capping tripodal ligand, with the methyl groups adopting the *syn* arrangement to form a five-coordinate complex cation (Figure 1.5). Rhodium-tellurium bond lengths are 2.6226(8), 2.5786(8) and 2.6924(7) Å, thus one Rh-Te bond is significantly longer than the other two. The Te-Rh-Te angles are all close to 90°, and the Te-Rh-C angles are between 83.5(3) and 167.9(2)°. The structure is therefore square pyramidal, with the longer R-Te bond axial and the shorter bonds being *trans* to the COD ligand.

Figure 1.5 - Crystal structure of $[Rh(COD)\{MeC(CH_2TeMe)_3\}]^{+}$[61]

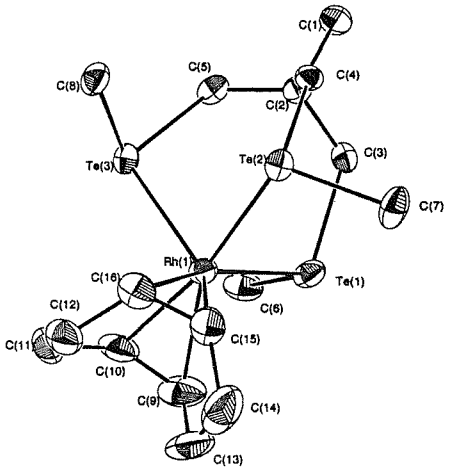

The reaction of $[MCl_2(NCMe)_2]$ (M = Pd or Pt) with two equivalents of L_3 (L_3 = $MeC(CH_2SeMe)_3$, $MeC(CH_2TeMe)_3$ or $MeC(CH_2TePh)_3$) and $TlPF_6$ in acetonitrile form the complexes $[M(L_3)_2][PF_6]_2$.[56] These have been shown to be fluxional in solution at room temperature by their simple ^1H NMR spectra, and a crystal structure of $[Pt\{MeC(CH_2SeMe)_3\}_2][PF_6]_2$ shows a square planar Se_4 donor set around the Pt(II) centre. The methyl groups adopt the DL configuration, with the uncoordinated arm of each tripod pointing away from the metal centre on opposite sides. The octahedral bis tripod complexes $[Ru\{MeC(CH_2TeR)_3\}_2][CF_3SO_3]_2$ have also been prepared from $[Ru(dmf)_6][CF_3SO_3]$ and the ligands in EtOH solution.[56]

1.4 Metal-ligand bonding

The bonding of tertiary phosphines to metal centres has been reviewed a number of times in the literature,[62] but relatively little work has been undertaken to determine the factors influencing the bonding of neutral group 16 donor ligands (and most of this has involved the lighter thioethers). A 1981 review by Murray and Hartley[4] summarised all of the known data on the structural and bonding characteristics of thio-, seleno- and telluroether complexes, but data on the heavier chalcogenide ligands were limited to only 4 crystal structures. The bonding of M-Se and M-Te remains relatively rather poorly understood, however, despite the structural characterisation of many more complexes since.[5]

Unlike for phosphines, arsines *etc.*, steric effects are not usually important for chalcogenoethers, since they may only have two substituent R groups. The presence of a second lone pair in an sp^3 hybrid orbital on the chalcogen atom complicates matters however, in that it may participate in π-donation to the metal centre, or be a source of π-repulsion. This is not a problem for group 15, where the only lone pair contributes to the metal-ligand bonding. Also, π-acceptance is possible, but as with tertiary phosphine ligand complexes, this is difficult to establish.[62]

Early work with metal-chalcogenoether complexes assumed that the acceptor orbital was the (S, Se or Te)*n*d orbital. This assumption, however, is subject to the same criticism encountered for group 15 ligands, since the *nd* orbital is considered to be too

high in energy to contribute significantly to the bonding. It was therefore concluded that the acceptor orbitals must be mainly the (E-C)σ^* combinations (where E = S, Se or Te).

Schumann and co-workers have reported structural data and Hückel molecular orbital calculations on the species $[CpFe(CO)_2EMe_2]^+$ (E = S, Se, Te),[63] the results of which showed that the inertness and stability of the Fe-E bonds lie in the order Te >> Se > S. Calculations on group 15 analogues and Fe-EH_3 systems have shown that π-bonding in these group 16 complexes is negligible. The increased σ-donation from S $\rightarrow$ Se $\rightarrow$ Te is consistent with the converse decrease in electronegativity (S = 2.58, Se = 2.55 and Te = 2.10 on the Pauling Scale). This generally applies to low oxidation state metal complexes where the greater spatial extension of the d-orbitals provides a better overlap with the large tellurium σ-orbital. The trend has been verified by a study into ^{77}Se-{^{1}H} and ^{125}Te-{^{1}H} NMR coordination shifts in the M(I) systems $[M(COD)\{MeC(CH_2EMe)_3\}]^+$, where M = Rh or Ir and COD = cyclooctadiene.[61] The major evidence from the Southampton laboratory for the enhanced σ-donating properties of telluroethers in comparison to the lighter group 16 analogues was provided by a study of the systems $[Mn(CO)_3X(L\text{-}L)]$ (X = Cl, Br, I; L-L = $RTe(CH_2)_3TeR$ (R = Me, Ph) and *o*-$C_6H_4(TeMe)_2$) which gave a series of complexes containing five and six-membered chelate rings suitable for comparison with the analogous thio- and selenoether complexes. The ^{55}Mn chemical shifts were found to move progressively to lower frequency as the group 16 donor was changed from S $\rightarrow$ Se $\rightarrow$ Te. The increased shielding paralleled the decrease in ν(CO), therefore providing evidence that σ-donation from the chalcogen to Mn(I) increases in the same direction.[8] For many comparable organoselenium and organotellurium compounds the ^{77}Se and ^{125}Te chemical shifts show consistent trends and often the δ(Te) : δ(Se) ratio is 1.7 – 1.8 and the $^1J_{(Te\text{-}X)}$: $^1J_{(Se\text{-}X)}$ ratio is *ca.* 2 – 3.[8] For the Mn(I) complexes above, the averaged chemical shifts for the different invertomers of each complex gave a δ(Te) : δ(Se) ratio between 2.1 and 2.9. These values are much more positive than expected, either by comparison with the ^{77}Se chemical shifts in the selenoether analogues or with the same ligands bonded to medium-oxidation state metal centres.[8] In medium to high oxidation state complexes there is a poorer orbital match (both in size and energy) between the large, soft, Te orbital and the contracted

orbitals of the hard metal centre. This has led to the observation that telluroether complexes of hard metals are much less stable than their selenoether and thioether analogues. This has also been demonstrated by studies of the NMR coordination shifts of ^{77}Se and ^{125}Te in the Rh(III)/Ir(III) systems $[(\eta^5\text{-cp}^*)M\{MeC(CH_2EMe)_3\}][PF_6]_2$, where $cp^* = C_5Me_5$ and M = Rh or Ir.[61] The greater stability of Se over S in these medium to high oxidation state complexes remains, however, due to the enhanced σ-donation by Se.[5] The inability of telluroethers to bond to high oxidation states of the platinum group metals, while the S and Se complexes of Pt(IV), Ru(III) and Os(IV) are known[64] may therefore be explained, since there is much poorer overlap between the large Te σ-donor orbital and the contracted metal orbitals.

1.5 The stereochemistry of the M-E Bond (E = S, Se, Te) and pyramidal inversion

Single crystal X-ray diffraction studies of thio-, seleno- and telluroether ligand complexes show the coordinated chalcogen atom (E) to be in a pyramidal environment. This means that the bond angles about E are near tetrahedral, with the remaining lone pair (the first participates in the bonding to M) in an sp^3 hybrid orbital (Figure 1.6).

Figure 1.6 - The stereochemistry of a group 16 ligand coordinated to a metal (M) centre (E = S, Se or Te)

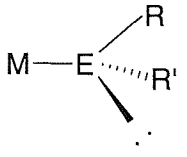

A consequence of this is that a ligand with substituents R' ≠ R becomes chiral upon coordination to M, and for simple RER' ligands this produces two possible enantiomers. For monodentate ligands, rotation about the M-E bond is a low energy process, and therefore the enantiomers are indistinguishable by NMR, even at low temperatures. For chelating ligands, however, rotation about the M-E bond is energetically less favourable, and therefore by using NMR spectroscopy it is possible to observe the different invertomers providing that they are not interconverting *via* rapid pyramidal inversion

(shown for a tridentate chalcogen ligand-metal complex in Figure 1.7). The DL pair are enantiomers and are therefore equivalent by NMR spectroscopy. The various invertomers may be present in different proportions in solution, which may be determined semi-quantitatively from the NMR spectra. Pyramidal inversion is explored in more detail in Chapter 4.

Figure 1.7 - The different invertomers possible for a tridentate chalcogen ligand-metal complex

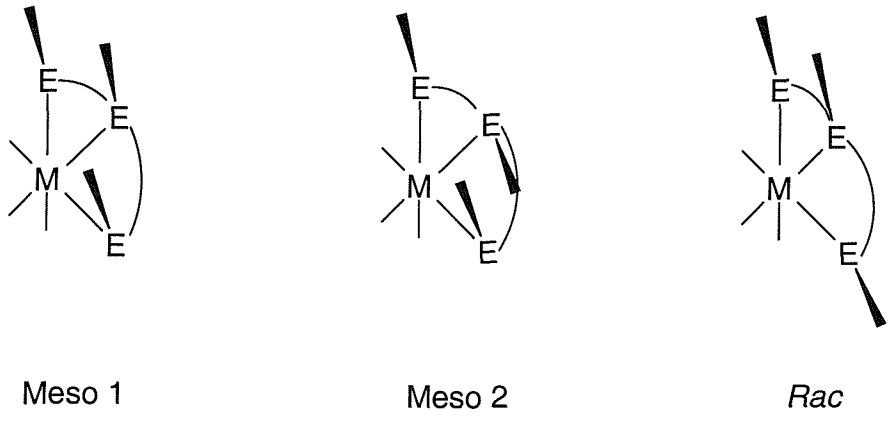

E = chalcogen

The most common mechanism of pyramidal atomic inversion is *via* a planar transition state (B) that involves the interchange of two energetically equivalent configurations (A and C) (Figure 1.8).

Figure 1.8 - Pyramidal inversion via a planar intermediate

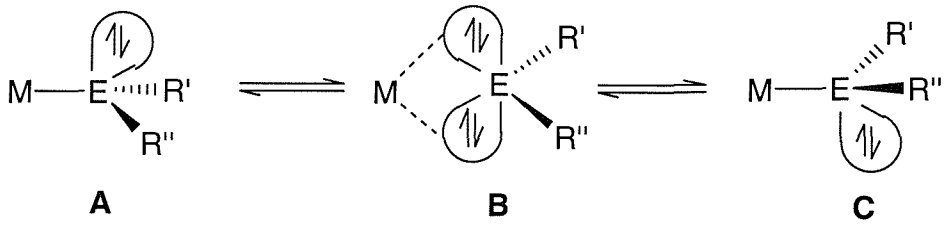

E = chalcogen atom, M = metal centre

R' and R'' = ligand backbone

This process does not involve the cleavage of any bonds, and is considered to be the most common mechanism for chalcogen complexes.[65] Other mechanisms include the dissociation and recombination of one or more of the 3 substituents on the central atom, and binuclear exchange.[65] Both of the latter mechanisms involve cleavage of the strong metal-chalcogen bonds, however, and are therefore thought to be unimportant in the systems described in this thesis.

Studies on pyramidal inversion in chalcogen-transition metal complexes have revealed the factors that influence atomic inversion energies.[65] These include:

- ***The nature of the inverting centre***[66-69]
  - Inversion barriers generally lie in the order Te > Se > S, although quantitative data for telluroethers are scarce.

- ***The nature of the metal centre***[70]
  - Coordination of a chalcogen-based lone pair of electrons to a metal centre significantly reduces its barrier to pyramidal inversion, and easier access to the planar transition state is facilitated as the bond strength between the chalcogen and the metal decreases (*i.e.* as the electronegativity of the metal increases.) For example in Pt-S and Pd-S systems the former has a higher inversion barrier as a result of the stronger metal-chalcogen bond. Also, the influence of (p-d)π conjugation between the chalcogen and the metal contributes to the stabilization of the transition state.

- ***π – conjugation effects in the ligands***[70]
  - There is a fall in pyramidal inversion energy when conjugation is present in the organic moiety of the ligand due to (2p)π conjugation effects between the chalcogen lone pair and the ligand backbone. These effects are more significant in the planar transition state than in the pyramidal ground state, therefore favouring inversion.

- *Ligand chelate ring effects*[67-69]
  - There is generally a fall in the inversion energy barrier between five- and six-membered chelate ring complexes as a result of the decreased angle constraint for access to the planar transition state.

- *Influence of trans ligands*[71]
  - The *trans* influence is essentially inductive and is attributed to a weakening of the metal-chalcogen bond. For the halogen co-ligands inversion energies for a given M-ER_2 complex decrease in the order Cl > Br > I.

1.6 Macrocyclic ligands and synthesis

Mono- and bidentate ligands form the majority of the tellurium containing ligands reported in the literature as a result of the synthetic difficulties involved in their synthesis. Tridentate ligands are scarce, and only one homoleptic tellurium macrocycle, [12]aneTe_3 has been reported to date, although no work has been reported exploring its coordination chemistry.[72]

Our group has been interested in the synthesis of novel, mixed-donor Se/Te and S/Te macrocyclic and acyclic ligands, since these will allow tellurium to be studied in new coordination environments (for example high oxidation state complexes) if facilitated by the additional donor(s). Also, direct comparisons of the electronic properties of Te and S/Se within the same complex will be possible.

The preparation of new macrocyclic telluroethers would allow tellurium to be studied within a macrocyclic environment and may lead to complexes with novel properties as a consequence of the enhanced thermodynamic and kinetic stability associated with the macrocyclic effect. It is also expected that the macrocyclic environment will enhance the σ-donating ability of Te to metal centres. Other macrocyclic complexes have applications in many diverse fields, although the applications of macrocyclic telluroether ligand complexes have not been studied in detail. These include:

- Catalysis: Electrochemical studies on thioether macrocyclic complexes have shown that unusual oxidation states may be accessed and stablisised that are often not possible with their acyclic analogues. An example is the paramagnetic Pd(III) ion which is stablisised in $[Pd([9]aneS_3)_2]^{3+}$.[73] The accessibility of such uncommon oxidation states suggests that some systems may have potential applications in electrocatalytic pathways. The complex $[Rh(PPh_3)_2([9]aneS_3)][PF_6]$ has been shown to undergo ligand substitution and catalyse the demurcuration of bis(alkynyl)mercurials.[74]

- Selectivity: Macrocycles are capable of extracting certain metal ions from a mixture depending on their donor atoms and ring size. This is particularly the case for crown ethers and their derivatives, where the hard oxygen donors preferentially bind group 1 and 2 metals. For example 18-crown-6 selectively binds K^+ over Na^+.[10]

- Tumour imaging: Macrocycles are potential carriers for β and γ emitters such as ^{64}Cu, which is of interest to the radiopharmaceutical industry. The strong coordinating ability of the macrocycle ensures that the metal centre remains complexed to the imaging agent.[75]

The preparation of thioether macrocycles is well established, with the ligands $[9]aneS_3$, $[14]aneS_4$, $[16]aneS_4$, and $[18]aneS_6$ being available from commercial suppliers. This reflects the significant amount of interest into their chemical and complexation behaviour. Of particular interest is the macrocycle $[9]aneS_3$, as a result of the preorganisation of its lone pairs for facial (*fac*) coordination, and the C_2 linkages between donor atoms. This last feature causes 5-membered chelate rings to be formed upon coordination to a metal centre. Complexes include the Pd and Pt species $[Pd([9]aneS_3)_2]^{3+}$ and $[Pt([9]aneS_3)_2]$,$^{3+}$ in which the unusual oxidation states Pd(III) and Pt(III) are stabilized by the ligand.[76] Other complexes with the ligand include Ag(II) and Rh(II) species. The compound $[Au([9]aneS_3)_2]^{2+}$ is a very rare example of a mononuclear Au(II) complex, and was the first such complex to be structurally

characterised. The structure confirms binding of two [9]aneS$_3$ macrocycles to the d^9 Au(II) centre, with a tetragonally elongated stereochemistry.[77] The reaction of $[Rh(OH_2)_6]^{3+}$ or $[Rh(CF_3SO_3)_3]$ with two molar equivalents of [9]aneS$_3$ affords $[Rh([9]aneS_3)_2]^{3+}$, which can be converted by controlled potential electrolysis into the monomeric d^7 species $[Rh([9]aneS_3)_2]^{2+}$.[78] This species is a rare example of a genuine, mononuclear Rh(II) complex, further demonstrating the ability of the trithia crown to stabilise unusual oxidation states.

Macrocycles are often synthesised by one of two main strategies: (i) metal template and (ii) high dilution synthesis, although the preparation of such compounds are generally more problematic and challenging than their corresponding acyclic derivatives. The first high yield (> 60%) synthesis of the macrocyclic thioether compound [9]aneS$_3$ by Sellmann and Zapf was *via* the cyclisation of the open chain dithiolate $^-S(CH_2)_2S(CH_2)_2S^-$ and 1,2-dibromoethane, using the Mo(CO)$_3$ fragment as a template for the reaction.[79] (Figure 1.9). This metal template technique binds the precursors together in close proximity, thereby favouring ring closure over polymerisation. Disadvantages of this technique are that demetallation is necessary to obtain the free ligand (which is not always trivial) and that problems are often encountered when trying to identify suitable metal templates, since the ion size is extremely important.[10] The high dilution method uses a very large excess of solvent in the reaction and therefore keeps the reactants at low concentrations, favouring ring closure over polymerisation. Disadvantages of this method include the likely occurrence of side reactions, which lower the yields substantially and can lead to long reaction times. The latter can be a problem when dealing with air or moisture sensitive materials.

Recently within the Southampton group a number of mixed donor thia-telluroether macrocycles, [9]aneS$_2$Te, [11]aneS$_2$Te, [12]aneS$_2$Te and [14]aneS$_3$Te, were synthesised *via* a high dilution method.[80] Very little work has been undertaken on the coordination chemistry of these ligands, however the mixed donor macrocycles (L) have been shown to react with one equivalent of silver trifluoromethanesulfonate, $AgCF_3SO_3$, in dichloromethane at room temperature to form the very poorly soluble complexes $[Ag(L)][CF_3SO_3]$.

Figure 1.9 - The synthesis of [9]aneS$_3$[79]

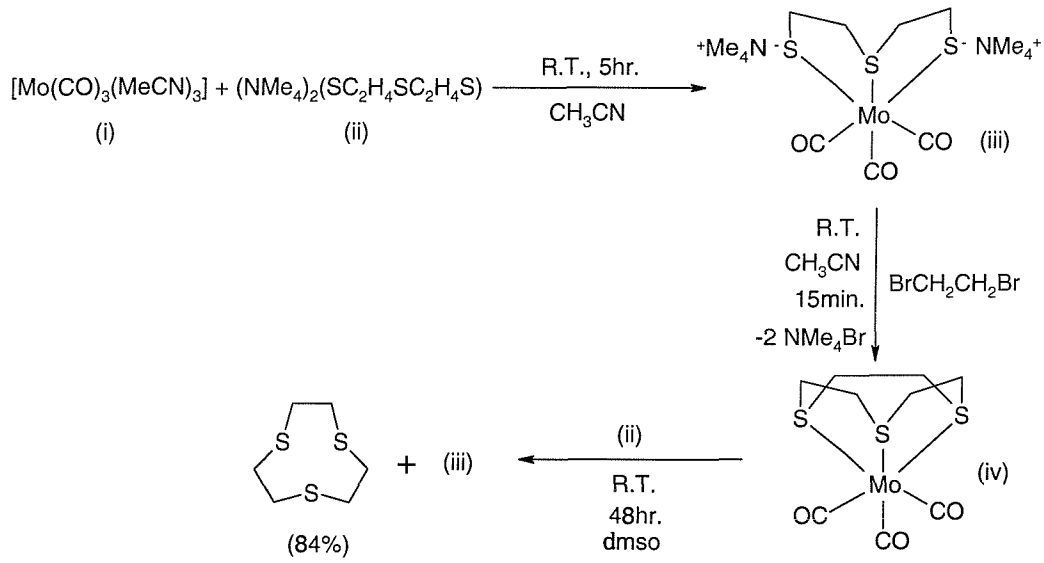

A crystal structure of the tetrafluoroborate salt [Ag([11]aneS$_2$Te)][BF$_4$] revealed a cationic one-dimensional polymeric structure, in which the silver(I) centres are bridged by the ligand, with a silver cation coordinated to each of the macrocyclic donor atoms.[80] (Figure 1.10). The synthesis and coordination chemistry of [9]- [11]- and [12]aneS$_2$Te have been investigated in detail in this work (Chapter 2).

Figure 1.10 - Crystal structure of [Ag([11]aneS$_2$Te)][BF$_4$][80]

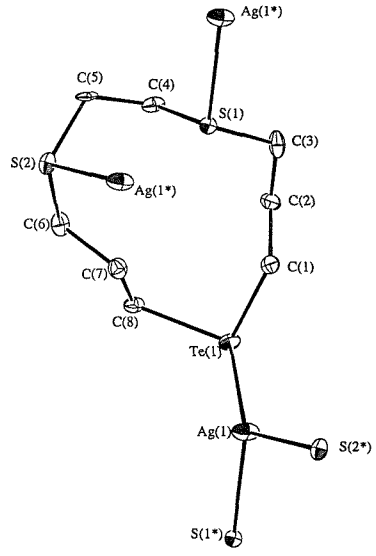

1.7 The macrocyclic effect

Cabbiness and Margerum first proposed the term 'macrocyclic effect' in 1970.[81,82] They demonstrated that the stability constant for the Cu(II) complex of the reduced Curtis macrocycle, tet-a (Figure 1.11, (i)) was approximately 10^4 times higher than for the related complex of the open-chain tetramine, 2.3.2-tet (Figure 1.11, (ii)). It was also noted that the rate of coordination of tet-a was about 10^3-10^4 times slower than that of 2.3.2-tet. Although it is expected that the stability of a particular complex type will increase as the number of chelate rings increases (the chelate effect), the additional stability observed for the macrocyclic complex was an order of magnitude greater than that expected purely from the presence of an additional chelate ring. Cabbiness and Margerum used the term 'macrocyclic effect' to describe the unexpected additional stability for the macrocyclic Cu(II) complex. This effect has been found to be general, with macrocyclic compounds being almost invariably more stable than those with equivalent open-chain ligands. For very large flexible rings incorporating many donors, however, the effect becomes insignificant.

Figure 1.11 - Cu(II) complexes of 'tet-a' (i) and '2.3.2-tet' (ii)

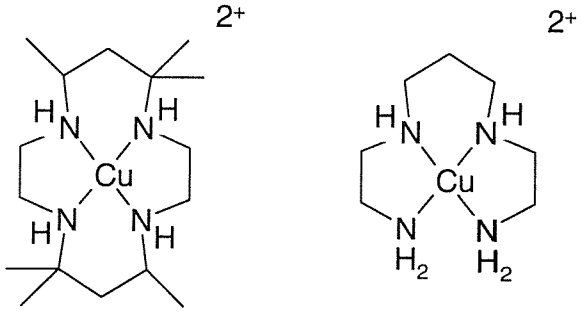

(i) (ii)

The origins of the macrocyclic effect, especially involving complexes of tetraaza ligands, has been the subject of many investigations. Early studies were contradictory, however, with the additional stability being assigned wholly to entropic factors[83] or to enthalpic factors.[84] This partly reflected the experimental difficulties that are encountered when trying to undertake such studies. Firstly, some reaction systems may take many days or

weeks to reach equilibrium, therefore pushing calorimetric methods to their limits. With some metal ions, various solution species may exist, differing in coordination number and/or spin state. Another problem may arise when choosing a suitable equivalent open-chain ligand. This should clearly contain the same number and type of donor atoms as the macrocyclic ligand, but also the nature of the spacer groups must be carefully considered. The various components of a typical complexation reaction are shown by the Born-Haber cycle (Figure 1.12), where each of the steps 1 – 5 has ΔG, ΔH and ΔS terms associated with it. The overall values of these parameters for the complexation reaction are the respective sums of the individual components. To fully understand the nature of a particular macrocyclic effect, it is therefore necessary to have full data for both the macrocyclic and open-chain systems. The general absence of unambiguous data for each of the steps for particular systems has been the major difficulty in defining precisely the nature of particular macrocyclic effects, however both the entropic (ΔS) and enthalpic (ΔH) terms contribute to the macrocyclic effect (*i.e.* ΔG for the formation of macrocyclic complexes are more negative than for the analogous open-chain ligand complexes).

Figure 1.12 - Born-Haber cycle for a typical complexation reaction

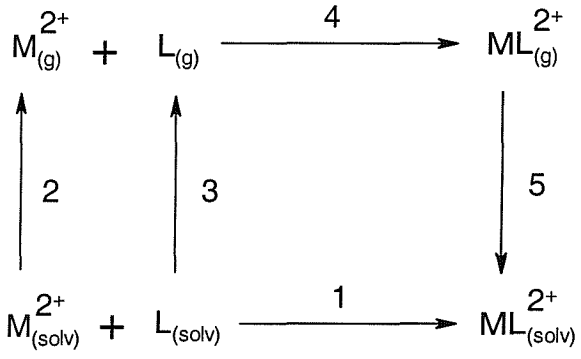

Solvation effects may play an important role in certain cases, *e.g.* the desolvation of the metal ion and ligand (steps 2 and 3) will result in positive changes for ΔH and ΔS. If it is assumed that a similar desolvation of the metal ion occurs on its reaction with either the macrocyclic or open-chain ligand, then it is the difference in the ligand desolvation terms that will contribute to the macrocyclic effect. It has also been argued that solvation

effects are less significant for macrocyclic ligands than for their acyclic counterparts because the former are more compact.[85] If this is the case, then ligand desolvation enthalpies would be expected to be less for the macrocyclic ligand, therefore contributing to the enhanced thermodynamic stability relative to the open-chain analogue.

The entropic component of the macrocyclic effect is harder to interpret, however cyclic ligands have fewer rotational and translational degrees of freedom than their open-chain analogues, and therefore there will be a less dramatic ordering effect upon coordination of the macrocycles to a metal centre than for the open-chain ligands. The preorganisation of macrocyclic ligands for coordination to metal centres reduces the unfavourable entropy loss compared with acyclic ligands, therefore contributing to the macrocyclic effect.

Thioether macrocyclic ligands have also proven useful for probing the nature of the macrocyclic effect, as metal complexation is not complicated by competing protonation equilibria as is the case for aza-macrocycles, and their generally lower polarity tends to result in ligand solvation effects being less important. For such systems, the observed macrocyclic effect appears to be attributable to a more favourable entropic component, perhaps reflecting the greater preorganisation of the macrocyclic systems versus their acyclic analogues.[86,87] In contrast, crown polyether macrocyclic complexes have been found to be enthalpy stabilised, with the entropy term also contributing to the stability in a number of cases.[88]

The cavity size of the macrocycle is also important when considering the stability of a given complex (and therefore contributes to the magnitude of the macrocyclic effect). A close match between the metal-ion radius and the cavity size tends to be associated with an enhanced stability for the system. Cavity size effects tend to be more dominant when the macrocyclic system involved is fairly rigid (*e.g.* porphyrin ligands), since rigid ligands of this type are less able to compensate for any size mismatch between the size of the central cavity and the metal-ion involved. If the metal ion is too small, complex formation may lead to elongated (weaker) ligand-metal bonds and the resultant complexes will be less stable and more prone to dissociative processes. Conversely, if the metal ion is too large, the result may either be compressed bond lengths or the metal

ion being displaced from the plane of the donor atom set, which also leads to decreased complex stability.[10]

Both coordination and ligand dissociation reactions of macrocyclic ligand complexes are usually slower than their open-chain analogues, this being especially true for macrocycles incorporating rigid backbones or having a greater steric bulk. The rate of complex formation is often almost independent of ring size, however. The origin of this observation lies in the greater flexibility of open-chain ligands versus their macrocyclic analogues. During complexation reactions, the reduced flexibility of macrocyclic ligands means that the ligands are often forced into high-energy conformations when positioning their donors for complexation, whereas the flexibility of open-chain ligands usually overcomes this problem.[89] For tetraaza macrocyclic ligand complexes, the high stabilities are due to extremely slow dissociation reactions, which are typically $10^5 - 10^7$ times slower than those of open-chain analogues.[90]

1.8 Characterisation techniques

A wide range of characterisation techniques are available to the analytical chemist for the study of new ligands and their coordination compounds, including ^{1}H, ^{13}C-{^{1}H} and multinuclear NMR spectroscopy, IR and UV-visible spectroscopy, mass spectrometry, single crystal X-ray diffraction and elemental analysis. A short account of mass spectrometry and ^{77}Se-{^{1}H}, ^{125}Te-{^{1}H}, ^{55}Mn and ^{195}Pt spectroscopies will be discussed in the next section.

1.8.1 Mass spectrometry

The study of tellurium-containing species by mass spectrometry is aided by the large number of different Te isotopes (eight of reasonable abundance, shown in Table 1.0).

Table 1.0 - Tellurium isotopes: relative abundance and nuclear spin values[91]

Isotope	Abundance/%	I	Isotope	Abundance/%	I
120	0.09	0	125	7.07	½
122	2.55	0	126	18.84	0
123	0.89	½	128	31.74	0
124	4.74	0	130	34.08	0

It is therefore straightforward to identify a tellurium-containing fragment from its characteristic isotope pattern (Figure 1.13) although fragments may have overlapping patterns, thereby complicating the analysis. For simplicity in this thesis, all calculated *m/z* values use the most abundant isotope, ^{130}Te. Another notable feature of the mass spectra is the inherent weakness of the Te-C bond compared with those of O-C, S-C and Se-C, therefore causing more prolific fragmentation. A detailed review of the mass spectrometry of tellurium-containing compounds is available.[92] For the ligands studied in this thesis, EI (or GC-EI mass spectrometry for volatile ligands) is generally appropriate, with fragmentation generally not precluding the observation of the parent ions. For metal complexes, electrospray mass spectrometry (ESMS) is extensively used in this work.

Figure 1.13 - Isotope patterns for 1 (i), 2 (ii) and 3 (iii) Te atoms

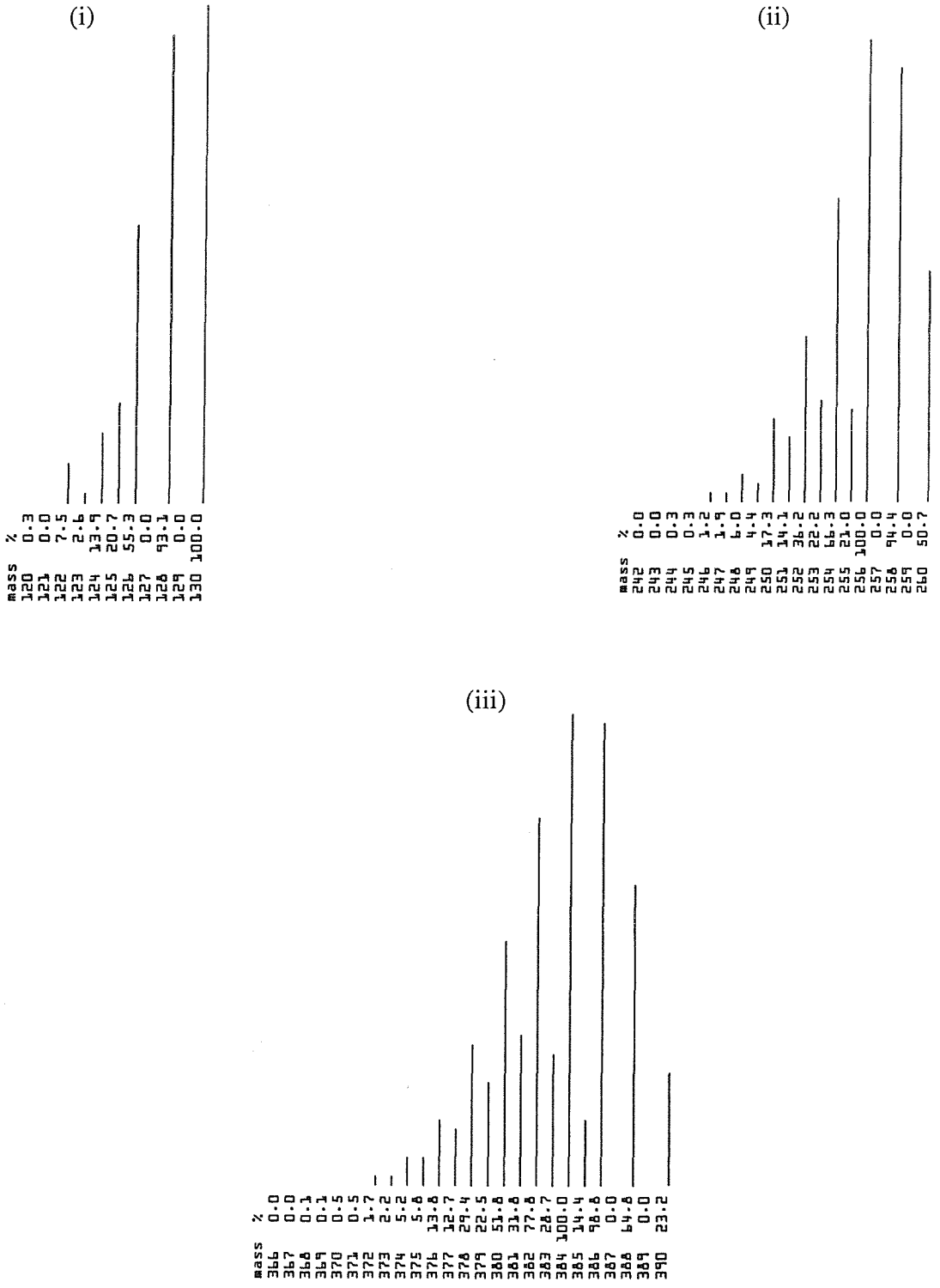

1.8.2 NMR spectroscopy

^{55}Mn NMR spectroscopy

Manganese-55 (100% abundant, I = 5/2) has a moderately high quadrupole moment (Q = 0.55×10^{-28} m^2) and therefore for complexes having lower than octahedral or tetrahedral symmetry the considerable electric field gradient results in significant broadening of the resonances.[93] Despite this, however, ^{55}Mn is a very sensitive nucleus having a relative receptivity (compared to ^{1}H) of 0.175 therefore making spectral acquisition straightforward. The total range of known ^{55}Mn chemical shifts covers a range of *ca.* 3500 ppm, from *ca.* -3000 ppm (*e.g.* $[Mn(CO)_5]^-$) to *ca.* +500 ppm (*e.g.* $[Mn(CO)_3(MeCN)_3]^+$).[93] The widely used reference for ^{55}Mn NMR spectroscopy is aqueous $KMnO_4$.[93]

^{77}Se-{^{1}H} and ^{125}Te-{^{1}H} NMR spectroscopy

The ^{77}Se and ^{125}Te nuclei are of moderate and good receptivity respectively, although there have been more studies with the former due to the greater overall activity in selenium chemistry. Table 1.0 outlines the nuclear spin values of the eight major Te isotopes, and although ^{123}Te has I = ½, its natural abundance of only 0.89% makes it difficult to study by NMR. ^{125}Te has a much larger natural abundance (7.07%) however, which means that it is much more easily studied. It has a negative magnetogyric ratio ($\gamma = -8.498 \times 10^7$ Rad T^{-1} s^{-1})[91] however H-Te distances are usually so great that the Nuclear Overhauser Effect is negligible. Therefore standard spin-½ techniques may be used for this nucleus and for ^{77}Se (*i.e.* proton decoupling, moderate pulse angles and pulse repetition rates from 0.5 to a few seconds). The receptivity relative to carbon is 13.1 for ^{125}Te, which indicates that it is of adequate sensitivity for NMR. Several reference compounds have been used for ^{77}Se and ^{125}Te NMR spectroscopy (*e.g.* SeO_2 and $Te(OH)_6$) but now Me_2Te (and Me_2Se for ^{77}Se NMR) are generally used as standard.[94] These compounds are, however, sensitive to changes in both solvent and concentration, so chemical shifts are reported relative to the neat reference samples. It is known that

variations of *ca.* 20 ppm may occur for any ^{125}Te resonance with changes in solvent, concentration and temperature, while this figure is approximately 10 ppm for ^{77}Se.[94] The overall chemical shift range for ^{125}Te is greater than 4000 ppm (*ca.* –1000 to 3000 ppm) while the chemical shift for ^{77}Se ranges from *ca.* –400 to 2000 ppm, with electron withdrawal from selenium or tellurium leading to decreased shielding and more positive chemical shifts.[95]

^{195}Pt NMR spectroscopy

The only NMR active isotope, ^{195}Pt, is 33.8% abundant and has I = ½. The receptivity (relative to ^{13}C) is good (19.9).[96] The widely used reference for ^{195}Pt NMR spectroscopy is aqueous 1 mol dm^{-3} $[PtCl_6]^{2-}$ in D_2O, for which $\delta = 0$. The relatively high resonance frequency of ^{195}Pt (21.4 MHz) makes it impractical to cover the whole of the very large chemical shift range in a single frequency width; therefore an educated assessment as to roughly where a resonance will occur must be made before the start of an NMR experiment.[96] The chemical shift range for ^{195}Pt NMR spectroscopy is very large – for example Pt(II)P_4 species have $\delta(^{195}Pt)$ *ca.* –5500 ppm while $[PtF_6]^{2-}$ has $\delta(^{195}Pt)$ *ca.* 12 000 ppm.[96] The rapid relaxation times for ^{195}Pt in fairly asymmetric environments allows for fast pulsing rates and therefore fairly short acquisition times. Chemical shift (δ) values and coupling constants (J) are very sensitive to the oxidation state and donor set around Pt, together with changes in the *trans* ligand. The geometry about ^{195}Pt is also very important (*e.g. cis* and *trans* isomers can have significantly different chemical shifts).[96]

1.9 Aims of this study

This thesis investigates the synthesis and coordination chemistry of new and recently reported telluroether ligands, both acyclic and macrocyclic, and is divided into 5 chapters.

Chapter 2

The syntheses of the recently reported mixed donor macrocyclic ligands [9]-, [11]- and [12]-aneS_2Te are explored in more detail and their coordination chemistry is investigated with a variety of low to medium oxidation state transition metal ions.

Chapter 3

We wished to investigate the effects of incorporating donors other than sulfur within a tellurium-containing macrocycle, and this chapter reports our attempts to synthesise the new mixed-donor macrocyclic ligands [9]aneO_2Te and [18]aneO_4Te_2, and to compare them with the previously reported [9]aneO_2Se and [18]aneO_4Se_2.

Chapter 4

In order to provide comparisons with the mixed donor macrocyclic ligands [9]-, [11]- and [12]-aneS_2Te (Chapter 2) we set out to explore the coordination chemistry of the recently synthesised $MeS(CH_2)_3Te(CH_2)_3SMe$ ligand with a variety of transition metals ions, including Mn(I), Rh(III), Cu(I), Ag(I), Pt(II) and Pd(II).

Chapter 5

Finally, Chapter 5 reports our results from an investigation into the synthesis and organo-derivatives of a number of xylyl-based telluroether ligands, including the new ligands *m*- and *p*-$C_6H_4(CH_2TeMe)_2$, and also the attempted syntheses of tellurium-containing cyclophane compounds.

1.10 References

1. M. E. Weeks, *Discovery of the Elements*, 6th edn., *Journal of Chemical Education*, Easton, Pa., 1956: Selenium and Tellurium, pp. 303-319; Klaproth-Kitaibel letters on tellurium, pp. 320-37.
2. F. Wohler, *Ann. Chem.*, 1840, **35**, 111.
3. S. E. Livingstone, *Q. Rev. Chem. Soc.*, 1965, **19**, 386.
4. S. G. Murray and F. R. Hartley, *Chem. Rev.*, 1981, **81**, 365.
5. E. G. Hope and W. Levason, *Coord. Chem. Rev.*, 1993, **122**, 109.
6. A. K. Singh and S. Sharma, *Coord. Chem. Rev.*, 2000, **209**, 49.
7. W. Levason, S. D. Orchard and G. Reid, *Coord. Chem. Rev.*, 2002, **225**, 159.
8. W. Levason, S. D. Orchard and G. Reid, *Organometallics*, 1999, **18**, 1275.
9. T. Yoshida, T. Adachi, T. Ueda, M. Kaminaka, N. Sasaki, T. Higuchi, T. Aoshima, I. Mega, Y. Mizobe and M. Hidai, *Angew. Chem. Int. Ed. Eng.*, 1989, **28**, 1040.
10. L. F. Lindoy, *The Chemistry of Macrocyclic Ligand Complexes*, Cambridge University Press, Cambridge, 1989.
11. H. J. Glysing, M. Lelental, M. G. Mason and L. J. Gerenser, *J. Photogr. Sci.*, 1982, **30**, 55.
12. M. B. Dines and M. Marrocco, in *Extended Linear Chain Compounds*, J. S. Miller (ed.), Plenum, New York, 1982, Vol. 2.
13. S. W. Burchiel and B. A. Rhodes (eds.), *Radioimmunoimaging and Radioimmunotherapy*, Elsevier, Essex, U.K.
14. A. F. Hill and J. D. E. T. Wilton-Ely, *Organometallics*, 1997, **16**, 4517.
15. H. A. Tayim and J. C. Bailar, Jr., *J. Am. Chem. Soc.*, 1967, **89**, 4330.
16. H. J. Gysing, *Coord. Chem. Rev.*, 1982, **42**, 133.
17. H. J. Gysing, in '*Proceedings of the Fourth International Conference on the Organic Chemistry of Selenium and Tellurium*', F. J. Berry and W. R. McWhinnie (eds.), The University of Aston, Birmingham, 1983, pp. 32.
18. W. S. Haller and K. J. Irgolic, *J. Organomet. Chem.*, 1972, **38**, 97.
19. N. Petragnani and M. de Moura Campos, *Chem. Ber.*, 1963, **96**, 249.

20. Yu. A. Boiko, B. S. Kupin and A. A. Petrov, *Zh. Org. Khim.*, 1969, **5**, 1553.
21. L. Tschugaeff and W. Chlopin, *Chem. Ber.*, 1914, **47**, 1269.
22. L. Brandsma and H. E. Wijers, *Rec. Trav. Chim. Pays-Bas*, 1963, **82**, 68.
23. B. Grushkin and M. N. Saltzman, U. S. Patent 3965 049. (*Chem. Abs.*, 1976, **85**, 124606).
24. E. G. Hope, T. Kemmitt and W. Levason, *Organometallics*, 1988, **7**, 78.
25. *Methoden der Organischem Chemie (Houben-Weyl), Schwefel-, Selen-, Tellur-Verbingdungen*, E. Muller (ed.), Georg Thieme Verlag, Stuttgart, 1955, Ch. 5.
26. D. J. Gulliver, E. G. Hope, W. Levason, S. G. Murray, D. M. Potter and G. L. Marshall, *J. Chem. Soc., Perkin Trans. II*, 1984, 429.
27. T. Kemmitt, Ph.D. thesis, University of Southampton, 1989.
28. T. Kemmitt and W. Levason, *Organometallics*, 1989, **8**, 1303.
29. J. Connolly, A. R. J. Genge, W. Levason, S. D. Orchard, S. J. A. Pope and G. Reid, *J. Chem. Soc., Dalton Trans.*, 1999, 2343.
30. H. M. K. K. Pathirana, W. R. McWhinnie and F. J. Berry, *J. Organomet. Chem.*, 1986, **312**, 323.
31. E. Fritzman, *J. Russ. Phys. Chem. Soc.*, 1915, **47**, 588.
32. K. Ihmels and D. Rehder, *Organometallics*, 1985, **4**, 1340.
33. D. Rehder, K. Ihmels, D. Wenke and P. Oltmanns, *Inorg. Chim. Acta*, 1985, **100**, L13.
34. J. W. Freeman and F. Basolo, *Organometallics*, 1991, **10**, 256.
35. H. Hausmann, M. Hoefler, T. Kruck and H. W. Zimmermann, *Chem. Ber.*, 1981, **114**, 975.
36. N. Kuhn, H. Schumann and E. Zauder, *J. Organomet. Chem.*, 1988, **354**, 161.
37. H. Fischer and U. Gerbing, *J. Organomet. Chem.*, 1986, **299**, C7.
38. G. Bremer, R. Boese, M. Keddo and T. Kruck, *Z. Naturforsch. Teil B*, 1986, **41**, 981.
39. P. Jaiter and W. Winder, *Inorg. Chim. Acta*, 1987, **134**, 201.
40. N. Kuhn and H. Schumann, *J. Organomet. Chem.*, 1984, **276**, 55.
41. S. Rossi, J. Pursiainen and T. A. Pakkanen, *J. Organomet. Chem.*, 1990, **397**, 81.
42. T. Kemmitt and W. Levason, *Inorg. Chem.*, 1990, **29**, 731.

43. J. R. Black, N. R. Champness, W. Levason and G. Reid, *Inorg. Chem.*, 1996, **35**, 4432.

44. A. F. Chiffey, J. Evans, W. Levason and M. Webster, *J. Chem. Soc., Dalton Trans.*, 1964, 2835.

45. W-F. Liaw, C-H. Lai, S-J. Chiou, Y-C. Horng, C-C. Chou, M-C. Liaw, G-H. Lee and S-M. Peng, *Inorg. Chem.*, 1995, **34**, 3755.

46. A. R. J. Genge, W. Levason and G. Reid, *J. Chem. Soc., Dalton Trans.*, 1997, 4479.

47. A. R. J. Genge, W. Levason and G. Reid, *J. Chem. Soc., Dalton Trans.*, 1997, 4549.

48. W. Levason, N. J. Hill and G. Reid, *J. Chem. Soc., Dalton Trans.*, 2002, 4316.

49. S. P. Wuller, A. L. Seligson, G. P. Mitchell and J. Arnold, *Inorg. Chem.*, 1995, **34**, 4854.

50. J. L. Brown, T. Kemmitt and W. Levason, *J. Chem. Soc., Dalton Trans.*, 1990, 1513.

51. T. Kemmitt and W. Levason, unpublished results, 1987-1988.

52. T. Kemmitt, W. Levason and M. Webster, *Inorg. Chem.*, 1989, **28**, 692.

53. P. W. Downs, P. Granger, W. R. McWhinnie and H. M. K. K. Pathirana, *Inorg. Chim. Acta*, 1988, **143**, 161.

54. W. Levason, S. D. Orchard, G. Reid and V-A. Tolhurst, *J. Chem. Soc., Dalton Trans.*, 1999, 2071.

55. A. J. Barton, W. Levason, G. Reid and V-A. Tolhurst, *Polyhedron*, 2000, **19**, 235.

56. W. Levason, S. D. Orchard and G. Reid, *Inorg. Chem.*, 2000, **39**, 3853.

57. A. J. Barton, W. Levason, G. Reid and A. J. Ward, *Organometallics*, 2001, **20**, 3644.

58. H. A. Mayer and W. C. Kaska, *Chem. Rev.*, 1994, **94**, 1239.

59. C. Bianchini, A. Meli, S. Moneti, W. Oberhauser, F. Vizza, V. Herrera, A. Fuentes and R. A. Sánchez-Delgado, *J. Am. Chem. Soc.*, 1999, **121**, 7071.

60. C. Bianchini, A. Meli, M. Peruzzini, F. Vizza, S. Moneti, V. Herrera and R. A. Sánchez-Delgado, *J. Am. Chem. Soc.*, 1994, **116**, 4370.

61. W. Levason, S. D. Orchard, G. Reid and J. M. Street, *J. Chem. Soc., Dalton Trans.*, 2000, 2537.
62. W. Levason, *The Chemistry of Organophosphorus Compounds*, F. R. Hartley (ed.), Wiley, New York, 1990, Vol. 1, Ch. 15.
63. H. Schumann, A. A. Arif, A. L. Rheingold, C. Janiak, R. Hoffmann and N. Kuhn, *Inorg. Chem.*, 1991, **30**, 1618.
64. A. J. Barton, W. Levason, G. Reid and V-A. Tolhurst, *Polyhedron*, 2000, **19**, 235.
65. E. W. Abel, S. K. Bhargava and K. G. Orrell, *Progr. Inorg. Chem.*, 1984, **32**, 1.
66. R. J. Cross, T. H. Green and R. Keat, *J. Chem. Soc., Dalton Trans.*, 1976, 1150.
67. E. W. Abel, S. K. Bhargava, K. Kite, K. G. Orrell, V. Šic and B. L. Williams, *J. Chem. Soc., Dalton Trans.*, 1982, 583.
68. E. W. Abel, A. R. Khan, K. Kite, K. G. Orrell and V. Šic, *J. Chem. Soc., Dalton Trans.*, 1980, 1175.
69. E. W. Abel, K. G. Orrell, S. P. Scanlan, D. Stephenson, T. Kemmitt and W. Levason, *J. Chem. Soc., Dalton Trans.*, 1991, 591.
70. E. W. Abel, S. K. Bhargava, K. Kite, K. G. Orrell, V. Šic and B. L. Williams, *Polyhedron*, 1982, **1**, 289.
71. P. C. Turley and P. Haake, *J. Am. Chem. Soc.*, 1967, **89**, 4617.
72. Y. Takaguchi, E. Horn and N. Furukawa, *Organometallics*, 1996, **15**, 5112.
73. A. J. Blake, A. J. Holder, T. I. Hyde and M. Schröder, *J. Chem. Soc., Chem. Commun.*, 1989, 1433.
74. A. F. Hill and J. D. E. T. Wilton-Ely, *Organometallics*, 1997, **16**, 4517.
75. R. B. Lauffer, *Chem. Rev.*, 1987, **87**, 901.
76. A. J. Blake and M. Schröder, *Adv. Inorg. Chem.*, 1990, **35**, 1.
77. A. J. Blake, R. O. Gould, J. A. Greig, A. J. Holder, T. I. Hyde and M. Schröder, *J. Chem. Soc., Chem. Commun.*, 1989, 876.
78. S. C. Rawle, R. Yagbasan, K. Prout and S. R. Cooper, *J. Am. Chem. Soc.*, 1987, **109**, 6181.
79. D. Sellmann and L. Zapf, *Angew. Chem. Int. Ed. Engl.*, 1984, **23**, 807.
80. W. Levason, S. D. Orchard and G. Reid, *Chem. Commun.*, 2001, **5**, 427.

81. D. K. Cabbiness and D. W. Margerum, *J. Am. Chem. Soc.*, 1969, **91**, 6540.

82. D. K. Cabbiness and D. W. Margerum, *J. Am. Chem. Soc.*, 1970, **92**, 2151.

83. M. Kodama and E. Kimura, *J. Chem. Soc., Dalton Trans.*, 1976, 2341.

84. F. P. Hinz and D. W. Margerum, *Inorg. Chem.*, 1974, **13**, 2941.

85. R. M. Clay, M. Micheloni, P. Paoletti and W. V. Steele, *J. Am. Chem. Soc.*, 1979, **101**, 4119.

86. L. L. Diaddario, L. L. Zimmer, T. E. Jones, L. S. W. L. Sokol, R. B. Cruz, E. L. Yee, L. A. Ochrymowycz and D. B. Rorabacher, *J. Am. Chem. Soc.*, 1979, **101**, 3511.

87. L. S. W. L. Sokol, L. A. Ochrymowycz and D. B. Rorabacher, *Inorg. Chem.*, 1981, **20**, 3189.

88. R. M. Izatt, J. S. Bradshaw, S. A. Nielsen, J. D. Lamb, J. J. Christensen and D. Sen, *Chem. Rev.*, 1985, **85**, 271.

89. D. W. Margerum, D. B. Rorabacher and J. F. G. Clarke, *Inorg. Chem.*, 1963, **2**, 667.

90. D. W. Margerum, G. R. Cayley, D. C. Weatherburn and G. K. Pagenkopf, *Adv. Chem. Ser.*, 1978, **174**, 1.

91. G. H. Fuller, *J. Phys. Chem. Ref. Data 5*, 1976, 835.

92. G. D. Sturgeon and M. L. Gross, in *The Chemistry of Organic Selenium and Tellurium Compounds*, S. Patai and Z. Rappoport (eds.), Wiley, New York, 1986, Vol. 1, pp. 243 – 286.

93. D. Rehder, in *Multinuclear NMR*, J. Mason (ed.), Plenum, New York, 1987, Ch. 19.

94. H. C. E. McFarlane and W. McFarlane, in *Multinuclear NMR*, J. Mason (ed.), Plenum, New York, 1987, Ch. 15.

95. D. H. O'Brien, K. J. Irgolic and C-K. Huang, *Proc. Int. Conf. Org. Chem. Selenium, Tellurium*, 4th, 1983, 469.

96. R. J. Goodfellow, in *Multinuclear NMR*, J. Mason (ed.), Plenum, New York, 1987, Ch. 20.

Chapter 2:

Synthesis and Coordination Chemistry of [9]-, [11]- and [12]aneS_2Te

2.0 Introduction

The preparation of new telluroether ligands is an area of significant interest due to their rich coordination chemistry, this being a function of their enhanced σ-donating properties to low valent transition metal centres[1] (Chapter 1). Of such compounds, medium to large ring organo-tellurium ligands are of particular interest, since these will allow tellurium to be studied in a macrocyclic environment. There are many examples of telluracycles (cyclic Te-containing compounds which may or may not incorporate other donor atoms) in the literature, and the preparations, derivatives and complexes of many are discussed here.

The small ring telluracycles telluracyclopentane and telluracyclohexane (Figure 2.0) were first reported many years ago,[2,3] with, for example, telluracyclohexane being synthesised from the condensation between α,ω-pentamethylene dihalides and Al_2Te_3.[2] A more convienient synthetic route from Na_2Te and $Br(CH_2)_nBr$ (n = 4 or 5) in water was described later[4] and a more recent preparation was reported *via* the reaction of MeTeLi with $Cl(CH_2)_nCl$ (n = 4 or 5), which also formed Me_2Te.[5]

Figure 2.0 - Telluracyclopentane (i) and telluracyclohexane (ii)

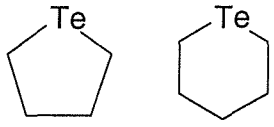

(i) (ii)

The diiodides of both species have been reported and the crystal structures reveal distorted trigonal bipyramidal geometries around Te(IV). Both structures show secondary Te···I interactions, with the five membered ring forming a zigzag ribbon structure in the solid state and the six membered ring (Figure 2.1) forming trimeric assemblies.[6] The analogous 1,1-dibromotelluracyclopentane, together with other organoderivatives have also been reported,[7,8] although no structural data has been obtained. A number of 2-methyl-1-organo-1-telluracyclopentane compounds and other derivatives have also been reported[9] and the compounds 1-telluracyclohexane-3,5-dione and 1-telluracyclohexane-2,6-dione are also known, with the crystal structure of the

former showing the ligand adopting the chair conformation. A crystal structure of the dichloride derivative has also been published.[10] Telluracyclopentane forms complexes of the type $[ML_2X_2]$ (where M = Pd or Pt and X = Cl, Br or I) and $[RhL_3Cl_3]$.[11] The $[PtL_2Cl_2]$ was shown to be *cis* in the solid state with both *cis* and *trans* isomers present in solution. The other Pd and Pt complexes are exclusively *trans* isomers, with the structure of the $PdCl_2$ complex having d(Pd-Cl) = 2.322 Å (av.) and d(Pd-Te) = 2.593 Å (av.). It was concluded that the telluracyclopentane complexes favoured *trans* geometries more than those of the simple R_2Te ligands. A rhodium complex $[RhL_3Cl_3]$, formed *via* the reaction of $RhCl_3.3H_2O$ with three equivalents of telluracyclopentane in ethanol solution was shown from its ^{125}Te-{^1H} NMR spectrum and by IR spectroscopy to exist as a mixture of *mer* and *fac* isomers in solution.

Figure 2.1 - Crystal structure of telluracyclohexanediiodide[6]

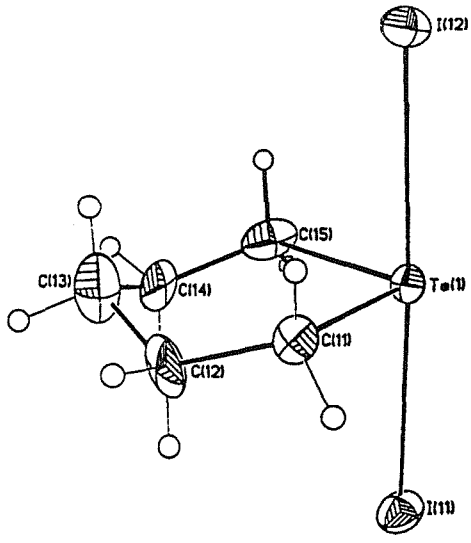

The small ring mixed donor telluracycles 1-oxa-4-telluracyclohexane and 1-thia-4-telluracyclohexane (Figure 2.2) have been reported. The compound 1-oxa-4-telluracyclohexane was first reported in 1945 *via* the reaction of $O(CH_2CH_2Cl)_2$ and Na_2Te in methanol[12], but a more recent synthetic route was published in 1987, in which bis(β-chloroethyl)ether, tellurium powder and sodium iodide were heated in 2-butoxyethanol to form 1-oxa-4-telluracyclohexane-4,4-diiodide. This compound, when refluxed in methanol with hydrazine hydrate gave 1-oxa-4-telluracyclohexane.[13]

Figure 2.2 - 1,4-oxatellurane (i) and 1-thia-4-telluracyclohexane (ii)

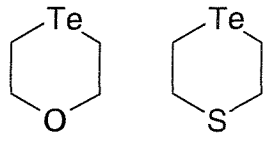

(i) (ii)

The 1-thia-4-telluracyclohexane was reported by McCullough and co-workers, whereby the high dilution reaction of bis(2-chloroethyl)sulfide with Na_2Te in water gave the product in under 7% yield.[14] Organo-derivatives of both telluracycles have been reported, for example the diiodide, dichloride and methyl iodide derivatives.[13,14] The crystal structure of 1-thia-4-telluracyclohexane was first reported by McCullough,[14] however complete refinement was not pursued and he opted to structurally characterise its diiodide derivative instead.[15] The transition metal chemistry of these compounds have been very little studied (in contrast to 1,4-dioxane and 1,4-dithiane) which are well established as ligands. Studies are limited to $[MCl_2L_2]$ complexes of 1-oxa-4-telluracyclohexane (M = Pd or Pt). Reaction of potassium tetrachloroplatinate(II) or potassium tetrachloropalladate(II) with the ligand in an acetone/water mixture, followed by extraction with CH_2Cl_2, produced the complexes in good yield (69-79%).[16] The structure of the Pt complex (Figure 2.3) showed a *trans* geometry around Pt(II), with d(Pt-Te) = 2.5945(3) Å, and d(Pt-Cl) = 2.3169(9) Å, both fairly typical values. The Te-Pt-Te and Cl-Pt-Cl angles were quoted as 180°, thereby confirming the square planar geometry around Pt(II).[16]

Figure 2.3 - Crystal structure of trans-[$PtCl_2$(1,4-oxatellurane)$_2$][16]

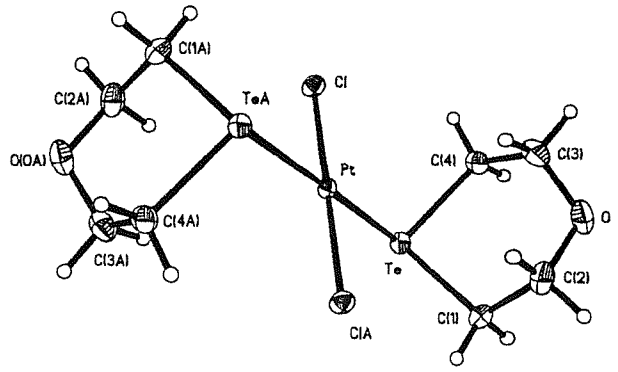

The compound 1,3-dihydrobenzo[*c*]tellurophene (Figure 2.4) was first reported in 1978 by Ziolo and Gunther *via* the reaction of α,α'-dichloro-*o*-xylene with Te and NaI in 2-methoxyethanol.[17] More recently, the ligand was obtained in low yield as a by-product of the attempted preparation of 2,11-ditellura[3.3]orthocyclophane.[18] This procedure involved the treatment of α,α'-dichloro-*o*-xylene with two molar equivalents of KTeCN in dmso solution. Addition of this solution and a solution of α,α'-dichloro-*o*-xylene in thf-EtOH dropwise to an $NaBH_4$ suspension in thf-EtOH over *ca.* 20 hours, gave the ligand as a yellow solid.

Figure 2.4 - 1,3-dihydrobenzo[c]tellurophene

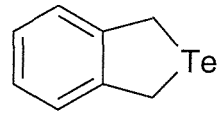

Reaction of the ligand with $[Rh(cp^*)Cl_2]_2$ was shown to form the complex $[Rh(cp^*)Cl_2L]$. When this reaction was carried out in the presence of $AgCF_3SO_3$, the complex $[Rh(cp^*)L][CF_3SO_3]_2$ was obtained.[19] More recently, the ligand has been reacted with a variety of transition metal ions in order to investigate its coordination behaviour. Complexes prepared were $[CuL_4][PF_6]$, $[AgL_4][BF_4]$, $[MCl_2L_2]$ (M = Pd and Pt), $[RhCl_3L_3]$, $[RuCl_2L_4]$, $[MnCl(CO)_3L_2]$, $[Mo(CO)_5L]$ and $[Mo(CO)_4L_2]$, with the crystal structures of the Cu(I), Ag(I) and $[Mo(CO)_4L_2]$ complexes having been reported.[18] $[CuL_4][PF_6]$ was shown to adopt a slightly distorted tetrahedral arrangement, with the four telluroether ligands bonded through Te to the central Cu(I) centre. This was very similar to the Ag(I) structure, which also displayed a slightly distorted tetrahedral geometry about the metal centre. The structure of $[Mo(CO)_4L_2]$ (Figure 2.5) showed the telluoether ligands adopting mutually *cis* positions in the distorted octahedral molecule, with d(Mo-Te(1)) = 2.814(1) Å and d(Mo-Te(2)) = 2.820(2) Å.[18] A poor quality X-ray crystallographic data set was also collected for a crystal of $[MnCl(CO)_3L_2]$, which showed Mn(I) octahedrally coordinated through three mutually *fac* carbonyls, a Cl and two tellurophene ligands. This study showed that for these complexes, coordination of the 1,3-dihydrobenzo[*c*]tellurophene ligand was *via* the lone pair on the Te atom.[18]

Figure 2.5 - Crystal structure of [Mo(CO)$_4$(1,3-dihydrobenzo[c]tellurophene)$_2$][18]

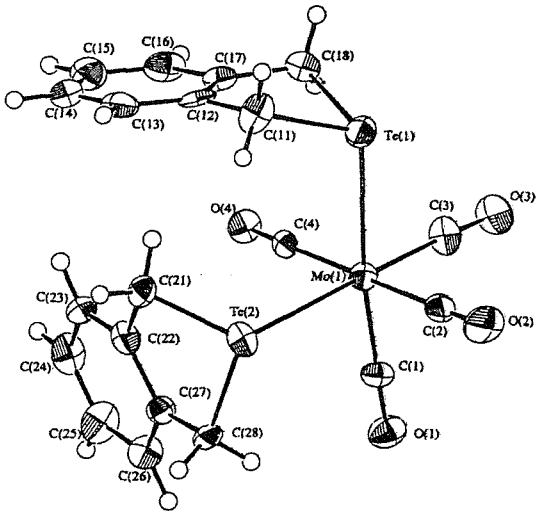

The related compound, 3,4-quinoxalino-1-telluracyclopentane (Figure 2.6) was prepared by the reduction of 1,1-diiodo-3,4-quinoxalino-1-tellura(IV)cyclopentane with hydrazine hydrate, and recrystallisation from diethyl ether gave fine yellow needles suitable for X-ray crystallographic studies.[20] The structure (Figure 2.7) revealed an almost planar molecule, but with the Te atom angled at 22° from the aromatic backbone.

Figure 2.6 - 3,4-quinoxalino-1-telluracyclopentane

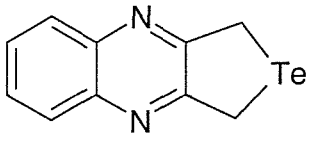

The tellurium atoms were observed to be arranged in layers, with short intermolecular bonds between some tellurium atoms – this being used to explain the poor solubility and high melting point of the compound. There was no evidence for secondary Te-N interactions, however, unlike that found in 1,2-benzoisotellurozole[21] (Figure 2.8).

Figure 2.7 - Crystal structure of 3,4-quinoxalino-1-telluracyclopentane[20]

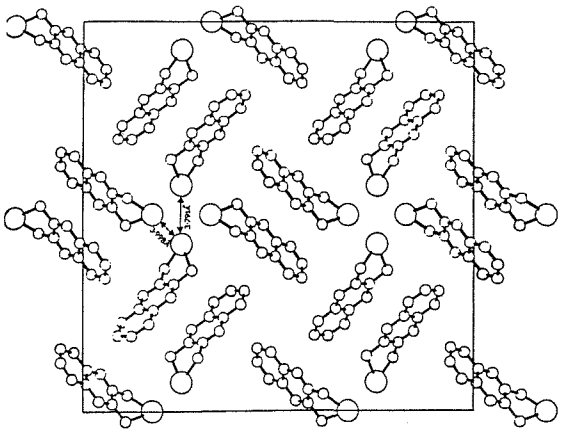

Figure 2.8 - Benzoisotellurazole

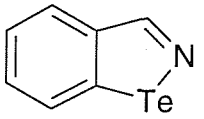

The unusual compound 2,7-dihydro-1 *H*-dibenzo[*c,e*]tellurepin was first reported by Al-Rubaie and co-workers in 1992 *via* the reaction of 2,2'-bis(bromomethyl)biphenyl with Te and NaI, followed by reduction of the diiodo derivative with hydrazine hydrate.[22] An improved synthesis (also by Al-Rubaie and co-workers) was reported in 1996, as shown in Figure 2.9.[23]

Figure 2.9 - Synthesis of 2,7-dihydro-1 H-dibenzo[c,e]tellurepin[23]

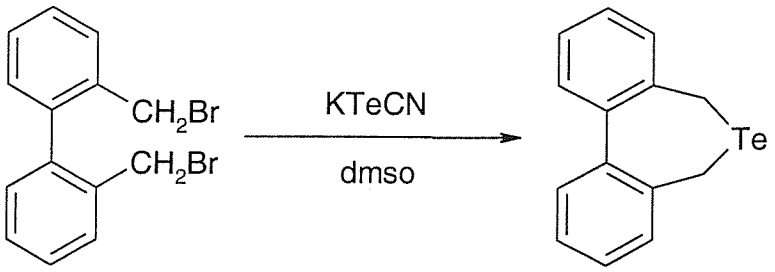

The compound was found to readily form organo-derivatives of the type LX_2 (X = Cl, Br, I), whilst treatment of the ligand with methyl iodide and ethyl iodide gave the methyltellurepinium and ethyltellurepinium salts respectively.[23] Several transition metal compounds have also been reported – for example reaction with Na_2PdCl_4 in $CHCl_3$ solution gave $[Pd_2Cl_4L_2]$, a chloro-bridged dinuclear complex, whilst reaction with $[PdCl_2(PhCN)_2]$ gave *trans*-$[PdCl_2L_2]$. Reaction of $RhCl_3.3H_2O$ with excess ligand in ethanol gave the square planar complex $[RhClL_3]$.[23]

The related compounds tellurophene and dibenzotellurophene (Figure 2.10) were first reported in 1978[24] and 1975[25] respectively. Dibenzotellurophene has been shown to react with triiron dodecacarbonyl, resulting in the removal of tellurium from the aromatic system and the isolation of ferrole, $[C_{12}H_8Fe_2(CO)_6]$. This is in contrast to the lack of reactivity of dibenzothiophene.[26] Also, McWhinnie and co-workers showed that the ligands reacted with $[Rh(cp^*)Cl_2]_2$ in the presence of $AgCF_3SO_3$ to form the species $[Rh(cp^*)(\eta^5\text{-}C_4H_4Te)][CF_3SO_3]_2$ and $[Rh(cp^*)(\text{dibenzothiophene})][CF_3SO_3]_2$, the latter showing η^1-coordination of the ligand to the Rh centre.[27] Tellurophenes and their derivatives are industrially important, since their addition to hydraulic fluids increases their fire resistance,[28] whilst supramolecular associations in organometallic compounds are a field of recent interest.[29]

Figure 2.10 - Tellurophene (i) and dibenzotellurophene (ii)

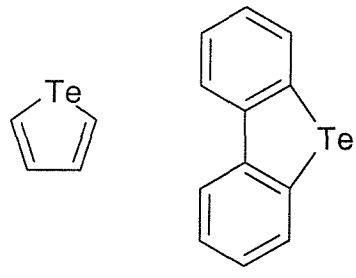

(i) (ii)

The related compound 3,5-naptho-1-telluracyclohexane is also known (Figure 2.11, (i)) which was prepared *via* the reaction of 1,8-bis(bromomethyl)naphthalene with elemental

Te and NaI in 2-methoxyethanol. Reduction of the resulting diiodo species with hydrazine hydrate gave the telluracycle, of which a charge transfer complex with 7,7,8,8-tetracyanoquinodimethane was prepared.[30] The same authors also reported the formation of 1,2,4,5-bis(diiodotelluracyclopentano)benzene (Figure 2.11, (ii)) from the reaction of 1,2,4,5-tetrakis(bromomethyl)benzene with elemental tellurium and NaI, however the analogous reduction with hydrazine hydrate failed to give the free ligand.

Figure 2.11 - 3,5-naptho-1-telluracyclohexane (i) and 1,2,4,5-bis(diiodotelluracyclopentano)benzene (ii)

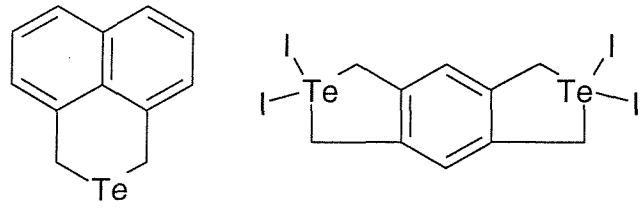

(i) (ii)

Later, Al-Shirayda reported the formation of 1,2,4,5-bis(telluracyclopentano)benzene *via* the reduction of the bis(diiodide) compound as a light and air sensitive solid. Treatment of the compound with ethyl bromide formed the bromo-methyl telluronium salt.[31]

There are also numerous tellurocycles based on naphthalene, for example Figure 2.12 shows the structures of telluranthrene (i), telluraxanthene (ii) and phenoxatellurine (iii). Telluranthrene was first reported in 1964 by the reaction of tetraphenyltin with tellurium metal,[32] and later from the reaction of $[(C_6H_4)_6Hg_6]$ with tellurium metal.[33] No transition metal chemistry with these compounds has been reported however. The selenium, sulfur and nitrogen donor analogues of (iii) are also known,[34] together with many variations of structure (ii) for example, having slightly differing organic backbones.[35]

Figure 2.12 - Telluranthrene (i), telluraxanthene (ii) and phenoxatellurine (iii)

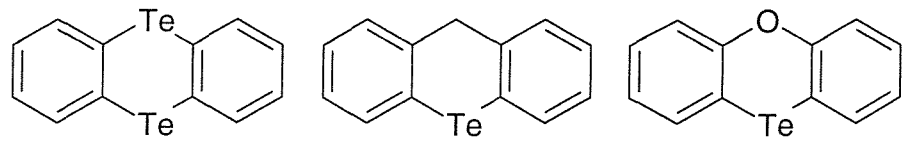

(i) (ii) (iii)

The 8-membered ring compound 1,5-ditelluracyclooctane (Figure 2.13, (iii)) was first reported by Furukawa and co-workers in 1991.[36] Reaction of 1,3-dibromopropane, (i), with Na_2Te in benzene/ethanol solution, followed by treatment with sodium borohydride formed sodium propane-1,3-ditellurolate (ii).

Figure 2.13 - Synthesis of 1,5-ditelluracyclooctane[36]

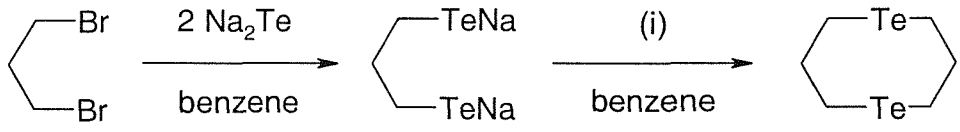

(i) (ii) (iii)

Reaction of this species with further 1,3-dibromopropane, followed by work-up and purification by silica-gel column chromatography yielded 1,5-ditelluracyclooctane (iii). This compound was shown to form dication salts upon reaction with $NOBF_4$ or $NOPF_6$, forming the corresponding dicationic BF_4^- or PF_6^- salts.[36] There are few known macrocyclic telluroether ligands, and only one report of a homoleptic tritelluroether, [12]aneTe_3 (1,5,9-tritelluracyclododecane), which was formed from 1,5-ditelluracyclooctane (Figure 2.14).[37]

Figure 2.14 - The Synthesis of [12]aneTe_3[37]

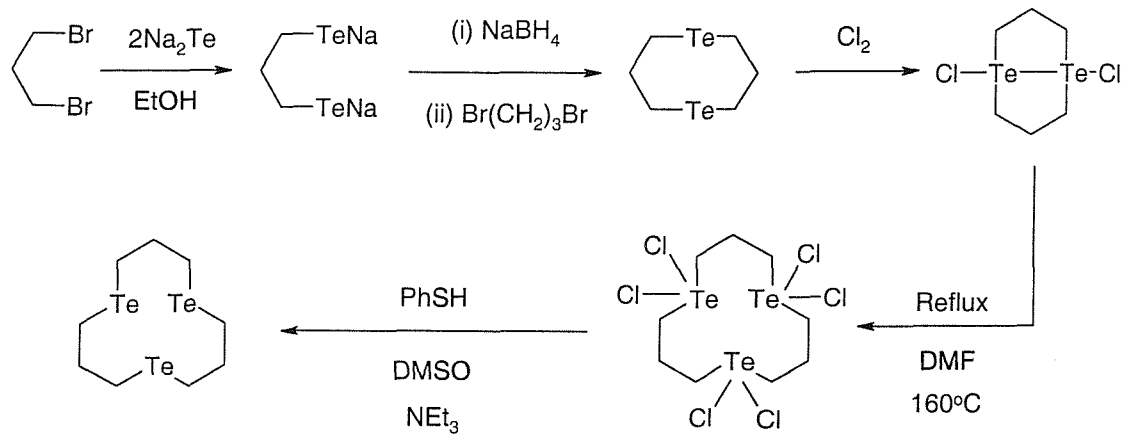

No data have been published on its coordination chemistry, however.[37] A crystal structure of the [12]aneTe_3Cl_6 species was reported (Figure 2.15) showing a *pseudo*-trigonal bipyramidal geometry about the Te donors, with the Cl atoms in apical positions.

Figure 2.15 - Crystal structure of [12]aneTe_3Cl_6[37]

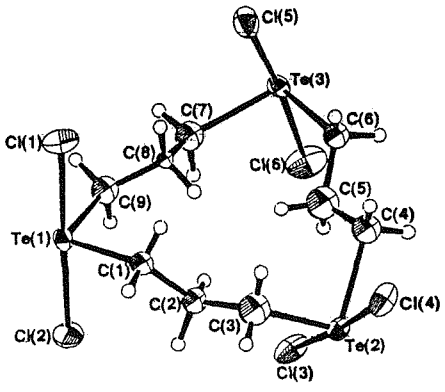

Cl-Te-Cl bond angles lay in the range 178.2(2) - 173.5(5)°, whilst Cl-Te-C bond angles were nearly 90°. Te-C bond distances lay in the range 2.10(5) – 2.26(4) Å, and d(Te-Cl) were 2.45(1) – 2.58(1) Å. It was concluded that there were no transannular Te···Te interactions due to the relatively long Te···Te transannular distances (6.185(3) – 6.299(3) Å) which are notably longer than the sum of the van der Waals radii (4.4 Å). The

structure does reveal a number of intermolecular Te···Cl interactions, however, with Te···Cl distances in the range 3.35(1) – 3.81(1) Å.[37]

The first Schiff base telluroether macrocycle, a 22-membered ring incorporating a Te_2N_4 donor set (Figure 2.16) was reported by Menon and co-workers in 1996.[38] Reaction of bis(2-formylphenyl)telluride and ethane-1,2-diamine in acetonitrile afforded the macrocyclic compound, which could then be reduced to the –NH- species using $NaBH_4$. The Schiff base also forms a hydrobromide salt, and reaction with two equivalents of $HgCl_2$ and $[PdCl_2(PhCN)_2]$ form the corresponding $[M_2Cl_4L]$ complexes (M = Hg or Pd), with bonding of the metal centre to adjacent Te and N donors in each case. The crystal structure of the Schiff base shows the molecule lying across a crystallographic inversion centre, with the two opposite aromatic rings being coplanar. A later study by Menon and co-workers described the reaction of the Schiff base with 1 equivalent of $[Pd(PhCN)_2Cl_2]$ and NH_4PF_6 in $CHCl_3$ solution, forming $[PdL][PF_6]_2$, with coordination of the macrocycle to Pd through both Te donors and two adjacent N donors. Reaction of $[Pt(COD)Cl_2]$ and NH_4PF_6 with the macrocycle in CH_2Cl_2 solution formed an unusual complex in which facile C-Te bond cleavage and transmetallation had occurred. Both complexes were characterised by X-ray studies.[39]

Figure 2.16 - The first Te-containing Schiff base macrocycle

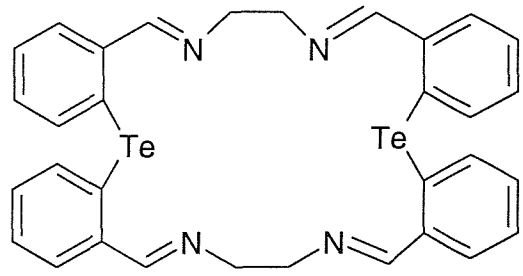

An additional Te-containing Schiff base macrocycle has been reported recently *via* the reaction shown in Figure 2.17. The poor solubility of the compound, however, meant that the acquisition of spectroscopic data was limited, and no coordination compounds have been reported.[40]

Figure 2.17 - Synthesis of the new Te-containing Schiff base macrocycle[40]

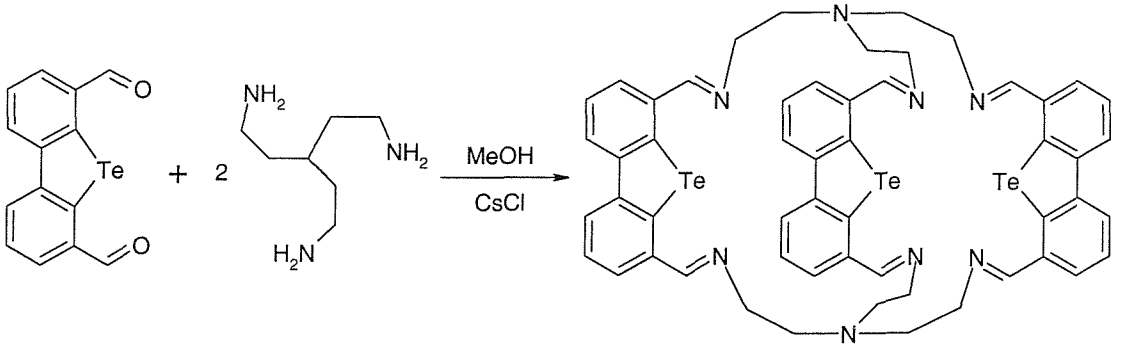

A number of tellura-crown macrocycles based on 10-tellurabenzo-15-crown-5 were reported fairly recently by Wing-Wah Yam and co-workers, the structures of which are outlined in Figure 2.18.[41]

Figure 2.18 - Tellura-crown macrocycles[41]

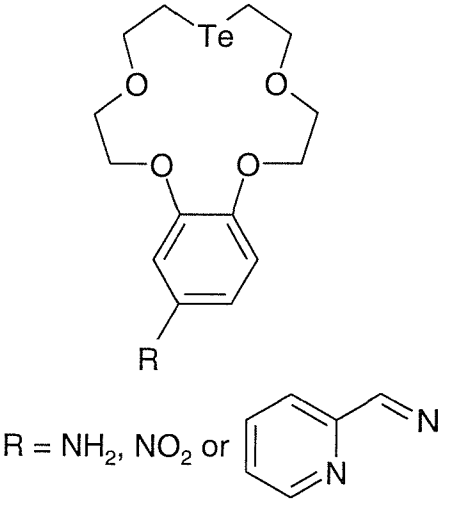

The synthesis of 4'-nitrobenzo-10-tellura-15-crown-5 (R = NO_2) was accomplished by the addition of bis(2-hydroxyethyl)telluride to a solution of sodium in *tert*-butyl alcohol, followed by reaction with 1,2-bis[2-(*p*-tosyloxy)ethoxy]-4-nitrobenzene. Conversion of the compound into the -NH_2 (amino) derivative was accomplished by reduction with hydrazine hydrate, whilst treatment of this species with 2-pyridinecarbaldehyde in ethanol yielded the third crown ether compound. A single copper complex of the tellura-

crown macrocycle with R = $C_6H_5N_2$, $[Cu(PPh_3)_2L][BF_4]$ was reported, with coordination of the Cu centre to the two N donors of the ligand.[41]

Previous to the work by Wing-Wah Yam and co-workers, a series of tellura-crown ethers were reported by Xu and co-workers, including 1,13-ditellura-24-crown-8 (Figure 2.19) and 10-tellurabenzo-15-crown-5.[42,43] No ^{125}Te-{^{1}H} NMR data were gathered on the compounds, however, and only one coordination compound, $[PtCl_2$(10-tellurabenzo-18-crown-6)] has been reported. The tellura-crown ether series, including their syntheses, will be examined in greater detail in Chapter 3.

Figure 2.19 - 1,13-ditellura-24-crown-8

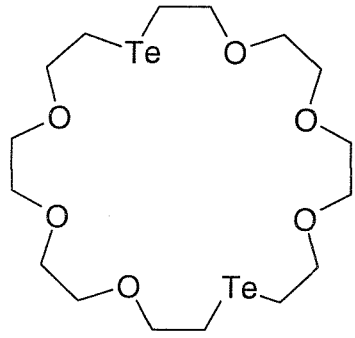

Previous to this work, the synthesis of the macrocyclic telluroether ligands [9]-, [11]- and [12]-aneS$_2$Te (1,4-dithia-7-telluracyclononane, 1,4-dithia-8-telluracycloundecane and 1,5-dithia-9-telluracyclododecane respectively) had been reported,[44,45] although, apart from the crystal structures of $[Ag(11]aneS_2Te)][BF_4]$ and the analogous CF_3SO_3 salt, no studies into the coordination chemistry of the ligands had been undertaken.[44,45] The ligands were synthesised *via* a 'disguised dilution' reaction, whereby the limited solubility of the precursors at the low temperatures employed (*ca.* -78°C) and the moderately large volumes of solvent ensured that cyclisation was favoured over polymerisation processes.

In contrast, the much studied analogue to [9]aneS$_2$Te, [9]aneS$_3$, was first synthesised in high yield by Sellmann and Zapf by the cyclisation of the open chain dithiolate $S^-(CH_2)_2S(CH_2)_2S^-$ and 1,2-dibromoethane, using the $Mo(CO)_3$ fragment as a

template for the reaction[46] (Chapter 1). This metal template technique binds the precursors together in close proximity, thereby favouring ring closure over polymerisation. The metal ion size is thought to be very important in this reaction, and a disadvantage of this technique is that to obtain the free ligand, demetallation is necessary (which is not always trivial). The high dilution method uses a very large excess of solvent in the reaction and keeps the reactants at low concentrations.

This chapter explores the syntheses of [9], [11]- and [12]-aneS_2Te in more detail, reporting improved yields for the [11]- and [12]-membered ring macrocyclic compounds. In particular, the synthesis of [9]aneS_2Te is explored in detail and has been found to be much more temperamental than the syntheses of [11]- and [12]-aneS_2Te, with the identification of several reaction by-products. X-ray crystallographic studies on two of the ligands and one of their organo-derivatives have confirmed their identities. Also reported here are investigations into the ligating properties of the dithiatellura-macrocycles with a variety of transition metal ions, including Cu(I), Ag(I), Mo(0), Mn(I), Rh(III), Pd(II) and Pt(II). The range of transition metals employed has allowed the coordination modes of the macrocycles to a range of different metals in different oxidation states to be studied. Where it has been possible to do so, the mode of coordination has been established spectroscopically, and the effect of changing the ring size from 9 to 11 to 12 established. The data gathered on the complexes have also been compared with other related systems, including complexes of the linear analogue, $MeS(CH_2)_3Te(CH_2)_3SMe$ (Chapter 4).

2.1 Results and discussion

2.2 Ligand syntheses

2.2.1 Synthesis of [11]- and [12]-aneS$_2$Te and their crystal structures

The ligands [11]aneS$_2$Te (1,4-dithia-8-telluracycloundecane) and [12]aneS$_2$Te (1,5-dithia-9-telluracyclododecane) were synthesised according to a recently established procedure developed in our laboratory[44] (Figure 2.20).

Figure 2.20 - Synthesis of [11]- and [12]-aneS$_2$Te

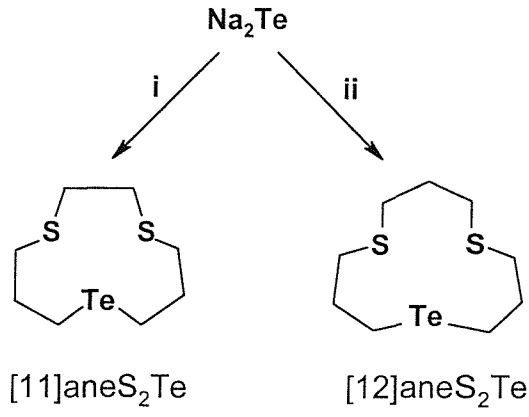

i $Cl(CH_2)_3S(CH_2)_2S(CH_2)_3Cl$ in thf, -78°C

ii $Cl(CH_2)_3S(CH_2)_3S(CH_2)_3Cl$ in thf, -78°C

The α,ω-dichlorodithioether precursors were synthesised according to the literature procedures[47] by addition of $HS(CH_2)_nSH$ (n = 2 or 3) to a solution of sodium in ethanol, followed by the dropwise addition of $Cl(CH_2)_3OH$ to give $HO(CH_2)_3S(CH_2)_nS(CH_2)_3OH$ (n = 2 or 3) respectively as white waxy solids. Treatment of $CHCl_3$ solutions of these with $SOCl_2$ gave the α,ω-dichlorodithioether precursors, $Cl(CH_2)_3S(CH_2)_nS(CH_2)_3Cl$ respectively as brown oils. ***[CARE: - the α,ω-dichlorodithioether precursors are powerful vesiccants and may cause severe blistering upon skin contact].** The

appropriate α,ω-dichlorodithioether, Cl(CH$_2$)$_3$S(CH$_2$)$_n$S(CH$_2$)$_3$Cl (n = 2 for [11]aneS$_2$Te and 3 for [12]aneS$_2$Te) in thf were added dropwise to a fresh solution of Na$_2$Te in NH$_{3(l)}$ at -78°C (see Scheme 2.3) thereby creating 'disguised high dilution' conditions. The ammonia was left to boil off overnight, and the resulting red/brown mixtures hydrolysed and extracted with CH_2Cl_2 to give red oily products after the removal of the solvent *in vacuo*. Purification of the ligands was achieved by flash column chromatography on silica using ethyl acetate: hexane 1:3 as eluent to give the pure ligands in 35% and 33% yield respectively for [11]- and [12]-aneS$_2$Te. The ligands were oxygen-sensitive, pale orange waxy solids, and were stored under an atmosphere of dinitrogen at –18°C in order to avoid decomposition. Solutions of the ligands in degassed solvents were found to be stable; however when exposed to air, tellurium deposition readily occurred. The purity of the ligands was confirmed by ^{1}H, ^{13}C-{^{1}H] and ^{125}Te-{^{1}H} NMR spectroscopy (see Table 2.0) and EI mass spectrometry.

Table 2.0 - ^{1}H, ^{13}C-{^{1}H} and ^{125}Te-{^{1}H} NMR data for [11]- and [12]aneS$_2$Te (CDCl$_3$)

Compound	^{1}H δ/ppm	Assignment	^{13}C-{^{1}H} δ/ppm	Assignment	^{125}Te-{^{1}H} δ/ppm
[11]aneS$_2$Te	2.05, quin.	CH$_2$C*H*$_2$CH$_2$	34.7	CH$_2$*C*H$_2$CH$_2$	234
	2.67, t	C*H*$_2$Te	2.2	*C*H$_2$Te	
	2.73, t	SC*H*$_2$CH$_2$CH$_2$Te	32.6	*C*H$_2$S	
	2.74, s	SC*H*$_2$CH$_2$S	32.9	*C*H$_2$S	
[12]aneS$_2$Te	1.86, quin.	SCH$_2$C*H*$_2$CH$_2$S	27.7	SCH$_2$*C*H$_2$CH$_2$S	217
	2.06, quin.	SCH$_2$C*H*$_2$CH$_2$Te	33.5	SCH$_2$*C*H$_2$CH$_2$Te	
	2.66, t	C*H*$_2$Te	1.0	*C*H$_2$Te	
	2.73, t	C*H*$_2$S	29.0	*C*H$_2$S	
	2.78, t	C*H*$_2$S	30.1	*C*H$_2$S	

The spectroscopic data gathered were all consistent with those previously reported,[44] with δ(^{125}Te) = 234 and 217 ppm for [11]- and [12]-aneS$_2$Te being a particularly useful reference. The ^{125}Te-{^{1}H} NMR spectrum of [12]-aneS$_2$Te is shown in Figure 2.21.

Figure 2.21 - ^{125}Te-{^{1}H} NMR spectrum of [12]aneS$_2$Te in CH$_2$Cl$_2$

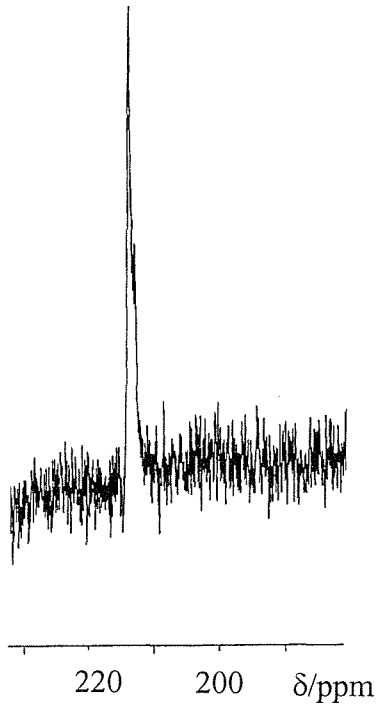

The δ(^{13}C(*C*H$_2$Te)) resonances for the two compounds were at 2.2 and 1.0 ppm respectively, which was typical of a *C*H$_2$Te moiety and consistent with the previously reported values.[44] IR spectra of the two macrocycles were also recorded (as thin films between CsI plates) in order to determine the free macrocycle absorptions. These data were obtained in order to aid characterisation of the complexes (see later). It should be noted that low resolution GC-EI mass spectrometry of the crude products identified the monocationic [11]aneS$_2$^{130}Te$^+$ and [12]aneS$_2$^{130}Te$^+$ as the highest mass species, with no evidence for larger ring systems (for example the [2+2] cyclisation products [22]aneS$_4$Te$_2$ and [24]aneS$_4$Te$_2$). A side-product of the [12]aneS$_2$Te synthesis in particular was observed in the crude reaction mixture, this being the dominant species in some preparations. The proposed structure is shown in Figure 2.22. The ^{125}Te-{^{1}H} NMR of this species (δ(^{125}Te) = 126 ppm) was consistent with a ditelluride unit of the type -(CH$_2$)$_3$TeTe(CH$_2$)$_3$-.[48] The EI mass spectrum (EIMS) of the impurity (Figure 2.23) showed a major species corresponding to the cation [C$_9$H$_{18}$S$_2$^{130}Te$_2$]$^+$ (*m/z* = 446) and so on the basis of this and the ^{125}Te-{^{1}H} NMR data the by-product may be tentatively assigned as the ditelluride [12]aneS$_2$Te$_2$ (Figure 2.22).

Figure 2.22 - Proposed structure of the ditelluride [12]aneS$_2$Te$_2$

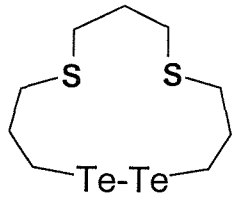

A minor species in some of the [11]aneS$_2$Te preparations with ($\delta(^{125}Te)$ = 126) was also observed, but not pursued. It is possible that this could be the analogous [11]aneS$_2$Te$_2$ ditelluride species.

Figure 2.23 - EIMS of the ditelluride from the [12]aneS$_2$Te preparation

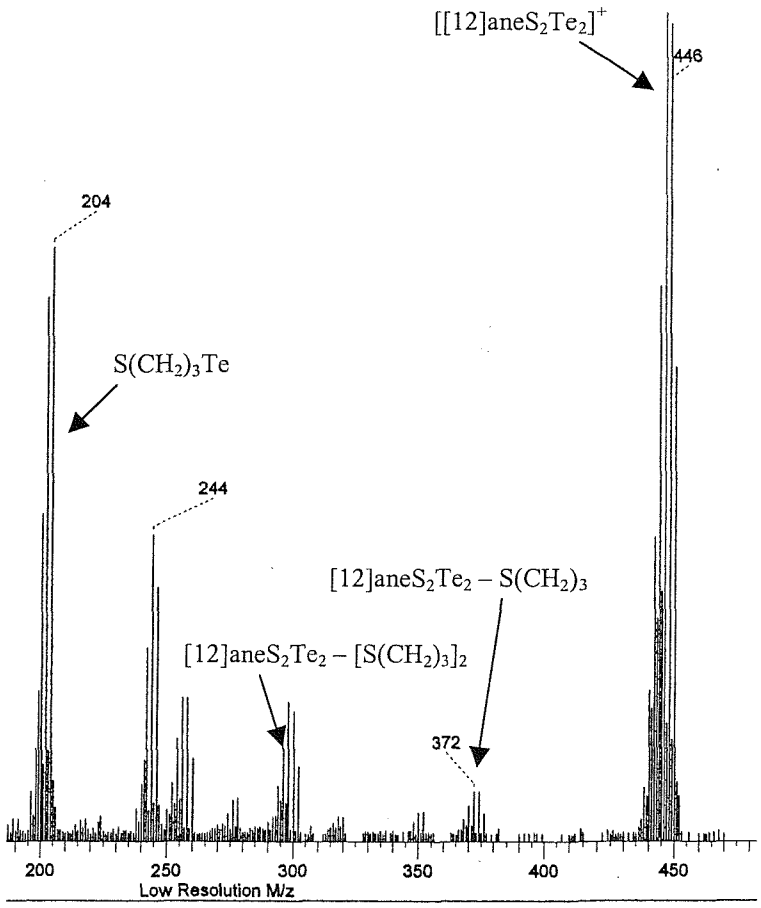

The crystal structures of [11]aneS_2Te (Figure 2.24, Table 2.1) and [12]aneS_2Te (Figure 2.25, Table 2.2) were obtained from crystals grown from the slow evaporation of solutions of the respective ligands in CH_2Cl_2/Et_2O.

The structures unambiguously confirm the formation of the [1+1] cyclisation products in the above reactions, showing discrete, molecular species that have no significant intermolecular contacts. [12]aneS_2Te adopts an approximately square arrangement, with a study of the torsion angles revealing one *gauche* and one *anti* CTeCC torsion and three of the four CSCC torsions being *gauche*. One S atom was observed to occupy a corner position, whereas the remaining S and Te donor atoms occupy side positions in the solid state.

Figure 2.24 - Crystal structure of [11]aneS_2Te with numbering scheme adopted. Ellipsoids are drawn at the 40% probability level and H atoms are omitted for clarity

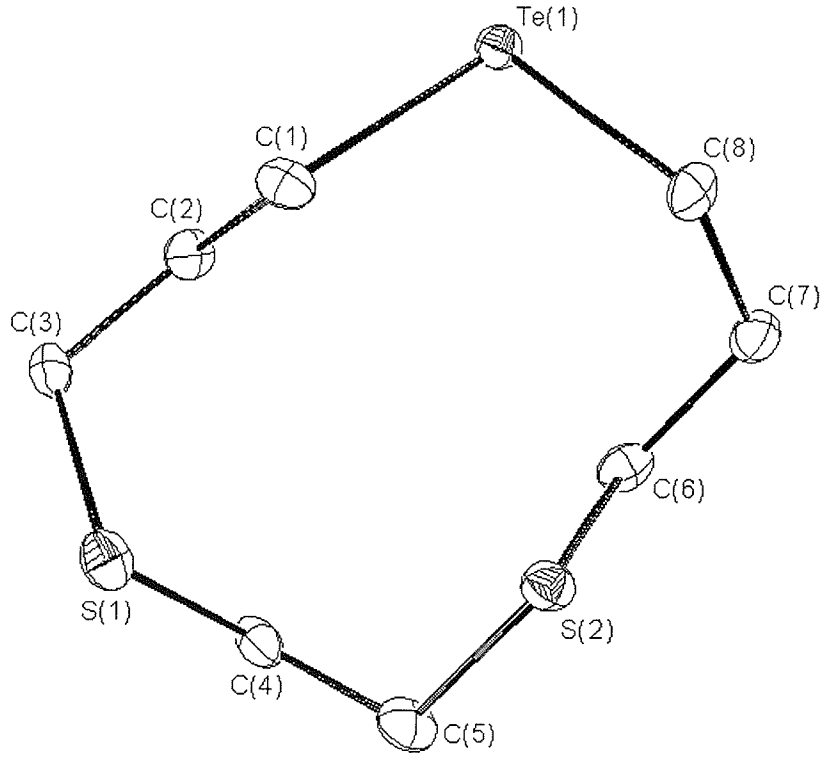

Table 2.1 - Selected bond lengths (Å), angles (°) and torsion angles (°) for [11]aneS_2Te

Bond lengths			
Te(1)-C(1)	2.151(6)	Te(1)-C(8)	2.158(5)
S(1)-C(3)	1.821(6)	S(1)-C(4)	1.812(7)
S(2)-C(5)	1.807(6)	S(2)-C(6)	1.813(7)
C(1)-C(2)	1.512(8)	C(2)-C(3)	1.530(9)
C(4)-C(5)	1.536(9)	C(6)-C(7)	1.531(8)
C(7)-C(8)	1.521(9)		
Bond angles			
C(1)-Te(1)-C(8)	95.5(2)	C(3)-S(1)-C(4)	103.4(3)
C(5)-S(2)-C(6)	100.1(3)	Te(1)-C(1)-C(2)	113.9(5)
C(1)-C(2)-C(3)	113.4(6)	S(1)-C(3)-C(2)	115.8(4)
S(1)-C(4)-C(5)	111.8(5)	S(2)-C(5)-C(4)	116.2(4)
S(2)-C(6)-C(7)	110.7(4)	C(6)-C(7)-C(8)	114.8(5)
Te(1)-C(8)-C(7)	116.3(4)		
Torsion angles			
Te(1)-C(1)-C(2)-C(3)	172.6(4)	Te(1)-C(8)-C(7)-C(6)	-63.9(6)
S(1)-C(3)-C(2)-C(1)	-59.1(7)	S(1)-C(4)-C(5)-S(2)	-65.3(6)
S(2)-C(6)-C(7)-C(8)	-64.2(6)	C(1)-Te(1)-C(8)-C(7)	91.8(5)
C(2)-C(1)-Te(1)-C(8)	-122.6(4)	C(2)-C(3)-S(1)-C(4)	-56.4(5)
C(3)-S(1)-C(4)-C(5)	140.7(4)	C(4)-C(5)-S(2)-C(6)	-67.9(6)
C(5)-S(2)-C(6)-C(7)	-179.2(4)		

The structure is similar to that reported for [12]aneS_3 (1,5,9-trithiacyclododecane – (Figure 2.26)[49] which also adopts an approximately square arrangement.

Figure 2.25 - Crystal structure of [12]aneS$_2$Te with numbering scheme adopted. Ellipsoids are drawn at the 40% probability level and H atoms are omitted for clarity

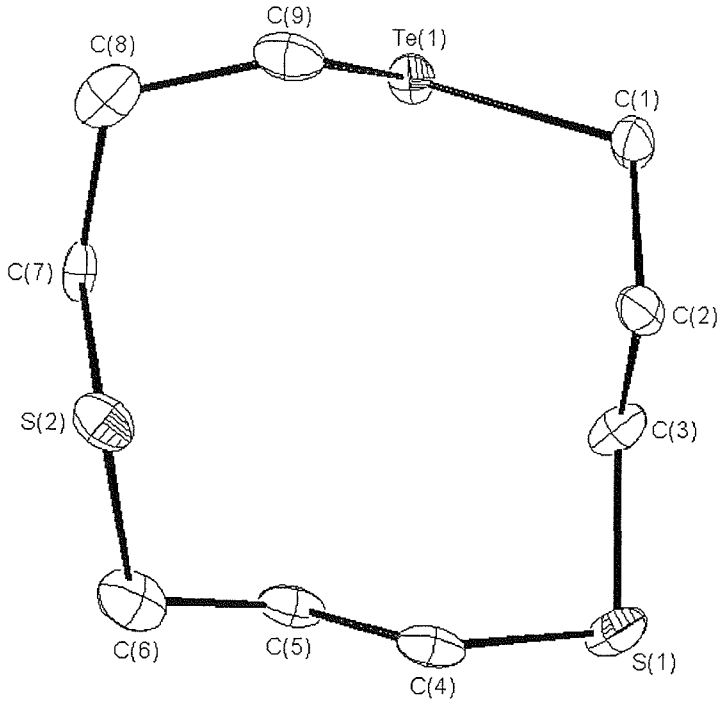

Figure 2.26 - [12]aneS$_3$

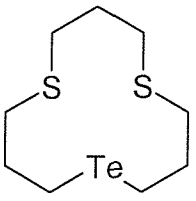

In [12]aneS$_3$, four out of the six CSCC torsions and four out of six SCCC torsions adopt *gauche* (approximately 60°) arrangements, with the rest being *anti* (approximately 180°). The [12]aneS$_2$Te analogue possesses a very similar distribution of torsion angles in the solid state, with three *gauche* and one *anti* CSCC torsions and one *gauche* and one *anti* CTeCC torsion. The C-S-C angles in [12]aneS$_2$Te (100.4(3) and 101.3(2)°) are significantly greater than the C(1)-Te(1)-C(9) angle (94.2(2)°), which follows from the larger energy gap between the s and p orbitals on Te compared to S leading to less s-orbital character in the Te-C bonding.

Table 2.2 - Selected bond lengths (Å), angles (°) and torsion angles (°) for [12]aneS_2Te

Bond lengths			
Te(1)-C(1)	2.163(5)	Te(1)-C(9)	2.148(6)
S(1)-C(3)	1.814(6)	S(1)-C(4)	1.820(6)
S(2)-C(6)	1.810(7)	S(2)-C(7)	1.818(5)
C(1)-C(2)	1.521(8)	C(2)-C(3)	1.511(10)
C(4)-C(5)	1.510(8)	C(5)-C(6)	1.525(9)
C(7)-C(8)	1.518(8)	C(8)-C(9)	1.533(8)
Bond angles			
C(1)-Te(1)-C(9)	94.2(2)	C(3)-S(1)-C(4)	101.3(2)
C(6)-S(2)-C(7)	100.4(3)	Te(1)-C(1)-C(2)	114.8(4)
C(1)-C(2)-C(3)	113.3(6)	S(1)-C(3)-C(2)	114.3(4)
S(1)-C(4)-C(5)	113.1(4)	C(4)-C(5)-C(6)	113.1(5)
S(2)-C(6)-C(5)	113.7(4)	S(2)-C(7)-C(8)	110.6(4)
C(7)-C(8)-C(9)	113.9(5)	Te(1)-C(9)-C(8)	113.8(4)
Torsion angles			
Te(1)-C(1)-C(2)-C(3)	-68.6(6)	Te(1)-C(9)-C(8)-C(7)	-65.0(5)
S(1)-C(3)-C(2)-C(1)	177.0(3)	S(1)-C(4)-C(5)-C(6)	174.4(4)
S(2)-C(6)-C(5)-C(4)	-70.3(5)	S(2)-C(7)-C(8)-C(9)	-73.2(5)
C(1)-Te(1)-C(9)-C(8)	149.6(4)	C(2)-C(1)-Te(1)-C(9)	-69.8(5)
C(2)-C(3)-S(1)-C(4)	-64.1(5)	C(3)-S(1)-C(4)-C(5)	-64.1(5)
C(5)-C(6)-S(2)-C(7)	-76.3(4)	C(6)-S(2)-C(7)-C(8)	161.5(4)

A similar trend in bond angles is also observed in the structure of [11]aneS$_2$Te, however in this case the torsion angles display greater deviations from strictly *gauche* or *anti* – this observation most probably arising from the smaller ring size of the molecule imposing restrictions on the structural geometry. In this case, as for the [12]aneS$_2$Te analogue, there are three *gauche* and one *anti* CSCC torsions and one *gauche* and one *anti* CTeCC torsion. As observed for [12]aneS$_2$Te, in the solid state [11]aneS$_2$Te adopts an approximate square geometry, but unlike [12]aneS$_2$Te the Te donor atom occupies a corner position, with the S atoms assuming positions on the edges.

2.2.2 Synthesis of [9]aneS$_2$Te

The smaller analogue of [11]aneS$_2$Te and [12]aneS$_2$Te was obtained similarly from the α,ω-dichlorodithioether, Cl(CH$_2$)$_2$S(CH$_2$)$_2$S(CH$_2$)$_2$Cl (Figure 2.27). The reaction was found to be much more dependent on the exact reaction conditions than the [11]- and [12]-aneS$_2$Te preparations.

Figure 2.27 - Synthesis of [9]aneS$_2$Te

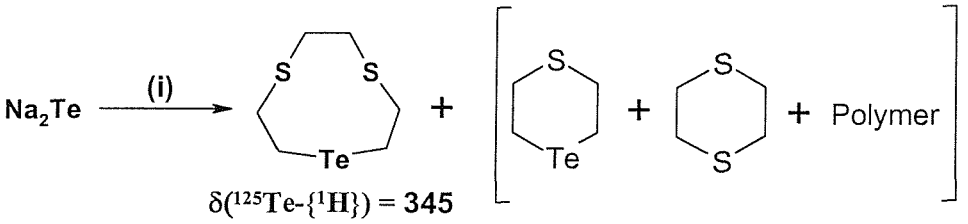

(i) Cl(CH$_2$)$_2$S(CH$_2$)$_2$S(CH$_2$)$_2$Cl in thf, -45°C

[CARE: the α,ω-dichlorodithioether precursors, especially Cl(CH$_2$)$_2$S(CH$_2$)$_2$S(CH$_2$)$_2$Cl, are powerful vesiccants and may cause severe blistering upon skin contact]. The reaction was initially carried out using the same conditions as those employed for the [11]- and [12]-aneS$_2$Te syntheses, but it was found to be much more more sensitive to the reaction temperature during the addition of the dichloro-precursor to Na$_2$Te in NH$_{3(l)}$.

When the addition was carried out at -78°C, as per the [11]- and [12]-aneS_2Te preparations, the product isolated was largely highly insoluble and concluded to be polymeric in nature, with a likely structure being $[Te(CH_2)_2S(CH_2)_2S(CH_2)_2]_n$. ^{125}Te-{^{1}H} NMR spectroscopy showed a minor resonance at δ 176 ppm, however, this being consistent with 1-thia-4-telluracyclohexane (see below). It is reasonable to conclude that this was a fairly small constituent of the bulk material due to the insolubility of the solid and the high solubility of 1-thia-4-telluracyclohexane in chlorinated solvents. Polymer formation may have arisen from the low solubility of the sulfur mustard precursor in the $NH_{3(l)}$/thf mixture at -78°C, resulting in a much less controlled reaction as the $NH_{3(l)}$ boiled off and the reaction warmed to room temperature.

The synthesis was attempted again, but carrying out the addition of the sulfur mustard precursor to the Na_2Te solution at the higher temperature of -45°C in order to increase its solubility during the addition and to speed up the reaction. This time, [9]aneS_2Te was isolated as a pale orange solid in approximately 20% yield, after recrystallisation of the crude solid from CH_2Cl_2/MeOH and CH_2Cl_2/hexane, and was fully characterised spectroscopically. The ^{1}H NMR spectrum showed a singlet resonance at δ 2.84 that was assigned to the S*C*H_2*C*H_2S resonances, and two triplets at δ 2.93 and 3.06 that were attributed to the S*C*H_2CH$_2$Te and *C*H_2Te protons respectively. The ^{13}C-{^{1}H} NMR spectrum displayed resonances assigned to the *C*H_2S environments at δ 38.9 and 32.9 ppm, with the *C*H_2Te resonance identified at δ 2.9 ppm; this being similar to the values reported for [11]- and [12]-aneS_2Te (δ 2.2 and 1.0 ppm respectively). The ^{125}Te-{^{1}H} NMR spectrum showed a single resonance at δ 345, the chemical shift being significantly to high frequency of [11]- and [12]-aneS_2Te (δ 234 and 217 respectively). The reasons for this are not clear, but the smaller ring size may mean that ring strain and transannular effects are much more significant than in the larger [11]- and [12]-aneS_2Te rings. The identity of the macrocycle was also confirmed by EI mass spectrometry, which revealed a cluster of peaks for the molecular ion $[C_6H_{12}S_2{}^{130}Te]^+$ at *m/z* = 278, together with several fragmentation products at lower *m/z* arising from the successive loss of C_2H_4 and S from the parent monocation.

A number of by-products from the reaction of the precursors at -45°C were also isolated, and in order to try to understand the reaction chemistry in more detail we were keen to identify some of the by-products from this rather temperamental reaction. The first by-product to be isolated was a highly insoluble solid from the crude, hydrolysed reaction mixture. This was thought to be polymeric in nature due to its insolubility, and similar to that formed from the reaction at -78°C. The very poor solubility of the solid, however, precluded the accumulation of spectroscopic data. The CH_2Cl_2/MeOH filtrate from the recrystallisation of crude [9]aneS_2Te was allowed to evaporate, forming a crop of orange crystals in approximately 15% yield. This was found to be largely 1-thia-4-telluracyclohexane on the basis of the spectroscopic data and an X-ray crystallographic study (Figure 2.28). This compound had previously been reported by McCullough and co-workers, where the high dilution reaction of bis(2-chloroethyl)sulfide with Na_2Te in water gave the product in under 7% yield.[14] McCullough and co-workers reported the analytical data and melting point for 1-thia-4-telluracyclohexane, but additional spectroscopic data were needed in order to provide comparisons with the larger [9]-, [11]- and [12]-aneS_2Te compounds. The crystals were found to have $\delta(^{125}Te) = 254$ ppm and $\delta(^{13}C\text{-}\{^1H\}) = 30.1$ and -5.8 ppm, these being assigned to the CH_2S and CH_2Te moieties respectively. The ^1H, $^{13}C\text{-}\{^1H\}$ and $^{125}Te\text{-}\{^1H\}$ spectroscopic data for the compound are given in Table 2.3.

Table 2.3 - ^1H, $^{13}C\text{-}\{^1H\}$ and $^{125}Te\text{-}\{^1H\}$ NMR data for 1-thia-4-telluracyclohexane

Compound	**^1H δ/ppm[a]**	**Assignment**	**$^{13}C\text{-}\{^1H\}$ δ/ppm[b]**	**Assignment**	**$^{125}Te\text{-}\{^1H\}$ δ/ppm[b]**
1-thia-4-telluracyclohexane	3.08[c]	CH_2Te	-5.8	CH_2Te	264
	2.93, t	CH_2S	30.1	CH_2S	

[a] $CDCl_3$ solution [b] $CH_2Cl_2/CDCl_3$ solution [c] AA'BB' multiplet

The GC-EI mass spectrum of the 1-thia-4-telluracyclohexane crystals showed a major cluster of peaks at *m/z* = 218 (consistent with the monocation $[C_4H_8S^{130}Te]^+$) together with fragmentation peaks resulting from the successive loss of the C_2H_4 inter-donor linkages.

The ^{1}H NMR spectrum of the 1-thia-4-telluracyclohexane crystals revealed a minor impurity (estimated by integration as *ca.* 5%) at δ 2.85 ppm that was tentatively assigned as 1,4-dithiane. A low resolution EI mass spectrum of the 1-thia-4-telluracyclohexane crystals showed the major species at *m/z* = 218 (consistent with $[C_4H_8STe]^+$) together with fragments associated with the successive loss of C_2H_4 units. A minor species at *m/z* = 120 was identified as 1,4-dithiane, therefore confirming it as the species observed at δ 2.85 ppm in the ^{1}H NMR spectrum. Dimethylene (C_2H_4) linkages between S and Te atoms are unknown in di- and tri-telluroethers due to their susceptibility to eliminate ethene and form ditellurides, RTeTeR, (Chapter 1) and therefore 1,4-dithiane is a likely by-product in the [9]aneS_2Te synthesis. The reasons for the presence of 1-thia-4-telluracyclohexane are less clear, however. The Te-C bonds are known to be weak, therefore leading to the decompositon of telluroether compounds upon exposure to air, but S-C bonds are much stronger, and there are many examples of C_2H_4 linkages in acyclic and macrocyclic thioether ligands – for example the macrocyclic compound [9]aneS_3.[46] Despite this, significant S-C bond cleavage must have occurred during the reaction in order to produce 1,4-dithiane.

The crystal structure (Figure 2.28) of 1-thia-4-telluracyclohexane shows it disordered over a crystallographic inversion centre at the centre of the ring, which adopts a chair conformation. The disorder was modeled successfully using a 50 : 50 split occupancy for the S and Te atoms. This means that detailed comparisons of S-C and Te-C bond lengths with [11]- and [12]-aneS_2Te are not possible, since the values for 1-thia-4-telluracyclohexane are averages.

Figure 2.28 - Crystal structure of 1-thia-4-telluracyclohexane with numbering scheme adopted. Ellipsoids are drawn at the 40% probability level and H atoms are omitted for clarity. The ring is disordered over a crystallographic inversion centre and atoms S(1^3), C(1^3) and C(2^3) are related by the operation –x, -y, -z

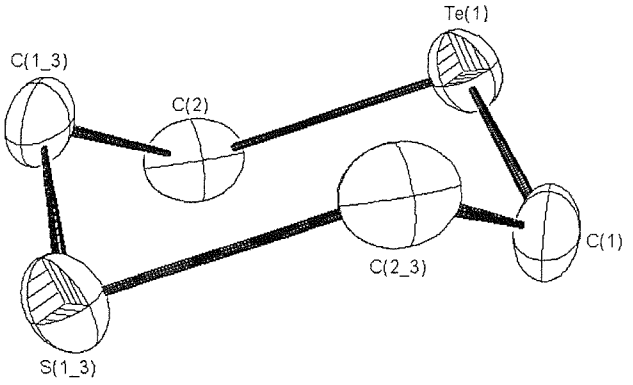

The crystals were found to have the same space group and unit cell parameters as those reported by McCullough,[14] although he chose not to fully refine the structure, opting to structurally characterize the 1-thia-4-telluracyclohexane-4,4-diiodide derivative instead.[15] The presence of the ring contraction product in the [9]aneS$_2$Te synthesis contrasts with the syntheses of the [11]- and [12]-membered S$_2$Te rings, in that no evidence for ring contraction was observed for the latter systems. The reason for its occurrence in the [9]aneS$_2$Te synthesis may be due to the presence of the C_2H_4 linkages between the S and Te donor atoms.

2.3 Organo-derivatives of [9]-, [11]- and [12]-aneS$_2$Te and C$_4$H$_8$STe

The preparation of derivatives (for example methiodides, dichlorides or diiodides) to form white or cream coloured solids (telluronium salts) can be very useful when characterising new tellurium-containing compounds. The Te(II) compounds are easily oxidised to formally Te(IV) species upon reaction with MeI, Cl_2 or I_2, and the compounds thus formed are air stable and therefore easy to characterise. The resulting deshielding of

the tellurium nucleus may be easily observed as a significant shift to high frequency in the ^{125}Te-{^{1}H} NMR spectrum.[50]

Reaction of the macrocycles and 1-thia-4-telluracyclohexane with excess MeI in CH_2Cl_2 solution, affords, after work up, their respective air-stable methiodide derivatives in high yield. The ^{125}Te-{^{1}H} and ^{13}C-{^{1}H} NMR spectra of the products were recorded in d_6-dmso owing to their very poor solubilities in non-coordinating solvents. Significant high frequency shifts for the CH_2Te moieties in the ^{13}C-{^{1}H} NMR spectra (Figure 2.29 – [11]aneS$_2$TeMeI) and in the ^{125}Te-{^{1}H} NMR spectra (Figure 2.30) confirmed that quaternisation had occurred at Te, this being paralleled by the appearance of a single TeCH_3 resonance in each case. Such high frequency shifts are typical of Te methiodide derivatives, for example Me_3TeI,[51] which has $\delta(^{125}Te) = 418$ ppm. This is compared with the shifts on quaternisation of 74 ppm for [9]aneS$_2$TeMeI, 308 and 326 ppm for [11]- and [12]-aneS$_2$TeMeI respectively and 170 ppm for 1-thia-4-telluracyclohexanemethiodide with respect to the free ligands.

Figure 2.29 - ^{13}C-{^{1}H} NMR spectrum of [11]aneS$_2$TeMeI in d_6-dmso

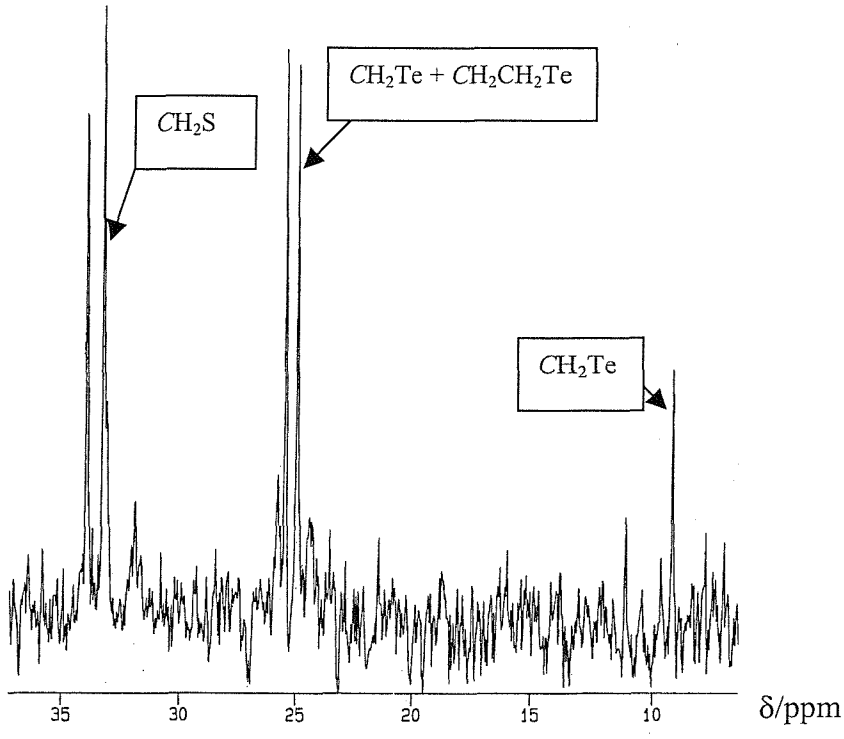

Electrospray mass spectra of the [11]- and [12]-aneS$_2$Te methiodides and 1-thia-4-telluracyclohexanemethiodide all display a single cluster of peaks with the correct isotopic distribution at the expected *m/z* for [ligand+Me]$^+$, which provides further evidence that the macrocyclic products are indeed the [1+1] cyclisation species. If the species present were in fact the dicationic [2+2] methiodides, the *m/z* values and isotopic distributions would be notably different owing to the presence of an additional Te atom. (Figure 1.13, Chapter 1). Due to the very poor solubility of [9]aneS$_2$TeMeI in MeCN (which is used for electrospray mass spectrometry) no mass spectrum was obtained.

Figure 2.30 - ^{125}Te-{^{1}H} NMR Spectrum of [12]aneS$_2$TeMeI in d_6-dmso

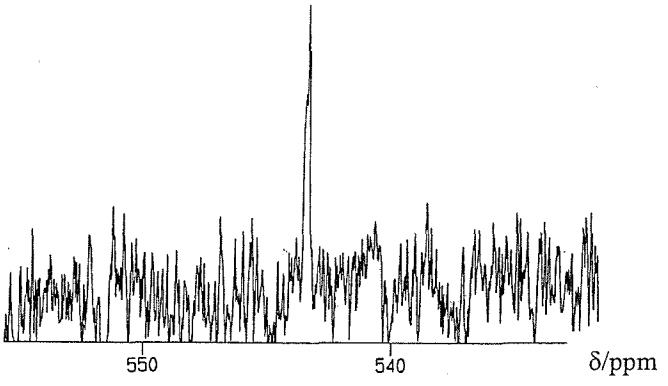

[11]- and [12]-aneS$_2$Te were also treated with one equivalent of I_2 in thf-CH_2Cl_2 solution, which provided, after work up, the air stable Te(IV) diiodides as brick red powdery solids. Iodination was chosen in preference to chlorination, since Cl_2 would attack the thioether donors, as was observed, for example, in the chlorination of [14]aneS$_4$-ol, $C_{10}H_{20}OS_4$.[52] Electrospray mass spectra of the derivatives reveal the major cluster of peaks as [[n]aneS$_2$TeI]$^+$. The ^{13}C-{^{1}H} and ^{125}Te-{^{1}H} NMR spectra of the derivatives failed to give sensible data, which we speculate may be due to ring opening or decomposition processes occurring in solution over the extended accumulation times. The ^{1}H NMR spectra of the products were recorded, however, and are consistent with the proposed formulations, showing significant high frequency shifts for the TeC*H*$_2$

functionalities to δ 3.50 and 3.60 ppm from δ 2.67 and 2.66 ppm respectively for [11]aneS_2TeI_2 and [12]aneS_2TeI_2.

Crystals of [12]aneS_2TeI_2 were grown from CH_2Cl_2-$CDCl_3$ solution by slow evaporation. The structure (Figure 2.31 and Table 2.4) shows a molecular, Te(IV) species with a distorted *pseudo*-trigonal bipyramidal geometry about Te, with axial iodines. The open, fifth vertex, is assumed to host the lone pair of electrons.

Figure 2.31 - Crystal structure of [12]aneS_2TeI_2 with numbering scheme adopted. Ellipsoids are drawn at the 40% probability level and H atoms are omitted for clarity

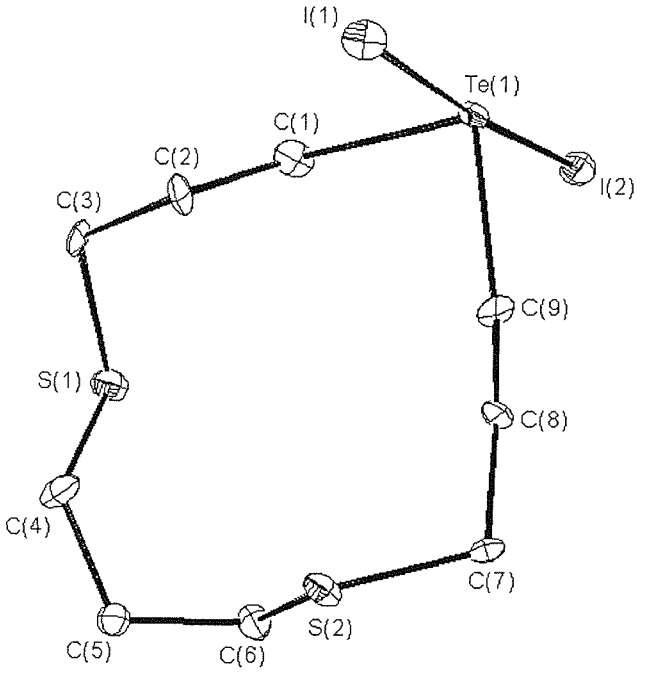

The geometry about Te is very similar to that reported for Me_2TeI_2,[53] which suggests that the presence of the ring does not impose any constraints upon the structure. The geometry is also similar to that of the parent macrocycle, [12]aneS_2Te, however this time the Te donor occupies a corner position rather than a S atom. The similarity is confirmed by an analysis of the distribution of torsion angles, which reveals both CTeCC torsions as being *gauche* (one being *anti* and one *gauche* for the parent macrocycle) and two CSCC torsions also being *gauche* and the remaining two *anti*. This compares with three *gauche* CSCC torsions in [12]aneS_2Te. Of the four ITeCC torsions, two are *anti* and two *gauche*.

Table 2.4 - Selected bond lengths (Å), angles (°) and torsion angles (°) for [12]aneS_2TeI_2

Bond lengths			
(I)1-Te(1)	2.8990(9)	I(2)-Te(1)	2.9179(9)
Te(1)-C(1)	2.189(9)	Te(1)-C(9)	2.155(9)
S(1)-C(3)	1.819(11)	S(1)-C(4)	1.829(11)
S(2)-C(6)	1.815(10)	S(2)-C(7)	1.820(10)
C(1)-C(2)	1.50(1)	C(2)-C(3)	1.528(12)
C(4)-C(5)	1.52(1)	C(5)-C(6)	1.516(12)
C(7)-C(8)	1.54(1)	C(8)-C(9)	1.50(1)
Bond angles			
I(1)-Te(1)-I(2)	176.77(3)	I(1)-Te(1)-C(1)	96.0(3)
I(1)-Te(1)-C(9)	86.3(3)	I(2)-Te(1)-C(1)	86.8(3)
I(2)-Te(1)-C(9)	95.2(3)	C(1)-Te(1)-C(9)	93.3(4)
C(3)-S(1)-C(4)	99.7(5)	C(6)-S(2)-C(7)	98.9(5)
Te(1)-C(1)-C(2)	117.2(6)	C(1)-C(2)-C(3)	110.7(8)
S(1)-C(3)-C(2)	112.4(6)	S(1)-C(4)-C(5)	110.5(7)
C(4)-C(5)-C(6)	112.9(8)	S(2)-C(6)-C(5)	111.9(7)
S(2)-C(7)-C(8)	113.1(6)	C(7)-C(8)-C(9)	110.0(9)
Te(1)-C(9)-C(8)	119.6(7)		
Torsion angles			
I(1)-Te(1)-C(1)-C(2)	-22.7(8)	I(1)-Te(1)-C(9)-C(8)	156.3(7)
I(2)-Te(1)-C(1)-C(2)	159.0(7)	I(2)-Te(1)-C(9)-C(8)	-26.6(7)
Te(1)-C(1)-C(2)-C(3)	-170.9(7)	Te(1)-C(9)-C(8)-C(7)	-168.9(6)
S(1)-C(3)-C(2)-C(1)	74.0(10)	S(1)-C(4)-C(5)-C(6)	65.6(9)
S(2)-C(6)-C(5)-C(4)	62.2(10)	S(2)-C(7)-C(8)-C(9)	72.0(9)
C(1)-Te(1)-C(9)-C(8)	60.5(7)	C(2)-C(1)-Te(1)-C(9)	63.9(8)
C(2)-C(3)-S(1)-C(4)	78.8(8)	C(3)-S(1)-C(4)-C(5)	-162.8(7)
C(5)-C(6)-S(2)-C(7)	-162.8(7)	C(6)-S(2)-C(7)-C(8)	80.6(8)

Te-I bond distances in [12]aneS$_2$TeI$_2$ (2.8990(9) and 2.9179(9) Å) are similar to those reported for the α-form of 1-thia-4-telluracyclohexanediiodide, which has two independent molecules in the unit cell (d(Te-I) = 2.884(2), 2.939(2), 2.985(2) and 2.851(2) Å.[15] The Te-C bond lengths in [12]aneS$_2$Te (2.189(9) and 2.155(9) Å) are also comparable to those reported for 1-thia-4-telluracyclohexanediiodide, which has d(Te-C) = 2.155(2) Å (av.). The I-Te-I bond angles in 1-thia-4-telluracyclohexanediiodide are 174.9(1) and 178.1(1)° with the I-Te-C bond angles being 88.3(6), 91.6(6), 91.6(6), 89.6(6), 87.4(6), 88.9(6), 91.8(6) and 88.5(6)° for the two independent molecules. These are comparable to the angles around Te in [12]aneS$_2$TeI$_2$, which has an I-Te-I bond angle of 176.77(3)° and I-Te-C angles of 86.3(3), 86.8(3), 95.2(3) and 93.3(4)°. The bond angles for both molecules confirm the *pseudo*-trigonal bipyramidal geometries about Te.

2.4 Transition metal complexes

2.4.1 [Mn(CO)$_3$([n]aneS$_2$Te)][CF$_3$SO$_3$] (n = 9, 11 and 12)

[Mn(CO)$_5$Cl] was refluxed in acetone solution with AgCF$_3$SO$_3$ to form the *in situ* intermediate [Mn(CO)$_3$(Me$_2$CO)$_3$][CF$_3$SO$_3$][54] which has ν(CO) = 2054 and 1974 cm^{-1}. The AgCl precipitate was filtered off in each case, and solutions of [n]aneS$_2$Te (n = 9, 11 and 12) in acetone added. The solutions were stirred at room temperature for *ca.* two hours, and monitored by solution IR spectroscopy to ensure reaction completeness. The Mn(I) tricarbonyl species *fac*-[Mn(CO)$_3$([n]aneS$_2$Te)][CF$_3$SO$_3$] were isolated by adding Et$_2$O to the concentrated reaction mixtures and subsequently filtering the resultant solids and washing them with Et$_2$O. The products were isolated as pale yellow solids in reasonable yield, with the exception of the [12]aneS$_2$Te complex, which was obtained only in low yield. IR spectra of the solids as CsI disks revealed two strong ν(CO) stretching vibrations in each case (Figure 2.32 and Table 2.5). The cationic *fac*-tricarbonyl moieties have effective *Cs* symmetry, for which 3 IR active CO stretches (2A' + A") are predicted by group theory. The observation of two bands (one of which is very broad – see Figure 2.32) suggests that the CO co-ligands do not 'observe' the difference between the S and Te donors, and therefore the complex appears to be C_{3v} (with visible

A_1 + E bands). The confirmation of the complexes as *fac*-Mn(I) species is consistent with coordination of the macrocycles to the Mn(I) centre through all three donor atoms; *i.e.* using S_2Te donor sets. ES mass spectrometry of the products revealed major clusters of peaks consistent with $[Mn(CO_3)([n]aneS_2Te)]^+$ for n = 11 and 12.

Figure 2.32 - IR spectrum (CsI disk, CO Region) of [Mn(CO)$_3$([11]aneS$_2$Te)][CF$_3$SO$_3$]

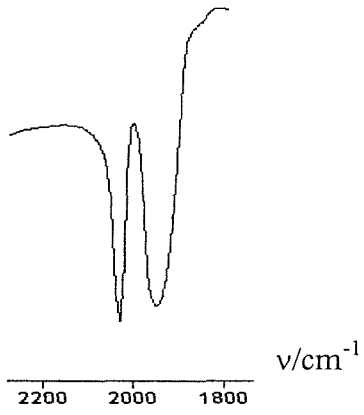

The decrease in ν(CO) in the order $[Mn(CO)_3([9]aneS_2Te)][CF_3SO_3]$ > $[Mn(CO)_3([11]aneS_2Te)][CF_3SO_3]$ > $[Mn(CO)_3([12]aneS_2Te)][CF_3SO_3]$ is indicative of increasing L → Mn σ-donation in the same direction. The ν(CO) frequencies for these complexes (see Table 2.5) may be compared with those in *fac*-$[Mn(CO_3)(MeC(CH_2TeR)_3)][CF_3SO_3]$ (for R = Me, ν(CO) = 2023, 1947 cm^{-1}, and for R = Ph, ν(CO) = 2028, 1959 cm^{-1}).[55]

Table 2.5 - ν(CO)/cm^{-1} for [Mn(CO)$_3$([n]aneS$_2$Te)][CF$_3$SO$_3$]

Complex	ν(CO)/cm^{-1}
$[Mn(CO)_3([9]aneS_2Te)][CF_3SO_3]$	2042s, 1963s br
$[Mn(CO)_3([11]aneS_2Te)][CF_3SO_3]$	2033s, 1950s br
$[Mn(CO)_3([12]aneS_2Te)][CF_3SO_3]$	2028s, 1945s br

The [Mn(CO)$_3$([12]aneS$_2$Te)][CF$_3$SO$_3$] readily decomposed even in the solid state and precluded the acquisition of ^{13}C-{^{1}H}, ^{55}Mn and ^{125}Te-{^{1}H} NMR data. In addition, even though stable in the solid state, the [11]aneS$_2$Te complex decomposed in solution, which meant that ^{13}C-{^{1}H} NMR data acquisition was not possible. The ^{1}H NMR spectra for the complexes, however, all displayed very broad, unresolved resonances to high frequency of free ligand, as was expected upon coordination of the ligands to the Mn(I) centre. The ^{55}Mn NMR spectra showed fairly sharp resonances at -821 and -817 ppm for the [9]- and [11]-membered ring complexes respectively (Figure 2.33). These may be compared with the corresponding resonances for the acyclic complex *fac*-[Mn(CO)$_3$(MeS(CH$_2$)$_3$Te(CH$_2$)$_3$SMe)][CF$_3$SO$_3$], which had δ(^{55}Mn) = -645 (Chapter 4) and *fac*-[Mn(CO)$_3$([n]aneS$_3$)][CF$_3$SO$_3$] which, for n = 9 and 10, have δ(^{55}Mn) = -963 and –764 ppm respectively.[55] These data reveal the significant dependence of δ(^{55}Mn) upon the ring size and donor atom type of the coordinated ligand.[55] The single resonances observed in the ^{125}Te-{^{1}H} NMR spectra of [Mn(CO)$_3$([9]aneS$_2$Te)][CF$_3$SO$_3$] and [Mn(CO)$_3$([11]aneS$_2$Te)][CF$_3$SO$_3$] at δ 214 and 110 ppm respectively were to low frequency of free ligand, as was also the case for the linear MeS(CH$_2$)$_3$Te(CH$_2$)$_3$SMe analogue (Chapter 4).

Figure 2.33 - ^{55}Mn NMR spectrum of [Mn(CO)$_3$([11]aneS$_2$Te)][CF$_3$SO$_3$] in d_6-Me$_2$CO

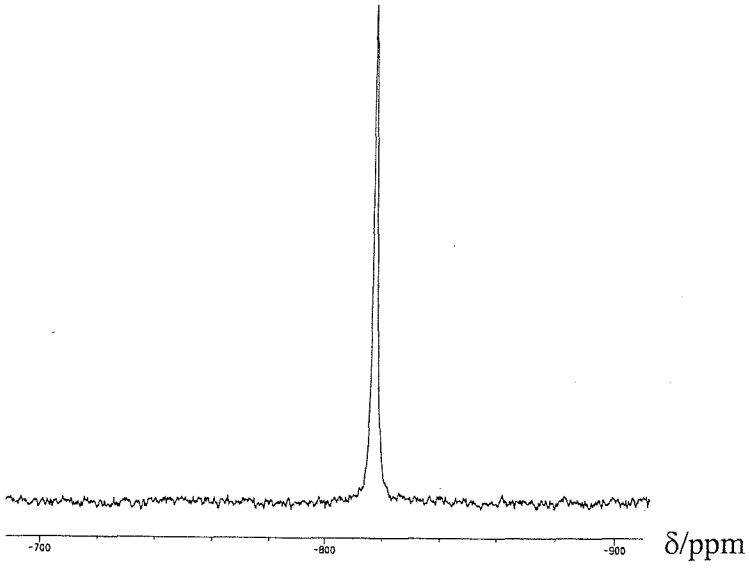

2.4.2 [Mo(CO)$_4$([n]aneS$_2$Te)] (n = 11 or 12)

Reaction of [11]aneS$_2$Te with either [Mo(CO)$_3$(MeCN)$_3$][56] in refluxing MeCN or [Mo(CO)$_6$] in MeNO$_2$ failed to produce the target *fac*-tricarbonyl complex [Mo(CO)$_3$([11]aneS$_2$Te)]. In each case, the IR spectra revealed the presence of a *cis*-tetracarbonyl species only. The complex [Mo(CO)$_3$([9]aneS$_3$)] has previously been reported,[57] and appears to be quite robust. This is in contrast to [Mo(CO)$_3$(MeC(CH$_2$EMe)$_3$)] (E = S, Se or Te), which are prone to decomposition in solution, forming tetracarbonyl species.[57] A subsequent attempt to synthesise the *cis*-tetracarbonyl complex [Mo(CO)$_4$([11]aneS$_2$Te)] from the reaction of [Mo(CO)$_4$(nbd)][58] (nbd = norbornadiene) and the ligand in CH$_2$Cl$_2$ was more successful. IR spectroscopy of the solid product revealed three ν(CO) stretching vibrations at 2021, 1900 and 1846 cm^{-1}, the failure to observe the four bands for the C_{2v} complex predicted by Group Theory was probably due to the A$_1$ and B$_1$ modes at *ca.* 1900 cm^{-1} being poorly resolved. The donor set is unclear on the basis of these data alone, however, since bidentate coordination of the macrocycle through either STe or SS donor sets are not expected to produce significantly different values for ν(CO).[59] The ^{125}Te-{^{1}H} NMR spectrum, however, facilitates an unambiguous determination of the donor set at Mo(0), displaying a single resonance at 282 ppm. This is significantly shifted to high frequency of the free ligand (δ(^{125}Te) = 234) and therefore clearly demonstrates that the only isomer present in solution in significant quantity involves coordination through the Te donor, and therefore an STe donor set. The compound was found to decompose slowly in solution. This is confirmed by the presence of precipitated dark solid in the NMR sample, together with the appearance over time of a second ^{125}Te-{^{1}H} NMR resonance at 194 ppm. This meant that the acquisition of reliable ^{13}C-{^{1}H} NMR data for the complex was not possible.

Reaction of [12]aneS$_2$Tee with [Mo(CO)$_4$(nbd)] in CH$_2$Cl$_2$ produced a low yield of an uncharacterised, insoluble brown solid, which rapidly turned black even when stored under dinitrogen. This result parallels the observed lower stability of [Mn(CO)$_3$([12]aneS$_2$Te)][CF$_3$SO$_3$] compared with the [9]- and [11]-membered ring

analogues, and the coordination chemistry of the ligand with Mo(0) was therefore not pursued.

2.4.3 [MCl$_2$([n]aneS$_2$Te)] (M = Pd or Pt; n = 11 or 12)

The Pd(II) and Pt(II) complexes [MCl$_2$([n]aneS$_2$Te)] (M = Pd or Pt; n = 11 or 12) were synthesised by the direct reaction of the corresponding macrocycle in CH_2Cl_2 solution with [MCl$_2$(NCMe)$_2$] (formed from refluxing MCl$_2$ in MeCN)[60] to give yellow solids in good yield. The IR spectra of the solids reveal weak absorptions between 300 and 320 cm^{-1}, which were assigned to ν(M-Cl) stretching vibrations. For a *cis* square planar [MCl$_2$L] complex, two ν(M-Cl) vibrations are expected, for example [PdCl$_2${*o*-C$_6$H$_4$(TeMe)$_2$}] has ν(Pd-Cl) = 295 and 284 cm^{-1} and [PtCl$_2${*o*-C$_6$H$_4$(TeMe)$_2$}] has ν(Pt-Cl) = 329 and 306 cm^{-1}.[61] The additional presence of coordinated macrocycle absorptions in this region, however, preclude the assignment of the complexes as either *trans* or *cis* (one or two bands respectively) on the basis of these data alone. The low solubility of the Pt(II) complexes in non-coordinating solvents meant that NMR data was only obtainable from d$_6$-dmf or d$_6$-dmso solution, whereas the Pd(II) complexes were more readily soluble in CH_2Cl_2 or $CDCl_3$. The ^{125}Te-{^{1}H} NMR spectra of the Pd(II) complexes displayed single resonances at δ 330 and 387 ppm, while the analogous Pt(II) complexes had δ(^{125}Te) = 299 and 374 ppm for [11]- and [12]-aneS$_2$Te respectively. These data revealed significant high frequency shifts upon coordination of the macrocycle to Pd(II)/Pt(II), with slightly smaller shifts for the Pt(II) complexes as a result of the lower electronegativity of Pt(II). This confirmed the coordination of the macrocycles through an STe donor set to the M(II) centers in each case. This assignment is reinforced by the ^{195}Pt satellite couplings in the ^{125}Te-{^{1}H} NMR spectra ($^1J_{Pt\text{-}Te}$ = 753 and 1034 Hz for the [11]aneS$_2$Te and [12]aneS$_2$Te complexes respectively), the values being consistent with *cis*-dichloro species involving STe coordination. Likewise, the ^{195}Pt NMR shifts for the [11]- and [12]-aneS$_2$Te complexes (δ -3834 and -3890 ppm respectively) are representative of similar group 16 complexes. For example [PtCl$_2$(MeTe(CH$_2$)$_3$TeMe)] has δ(^{195}Pt) = δ -4434 and -4379 ppm ($^1J_{Pt\text{-}Te}$ = 1140, 820 Hz),[62] while

[$PtCl_2(MeS(CH_2)_3SMe)$] has $\delta(^{195}Pt) = \delta$ -3538 and -3570 ppm.[63] The two resonances for both of the complexes are due to the presence of *meso* and DL invertomers in solution.

Crystal structures of [PtX_2([9]aneS_3)], where X = Cl, Br or I[64] have shown the macrocycle coordinated *cis* to the Pt(II) centre, with the third sulfur atom of the macrocycle forming a long distance interaction with the metal. This results in an elongated square pyramidal structure with an S_2X_2+S_1 coordination geometry. The analogous complexation with [9]aneS_2Te was not attempted due to the low solubility of the Pt(II) complexes of [11]- and [12]-aneS_2Te, since the much lower solubility of the [9]aneS_2Te ligand would likely preclude the acquisition of spectroscopic data. On the basis of these data, the structures of the [11]- and [12]-aneS_2Te complexes with Pd(II) and Pt(II) are likely to be square planar, with bidentate coordination of the macrocycle to the metal(II) centre through an STe donor set.

2.4.4 [Rh(cp*)([n]aneS_2Te)][PF_6]$_2$ (n = 9, 11 or 12)

The reaction of [Rh(cp*)Cl_2]$_2$[65] with two equivalents of macrocycle and four equivalents of $TlPF_6$ in CH_2Cl_2 solution, afforded, in each case, after stirring at room temperature for *ca.* two hours, a bright yellow solution with a white precipitate of TlCl. These were filtered through celite to remove TlCl and the solvent removed *in vacuo*. The resulting residues were redissolved in acetone and filtered through celite for a second time to remove any remaining traces of TlCl. Concentration of the resultant clear yellow solutions followed by the addition of Et_2O precipitated the products, which were subsequently filtered, washed with Et_2O and dried *in vacuo*, giving bright yellow powdered solids in moderate yield (35 – 63%). The non-coordinating PF_6^- anion was chosen in order to avoid competition with the macrocycles for bonding to the Rh(III) centre. $TlPF_6$ was chosen as the source of PF_6^-, since the formation of the highly insoluble TlCl during the reaction provides a strong driving force. The IR spectrum revealed the presence of PF_6^- anion (two intense absorptions at *ca.* 835 and 560 cm^{-1}) coordinated macrocycle and cp* co-ligand, therefore confirming the distorted, *pseudo*-octahedral Rh(III) complexes. Electrospray mass spectrometry of the complexes showed, in each case, clusters of peaks with the correct *m/z* and isotopic distribution for the

species [[Rh(cp*)([n]aneS$_2$Te)][PF$_6$]]$^+$, although for n = 11 and 12 the most intense peaks corresponded to the dicationic [Rh(cp*)([n]aneS$_2$Te)]$^{2+}$. The latter species was not observed in the electrospray mass spectrum where n = 9, however. The ^{1}H and ^{13}C-{^{1}H} NMR spectra of the products were all consistent with the proposed formulations, showing cp* resonances at *ca.* 1.75 ppm in the ^{1}H NMR spectra, together with peaks shifted to high frequency of free ligand, consistent with coordination of the macrocycle to the Rh(III) centre. The C*H*$_2$Te resonances in the ^{13}C-{^{1}H} NMR spectra were observed at δ 24.7, 24.6 and 25.6 ppm for the [9]-, [11]- and [12]-aneS$_2$Te complexes respectively, these also being shifted significantly to high frequency of uncoordinated macrocycle (δ^{125}Te(C*H*$_2$Te) = 2.9, 2.2 and 1.0 ppm for [9]-, [11]- and [12]-aneS$_2$Te).

The ^{125}Te-{^{1}H} NMR spectra of the complexes all revealed doublet resonances to high frequency of uncoordinated ligand: [Rh(cp*)([9]aneS$_2$Te)][PF$_6$]$_2$ = δ 397 ($^1J_{\text{Rh-Te}}$ = 75 Hz); [Rh(cp*)([11]aneS$_2$Te)][PF$_6$]$_2$ = δ 282 ($^1J_{\text{Rh-Te}}$ = 106 Hz) (Figure 2.34) and [Rh(cp*)([12]aneS$_2$Te)][PF$_6$]$_2$ = δ 275 ppm ($^1J_{\text{Rh-Te}}$ = 102 Hz). The coupling constants are similar to those reported for [Rh(cp*)(RTe(CH$_2$)$_3$Te(CH$_2$)$_3$TeR)][PF$_6$]$_2$, where $^1J_{\text{Rh-Te}}$ = 80 Hz (av.) for R = Me and 90 Hz (av.) for R = Ph,[66] and [Rh(cp*)(MeS(CH$_2$)$_3$Te(CH$_2$)$_3$SMe)][PF$_6$]$_2$, which has $^1J_{\text{Rh-Te}}$ = 94 Hz (Chapter 4). The ^{125}Te-{^{1}H} NMR shift for the MeS(CH$_2$)$_3$Te(CH$_2$)$_3$SMe complex is to low frequency of uncoordinated ligand, but for RTe(CH$_2$)$_3$Te(CH$_2$)$_3$TeR the four resonances (consistent with the resolution of *meso* and DL invertomers in solution – Chapter 4) are shifted to high frequency of free ligand. This is also the case for the macrocyclic complexes described here.

The complexes are expected to have a distorted *pseudo*-octahedral geometry about Rh(III), with the macrocycle coordinated *fac* through an S$_2$Te donor set. (Figure 2.35).

Figure 2.34 - ^{125}Te-{^{1}H} NMR spectrum of [Rh(cp*)([11]aneS_2Te)][PF_6]$_2$ in d_6-Me_2CO

$^1J_{Rh\text{-}Te}$ = 106 Hz

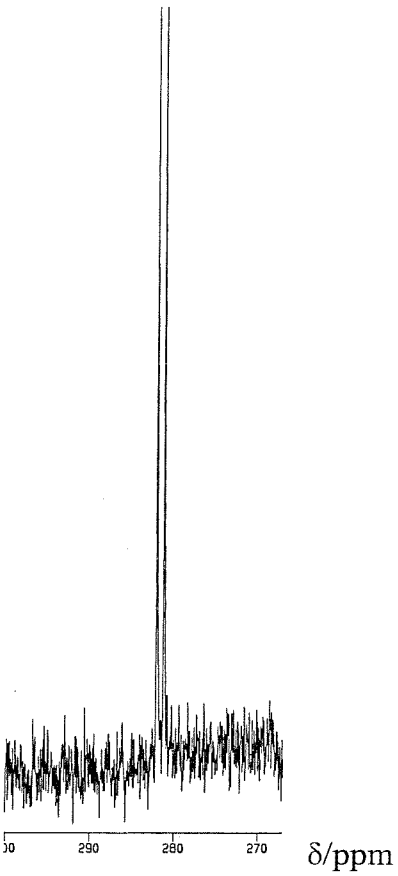

Figure 2.35 - Expected structure of [Rh(cp*)([9]aneS_2Te)][PF_6]$_2$

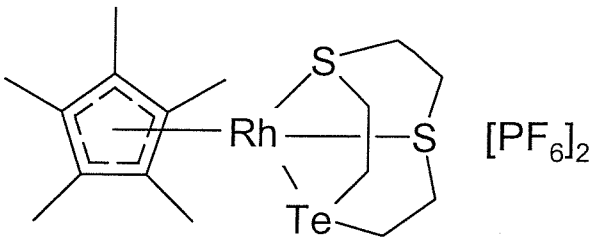

Crystal structures of the analogous [Rh(cp*)([9]aneS$_3$)][ClO$_4$]$_2$[67] and [Rh(cp*)([9]aneS$_3$)][CF$_3$SO$_3$]$_2$[68] have been reported and show distorted octahedral structures, with facial coordination of the trithia-macrocycle to Rh(III).

2.4.5 [Ag([n]aneS$_2$Te][X] (n = 9 or 11, X = CF$_3$SO$_3$; n = 12, X = CF$_3$SO$_3$ or BF$_4$

AgCF$_3$SO$_3$ reacted with one molar equivalent of macrocyclic ligand in CH$_2$Cl$_2$ solution to form the complexes as pale yellow to cream coloured solids, which were subsequently filtered and washed with Et$_2$O to remove any impurities. The complexes were found to be very poorly soluble, even in coordinating solvents; this presumably being due to the relative insolubility of the ligand (in the case of [9]aneS$_2$Te) and to the formation of an extended structural motif, as is common in Ag(I) chemistry. The presence of coordinated macrocycle and of CF$_3$SO$_3^-$ anion[69] was confirmed by IR spectroscopy of the solids. Electrospray mass spectra of the complexes showed clusters of peaks at the correct m/z and having isotopic distributions consistent with [Ag([n]aneS$_2$Te)$_2$]$^+$ for n = 9, 11 and 12, and also [Ag([n]aneS$_2$Te)]$^+$ for n = 11 and 12. These data also suggest the presence of extended structures for the complexes. The ^{1}H NMR spectra confirmed the presence of macrocyclic ligand in each case, the resonances of which being only slightly shifted to high frequency of free ligand. The small coordination shifts are typical of group 16 donor ligand complexes of Ag(I)[70,71] and this was also observed to be the case for the open chain analogue [Ag(MeS(CH$_2$)$_3$Te(CH$_2$)$_3$SMe)][CF$_3$SO$_3$] (Chapter 4).

Elemental analyses for the complexes [Ag([n]aneS$_2$Te)][CF$_3$SO$_3$] where n = 9 and 11 were consistent with the formation of 1:1 ligand : metal complexes, however due to the instability of the n = 12 complex, satisfactory elemental analysis was not obtainable. The latter complex rapidly turned from a pale yellow/cream solid after isolation to a black gum, even when stored under an atmosphere of dinitrogen and shielded from light. The analogous BF$_4^-$ salt, [Ag([12]aneS$_2$Te)][BF$_4$], however, was found to be much more stable and displayed very similar spectroscopic properties, and elemental analysis confirmed the 1:1 stoichiometry.

The crystal structure of [Ag([11]aneS$_2$Te)][BF$_4$] has been reported previously[44] and shows the cation adopting a one-dimensional polymeric structure, where the Ag(I)

centres are bridged by [11]aneS$_2$Te ligands, and a Ag(I) ion coordinated to each macrocyclic donor in a distorted trigonal planar coordination geometry (Figure 1.10, page 21). Ag-S bond lengths are 2.521(3) and 2.634(3) Å, with d(Ag-Te) = 2.674(1) Å. The Ag-Te bond distance is slightly shorter than those reported for [Ag(MeTe(CH$_2$)$_3$TeMe)$_2$][BF$_4$] (d(Ag-Te) = 2.785(2) – 2.837(2) Å,[72] whilst the Ag-S bond lengths are similar to those in [Ag(PhS(CH$_2$)$_3$SPh)$_2$][BF$_4$] (d(Ag-S) = 2.573(3) – 2.623(3) Å),[70] both of which also adopt infinite structures. It is likely that similar polymeric structural motifs exist for the Ag(I) complexes reported here.

2.4.6 [Cu([n]aneS$_2$Te)][BF$_4$], n = 11 or 12

The complexes were formed from solutions of the ligand and [Cu(MeCN)$_4$][BF$_4$][73] in CH$_2$Cl$_2$, and the solids which precipitated were filtered and washed with Et$_2$O to give cream coloured products. Electrospray mass spectra of the complexes were very similar to those observed for the [Ag([n]aneS$_2$Te][CF$_3$SO$_3$] analogues, showing clusters of peaks consistent with the species [Cu([n]aneS$_2$Te)$_2$]$^+$ and [Cu([n]aneS$_2$Te)]$^+$. These data suggest that the Cu(I) complexes may, as in the case of the Ag(I) analogues, adopt extended or polymeric structures, but the absence of X-ray crystallographic data preclude confirmation of this. The IR spectra also confirm the presence of BF$_4^-$ anion, together with that of coordinated macrocycle, while elemental analyses were consistent with the formation of 1:1 complexes.

2.5 Conclusions

The syntheses of the previously reported ligands [11]aneS_2Te and [12]aneS_2Te have been investigated in some detail and found to be reproducible, with slightly increased yields resulting from the modification of the reaction conditions. In each preparation, the formation of a ditelluride species, tentatively assigned as [n]aneS_2Te_2, where [n] = 11 and 12 was identified, these being straightforwardly removed by flash column chromatography of the crude macrocycles on silica, using hexane : ethyl acetate 3:1 as eluent. The synthesis of the 9-membered analogue of [9]aneS_3, [9]aneS_2Te, has also been investigated in much greater detail, with full spectroscopic data having been acquired for the pure macrocycle. The synthesis of the 9-membered ring was found to be much more temperamental than those of the [11]- and [12]-membered rings, but addition of the dichloro-precursor at a slightly elevated temperature (*ca.* -45°C) maximised the formation of the desired product. Even so, several reaction by-products were isolated, these being a highly insoluble (presumably polymeric) species, together with the ring contraction products 1-thia-4-telluracyclohexane and 1,4-dithiane. The former has been unambiguously identified from an X-ray crystallographic study, with the latter, minor by-product, assigned on the basis of ^{1}H NMR spectroscopy and EI mass spectrometry.

Crystal structures of [11]aneS_2Te and [12]aneS_2Te confirmed the presence of the [1+1] cyclisation products, with no evidence for [2+2] species or ring contraction products in any of the spectroscopic data that were accumulated. This is in contrast to the analogous reaction of Na_2Te with $Cl(CH_2)_2O(CH_2)_2O(CH_2)_2Cl$, which gives the [2+2] cyclisation product [18]aneO_4Te_2 as the major species, with the [1+1] product, [9]aneO_2Te being isolated in much lower yield (Chapter 3). The more temperamental nature of the [9]aneS_2Te synthesis may be attributed to the susceptibility of the dimethylene linkages adjacent to Te to elimination, together with the low solubility of $Cl(CH_2)_2S(CH_2)_2S(CH_2)_2Cl$ in $NH_{3(l)}$. The crystal structures of the free ligands are similar to both parent cyclohydrocarbons (and [12]aneS_3 in the case of [12]aneS_2Te). This is despite the introduction of the heavy (and large) Te atom and the resulting changes in the distribution of Te-C and C-Te-C angles.

It has been demonstrated that the macrocycles readily form organo-derivatives of the type [n]aneS_2TeMeI for n = 9, 11 and 12, and the Te(IV) diiodide species [n]aneS_2TeI_2 for n = 11 and 12 have also been prepared. An X-ray crystallographic study of [12]aneS_2TeI_2 has shown the molecule adopting a distorted *pseudo*-trigonal bipyramidal geometry about Te, with *trans* (axial) iodines.

The macrocycles also readily coordinate to a variety of low and medium oxidation state transition metal ions, functioning as either bidentate ligands through an STe donor set in *e.g.* [MCl_2([n]aneS_2Te)] (M = Pd or Pt; n = 11 or 12) or as tridentate (face-capping) ligands, *e.g.* in [$Mn(CO)_3$([n]aneS_2Te)][CF_3SO_3] (n = 9, 11 or 12). The complexes of [12]aneS_2Te were found to be much less stable, both in the solid state and in solution, than the 9- and 11-membered analogues. This parallels the results reported by Cooper and co-workers[74] who demonstrated the lower stability of 3d and 4d transition metal complexes of [12]aneS_3 compared with smaller ring thioether macrocycles. These complexes were found to be susceptible to dissociaton or solvolysis. In contrast, complexes with [9]aneS_3 are known to be very stable and resistant to such processes. It is highly likely that the stability of the macrocyclic complexes is a function of the macrocycle size – in the case of [9]aneS_2Te, the apparently stable complexes are probably due to the macrocycle possessing an optimal ring size for *fac*-coordination. In the case of [12]aneS_2Te, however, the much larger ring probably leads to complexes where ring strain lowers the complex stability.

Table 2.6 - Crystallographic parameters[a]

	[11]aneS$_2$Te	**[12]aneS$_2$Te**	**1-thia-4-telluracyclohexane**	**[12]aneS$_2$TeI$_2$**
Formula	$C_8H_{16}S_2Te$	$C_9H_{18}S_2Te$	C_4H_8STe	$C_9H_{18}I_2S_2Te$
M	303.93	317.96	215.76	571.77
Crystal system	orthorhombic	monoclinic	monoclinic	monoclinic
Space group	$Pna2_1$	$P2_1$	$P2_1/n$	$P2_1/c$
a/Å	15.3529(4)	7.7448(3)	7.020(2)	10.4800(3)
b/Å	12.6938(3)	5.5407(3)	5.6344(15)	8.5703(3)
c/Å	5.50550(10)	13.7720(4)	8.009(3)	16.6779(5)
β/°	90	94.666(2)	93.635(10)	94.309(2)
U/Å^3	1072.95(4)	589.02(4)	316.13(16)	1493.72(7)
Z	4	2	2	4
μ(Mo-Kα)/mm^{-1}	3.104	2.832	4.899	6.375
Unique reflections	1452	1479	706	3494
Obs. reflections [I>2σ(I)]	1251	1437	650	2701
R	0.0340[a]	0.0315[a]	0.0266[b]	0.0563[a]
R_w	0.0410[a]	0.0380[a]	0.0683[b]	0.0700[a]

[a] $R = \sum (|F_{obs}|_i - |F_{calc}|_i)/\sum |F_{obs}|_i$; $R_w = \sqrt{[\sum w_i(|F_{obs}|_i - |F_{calc}|_i)^2/\sum w_i|F_{obs}|_i^2}$.

[b] R_1 ($I > 2\sigma(I)$); wR_2 ($I > 2\sigma(I)$) from SHELXL-97.[74] ($R_1 = \Sigma \; | \; |F_o| - |F_c| \; |_i \; / \; \Sigma |F_o|$; $wR_2 = [\Sigma_w(F_o^2 - F_c^2)^2 \; / \; \Sigma \; wF_{oi}^4]^{1/2}$)

2.6 Experimental

The compounds $Cl(CH_2)_2S(CH_2)_2S(CH_2)_2Cl$,[47] $Cl(CH_2)_3S(CH_2)_2S(CH_2)_3Cl$,[47] $Cl(CH_2)_3S(CH_2)_3S(CH_2)_3Cl$,[47] $[Mo(CO)_4(nbd)]$,[58] $[Rh(cp^*)Cl_2]_2$[65] and $[Cu(MeCN)_4][BF_4]$[73] were synthesised according to the literature procedures.

[11]aneS_2Te[44]

Procedure modified from the literature method.[44] Ammonia (600 cm^3) was condensed in a 1L flask at -78°C. Sodium metal (1.5g, 65 mmol) was added slowly, followed by freshly ground tellurium powder (3.87g, 30 mmol). The mixture was allowed to warm to the boiling point of ammonia until a white precipitate of Na_2Te was observed. The mixture was then re-cooled (-78°C) and a solution of $Cl(CH_2)_3S(CH_2)_2S(CH_2)_3Cl$ (7.03g, 30 mmol) in dry thf (*ca.* 100 cm^3) added slowly over a period of *ca.* 15 minutes. The mixture was allowed to warm to room temperature overnight and the ammonia boil off. The red-brown mixture was hydrolysed with water (150 cm^3) and extracted with CH_2Cl_2 (2 × 125 cm^3) and the combined organic extracts dried over anhydrous $MgSO_4$. Filtration and removal of the solvent *in vacuo* gave an orange/red waxy solid. Crude yield 79%. The crude product was purified by flash column chromatography on silica in two batches using hexane : ethyl acetate 3 : 1 as eluent to give the pure macrocycle as a pale yellow solid. Total yield 3.25g (35%). ^1H, ^{13}C-{^1H} and ^{125}Te-{^1H} NMR: see text. EIMS: found *m/z* = 306, 204; calculated for $[C_8H_{16}S_2{}^{130}Te]^+$ 306, calculated for $[C_3H_6S^{130}Te]^+$ 204. IR ν/cm^{-1} (thin film): 2963m, 2915m, 2847w, 1435s, 1414s, 1337w, 1289m, 1268m, 1246m, 1199s, 1102w, 1037w, 902w, 853w, 811m, 737w, 702m, 688m, 568w, 515w, 321w, 312w, 221w.

[12]aneS_2Te[44]

Procedure modified from the literature method.[44] Ammonia (600 cm^3) was condensed in a 1L flask at -78°C. Sodium metal (1.4g, 61 mmol) was added slowly, followed by freshly ground tellurium powder (1.89g, 15 mmol). The mixture was allowed to warm to the boiling point of ammonia until a white precipitate of Na_2Te was observed. The mixture was then re-cooled (-78°C) and a solution of $Cl(CH_2)_3S(CH_2)_3S(CH_2)_3Cl$ (3.86g,

15 mmol) in dry thf (*ca.* 100 cm^3) added slowly over a period of *ca.* 15 minutes. The mixture was allowed to warm to room temperature overnight and the ammonia boil off. The red-brown mixture was hydrolysed with water (150 cm^3) and extracted with CH_2Cl_2 (2 × 125 cm^3) and the combined organic extracts dried over anhydrous $MgSO_4$. Filtration and removal of the solvent gave a red oily solid. Crude yield 3.21g, 68%. The crude product was purified by flash column chromatography on silica using hexane : ethyl acetate 3 : 1 as eluent to give the pure macrocycle as a waxy orange solid, yield 1.53g, 33%. ^{1}H, ^{13}C-{^{1}H} and ^{125}Te-{^{1}H} NMR: see text. EIMS: found *m/z* = 320, 246, 204; calculated for $[C_9H_{18}S_2{}^{130}Te]^+$ 320, calculated for $[C_6H_{12}S{}^{130}Te]^+$ 246, calculated for $[C_3H_6S{}^{130}Te]^+$ 204. IR ν/cm^{-1} (thin film): 2958m, 2921m, 2851w, 1437s, 1414s, 1375w, 1338w, 1289m, 1260m, 1201m, 1174w, 1098s, 1021s, 800s, 754w, 693w, 519w, 500w, 395m.

[9]aneS$_2$Te/1-thia-4-telluracyclohexane

Ammonia (600 cm^3) was condensed in a 1L flask at -78°C and freshly cut Na (1.113g, 48 mmol) added over the course of several minutes to give a deep blue solution. Freshly ground Te powder (3.089g, 24 mmol) was added and the mixture allowed to warm until a blue solution with a white precipitate of Na_2Te was observed. The solution was re-cooled to -45°C and $Cl(CH_2)_2S(CH_2)_2S(CH_2)_2Cl$ (5.307g, 24 mmol) in thf (100 cm^3) added dropwise over 30 minutes to give a deep red solution. The reaction was allowed to slowly warm to room temperature and the ammonia boil off overnight to produce a red/brown mixture with a large amount of solid. This was hydrolysed (*ca.* 150 cm^3) and extracted with CH_2Cl_2 (*ca.* 800 cm^3) and the extracts transferred *via* cannula into a vessel containing $MgSO_4$. Some undissolved solid (very insoluble in CH_2Cl_2) was separated from the $MgSO_4$ and kept aside (0.751g). The remaining orange solution, after filtration, was concentrated (*ca.* 400 cm^3) and MeOH (*ca.* 50 cm^3) added before chilling at -18°C overnight. The resultant precipitate was filtered off and dried *in vacuo* to give a first crop of product (0.913g). The filtrate was concentrated further (*ca.* 300 cm^3), MeOH (*ca.* 50 cm^3) added and the mixture chilled at -18°C once more to produce a second crop of product that was subsequently filtered and dried *in vacuo* (0.414g). The pale yellow filtrate was left to slowly evaporate to produce a crop of orange crystals (largely 1-thia-4-

telluracyclohexane) that were suitable for X-ray diffraction studies (0.775g). Pure [9]aneS_2Te was obtained from the recrystallisation of crop 1 (0.913g) from CH_2Cl_2/hexane to give a pale orange solid (0.297g). The solid obtained from the remaining mother liquor was found to be a mixture of [9]aneS_2Te and 1-thia-4-telluracyclohexane (0.4057g). Crop 2 (0.414g) was likewise a mixture.

[9]aneS_2Te: yield 18%. Calc. for [$C_6H_{12}S_2Te$]: C, 26.1; H, 4.4%. Found C, 25.8; H, 3.9%. EIMS: found *m/z* = 278, 250, 222, 190; calculated for [$C_6H_{12}S_2{}^{130}Te]^+$ 278, calculated for [$C_4H_8S_2{}^{130}Te]^+$ 250, calculated for [$C_2H_4S_2{}^{130}Te]^+$ 222, calculated for [$C_2H_4S^{130}Te]^+$ 190. IR ν/cm^{-1} (CsI disk): 2966w, 2927m, 1423s, 1358m, 1261w, 1201m, 1138s, 1099s, 1022w, 869w, 834w, 803w, 713w, 676m, 613w, 575w, 550w, 318w, 309w, 300w, 246m, 223w.

1-thia-4-telluracyclohexane: yield 15%. GC-EIMS: found *m/z* = 218, 190, 162; calculated for [$C_4H_8S^{130}Te]^+$ 218, calculated for [$C_2H_4S^{130}Te]^+$ 190, calculated for [$S^{130}Te]^+$ 162. EIMS: found *m/z* = 218, 190, 162, 120; calculated for [$C_4H_8S^{130}Te]^+$ 218, calculated for [$C_2H_4S^{130}Te]^+$ 190, calculated for [$S^{130}Te]^+$ 162, calculated for [1,4-dithiane]$^+$ 120. IR ν/cm^{-1} (CsI disk): 2960w, 2921w, 2858w, 1458w, 1406m, 1365m, 1292w, 1263m, 1249m, 1216m, 1159w, 1111m, 992m, 905m, 849w, 821m, 663w, 630m, 509m, 419w, 294w, 224w, 221w.

1-thia-4-telluracyclohexanemethiodide

1-Thia-4-telluracyclohexane (0.145g, 0.672 mmol) was stirred with MeI (*ca.* 1 cm^3, excess) in CH_2Cl_2 for 1 hour and the resultant pale cream-yellow precipitate filtered off, washed with Et_2O and dried *in vacuo*. Yield 0.163g, 68%. Calc. for [$C_5H_{11}ISTe$]: C, 16.8; H, 3.1%. Found: C, 17.5; H, 2.7%. ESMS: found *m/z* = 233, 173; calculated for [$C_5H_{11}S^{130}Te]^+$ 233, calculated for [$CH_2CH_2{}^{130}TeMe]^+$ 173. ^{1}H NMR (d_6-dmso): δ 2.15 (s, TeCH_3), 2.8 – 3.1 (m). ^{13}C-{^{1}H} NMR (d_6-dmso): δ 24.0, 20.1 (CH_2), 1.9 (TeCH_3). ^{125}Te-{^{1}H} NMR (d_6-dmso): δ 434.

[9]aneS$_2$TeMeI

Method as above giving an orange solid. Yield 72%. Calc. for [$C_7H_{15}IS_2Te$]: C, 20.1; H, 3.6%. Found: C, 19.8; H, 3.4%. ^{1}H NMR (d_6-dmso): δ 2.2 (s, Te*Me*), 2.7 – 3.29 (m, CH_2S and CH_2Te). ^{13}C-{^{1}H} NMR (CH_2Cl_2-$CDCl_3$): δ 32.8, 32.4 (*C*H_2S), 28.8 (*C*H_2Te), 7.5 (Te*Me*). ^{125}Te-{^{1}H} NMR (CH_2Cl_2-$CDCl_3$): δ 419.

[11]aneS$_2$TeMeI

To a solution of [11]aneS$_2$Te (0.120g, 0.494 mmol) in CH_2Cl_2 (30 cm^3) was added MeI (1cm^3, excess). The solution was stirred and gently refluxed for one hour, allowed to cool, concentrated (*ca.* 10 cm^3) and pipetted into ice-cold Et_2O. The resultant precipitate was filtered, washed with Et_2O and dried *in vacuo* to produce a white solid that darkened to a red-brown colour and became sticky soon after isolation. The solid was kept under nitrogen in the freezer to avoid decomposition. Yield 0.159g, 72%. Calc. for [$C_9H_{19}IS_2Te$]: C, 24.2; H, 4.3%. Found C, 23.9; H, 3.9%. ESMS: found *m/z* = 321; calculated for [[11]aneS$_2$^{130}TeMe]$^+$ 321. ^{1}H NMR (d_6-dmso): δ 2.90 – 2.65 (m, S*C*H_2, 8H), 2.50 (t, Te*C*H_2, 4H), 2.13 (s, Te*Me*, 3H), 2.11 (m, SCH_2C*H*$_2$$CH_2Te$, 4H). ^{13}C-{^{1}H} NMR (d_6-dmso): δ 33.9, 33.2 (S*C*H_2), 25.5, 24.9 (Te*C*H_2, CH_2*C*H_2CH_2), 9.2 (Te*Me*). ^{125}Te-{^{1}H} NMR (d_6-dmso): δ 542.

[12]aneS$_2$TeMeI

This was prepared similarly, using [12]aneS$_2$Te (0.117g, 0.315 mmol) and MeI (1cm^3, excess) to give a white solid which also darkened and became sticky soon after isolation. The product was also stored at -18°C to avoid decomposition. Yield 0.132g, 91%). Calc. for [$C_{10}H_{21}IS_2Te$].CH_2Cl_2: C, 24.2; H, 4.2%. Found: C, 24.5; H, 4.2%. ESMS: found *m/z* = 335; calculated for [[12]aneS$_2$^{130}Te]$^+$ 335. ^{1}H NMR (d_6-dmso): δ 2.95 – 2.72 (m, S*C*H_2, 8H), 2.60 (t, Te*C*H_2, 4H), 2.13 (s, Te*Me*, 3H), 2.00 (m, SCH_2C*H*$_2$$CH_2Te$, 4H), 1.78 (quin., SCH_2C*H*$_2$$CH_2S$, 2H). ^{13}C-{^{1}H} NMR (d_6-dmso): δ 33.7, 29.6 (S*C*H_2), 28.3 (SCH_2*C*H_2CH_2S), 24.0 ($TeCH_2$*C*H_2CH_2S), 20.4 (Te*C*H_2), 4.5 (Te*Me*). ^{125}Te-{^{1}H} NMR (d_6-dmso): δ 543.

[12]aneS$_2$TeI$_2$

I_2 (0.056g, 0.22 mmol) was dissolved in THF (*ca.* 30 cm^3) and [12]aneS$_2$Te (0.070g, 0.22 mmol) in CH_2Cl_2 (*ca.* 10 cm^3) added. The reaction was stirred in a foil-wrapped vessel for two hours, concentrated to half volume and Et_2O added to produce a brick red precipitate that was filtered, washed with Et_2O and dried *in vacuo*. Yield 0.104g, 83%. Calc. for $[C_9H_{18}I_2S_2Te].1/4thf$: C, 20.4; H, 3.5%. Found: C, 20.7; H, 4.7%. ESMS: found *m/z* = 447; calculated for [[12]aneS$_2$^{130}TeI]$^+$ 447. ^{1}H NMR ($CDCl_3$): δ 3.6 (t, TeC*H*$_2$), 2.75 (t, SC*H*$_2$), 2.62 (t, SC*H*$_2$), 2.40 (m, TeCH$_2$C*H*$_2$CH$_2$), 1.80 (quin., SCH$_2$C*H*$_2$CH$_2$). IR ν/cm^{-1} (CsI disk): 2932w, 2923w, 2858w, 1428m, 1412m, 1359s, 1246w, 1107m, 1067m, 997w, 959w, 835w, 729w, 661w, 541w, 510w, 393w, 311w, 244w, 224w.

[11]aneS$_2$TeI$_2$

Procedure as above, using I_2 (0.353g, 1.39 mmol) and [11]aneS$_2$Te (0.423g, 1.39 mmol). Yield 0.582g, 75%. Calc. for $[C_8H_{16}I_2S_2Te].CH_2Cl_2$: C, 16.8; H, 2.8%. Found: C, 17.2; H, 2.9%. ESMS: found *m/z* = 433; calculated for [[11]aneS$_2$^{130}TeI]$^+$ 433. ^{1}H NMR ($CDCl_3$): δ 3.50 (t, TeC*H*$_2$), 2.85 – 3.02 (m, SC*H*$_2$), 2.63 (m, CH$_2$C*H*$_2$CH$_2$). IR ν/cm^{-1} (CsI disk): 2963w, 2908w, 1428m, 1414m, 1400w, 1358s, 1261m, 1223w, 1205w, 1120m, 1096m, 1020w, 970w, 887w, 804m, 705w, 508w, 394w, 311w, 300w, 247w, 223w.

[Mn(CO)$_3$([9]aneS$_2$Te)][CF$_3$SO$_3$]

[Mn(CO)$_5$Cl] (0.063g, 0.27 mmol) and $AgCF_3SO_3$ (0.070g, 0.27 mmol) were refluxed in degassed acetone in a foil-wrapped vessel for one hour before being allowed to cool. The solution was then filtered to remove the AgCl precipitate and added to a solution of [9]aneS$_2$Te (0.075g, 0.27 mmol) in CH_2Cl_2 (*ca.* 100 cm^3). The solution was stirred in the dark for 20 hours, by which time solution IR spectroscopy indicated reaction completeness. The mixture was filtered to remove a small amount of insoluble material and the resulting clear yellow solution was concentrated (5 cm^3) and Et_2O added to produce a yellow/fawn precipitate. This was filtered and dried *in vacuo*. Yield 0.081g, 53%. Calc. for $[C_7H_{12}F_3MnO_6S_3Te].1/3Me_2CO$: C, 22.7; H, 2.4%. Found: C, 22.9; H,

2.3%. ^{1}H NMR (CD_2Cl_2): δ 2.4 – 3.5 (br, m). ^{125}Te-{^{1}H} NMR (CD_2Cl_2): δ 214 (br s). ^{55}Mn NMR (CD_2Cl_2): δ -821. IR ν(CO)/cm^{-1} (CsI disk): 2042s, 1963s br.

[Mn(CO)$_3$([11]aneS_2Te)][CF_3SO_3]

[Mn(CO)$_5$Cl] (0.038g, 0.165 mmol) and $AgCF_3SO_3$ (0.043g, 0.167 mmol) were refluxed in degassed acetone (*ca.* 20 cm^3) for 1 hour to form the *in situ* intermediate [Mn(CO)$_3$(Me_2CO)$_3$][CF_3SO_3]. The clear yellow solution was filtered to remove the AgCl precipitate and transferred into a vessel containing [11]aneS_2Te (0.051g, 0.166 mmol) in CH_2Cl_2 (10 cm^3). The reaction mixture was stirred for 20 hours at room temperature, after which time solution IR spectroscopy indicated reaction completeness. The solvent volume was reduced (*ca.* 10 cm^3) and the concentrate injected into ice-cold Et_2O. The precipitate generated was filtered and dried *in vacuo* to give a yellow solid, yield 0.083g, 85%. Calc. for [$C_{12}H_{16}F_3MnO_6S_3Te$]: C, 24.4; H, 2.7%. Found: C, 23.7; H, 2.9%. ESMS: found *m/z* = 443; calculated for [Mn(CO)$_3$([11]aneS_2^{130}Te)]$^+$ 445. ^{1}H NMR (d_6-Me_2CO): δ 2.0 – 3.5 (br m). ^{125}Te-{^{1}H} NMR (d_6-Me_2CO): δ 110 (br s). ^{55}Mn NMR (d_6-Me_2CO): δ -817. IR ν(CO)/cm^{-1} (CsI disk): 2033s, 1950s br; (CH_2Cl_2): 2034s, 1952s br.

[Mn(CO)$_3$([12]aneS_2Te)][CF_3SO_3]

The reaction was carried out similarly, except [12]aneS_2Te (0.071g, 0.225 mmol) in CH_2Cl_2 (*ca.* 10 cm^3) was added to a solution of [Mn(CO)$_3$(Me_2CO)$_3$][CF_3SO_3] generated from [Mn(CO)$_5$Cl] (0.0517g, 0.225 mmol) and $AgCF_3SO_3$ (0.058g, 0.225 mmol). After 20 hours, solution IR spectroscopy indicated a possible mixture of products/isomers. The solvent volume was reduced (*ca.* 10 cm^3) and Et_2O (*ca.* 5 cm^3) added to produce a yellow solid that was filtered and dried *in vacuo*. Yield 0.035g, 28%. Calc. for [$C_{13}H_{18}F_3MnO_6S_3Te$].$CH_2Cl_2$: C, 24.3; H, 2.9%. Found: C, 24.1; H, 2.6%. ESMS: found *m/z* = 459; calculated for [Mn(CO)$_3$([12]aneS_2^{130}Te)]$^+$ 459. ^{1}H NMR (d_6-Me_2CO): δ 1.9 – 3.6 (br m). IR ν(CO)/cm^{-1} (CsI disk): 2028s, 1945s br.

[Mo(CO)$_4$([11]aneS$_2$Te)]

To a solution of [Mo(CO)$_4$(nbd)] (0.148g, 0.493 mmol) in CH_2Cl_2 (40 cm^3) was added a solution of [11]aneS$_2$Te (0.149g, 0.49 mmol) in CH_2Cl_2 (*ca.* 10 cm^3). The reaction was stirred at room temperature overnight, by which time solution IR spectroscopy indicated reaction completeness. The solution was then concentrated (*ca.* 10 cm^3) and a brown solid precipitated by the addition of hexane. This was filtered off and dried *in vacuo*. Yield 0.042g, 17%. Calc. for [$C_{12}H_{16}MoO_4S_2Te$]: C, 28.2; H, 3.2%. Found: C, 28.3; H, 3.3%. ^{1}H NMR (d$_6$-Me_2CO): δ 2.6 – 3.2 (br m). ^{125}Te-{^{1}H} NMR (d$_6$-Me_2CO): δ 282. IR ν(CO)/cm^{-1} (CsI disk): 2021s, 1900s br, 1846s.

[PdCl$_2$([12]aneS$_2$Te)]

[$PdCl_2(NCMe)_2$] (0.079g, 0.303 mmol) was dissolved in CH_2Cl_2 (*ca.* 40 cm^3) and [12]aneS$_2$Te (0.096g, 0.303 mmol) in CH_2Cl_2 (10 cm^3) added. The solution was stirred at room temperature for two hours, followed by the addition of Et_2O (*ca.* 10 cm^3) to produce a yellow precipitate that was washed with Et_2O, filtered and dried *in vacuo*. Yield 0.090g, 60%. Calc. for [$C_9H_{18}Cl_2PdS_2Te$].2CH_2Cl_2: C, 19.9; H, 3.3%. Found: C, 19.4; H, 3.0%. ^{1}H NMR (d$_6$-dmso): δ 2.0 – 3.5 (br m). ^{125}Te-{^{1}H} NMR (CH_2Cl_2-$CDCl_3$): δ 387. IR ν/cm^{-1} (CsI disk): 2962w, 2938w, 2921w, 1480w, 1430sh, 1416m, 1356m, 1341m, 1290w, 1256m, 1245m, 1229w, 1207m, 1134w, 1107m, 1085w, 1013w, 853w, 782w, 721m, 616w, 352m, 300w.

PdCl$_2$([11]aneS$_2$Te)]

The reaction was carried out as above using [$PdCl_2(NCMe)_2$] (0.066g, 0.254 mmol) and [11]aneS$_2$Te (0.0773g, 0.254 mmol). The solution was filtered after stirring for two hours at room temperature in order to remove a small amount of brown solid, and the remaining clear yellow solution reduced in volume (*ca.* 10 cm^3). Et_2O (*ca.* 10 cm^3) was added to the concentrate and the mixture chilled at -18°C to form a yellow precipitate that was subsequently filtered, washed with Et_2O and dried *in vacuo*. Yield 0.078g, 64%. Calc. for [$C_8H_{16}Cl_2PdS_2Te$]: C, 20.0; H, 3.3%. Found: C, 19.6%; H, 3.2%. ^{1}H NMR ($CDCl_3$): δ 2.0 – 3.5 (br, m). ^{125}Te NMR (CH_2Cl_2-$CDCl_3$): δ 330. IR ν/cm^{-1} (CsI disk):

2973w, 1422m, 1361s, 1262m, 1096s, 1024m, 859w, 804m, 616w, 544w, 348w, 322w, 311w, 300w, 240w, 225w.

[PtCl$_2$([12]aneS$_2$Te)]

[PtCl$_2$(NCMe)$_2$] was generated by refluxing PtCl$_2$ (0.126g, 0.472 mmol) in MeCN (*ca.* 30 cm^3) to form a clear, yellow solution. This was allowed to cool, filtered (celite) and [12]aneS$_2$Te (0.150g, 0.472 mmol) in CH_2Cl_2 (*ca.* 10 cm^3) added *via* syringe. The mixture was stirred at room temperature for two hours and a small amount of dark material filtered off. The remaining yellow solution was concentrated (*ca.* 10 cm^3) and Et_2O added. The resultant precipitate was filtered off and dried *in vacuo* to give a bright yellow, powdery solid. Yield 0.132g, 48%. Calc. for [$C_9H_{18}Cl_2PtS_2Te$].2CH_2Cl_2: C, 17.5; H, 2.9%. Found: C, 17.1; H, 2.9%. ESMS: found *m/z* = 551; calculated for [^{195}Pt^{35}Cl([12]aneS$_2$^{130}Te)]$^+$ 550. ^{1}H NMR (d$_6$-dmso): δ 2.2 – 3.4 (br, m). ^{125}Te-{^{1}H} NMR (d$_6$-dmf): δ 374 ($^1J_{Pt\text{-}Te}$ = 1034 Hz). ^{195}Pt NMR (d$_6$-dmf): δ -3890. IR ν/cm^{-1} (CsI disk): 3032w, 2978w, 1430m, 1365m, 1307w, 1264w, 1221w, 1109m, 907w, 841w, 806w, 754w, 482w, 354w, 322m br.

[PtCl$_2$([11]aneS$_2$Te)]

The reaction was carried out similarly, using PtCl$_2$ (0.131g, 0.494 mmol) and [11]aneS$_2$Te (0.150g, 0.494 mmol). The yellow precipitate obtained after stirring at room temperature for two hours was filtered off, washed with Et_2O and dried *in vacuo*. Yield 0.092g, 33%. Calc. for [$C_8H_{16}Cl_2PtS_2Te$]: C, 16.9; H, 2.8%. Found: C, 16.9; H, 2.6%. ESMS: found *m/z* = 534; calculated for [^{195}Pt^{35}Cl([11]aneS$_2$Te)]$^+$ 536. ^{1}H NMR (d$_6$-dmso): δ 2.0 – 3.4 (br m). ^{125}Te-{^{1}H} NMR (d$_6$-dmf): δ 299 ($^1J_{Pt\text{-}Te}$ = 753 Hz). ^{195}Pt NMR (d$_6$-dmf): δ -3834. IR ν/cm^{-1} (CsI disk): 2958w, 2889w, 1410m, 1360m, 1295w, 1248m, 1154w, 1107m, 981m, 932w, 890w, 856m, 770w, 700w, 527w, 318m br.

[Rh(cp*)([9]aneS$_2$Te)][PF$_6$]$_2$

A solution of [Rh(cp*)Cl$_2$]$_2$ (0.032g, 0.05 mmol) in MeOH (*ca.* 20 cm^3) was added to [9]aneS$_2$Te (0.029g, 0.10 mmol) in CH_2Cl_2 (*ca.* 50 cm^3) and the mixture stirred at room temperature for 30 minutes. TlPF$_6$ (0.080g, 0.23 mmol) in MeOH (20 cm^3) was then added and the cloudy yellow mixture stirred for an hour at room temperature, refluxed for

30 minutes and then stirred for a further hour at room temperature. The solvent was removed and the residue taken up in acetone and filtered twice (celite) to remove the TlCl precipitate. The remaining clear orange solution was concentrated (5 cm^3) and Et_2O added to produce an orange gum that was triturated under petroleum ether to produce an orange-brown powdery solid. Yield 0.053g, 63%. Calc. for $[C_{16}H_{27}F_{12}P_2RhS_2Te].CH_2Cl_2$: C, 23.0; H, 3.3%. Found: C, 22.8; H, 3.1%. ESMS: found *m/z* = 515; calculated for $[Rh(cp^*)([9]aneS_2{}^{130}Te)]^+$ 515. ^{1}H NMR (d_6-Me_2CO): δ 3.0 – 3.7 (br m, [9]aneS$_2$Te), 1.72 (s, C_5Me_5). ^{13}C-{^{1}H} NMR (d_6-Me_2CO): 107.5 (C_5Me_5), 37.6, 32.9 (SCH_2), 24.7 (CH_2Te), 7.9 (C_5Me_5). ^{125}Te-{^{1}H} NMR (d_6-Me_2CO): δ 397 ($^1J_{Rh\text{-}Te}$ = 75Hz). IR ν/cm^{-1} (CsI disk): 2972w, 1473m, 1423m, 1382m, 1365m, 1227w, 1082m, 1024m, 838br s, 740w, 614w, 559s, 439w, 321w.

[Rh(cp*)([11]aneS$_2$Te)][PF$_6$]$_2$

$[Rh(cp^*)Cl_2]_2$ (0.055g, 0.089 mmol) was dissolved in MeOH (*ca.* 20 cm^3) and [11]aneS$_2$Te (0.054g, 0.178 mmol) added in CH_2Cl_2 (10 cm^3). $TlPF_6$ (0.137g, 0.392 mmol) was added to the solution, and the mixture stirred at room temperature overnight to form a clear orange mixture and a white precipitate of TlCl. The mixture was filtered and the solvent removed to give a residue that was then taken up in the minimum volume of acetone (*ca.* 5 cm^3), filtered again (celite) and injected into ice-cold Et_2O. The resultant precipitate was filtered and dried *in vacuo* to give a yellow solid. Yield 0.052g, 35%. Calc. for $[C_{18}H_{31}F_{12}P_2RhS_2Te].Me_2CO$: C, 28.3; H, 4.2%. Found C, 27.8; H, 3.7%. ESMS: found *m/z* = 689, 272; calculated for $[Rh(cp^*)([11]aneS_2{}^{130}Te)PF_6]^+$ 689, calculated for $[Rh(cp^*)([11]aneS_2Te)]^{2+}$ 272. ^{1}H NMR (d_6-Me_2CO): δ 2.5 –3.6 (br m, [11]aneS$_2$Te), 1.78 (s, cp*). ^{13}C-{^{1}H} NMR (d_6-Me_2CO): δ 106.4 (C_5Me_5), 37.0, 32.9, 32.7 (CH_2S and $CH_2CH_2CH_2$), 24.6 (CH_2Te), 8.5 (C_5Me_5). ^{125}Te-{^{1}H} NMR (d_6-Me_2CO): δ 282 ($^1J_{Rh\text{-}Te}$ = 106 Hz). IR ν/cm^{-1} (CsI disk): 3009w, 2976w, 1357m, 1261w, 1094m br, 997w, 835s, 731w, 613w, 560s, 476w, 322w.

[Rh(cp*)([12]aneS$_2$Te)][PF$_6$]$_2$

The reaction was carried out similarly, using $[Rh(cp^*)Cl_2]_2$ (0.113g, 0.184 mmol), [12]aneS$_2$Te (0.117g, 0.369 mmol) and $TlPF_6$ (0.567g, 0.811 mmol) to produce a yellow-

orange solid. Yield 0.131g, 42%. Calc. for $[C_{19}H_{33}F_{12}P_2RhS_2Te].Me_2CO$: C, 27.0; H, 3.9%. Found: C, 26.8; H, 3.7%. ESMS: found *m/z* = 701, 279; calculated for $[Rh(cp^*)([11]aneS_2{}^{130}Te)PF_6]^+$ 703, calculated for $[Rh(cp^*)([11]aneS_2{}^{130}Te)]^{2+}$ 279. ^{1}H NMR (d_6-Me_2CO): δ 2.6 – 3.5 (br, m, [11]aneS$_2$Te), 1.73 (s, cp^*). ^{13}C-{^{1}H} NMR (d_6-Me_2CO): δ 106.7 (C_5Me_5), 34.0, 33.2, 32.3 (SCH_2 and $SCH_2CH_2CH_2Te$), 27.1 ($SCH_2CH_2CH_2S$), 25.6 (CH_2Te), 8.7 (C_5Me_5). ^{125}Te-{^{1}H} NMR (d_6-Me_2CO): δ 275 ($^1J_{Rh\text{-}Te}$ = 102 Hz). IR ν/cm^{-1} (CsI disk): 2980w, 1481w, 1355m, 1260w, 1093m br, 1022w, 997w, 840s, 733w, 611w, 558s, 436w, 322w.

[Ag([11]aneS$_2$Te)][CF$_3$SO$_3$]

$AgCF_3SO_3$ (0.025g, 0.097 mmol) was added to a solution of [11]aneS$_2$Te (0.029g, 0.097 mmol) in CH_2Cl_2 (*ca.* 30 cm^3) and the reaction stirred for 1 hour. The resultant light yellow precipitate was filtered off, washed with Et_2O and dried *in vacuo*. Yield 0.030g, 63%. Calc. for $C_9H_{16}AgF_3O_3S_3Te$: C, 19.3; H, 2.9%. Found: C, 19.5; H, 3.0%. ESMS: found *m/z* = 717, 454, 413; calculated for $[^{107}Ag([11]aneS_2{}^{130}Te)_2]^+$ 719, calculated for $[^{107}Ag([11]aneS_2{}^{130}Te)MeCN]^+$ 454, calculated for $[^{107}Ag([11]aneS_2{}^{130}Te)]^+$ 413. ^{1}H NMR ($CDCl_3$): δ 2.2 (br, $TeCH_2CH_2CH_2S$), 2.7 (br, $TeCH_2$), 2.8 – 3.2 (m, SCH_2). IR ν/cm^{-1} (CsI disk): 2959w, 2948w, 1364m, 1263s, 1155m, 1098m, 1030m, 834w, 797w, 668w, 636m, 572w, 517w.

[Ag([9]aneS$_2$Te)][CF$_3$SO$_3$]

Method as above, but using [9]aneS$_2$Te to give a light yellow solid. Yield 60%. Calc. for $[C_7H_{12}AgF_3O_3S_3Te]$: C, 15.2; H, 2.3. Found: C, 15.4; H, 2.2%. ESMS: found *m/z* = 661, 382; calculated for $[^{107}Ag([9]aneS_2{}^{130}Te)_2]^+$ 663, $[^{107}Ag([9]aneS_2{}^{130}Te)]^+$ 385. ^{1}H NMR ($CDCl_3$): δ 2.2 (br, $TeCH_2$), 2.9 – 3.1 (m, SCH_2). IR ν/cm^{-1} (CsI disk): 2962w, 2946w, 1360s, 1263m, 1242w, 1150sh, 1096br s, 986m, 850w, 834w, 636m, 538w.

[Ag([12]aneS$_2$Te)][CF$_3$SO$_3$]

Method as above, but using [12]aneS$_2$Te to give a light yellow solid which decomposed rapidly giving a black sold. Yield 38%. Analysis: see text. ESMS: found *m/z* = 745, 427; calculated for $[^{107}Ag([12]aneS_2{}^{130}Te)_2]^+$ 747, calculated for $[^{107}Ag([12]aneS_2Te)]^+$

427. ^{1}H NMR ($CDCl_3$): δ 1.8 (br, $SCH_2CH_2CH_2S$), 2.1 (br, $TeCH_2CH_2CH_2S$), 2.4 – 3.0 (m, SCH_2, $TeCH_2$). IR ν/cm^{-1} (CsI disk): 2965w, 2945w, 1359s, 1275s, 1154m, 1090m, 1032m, 970w, 637m, 510w, 482w.

[Ag([12]aneS_2Te)][BF_4]

[12]aneS_2Te (0.141g, 0.444 mmol) and $AgBF_4$ (0.086g, 0.444 mmol) were stirred in CH_2Cl_2 (*ca.* 40 cm^3) in a foil-wrapped vessel for 1 hour at room temperature. The solution was then concentrated (*ca.* 10 cm^3) and injected into ice-cold Et_2O to form a creamy-yellow solid that was filtered and dried *in vacuo*. Yield 0.043g, 19%. Calc. for [$C_9H_{18}AgBF_4S_2Te$]: C, 21.1; H, 3.5%. Found: C, 20.8; H, 3.3%. ESMS: found *m/z* = 745, 427; calculated for [^{107}Ag([12]aneS_2^{130}Te)$_2$]$^+$ 747, calculated for [^{107}Ag([12]aneS_2^{130}Te)]$^+$ 427. ^{1}H NMR ($CDCl_3$): δ 1.8 (br, $SCH_2CH_2CH_2S$), 2.0 (br $TeCH_2CH_2CH_2S$), 2.55 – 2.95 (br, SCH_2, $TeCH_2$). IR ν/cm^{-1} (CsI disk): 2921m, 2843w, 1438, 1344m, 1291m, 1245m, 1209m, 1062br s, 768w, 729m, 667w, 520s.

[Cu([11]aneS_2Te)][BF_4]

[Cu(MeCN)$_4$][BF_4] (0.155g, 0.494 mmol) and [11]aneS_2Te (0.150g, 0.494 mmol) were stirred in MeOH (30 cm^3) and CH_2Cl_2 (*ca.* 10 cm^3) added to aid dissolution of the ligand. The solution was stirred at room temperature for two hours, concentrated (*ca.* 5 cm^3) and injected into ice-cold Et_2O to produce a cream solid that was filtered off and dried *in vacuo*. Yield 0.122g, 51%. Calc. for [$C_8H_{16}BCuF_4S_2Te$]: C, 21.2; H, 3.6%. Found: C, 21.3; H, 3.3%. ESMS: found *m/z* = 673, 410, 369; calculated for [^{63}Cu([11]aneS_2^{130}Te)$_2$]$^+$ 673, calculated for [^{63}Cu([11]aneS_2^{130}Te)MeCN]$^+$ 410, calculated for [^{63}Cu([11]aneS_2^{130}Te)]$^+$ 369. ^{1}H NMR (CD_3NO_2): δ 2.2 – 3.5 (br m, [11]aneS_2Te). IR ν/cm^{-1} (CsI disk): 2973w, 1437m, 1419m, 1356m, 1287w, 1250w, 1209w, 1060vs br, 913w, 839w, 736w, 521m, 223w.

[Cu([12]aneS_2Te)][BF_4]

The reaction was carried out similarly, using [12]aneS_2Te (0.098g, 0.315 mmol) and [Cu(MeCN)$_4$][BF]$_4$ (0.097g, 0.315 mmol). The reagents were stirred in CH_2Cl_2 (*ca.* 40 cm^3) for two hours and worked up similarly to produce a creamy-yellow solid. Yield

0.095g, 65%. Calc. for [$C_9H_{18}BCuF_4S_2Te$]: C, 23.1; H, 3.9%. Found: C, 22.5; H, 4.0%. ESMS: found *m/z* = 701, 424, 383; calculated for [^{63}Cu([12]aneS_2^{130}Te)$_2$]$^+$ 701, calculated for [^{63}Cu([12]aneS_2^{130}Te)MeCN]$^+$ 424, calculated for [^{63}Cu([12]aneS_2Te)]$^+$ 383. ^{1}H NMR ($CDCl_3$): δ 2.98 (br, SC*H*$_2$), 2.80 (m, TeC*H*$_2$), 2.10 (br, $CH_2CH_2CH_2$). IR ν/cm^{-1} (CsI disk): 2962w, 2926w, 1436m, 1355m, 1285m, 1251w, 1066br s, 905w, 847m, 824w, 804w, 763w, 519s.

X-ray crystallography

Details of the crystallographic data parameters are given in Table 2.2. Data were collected by Melissa Matthews, using a Nonius Kappa CCD diffractometer equipped with an Oxford Systems open-flow crysostat operating at 120K, with graphite-monochromated Mo-K$_\alpha$ X-radiation (λ = 0.71073 Å). Structure solution and refinement were routine except in the case of 1-thia-4-telluracyclohexane, which crystallises in space group *P*2$_1$/*n* with Z = 2 and the 6-membered ring disordered across a crystallographic inversion centre. Refinement used a 50:50 split occupancy for the S and Te atoms.[75-78] Selected bond lengths and angles are quoted in Tables 2.1, 2.2 and 2.3.

2.7 References

1. W. Levason, S. D. Orchard and G. Reid, *Organometallics*, 1999, **18**, 1275.
2. G. T. Morgan and H. Burgess, *J. Chem. Soc.*, 1928, 321.
3. G. T. Morgan and F. H. Burstall, *J. Chem. Soc.*, 1931, 180.
4. W. V. Farrar and J. M. Gulland, *J. Chem. Soc.*, 1945, 11.
5. E. G. Hope, T. Kemmitt and W. Levason, *Organometallics*, 1988, **7**, 78.
6. P. C. Srivastava, S. Bajpai, R. Lath and R. J. Butcher, *J. Organomet. Chem.*, 2000, **608**, 96.
7. T. N. Srivastava, R. C. Srivastava, H. B. Singh and M. Singh, *Ind. J. Chem., Sect. A*, 1979, **18A**, 367.
8. A. Z. Al-Rubaie, H. A. Y. AL-Shirayda, P. Granger and S. Chapelle, *J. Organomet. Chem.*, 1985, **287**, 321.
9. A. Z. AL-Rubaie, H. A. AL-Shirayda and A. I. Auoob, *J. Organomet. Chem.*, 1988, **356**, 49.
10. C. L. Raston, R. J. Secomb and A. H. White, *J. Chem. Soc., Dalton Trans.*, 1976, 2307.
11. T. Kemmitt, W. Levason, R. D. Oldroyd and M. Webster, *Polyhedron*, 1992, **11**, 2165.
12. W. Farrar and J. Gulland, *J. Chem. Soc.*, 1945, 11.
13. A. Z. AL-Rubaie, H. A. AL-Shirayda and A. I. Auoob, *Inorg. Chim. Acta*, 1987, **134**, 139.
14. J. D. McCullough, *Inorg. Chem.*, 1965, **4**, 862.
15. C. Knobler, J. D. McCullough and H. Hope, *Inorg. Chem.*, 1970, **9**, 797.
16. A. K. Singh, M. Kadarkaraisamy, S. Husebye and K. W. Tornroos, *J. Chem. Res., (S)*, 2000, 64.
17. R. F. Ziolo and W. H. H. Gunther, *J. Organomet. Chem.*, 1978, **146**, 245.
18. W. Levason, G. Reid and V-A. Tolhurst, *J. Chem. Soc., Dalton Trans.*, 1998, 3411.
19. K. Badyal, W. R. McWhinnie, J. Homer and M. C. Perry, *J. Organomet. Chem.*, 1998, **555**, 279.
20. A. E. McCarthy and H. B. Singh, *J. Organomet. Chem.*, 1984, **275**, 57.

21. H. Campsteyn, L. Dupont, J. Lamotte-Brasseur and M. Vermeire, *J. Heterocycl. Chem.*, 1978, **15**, 745.

22. A. Z. Al-Rubaie and A. F. Hassan, *Polyhedron*, 1992, **11**, 3155.

23. A. Z. Al-Rubaie, A. Y. Al-Marzook and S. A. N. Al-Jadaan, *Rec. Trav. Chim. Pays-Bas*, 1996, **115**, 427.

24. W. Lohner and K. Praefcke, *Chem. Ber.*, 1978, **111**, 3745.

25. J. D. McCullough, *Inorg. Chem.*, 1975, **14**, 2285.

26. K. Singh, W. R. McWhinnie, H. L. Chen, M. Sun and T. A. Hamor, *J. Chem. Soc., Dalton Trans.*, 1996, 1545.

27. K. Badyal, W. R. McWhinnie, H. L. Chen and T. A. Hamor, *J. Chem. Soc., Dalton Trans.*, 1997, 1579.

28. R. T. Morrison in, *Organic Chemistry*, R. N. Boyd (ed.), 6th edn., Prentice-Hall, Englewood Cliffs, NJ, 1997, p. 446.

29. C. V. K. Sharma and G. R. Desiraju, *Perspectives in supramolecular chemistry*, in, *The Crystal as a Supramolecular Entity*, G. R. Desiraju (ed.), Wiley, Chichester, 1996.

30. H. B. Singh, P. K. Khanna and S. K. Kumar, *J. Organomet. Chem.*, 1988, **338**, 1.

31. H. A. Al-Shirayda, *Heteroat. Chem.*, 1993, **4**, 537.

32. M. Schmidt and H. Schumann, *Z. Naturforsch. B*, 1964, **19**, 74.

33. N. L. M. Dereu and R. A. Zingaro, *J. Organomet. Chem.*, 1981, **212**, 141.

34. E. A. Meyers, K. J. Irgolic, R. A. Zingaro, T. Junk, R. Chakravorty, N. L. M. Dereu, K. French and G. C. Pappalardo, *Phosphorus, Sulfur, Silicon, Relat. Elem.*, 1988, **38**, 257.

35. A. Levy, P. U. Biedermann, S. Cohen and I. Agranat, *J. Chem. Soc., Perkin Trans. II*, 2001, **12**, 2329.

36. H. Fujihara, T. Ninoi, R. Akaishi, T. Erata and N. Furukawa, *Tetrahedron Lett.*, 1991, **32**, 4537.

37. Y. Takaguchi, E. Horn and N. Furukawa, *Organometallics*, 1996, **15**, 5112.

38. S. C. Menon, H. B. Singh, R. P. Patel and S. K. Kulshreshtha, *J. Chem. Soc., Dalton Trans.*, 1996, 1203.

39. S. C. Menon, A. Panda, H. B. Singh and R. J. Butcher, *J. Chem. Soc., Chem. Commun.*, 2000, 143.

40. A. Panda, S. C. Menon, H. B. Singh and R. J. Butcher, *J. Organomet. Chem.*, 2001, **623**, 87.

41. V. W-W. Yam, Y-L. Pui, W-P. Li, K. K-W. Lo and K-K. Cheung, *J. Chem. Soc., Dalton Trans.*, 1998, 3615.

42. X. Liu, W. Li, X. Lu and H. Xu, *Chin. Chem. Lett.*, 1992, **3**, 589. (*Chem. Abs.*, 1993, **118**, 39140a).

43. H. Xu, W. Li, X. Liu, L. Shen, X. Mao and M. Li, *Huaxue Xuebao*, 1994, **52**, 386. (*Chem. Abs.*, 1994, **121**, 25539n).

44. W. Levason, S. D. Orchard and G. Reid, *J. Chem. Soc., Chem. Comm.*, 2001, 427.

45. S. D. Orchard, Ph. D. Thesis, University of Southampton, 2000.

46. D. Sellmann and L. Zapf, *Angew. Chem. Int. Ed. Engl.*, 1984, **23**, 807.

47. W. Levason, C. A. McAuliffe and S. G. Murray, *Inorg. Chim. Acta*, 1976, **17**, 247.

48. N. P. Luthra and J. D. Odom, in *The Chemistry of Organic Selenium and Tellurium Compounds*, S. Patai and Z. Rappoport (eds.), Wiley, New York, 1986, Vol. 1, Ch. 6, pp.226.

49. S. C. Rawle, G. A. Admans and S. R. Cooper, *J. Chem. Soc., Dalton Trans.*, 1988, 93.

50. N. P. Luthra and J. D. Odom, in *The Chemistry of Organic Selenium and Tellurium Compounds*, S. Patai and Z. Rappoport (eds.), Wiley, New York, 1986, Vol. 1, Ch. 6, pp.229.

51. Z-L. Zhou, Y-Z. Huang, Y. Tang, Z-H. Chen, L-P. Shi, X-L. Jin and Q-C. Yang, *Organometallics*, 1994, **13**, 1575.

52. P. Comba, A. Fath, B. Nuber and A. Peters, *J. Org. Chem.*, 1997, **62**, 8459.

53. T. S. Cameron, R. B. Amero and R. E. Cordes, *Cryst. Struct. Commun.*, 1980, **9**, 533.

54. R. Usón, V. Riera, J. Gimeno, M. Laguna and M. P. Gamasa, *J. Chem. Soc., Dalton Trans.*, 1979, 996.

55. J. Connolly, A. R. J. Genge, W. Levason, S. D. Orchard, S. J. A. Pope and G. Reid, *J. Chem. Soc., Dalton Trans.*, 1999, 2343.

56. J. W. Faller and C. Lambert, *Tetrahedron Lett.*, 1985, **41**, 5755.

57. A. J. Barton, J. Connolly, W. Levason, A. Mendia-Jalon, S. D. Orchard and G. Reid, *Polyhedron*, 2000, **19**, 1373.

58. G. R. Dobson and G. C. Faber, *Inorg. Chim. Acta*, 1970, **4**, 87.

59. A. J. Barton, W. Levason and G. Reid, *J. Organomet. Chem.*, 1999, **579**, 235.

60. F. R. Hartley, S. Murray and C. A. McAuliffe, *Inorg. Chem.*, 1979, **18**, 1394.

61. T. Kemmitt and W. Levason, *Inorg. Chem.*, 1990, **29**, 731.

62. T. Kemmitt, W. Levason and M. Webster, *Inorg. Chem.*, 1989, **28**, 692.

63. E. G. Hope, W. Levason and N. A. Powell, *Inorg. Chim. Acta*, 1986, **115**, 187.

64. C. G. Brandow, J. P. Davis, D. F. Galas, G. J. Grant, W. T. Pennington, E. J. Valente and J. D. Zubkowski, *Polyhedron*, 2001, **20**, 3333.

65. J. W. Kang, K. Mosely, and P. M. Maitlis, *J. Am. Chem. Soc.*, 1969, **91**, 5970.

66. A. J. Barton, W. Levason, G. Reid and A. J. Ward, *Organometallics*, 2001, **20**, 3644.

67. Y. Do, J. H. Jeong and H. J. Kim, *Bull. Korean Chem. Soc.*, 1992, **13**, 463.

68. A. W. Cordes, M. Draganjac, M. Green and Y. Jiang, *J. Chem. Crystallogr.*, 1999, **29**, 273.

69. D. H. Johnston and D. F. Shriver, *Inorg. Chem.*, 1993, **32**, 1045.

70. J. R. Black and W. Levason, *J. Chem. Soc., Dalton Trans.*, 1994, 3225.

71. J. R. Black, N. R. Champness, W. Levason and G. Reid, *J. Chem. Soc., Dalton Trans.*, 1995, 3439.

72. W-F. Liaw, C-H. Lai, S-J. Chiou, Y-C. Horng, C-C. Chou, M-C. Liaw, G-S. Lee and S-M. Peng, *Inorg. Chem.*, 1995, **34**, 3755.

73. G. Kubas, *Inorg. Synth.*, 1990, **28**, 68.

74. S. R. Cooper and S. C. Rawle, *Struct. Bonding (Berlin)*, 1990, **72**, 1.

75. G. M. Sheldrick, SHELXL-97, Program for refinement of crystal structures, University of Göttingen, Germany, 1997.

76. P. T. Beurskens, G. Admiraal, G. Beurskens, W. P. Bosman, S. Garcia-Granda, R. O. Gould, J. M. M. Smits and C. Smykalla, PATTY, The DIRDIF program

system, Crystallography Laboratory, University of Nijmegen, The Netherlands, 1992.

77. TeXsan: Crystal Structure Analysis Package, Molecular Structure Corporation, The Woodlands, TX, 1995.
78. H. D. Flack, *Acta Crystallogr., Sect. A*, 1983, **39**, 876.

Chapter 3:

Synthesis and Coordination Chemistry of [9]aneO$_2$Te and [18]aneO$_4$Te$_2$

3.0 Introduction

Crown ether (macrocyclic polyether) compounds containing only oxygen donors were first reported by Lüttringhaus in 1937 during a study into medium/large ring compounds,[1] and the first stable crown ether complexes with alkali metals were reported in 1967 by Pedersen.[2] It was discovered that certain crown ether compounds had an affinity for a particular alkali metal cation, this being dependent on the cavity size of the crown ether and the ionic radius of the metal ion.[2] The optimal ring size was found to be 15-18 for Na^+, 18 for K^+ and 18-21 for Cs^+.[3] The stability of the complexes were also found to be dependent upon the number of O atoms in the polyether ring, the coplanarity of the O atoms and their symmetrical placement within the ring, the basicity of the O atoms, steric hindrance in the polyether ring, the tendency of the ion to associate with the solvent and the electrical charge on the ion.[2] Subsequent studies into the separation and solubilisation of alkali metals and ion transport were undertaken.[4] For example, the crown ether compound 18-crown-6 (cavity size 2.6 – 3.2 Å) was found to form much more stable complexes with K^+ which has an ionic diameter of 2.66 Å. (log K_1' (stability constant) for the K^+ complex = 6.10 L mol^{-1}) whereas the stability constants for the Na^+ and Cs^+ complexes were 4.32 and 4.62 L mol^{-1} respectively.[3]

Further studies into crown ether compounds revealed that the replacement of one or more O donor with, for example N or S donors, reduced their affinity for alkali metal cations, but increased their affinity for transition metal ions. For example the complexation of K^+ by 18-crown-6 was found to weaken appreciably following N or S substitution for one or more of the oxygen donors, with the stability constants falling in the order of decreasing heteroatom electronegativity *i.e.* O > NR > NH > S.[3] The first transition metal complexes of crown ether compounds were reported in 1967, with stable complexes of ionic compounds of Li^+, Na^+, NH_4^+, RNH_3^+, K^+, Rb^+, Cs^+, Ag^+, Ca^{2+}, Ba^{2+}, Cd^{2+}, Hg^+, Hg^{2+}, La^{3+}, Tl^+, Ce^{3+} and Pb^{2+} reported.[2] Many other examples have been reported to date, including complexes with BF_3, $BeCl_2$, $AlCl_3$, $TiCl_4$, $CrCl_3$ and $FeBr_2$.[5]

There is a wide variety of known crown ether macrocycles having mixed S/O and Se/O donors, and some of the most relevant systems will be described here. It is only in the last 40 years or so that the chemistry of mixed S/O donor macrocycles has been

extensively studied, and the number of known compounds is now quite large. The mixed S/O donor macrocycle, 1,10-dithia-4,7,13,16-tetraoxacyclooctadecane, [18]aneO$_4$S$_2$ (Figure 3.0) was first reported in 1960 by Dann and co-workers *via* the reaction of sodium sulfide with 1,2-bis(2-chloroethoxy)ethane in H$_2$O/EtOH. The yield was fairly low due to large amounts of polymer formation.[6]

Figure 3.0 - [18]aneO$_4$S$_2$

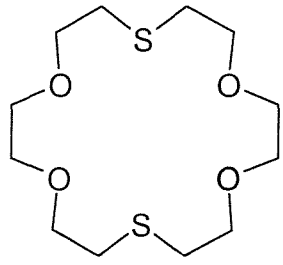

[18]aneO$_4$S$_2$

Also reported were the compounds 1-thia-4,7,10-trioxacyclododecane, 1,13-dithia-4,7,10,16,19,22-hexaoxacyclotetracosane and 1,7-dithia-4,10-dioxacyclododecane.[6] Various metal complexes of [18]aneO$_4$S$_2$ have been described, including the Pd(II) complex [Pd([18]aneO$_4$S$_2$)(NO$_3$)$_2$].[7] The crystal structure showed a square planar geometry about the metal centre, with the macrocycle coordinated to Pd(II) *via* the two sulfur donors only. Two nitrato co-ligands completed the square planar geometry, each bonding to the metal centre through an oxygen donor. The related complex [PdCl$_2$([18]aneO$_4$S$_2$)] was prepared by Metz and co-workers by the reaction of PdCl$_2$ with [18]aneO$_4$S$_2$ in acetone, and the crystal structure (Figure 3.1) showed a *cis* square planar geometry about the Pd(II) centre. As for [Pd([18]aneO$_4$S$_2$)(NO$_3$)$_2$], the macrocycle was coordinated to Pd(II) *via* the sulfur donors only.[8] The compound *cis*-[PtCl$_2$([18]aneO$_4$S$_2$)] has also been reported *via* the reaction of [18]aneO$_4$S$_2$ with K$_2$PtCl$_4$ in water, and the crystal structure is very similar to that of the Pd analogue.[9]

Figure 3.1 - Crystal structure of [PdCl$_2$([18]aneO$_4$S$_2$)][8]

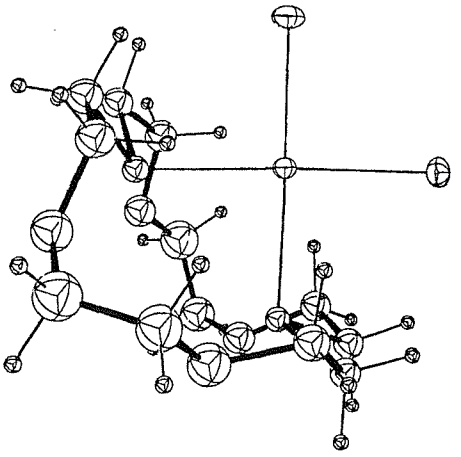

There are also many other known macrocyclic thia-oxa compounds, a number of which were reported by Bradshaw and co-workers in 1973 including the new compounds 1,4-dithia-7,10,13-trioxacyclopentadecane ([15]aneS$_2$O$_3$) (i), 1-thia-4,7-dioxacyclononane ([9]aneO$_2$S) (ii) and 1,4-dithia-7-oxacyclononane ([9]aneOS$_2$) (iii) (see Figure 3.2).[10] These were synthesised in low yields (*ca.* 5 – 30%) *via* the reactions of various oligoethylene glycol dichlorides with dithiolates or sodium sulfide, in a similar method to that used by Dann and co-workers to prepare [18]aneO$_4$S$_2$.

Figure 3.2 - 1,4-dithia-15-crown-5, 1-thia-9-crown-3 and 1,4-dithia-9-crown-3

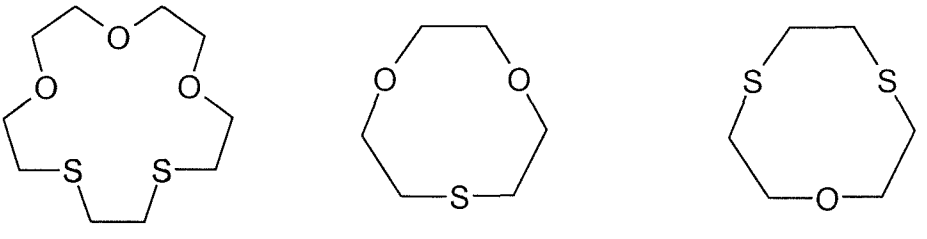

The selenium analogue, [9]aneO$_2$Se (1-selena-4,7-dioxacyclononane) has been observed as an unexpected ring contraction product of the reaction of Br(CH$_2$)$_2$O(CH$_2$)$_2$O(CH$_2$)$_2$Br,

NCSe(CH$_2$)$_2$SeCN and NaBH$_4$,[11] whilst the selenium analogue of [18]aneO$_4$S$_2$, [18]aneO$_4$Se$_2$, has also been described, although little studied.[11] There have been a number of other reports of Se/O containing macrocyclic compounds (mostly containing just one selenium atom) although studies into their coordination chemistry have been very limited.[12]

The first tellura-crown ether compound, 10-tellurabenzo-15-crown-5 (2,3-benzo-1,4,7,13-tetraoxa-10-telluracyclopentadeca-2-ene) was reported by Xu and co-workers in 1992 via the method shown in Figure 3.3.[13]

Figure 3.3 - Synthesis of 10-tellurabenzo-15-crown-5

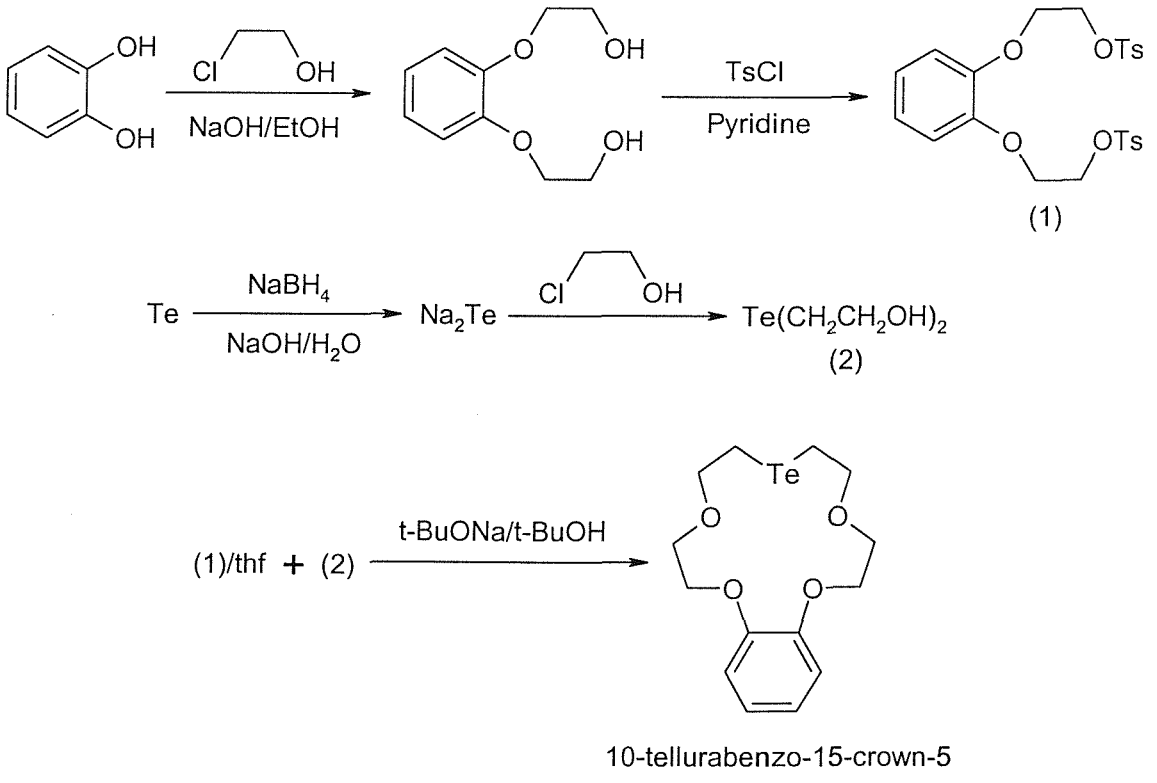

The compound was characterised by its IR spectrum, ^{1}H NMR spectroscopy and microanalysis, and reaction of two equivalents of 10-tellurabenzo-15-crown-5 (L) with K_2PtCl_4 in acetone solution formed the complex [PtCl$_2$L$_2$]. Little data were reported for the complex, however, apart from the melting point and microanalytical data. It has been reported, however, that the compound is an active catalyst in the hydrosilylation of olefins by triethoxysilane.[13] The compound was also reported to transport Na^+, K^+, Ag^+

and Pb^{2+} ions across liquid membranes, with the transport rates of the Na^+, K^+ and Pb^{2+} ions being greater than for the related S and Se compounds 10-thiabenzo-15-crown-5 and 10-selenabenzo-15-crown-5 respectively.[14]

The same laboratory reported an additional series of seven telluroether crown compounds in 1994 *via* the reactions of bis(2-hydroxyethyl)telluride with diol ditosylates in a similar method used to prepare 10-tellurabenzo-15-crown-5. These compounds were 19-telluradibenzo-24-crown-8 (i), 10-tellurabenzo-18-crown-6 (ii), 11-tellurabenzo-16-crown-5 (iii), 1-tellura-12-crown-4 (iv), 1-tellura-15-crown-5 (v), 1-tellura-18-crown-6 (vi) and 1,13-ditellura-24-crown-8 (vii), (Figure 3.4).[15]

Figure 3.4 - Tellura-crown ether compounds

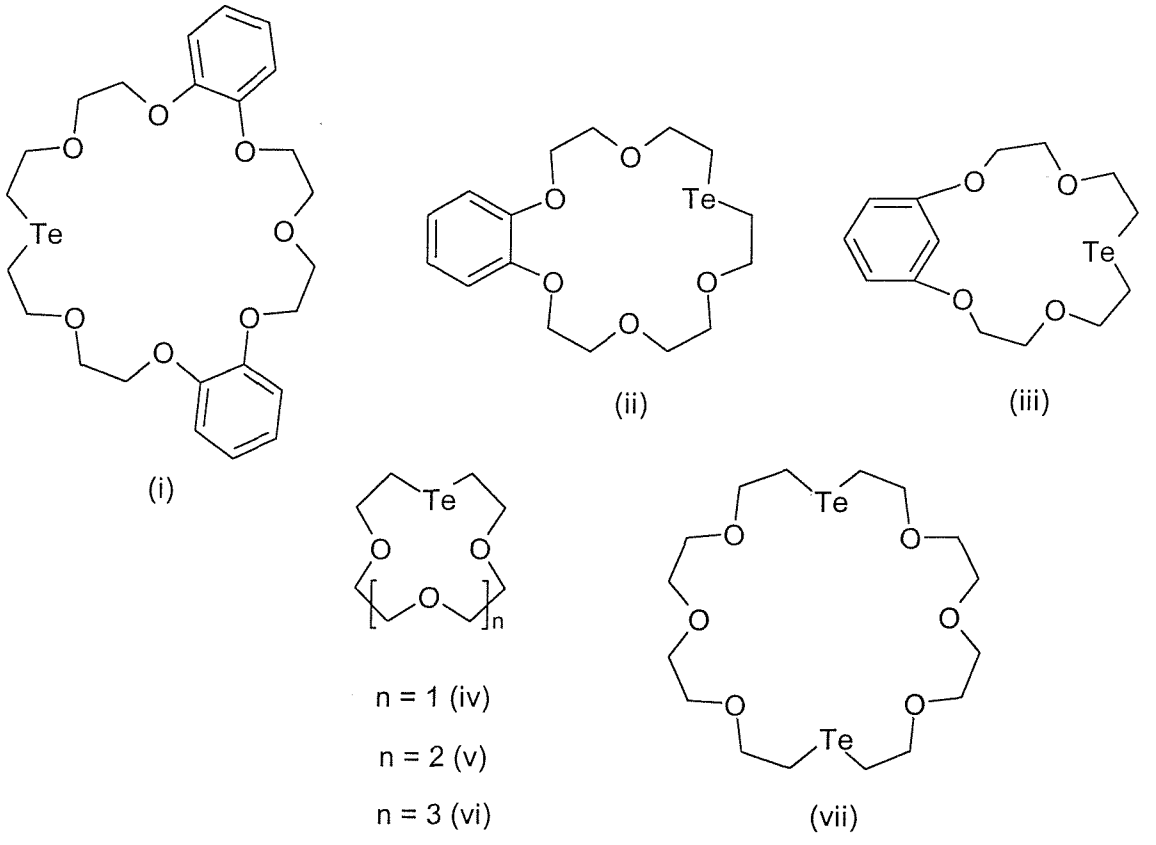

The authors report the microanalytical data for the proposed compounds, plus their IR and ^1H NMR spectra, melting points and mass spectra. No ^{13}C-{^1H} or ^{125}Te-{^1H} NMR data were quoted, however, and only one complex, $[PtCl_2L_2]$ (L = 10-tellurabenzo-18-crown-6) was prepared. In the absence of far-infrared, ^{125}Te-{^1H} or structural data,

however, it was unclear whether this was the *cis* or the *trans* isomer.[15] The yields reported for the compounds were very low to moderate ((i) = 1.4%, (ii) = 8.6%, (iii) = 12%, (iv) = 23%, (v) = 1.4%, (vi) = 30%, (vii) = 26%) and the lack of structural data means that their identity as macrocyclic compounds (rather than oligomeric species) has not been unambiguously determined.

An additional series of tellura-crown compounds based on 10-tellura-15-crown-5 were reported in 1998 by Yam and co-workers, the structures of which are depicted in Figure 3.5.[16]

Figure 3.5 - Tellura-crown macrocycles

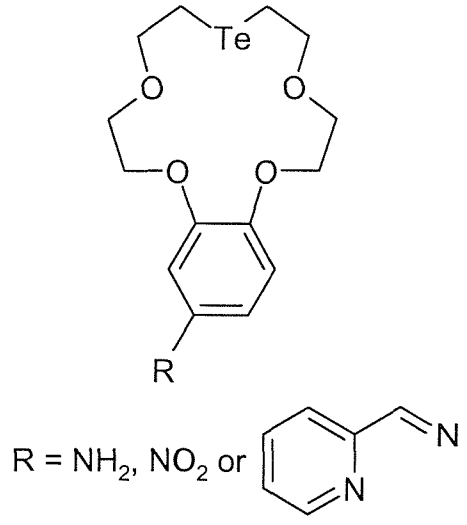

The synthesis of 4'-nitrobenzo-10-tellura-15-crown-5 (R = NO_2) was accomplished in low yield (9%) by the addition of bis(2-hydroxyethyl)telluride to a solution of sodium in *tert*-butyl alcohol, followed by reaction with 1,2-bis[2-(*p*-tosyloxy)ethoxy]-4-nitrobenzene. Conversion of the compound into the NH_2 (amino) derivative was accomplished in 70% yield by reduction with hydrazine hydrate, whilst treatment of this species with 2-pyridinecarbaldehyde in ethanol yielded the third crown ether compound in 93% yield. The compounds were characterized by their melting points, EI mass spectra, ^{1}H NMR spectra and microanalytical data, although no ^{13}C-{^{1}H} or ^{125}Te-{^{1}H} NMR data were quoted. A single copper complex of the tellura-crown macrocycle with R = $C_6H_5N_2$ (L), [Cu(PPh_3)$_2$L][BF_4] was reported, with coordination of the Cu(I) centre

assumed to be *via* the two N donors of the ligand, although no structural data were obtained.[16]

Following our investigations into the synthesis and coordination chemistry of the mixed donor thia-tellura macrocycles [9]-, [11]- and [12]-aneS$_2$Te (Chapter 2) we wished to investigate the effects of incorporating tellurium within a macrocyclic environment with donors other than sulfur, and how this would affect the coordinating properties of the compounds. We chose oxa-tellura systems specifically, due to the few reports of related compounds and the scarcity of NMR spectroscopic and structural data obtained for these. The coordination chemistry of oxa-tellura macrocycles, except for the poorly characterised complexes [PtCl$_2$L$_2$] (L = 10-tellurabenzo-15-crown-5 or 10-tellurabenzo-18-crown-6) and [Cu(PPh$_3$)$_2$L][BF$_4$] (L = 4'-(2-pyridylmethyleneamino)benzo-10-tellura-15-crown-5) has not been investigated. We therefore undertook the preparation of a new O/Te donor macrocycle *via* the reaction of Na$_2$Te with Cl(CH$_2$)$_2$O(CH$_2$)$_2$O(CH$_2$)$_2$Cl in a similar method used to prepare the mixed thia-tellura compounds (Chapter 2). This would allow for comparisons of their syntheses, and of the coordinating properties of the thia-tellura and oxa-tellura compounds.

3.1 Results and discussion

3.2 [9]aneO$_2$Te/[18]aneO$_4$Te$_2$

Addition of Cl(CH$_2$)$_2$O(CH$_2$)$_2$O(CH$_2$)$_2$Cl in dry thf over a period of 30 minutes to Na$_2$Te in NH$_{3(l)}$ (as in the [n]aneS$_2$Te ligand syntheses (n = 11 and 12, Chapter 2)), produced a yellow-orange mixture after being allowed to warm to room temperature overnight. The mixture was hydrolysed and extracted with CH$_2$Cl$_2$, and the combined extracts dried over anhydrous MgSO$_4$. Filtration and removal of the solvent *in vacuo* gave a waxy orange solid, having $\delta(^{125}Te)$ = 176 ppm, together with a minor species (*ca.* 10%) at δ 200 ppm. Recrystallisation of the crude material from CH$_2$Cl$_2$-Et$_2$O at -18°C produced a yellow solid. The $^{125}Te-\{^1H\}$ NMR spectrum of the recrystallised product showed a single resonance at δ 176 ppm only, confirming that the minor impurity had been removed during the recrystallisation. The EI mass spectrum of the solid revealed a cluster of peaks at *m/z* = 488, with the correct isotopic distribution for [[18]aneO$_4$Te$_2$]$^+$. This provided evidence for the isolation of the [2+2] cyclisation product [18]aneO$_4$Te$_2$ (1,10-ditellura-4,7,13,16-tetraoxacyclooctadecane, Figure 3.6).

Figure 3.6 - [18]aneO$_4$Te$_2$

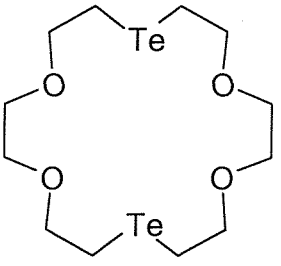

The yield of this species was remarkably high for a tellurium-containing macrocyclic compound (50-55%) and may be compared with the [n]aneS$_2$Te (n = 9, 11 and 12) compounds, which are isolated in typically 18 – 35% yield (Chapter 2).

The reaction was repeated under the same conditions in an attempt to identify the minor (*ca.* 10%) species that was present in the crude reaction mixture. The crude solid

obtained was dissolved in CH_2Cl_2 and adsorbed onto a silica column and eluted with hexane-ethyl acetate 3 : 1. The first fraction to elute was a small quantity of an orange oil with $\delta(^{125}Te)$ = 288 ppm. This was not observed in the crude reaction mixture by $^{125}Te-\{^1H\}$ NMR spectroscopy, presumably due to the very small quantity present. The remaining fractions were found to have identical $^{125}Te-\{^1H\}$ NMR spectra, with $\delta(^{125}Te)$ = 200 ppm. The chemical shift was identical to that observed for the minor species present in the crude solid. The fractions with $\delta(^{125}Te)$ = 200 ppm were combined, and removal of the solvent *in vacuo* produced a microcrystalline, pale yellow solid in 4% yield (based on Te). The bulk of the crude material ([18]aneO$_4$Te$_2$) did not elute, and remained adsorbed on the silica column. It was found that this could be partially recovered by extracting the silica with dmf overnight, followed by the removal of solvent by distillation, to give a yellow solid. Recrystallisation from CH_2Cl_2-Et_2O at -18° gave [18]aneO$_4$Te$_2$, which had identical ^1H, $^{13}C-\{^1H\}$ and $^{125}Te-\{^1H\}$ NMR spectra to those previously obtained. Substantial amounts of the 18-membered ring compound were lost in this process, although it would be possible to overcome this problem by firstly recrystallising [18]aneO$_4$Te$_2$ from the crude reaction mixture and then purifying the remaining solution by column chromatography. The EI mass spectrum of the solid revealed a cluster of peaks with the correct *m/z* and isotopic distribution for $[[9]aneO_2Te]^+$, *m/z* = 246. Therefore, from the EI mass spectrum, the [1+1] cyclisation product of the reaction, [9]aneO$_2$Te (1-tellura-4,7-dioxacyclononane) (Figure 3.7) had been isolated as a minor species from the reaction.

Figure 3.7 - [9]aneO$_2$Te

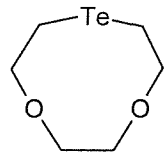

Figure 3.8 - EI Mass Spectra of [18]aneO$_4$Te$_2$ (i) and [9]aneO$_2$Te (ii)

(i) Theoretical (top) and actual (bottom) isotope patterns for [18]aneO$_4$Te$_2$

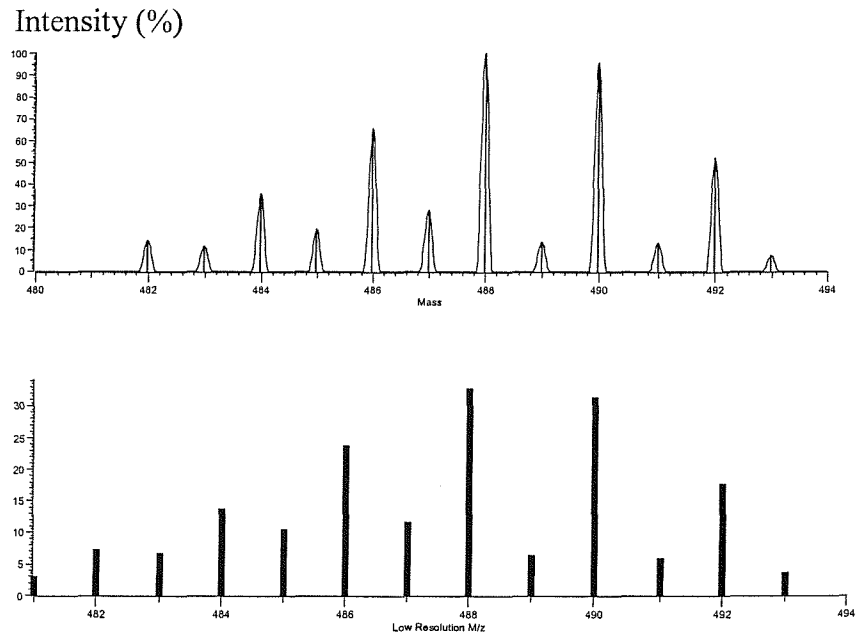

(ii) Theoretical (top) and actual (bottom) isotope patterns for [9]aneO$_2$Te

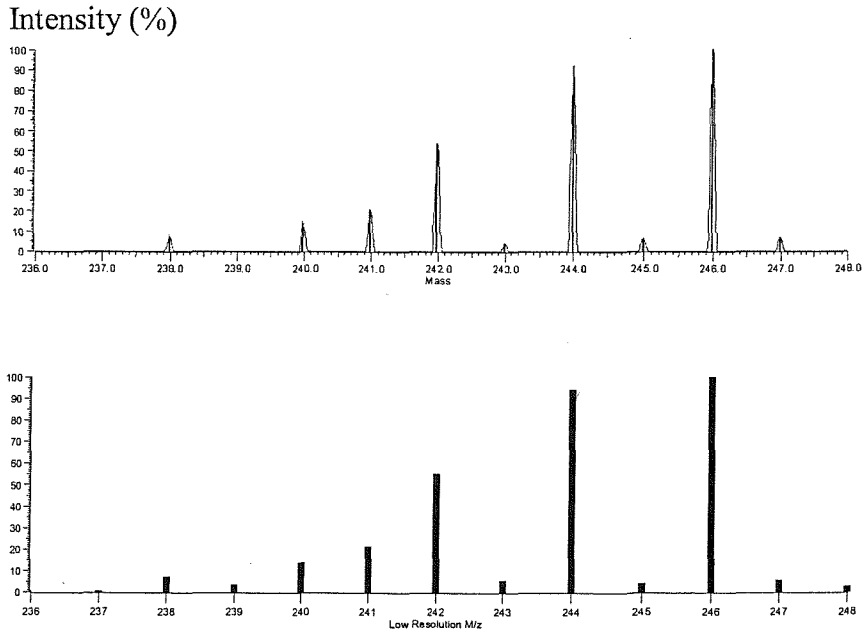

Figure 3.8 shows the EI mass spectra of the two compounds, which confirm their identities and illustrate the differences in isotopic distribution arising from the incorporation of an extra Te donor in the case of [18]aneO$_4$Te$_2$ (Chapter 1).

The ^{1}H and ^{13}C-{^{1}H} NMR spectra of both products were very similar, as was expected (Table 3.0). Resonance multiplicities and integrals were consistent with the proposed structures, with the most significant difference in the data being for the Te*C*H$_2$ resonances in the ^{13}C-{^{1}H} NMR spectra (δ 2.2 and 2.6 ppm for the [9]- and [18]-membered rings respectively). No ^{125}Te satellites could be observed for the Te*C*H$_2$ resonances however. The ^{13}C-{^{1}H} NMR spectrum of [18]aneO$_4$Te$_2$ is shown in Figure 3.9.

Figure 3.9 - ^{13}C-{^{1}H} NMR spectrum of [18]aneO$_4$Te$_2$ in CDCl$_3$

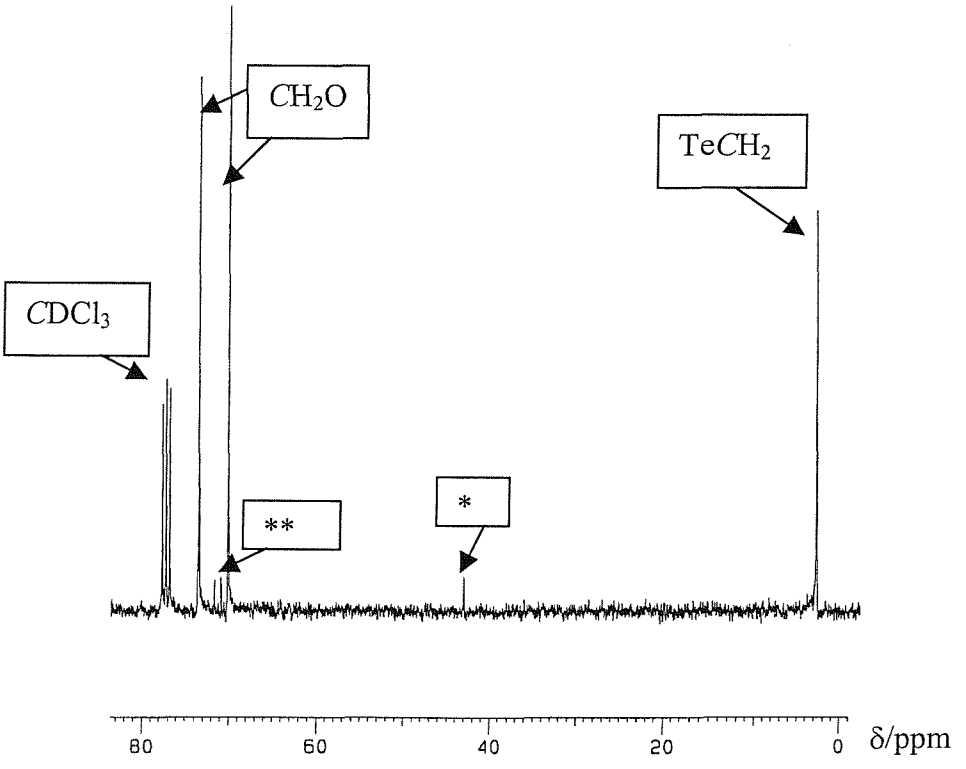

* = *C*H$_2$Cl resonance of Cl(CH$_2$)$_2$O(CH$_2$)$_2$O(CH$_2$)$_2$Cl precursor; ** = *C*H$_2$O resonances of Cl(CH$_2$)$_2$O(CH$_2$)$_2$O(CH$_2$)$_2$Cl precursor.

The shifts are reasonable when compared with δ(^{13}C-{^{1}H}) for the *C*H$_2$Te resonances in [9]-, [11]- and [12]-aneS$_2$Te (2.9, 2.2 and 1.0 ppm respectively, Chapter 2). The C*H*$_2$O resonances in the ^{1}H NMR spectra were similar to those reported for the analogous selenium-containing compounds [9]aneO$_2$Se (δ 3.65, 4.10 ppm) and [18]aneO$_4$Se$_2$ (δ 3.63, 3.79 ppm).[11] The ^{125}Te-{^{1}H} NMR shifts for the two compounds ([9]aneO$_2$Te = δ 200 ppm, [18]aneO$_4$Te$_2$ = δ 176 ppm) were found to differ by 24 ppm, which provides a convenient fingerprint for the identification of the two species.

Table 3.0 - ^{1}H, ^{13}C-{^{1}H} and ^{125}Te-{^{1}H} NMR data for [9]aneO$_2$Te and [18]aneO$_4$Te$_2$

Compound	^{1}H δ (ppm)[a]	Assignment	^{13}C-{^{1}H} δ (ppm)[a]	Assignment	^{125}Te-{^{1}H} δ (ppm)[b]
[9]aneO$_2$Te	2.85, t, 4H	C*H*$_2$Te	2.2	*C*H$_2$Te	200
	3.65, s, 4H	OCH$_2$C*H*$_2$O	70.3	*C*H$_2$O	
	3.80, t, 4H	TeCH$_2$C*H*$_2$O	70.4	*C*H$_2$O	
[18]aneO$_4$Te$_2$	2.80, t, 8H	C*H*$_2$Te	2.6	*C*H$_2$Te	176
	3.57, s, 8H	OCH$_2$C*H*$_2$O	70.0	*C*H$_2$O	
	3.85, t, 8H	TeCH$_2$C*H*$_2$O	73.4	*C*H$_2$O	

([a]: $CDCl_3$ solution; [b]: CH_2Cl_2 solution).

The melting points for the two compounds (70-72°C and 49°C for [9]aneO$_2$Te and [18]aneO$_4$Te$_2$ respectively) provided further evidence for the presence of two different compounds having differing ring sizes.

The isolation of the [2+2] cyclisation product [18]aneO$_4$Te$_2$ as the major species from the reaction of Cl(CH$_2$)$_2$O(CH$_2$)$_2$O(CH$_2$)$_2$Cl with Na$_2$Te is in contrast with the syntheses of [n]aneS$_2$Te (n = 9, 11 or 12), in which only the [1+1] cyclisation products were identified (Chapter 2). This may be due to a templating effect of Na^+ in the synthesis of the oxa-tellura-macrocycles, with interactions between the Na^+ cation and the ether functionalities of the precursor serving to prearrange the Cl(CH$_2$)$_2$O(CH$_2$)$_2$O(CH$_2$)$_2$Cl precursor molecules for reaction with Na$_2$Te. We conclude that the formation of the [18]-membered ring compound is favoured in this reaction, with only small amounts of the [1+1] cyclisation product, [9]aneO$_2$Te, being formed. This is likely to arise due to a combination of the ionic radius of Na^+ and steric factors associated

with the assembly of the precursor molecules around the alkali metal cation. Tentative evidence for the possible templating effect was observed in the electrospray mass spectrum (MeCN solution) of [18]aneO$_4$Te$_2$, which clearly displayed an intense cluster of peaks at *m/z* = 511, consistent with the monocationic [[18]aneO$_4$Te$_2$Na]$^+$. Addition of large excesses of other alkali metal cations (Li^+, K^+, Cs^+ or Rb^+) failed to show similar associations with the macrocycle, which may indicate that it selectively binds Na^+. The corresponding cyclisation reactions using the dichlorodithioether precursors Cl(CH$_2$)$_3$S(CH$_2$)$_n$S(CH$_2$)$_3$Cl (n = 2 or 3) give only the [1+1] cyclisation products, with no evidence for higher rings compounds, since the thioether functions are not expected to interact significantly with Na^+ (Chapter 2). It is possible that the relative ratios of [9]aneO$_2$Te and [18]aneO$_4$Te$_2$ formed in the reaction may be changed by using a different alkali metal precursor, for example Li_2Te in place of Na_2Te. In this case, the smaller Li^+ ion may favour the formation of the smaller ring. As expected, [9]aneO$_2$Te does not show any association with Na^+ due to the smaller cavity size of the compound.

The stability of the –Te(CH$_2$)$_2$O- linkages are notable, since –Te(CH$_2$)$_2$Te- moieties cannot be formed. This is exemplified by the attempted formation of RTe(CH$_2$)$_2$TeR whereby CH$_2$=CH$_2$ is eliminated and ditellurides are produced.[17] The six-membered heterocycle 1-thia-4-oxacyclohexane is known,[18] together with various tellurium containing crown-ether macrocycles[13-16] and therefore the strong –CH$_2$-OR bonds probably prevent the elimination of ethene from occurring.

3.2 Organo-derivatives

In order to fully characterise the new macrocyclic compounds, they were derivatised by quaternisation with MeI and also, for [18]aneO$_4$Te$_2$, by chlorination. In all cases reaction occurs exclusively at the Te centres, with no attack of the ether functionalities. The resulting formally Te(IV) derivatives are air stable and are therefore easy to characterise. The reaction of [18]aneO$_4$Te$_2$ with excess MeI in CH_2Cl_2 solution produced, after concentration of the reaction mixture and precipitation of the product with Et_2O, an air-stable yellow powdered solid. This quickly turned into a waxy orange solid when stored under dinitrogen. Microanalytical data were consistent with the formulation

[18]aneO$_4$Te$_2$Me$_2$I$_2$, with the ES mass spectrum showing a complex ion cluster at *m/z* = 645 and another intense feature at *m/z* = 259. These were attributed to the loss of one and two iodine atoms from the parent compound, giving the [P-I]$^+$ and [P-2I]$^{2+}$ cations respectively. The site of quaternisation was confirmed by characteristic, significant high frequency shifts of the CH$_2$Te resonances in the ^{1}H and ^{13}C-{^{1}H} NMR spectra, which was also observed for the methiodide derivatives of [9]-, [11]- and [12]- aneS$_2$Te (Chapter 2). The ^{125}Te-{^{1}H} NMR spectrum of the product (δ ^{125}Te = 506 ppm) represented a considerable high frequency shift (*ca.* 330 ppm) upon quaternisation of the formally R$_2$Te(II) centre, forming an R$_3$ITe(IV) species. This value is typical of an R$_3$TeI group – for example (CH$_3$)$_3$TeI has δ(^{125}Te) = 443 ppm.[19]

The [9]aneO$_2$Te reacted similarly with MeI in CH$_2$Cl$_2$ solution to form the corresponding methiodide derivative [9]aneO$_2$TeMeI. ^{1}H and ^{13}C-{^{1}H} NMR spectra were similar to those observed for [18]aneO$_4$Te$_2$Me$_2$I$_2$, with δ(^{125}Te) = 520 ppm. The electrospray mass spectrum showed an ion cluster at *m/z* = 261, which was consistent with the monocationic species [[9]aneO$_2$TeMeI]$^+$. This was easily distinguished from the [P-2I]$^{2+}$ species in the mass spectrum of [18]aneO$_4$Te$_2$Me$_2$I$_2$ by the significantly different isotope pattern (Chapter 1) and the half-mass separation between ion peaks.

The reaction of [18]aneO$_4$Te$_2$ with Cl$_2$ in CH$_2$Cl$_2$ solution produced the Te(IV) chloride derivative, [18]aneO$_4$Te$_2$Cl$_4$ as a white solid, which readily turned into a black waxy solid upon storage. The ^{1}H and ^{13}C-{^{1}H} NMR spectra of a freshly prepared sample again displayed high frequency shifts for the CH$_2$Te resonance (δ ^{1}H = 4.2 ppm and δ ^{13}C-{^{1}H} = 15.5) as expected upon oxidation of the formally Te(II) centre to Te(IV), thereby deshielding the proton and carbon environments. In addition, the ^{125}Te-{^{1}H} NMR spectrum (Figure 3.10) displayed a single resonance at δ 850 ppm, consistent with other known Te(IV) chloride derivatives, for example Me$_2$TeCl$_2$ has δ(^{125}Te) = 749 ppm.[19] The EI mass spectrum displayed a weak parent ion, consistent with the species [[18]aneO$_4$Te$_2$Cl$_4$]$^+$. The corresponding [[18]aneO$_4$Te$_2$Cl$_3$]$^+$ ion cluster at *m/z* = 595 was much more intense, with the *m/z* value and the isotopic distribution serving to confirm the identity of the species.

Figure 3.10 - ^{125}Te-{^{1}H} NMR spectrum of [18]aneO$_4$Te$_2$Cl$_4$ in CH$_2$Cl$_2$-CDCl$_3$

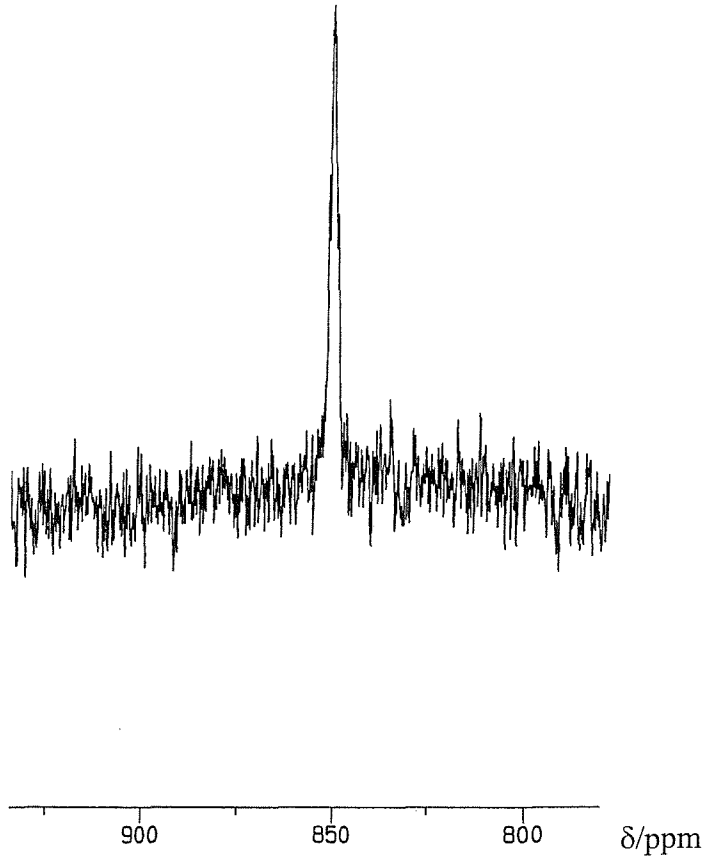

3.3 [9]aneO$_2$Se/[18]aneO$_4$Se$_2$

The direct analogues of the oxa-tellura macrocycles, [9]aneO$_2$Se and [18]aneO$_4$Se$_2$, have been reported, with the former being observed as an unexpected ring-contraction product of the reaction between Br(CH$_2$)$_2$O(CH$_2$)$_2$O(CH$_2$)$_2$Br, NCSe(CH$_2$)$_2$SeCN and NaBH$_4$.[11] No studies investigating their coordinating properties have been reported however. In order to directly compare the syntheses and coordination chemistry of the oxa-tellura and oxa-selena macrocycles, attempts were made to prepare [9]aneO$_2$Se/[18]aneO$_4$Se$_2$ from Na$_2$Se and Cl(CH$_2$)$_2$O(CH$_2$)$_2$O(CH$_2$)$_2$Cl as per the oxa-tellura compounds. A solution of Cl(CH$_2$)$_2$O(CH$_2$)$_2$O(CH$_2$)$_2$Cl in dry thf was added to Na$_2$Se in NH$_{3(l)}$ at -78°C over the course of approximately 30 minutes and then allowed to warm to room temperature. Work-up yielded recovery of the Cl(CH$_2$)$_2$O(CH$_2$)$_2$O(CH$_2$)$_2$Cl precursor. This was

confirmed by the ^{1}H and ^{13}C-{^{1}H} NMR spectra of the isolated material. We concluded that the recovery of the starting material may have been due to the lower nucleophilicity of Se^{2-} compared with Te^{2-}. The reaction was therefore attempted again, this time carrying out the addition of the precursor to Na_2Se at the boiling point of ammonia (-33°C). Under these conditions, varying amounts and ratios of the macrocycles were produced (together with large amounts of polymer and some $Cl(CH_2)_2O(CH_2)_2O(CH_2)_2Cl$) even from reactions performed under apparently identical conditions. A possible reason for this may be the lower nucleophilicity of Se^{2-}, resulting in an incomplete reaction at low temperature followed by uncontrolled reaction and polymerization upon warming. In a typical work up, the reaction mixture was hydrolysed and extracted with CH_2Cl_2. After drying the combined extracts ($MgSO_4$), filtering and removing the solvent *in vacuo*, yellow oily products were obtained. Kugelröhr distillation of the crude material (0.2 mmHg) produced low boiling point, non-selenium containing fractions, together with a yellow oil at 200°C and an involatile red-brown solid residue that did not distil. ^{77}Se-{^{1}H} NMR spectroscopy showed that the amounts of [9]aneO$_2$Se and [18]aneO$_4$Se$_2$ in the distilled yellow oil were highly variable, with only trace amounts of [9]aneO$_2$Se being present in some cases, and in others being the dominant product. Separation of the compounds was achieved by careful sublimation of the oil *in vacuo* onto an $N_{2(l)}$ cold finger, giving [9]aneO$_2$Se as a yellow oil and the less volatile [18]aneO$_4$Se$_2$ as a waxy yellow solid.

The identities of the two macrocycles were confirmed by their ^{1}H and ^{13}C-{^{1}H} NMR spectra, which were consistent with those previously reported,[11] while the EI mass spectra of the products displayed ion clusters at *ca.* *m/z* = 196 for [[9]aneO$_2$Se]$^+$ and *ca.* *m/z* = 392 for [[18]aneO$_4$Se$_2$]$^+$. ^{77}Se-{^{1}H} NMR spectra were recorded for the two compounds, since this data had not previously been reported[11] ($\delta(^{77}Se)$ = 204 and 144 ppm for [9]aneO$_2$Se and [18]aneO$_4$Se$_2$ respectively).

In an attempt to further explore the synthesis of the oxa-selena macrocycles from Na_2Se and to try to optimise their yields, the preparation was attempted *via* a different method, this time using high dilution conditions at room temperature. Freshly prepared Na_2Se was dissolved in dry EtOH (1000 cm^3) and a solution of $Cl(CH_2)_2O(CH_2)_2O(CH_2)_2Cl$ in EtOH (1000 cm^3) added dropwise over the course of 7

hours at room temperature. The reaction mixture was stirred for a further 20 hours at room temperature and refluxed gently for an hour, then allowed to cool, hydrolysed and filtered. The solvent was then removed to give a residue that was extracted with CH_2Cl_2, and the combined extracts were dried over anhydrous $MgSO_4$. Filtration and removal of the solvent *in vacuo* produced a viscous yellow oil. The ^{77}Se-{^{1}H} NMR spectrum of the crude product showed resonances at δ 204 and 144 ppm, consistent with [9]aneO$_2$Se and [18]aneO$_4$Se$_2$ respectively, together with several resonances in the range δ 123 – 131 ppm, which were concluded to be oligomeric compounds. Two additional resonances at δ 226 and 312 ppm were thought to be diselenide species. Recrystallisation of the oil from CH_2Cl_2-hexane at -18°C produced a yellow waxy solid, consisting of a mixture of [18]aneO$_4$Se$_2$ and oligomeric material. The mother-liquor was evaporated and the residue Kugelröhr distilled (2 mmHg) to produce four different fractions. The first to distill at ≤ 125°C was identified as [9]aneO$_2$Se (δ(^{77}Se) = 203 ppm), yield 0.25g, while the other two fractions both distilled at ≤ 200°C. Fraction 2 (yield 0.09g) was largely diselenide on the basis of its ^{77}Se-{^{1}H} NMR spectrum (δ 227 ppm) (although its identity is unclear) and fraction 3 (0.050g) was identified as [18]aneO$_4$Se$_2$ (δ(^{77}Se) = 144 ppm).

It may therefore be concluded that the syntheses of [9]aneO$_2$Se and [18]aneO$_4$Se$_2$ from the reaction of Cl(CH$_2$)$_2$O(CH$_2$)$_2$O(CH$_2$)$_2$Cl with Na$_2$Se is much lower yielding than the corresponding reaction with Na$_2$Te, producing large amounts of polymeric and oligomeric materials, with low and varying yields of the desired compounds. This may reflect the lower nucleophilicity of Se^{2-} compared with Te^{2-}. Electrospray mass spectrometry of [18]aneO$_4$Se$_2$ (MeCN solution) revealed, as observed for [18]aneO$_4$Te$_2$, an affinity of the compound for Na^+, with a strong ion multiplet at *m/z* = 413. This suggests that Na^+ may also play a templating role in the formation of [18]aneO$_4$Se$_2$.

3.4 [MX$_2$([18]aneO$_4$Te$_2$)] (M = Pd or Pt; X = Cl or Br)

We wished to explore the coordination behaviour of the new compounds, and decided that complexes with Pt(II) and Pd(II) halides would provide a good insight into the coordination behaviour of the new ligands, with the availability of ^{1}H, ^{125}Te-{^{1}H} and ^{195}Pt-{^{1}H} spectroscopic probes, together with UV/visible and IR spectroscopy and ES

mass spectrometry. The dropwise addition of dilute $[MX_2(MeCN)_2]$[20] (M = Pd or Pt, X = Cl or Br) solutions in MeCN to gently refluxing solutions of [18]aneO$_4$Te$_2$ (one molar equivalent) in CH_2Cl_2/MeCN produced yellow solutions, which were refluxed for a further hour before allowing to cool and stir at room temperature overnight. The solutions were then filtered to remove small amounts of precipitated solid (presumably oligomeric compounds), concentrated *in vacuo* and the products precipitated by the addition of Et_2O. The solids were then filtered, washed with Et_2O and dried *in vacuo* to produce yellow-orange powdered solids in moderate to high yield (36 – 80%). Dilute solutions of the precursors were used in order to favour the formation of chelate complexes while minimising the formation of oligomeric compounds. Microanalytical data for all the complexes were consistent with the stoichiometry $[MX_2([18]aneO_4Te_2)]$, and the complexes were moderately soluble in organic solvents (CH_2Cl_2 and $CHCl_3$).

The complexes all displayed two absorptions in their respective UV/visible spectra at 34 435 and 25 560 cm^{-1} for $[PtCl_2([18]aneO_4Te_2)]$, 36 075 and 30 980 cm^{-1} for $[PtBr_2([18]aneO_4Te_2)]$, 30 600 and 25 640 cm^{-1} for $[PdCl_2([18]aneO_4Te_2)]$ and 28 900 and 24 630 cm^{-1} for $[PdBr_2([18]aneO_4Te_2)]$. These were consistent with the formation of planar MX_2Te_2 species,[21,22] for example $[PtCl_2(MeTe(CH_2)_3TeMe)]$ has ν_{max} = 30 860 and 26 670 cm^{-1}, while $[PtBr_2(MeTe(CH_2)_3TeMe)]$ has ν_{max} = 30 120 and 25 640cm^{-1}.[22] All of the complexes were observed to have two ν(M-X) vibrations in their far IR spectra, which is consistent with the formation of *cis*-complexes. From Group Theory, for a *cis*-square planar MX_2Te_2 complex, two absorptions are expected ($A_1 + B_1$). For a *trans* complex, only one absorption is predicted (E_u). For example, $[PdX_2([18]aneO_4Te_2)]$ has ν(M-X) = 311, 301 cm^{-1} for X = Cl and 243, 221 cm^{-1} for X = Br. The corresponding $[PtCl_2([18]aneO_4Te_2)]$ complex was observed to have ν(M-X) = 308, 291 cm^{-1}, however $[PtBr_2([18]aneO_4Te_2)]$ had only one observable Pt-Br stretching vibration at 223 cm^{-1}. This may have been due to the coincidence of the two absorptions. The data are comparable with other planar *cis*-MX_2Te_2 compounds – for example *cis*-$[PdCl_2(PhTe(CH_2)_3TePh)]$ has ν(Pd-Cl) = 305 and 290 cm^{-1}, but $[PdBr_2(PhTe(CH_2)_3TePh)]$ was observed to have only one Pd-Br stretching vibration at 220 cm^{-1}, despite a crystal structure of the complex confirming the *cis* geometry.[22]

The ^{1}H NMR spectra of the complexes in $CDCl_3$ all contained overlapping multiplet resonances within the range δ 3.0 – 4.5 ppm, showing that the TeC*H*$_2$ resonance in uncoordinated [18]aneO$_4$Te$_2$ (δ(TeC*H*$_2$) = 2.8 ppm) had shifted to significantly higher frequency. This was also observed for the complexes [MCl$_2$([n]aneS$_2$Te)] where M = Pd or Pt, and n = 11 and 12 (Chapter 2). The C*H*$_2$O resonances in the complexes were essentially unshifted from those in uncoordinated [18]aneO$_4$Te$_2$, and therefore these data are consistent with the coordination of the macrocycle to the metal centres through the Te donor atoms only. The ^{125}Te-{^{1}H} NMR spectra of the complexes in $CH_2Cl_2/CDCl_3$ solution all showed significant high frequency coordination shifts compared to free [18]aneO$_4$Te$_2$, with δ(^{125}Te) = 393 ppm ($^1J_{Te-Pt}$ = 862 Hz) for [PtCl$_2$([18]aneO$_4$Te$_2$)] and 390 ppm ($^1J_{Te-Pt}$ = 690 Hz) for [PtBr$_2$([18]aneO$_4$Te$_2$)], while the complexes [PdX$_2$([18]aneO$_4$Te$_2$)] had δ(^{125}Te) = 375 and 370 ppm for X = Cl and Br respectively. The high frequency coordination shifts compared to free [18]aneO$_4$Te$_2$ (δ(^{125}Te) = 176 ppm) confirmed that the macrocyclic ligand was coordinated *via* the tellurium donors to the M(II) centers, with the coordination shift increasing in the order Pt(II) > Pd(II) and Cl > Br. This latter observation is consistent with a *trans* halide dependence on the ^{125}Te chemical shift (for example the complexes [PtX$_2$(PhMeTe)$_2$] have δ(^{125}Te) = 487, 460 and 391 ppm for X = Cl, Br and I respectively).[21] The $^1J_{Te-Pt}$ coupling constants decrease in the order Cl>Br, which is also consistent with a *trans* influence of the halogen co-ligands, for example [PtX$_2$(PhMeTe)$_2$] have $^1J_{Te-Pt}$ = 1257, 933 and 256 Hz for X = Cl, Br and I.[21] The coupling constants are similar to those previously reported for *cis*-PtX$_2$Te$_2$ moieties; for example *cis*-[PtBr$_2$(Ph$_2$Te)$_2$] has $^1J_{Te-Pt}$ = 933 Hz. The corresponding values for *trans*-PtX$_2$Te$_2$ complexes are lower, this being exemplified by the $^1J_{Te-Pt}$ value for *trans*-[PtBr$_2$(Ph$_2$Te)$_2$] (525 Hz).[21] It has been shown that the coordination shifts in the ^{125}Te-{^{1}H} NMR spectra of Pt(II) and Pd(II) telluroether complexes are sensitive to chelate ring size.[21] Using the compounds *cis*-[PtX$_2$(R$_2$Te)$_2$] as a reference, bidentate telluroether ligands (preferably where the R groups are similar) show very large, positive coordination shifts for five-membered chelate rings, markedly smaller coordination shifts for six-membered chelates and negative coordination shifts for four-membered chelate ring complexes. The high frequency coordination shifts observed here (*ca.* 200 – 220 ppm) are similar to those reported for [MX$_2$(Me$_2$Te)$_2$], which confirmed that the presence

of the 11-membered chelate rings in the [18]aneO$_4$Te$_2$ complexes have very little effect on the coordination shift, and therefore the chelate ring parameter is close to zero.[21] An exact comparision would require data on complexes of Te(CH$_2$CH$_2$OR)$_2$ (which are unavailable) since ^{125}Te-{^{1}H} NMR shifts are sensitive to substituent effects as remote as the γ-carbon.[23]

The ^{195}Pt NMR spectra of *cis*-[PtX$_2$([18]aneO$_4$Te$_2$)] showed resonances at δ -4257 and -4756 ppm for X = Cl and Br respectively. These are comparable to the values for other reported *cis*-PtX$_2$Te$_2$ complexes, for example [PtX$_2$(MeTe(CH$_2$)$_3$TeMe)] have δ(^{195}Pt) = -4434 and -4379 ppm for X = Cl, and -4846 and -4809 ppm for X = Br (the two values are due to the presence of both the *meso* and DL invertomers).[22] The corresponding *trans*-PtX$_2$Te$_2$ isomers have ^{195}Pt chemical shifts typically 400 – 500 ppm to higher frequency (for example *cis*-[PtCl$_2$(Me$_2$Te)$_2$] has δ(^{195}Pt) = -4351 ppm, whilst *trans*-[PtCl$_2$(Me$_2$Te)$_2$] has δ(^{195}Pt) = -3769 ppm.[21] The ^{125}Te-{^{1}H} and ^{195}Pt-{^{1}H} NMR spectra were recorded at -50°C, since good quality data were unobtainable at room temperature. The reasons for the poor data quality obtained at room temperature are unclear, although it may reflect dynamic processes occurring in solution, for example reversible chelate ring opening.

When the reactions between [MX$_2$(MeCN)$_2$] (M = Pd or Pt, X = Cl or Br) and [18]aneO$_4$Te$_2$ were carried out by rapidly mixing concentrated solutions of the reagents, the immediate precipitation of yellow-orange solid products occurred. Microanalytical data on these compounds were again consistent with the formulation [MX$_2$([18]aneO$_4$Te$_2$)], but they had only very limited solubility in CH$_2$Cl$_2$. The remainder of the samples were insoluble in chlorinated solvents, MeCN or acetone, but dissolved slowly, probably with reaction, in dmso. UV/visible and infrared spectra of the solids were almost identical to those of the soluble [MX$_2$([18]aneO$_4$Te$_2$)] complexes, except for differences in the far IR ν(M-X) region where they were more complicated. The insolubility of the compounds precluded their full characterisation, however it is highly likely that a mixture of *cis*-[MX$_2$([18]aneO$_4$Te$_2$)] (the small soluble component) and insoluble, oligomeric [MX$_2$([18]aneO$_4$Te$_2$)]$_n$ species were formed. This hypothesis is consistent with the microanalytical data and the insolubility of the bulk material.

3.5 [MCl$_2$([9]aneO$_2$Te)$_2$] (M = Pd or Pt)

The reaction of [9]aneO$_2$Te with one molar equivalent of [MCl$_2$(MeCN)$_2$] (M = Pd or Pt) produced yellow complexes of stoichiometry [MCl$_2$([9]aneO$_2$Te)$_2$] which was confirmed by the microanalytical data. The complexes were soluble in chlorinated solvents, and their UV/visible spectra were very similar to the analogous [MCl$_2$([18]aneO$_4$Te$_2$)] (M = Pd or Pt) complexes. For [PdCl$_2$([9]aneO$_2$Te)$_2$], two absorptions were observed at 30 490 and 26 710 cm^{-1} (compared with [PdCl$_2$([18]aneO$_4$Te$_2$)] which had ν_{max} = 30 600 and 25 640 cm^{-1}), while [PdCl$_2$([9]aneO$_2$Te)$_2$] had two absorptions at 30 490 and 26 710 cm^{-1} ([PtCl$_2$([18]aneO$_4$Te$_2$)], ν_{max} = 34 435 and 25 560 cm^{-1}). These data confirmed the presence of planar MX$_2$Te$_2$ moities, while the IR spectra showed two (M-Cl) stretching vibrations at 283, 305 cm^{-1} for M = Pd and 290, 311 cm^{-1} for M = Pd. On the basis of these data, therefore, the compounds were concluded to be *cis* in the solid state.

The ^{125}Te-{^{1}H} NMR spectra of the compounds showed single resonances at δ 387 and 394 ppm for [PdCl$_2$([9]aneO$_2$Te)$_2$] and [PtCl$_2$([9]aneO$_2$Te)$_2$] (Figure 3.11) respectively, which were very similar to the values for the corresponding [MCl$_2$([18]aneO$_4$Te$_2$)] which had δ(^{125}Te) = 375 and 393 ppm for M = Pd and Pt respectively. The ^{125}Te-{^{1}H} NMR spectrum of [PtCl$_2$([9]aneO$_2$Te)$_2$] had visible platinum satellites ($^1J_{Te\text{-}Pt}$ = 975 Hz). The value was similar to that obtained for the analogous [PtCl$_2$([18]aneO$_4$Te$_2$)] which had $^1J_{Te\text{-}Pt}$ = 862 Hz, consistent with a *cis* isomer in solution. For both ring sizes, the chemical shifts for the platinum complexes were slightly greater than in their palladium analogues due to the better σ-orbital overlap between the larger Pt(II) orbitals and Te, resulting in increased σ-donation from Te $\rightarrow$ Pt. The presence of single resonances in both cases indicated the presence of only one isomer in solution.

Figure 3.11 - ^{125}Te-{^{1}H} NMR spectrum of [PtCl$_2$([9]aneO$_2$Te)$_2$] in CH$_2$Cl$_2$-CDCl$_3$

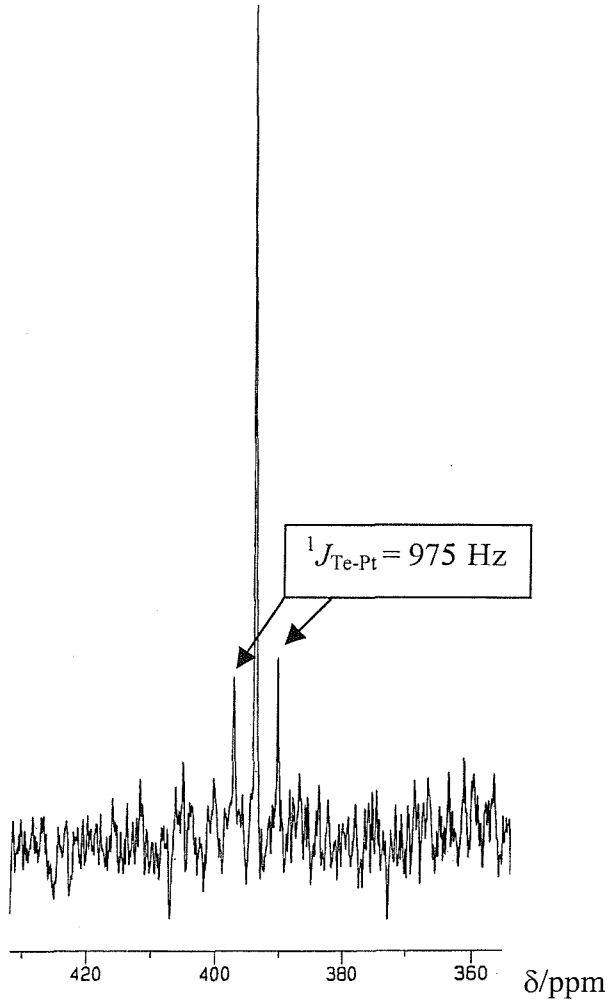

It is not possible, however, to distinguish between the possible *cis* and *trans* isomers of [PdCl$_2$([9]aneO$_2$Te)$_2$] from the ^{125}Te-{^{1}H} chemical shift, since the values for the related compounds [PdCl$_2$(R$_2$Te)$_2$] (R = Me or Ph) are very similar. For example *cis*-[PtCl$_2$(Me$_2$Te)$_2$] and *cis*-[PtCl$_2$(Ph$_2$Te)$_2$] have δ(^{125}Te) = 224 and 715 ppm, whereas *trans*-[PtCl$_2$(Me$_2$Te)$_2$] and *trans*-[PtCl$_2$(Ph$_2$Te)$_2$] have δ(^{125}Te) = 234 and 729 ppm respectively.[21] The two Pd-Cl stretches observed in the IR spectrum of [PdCl$_2$([9]aneO$_2$Te)$_2$] suggest that the *cis*-isomer is likely in the solid state, however. The ^{195}Pt NMR spectrum of [PtCl$_2$([9]aneO$_2$Te)$_2$] (Figure 3.12) showed a single

resonance at -4501 ppm, which was similar to the value obtained for the analogous [PtCl$_2$([18]aneO$_4$Te$_2$)] which had $\delta(^{195}Pt)$ = -4257 ppm.

Figure 3.12 - ^{195}Pt NMR spectrum of [PtCl$_2$([9]aneO$_2$Te)$_2$] in CH$_2$Cl$_2$-CDCl$_3$

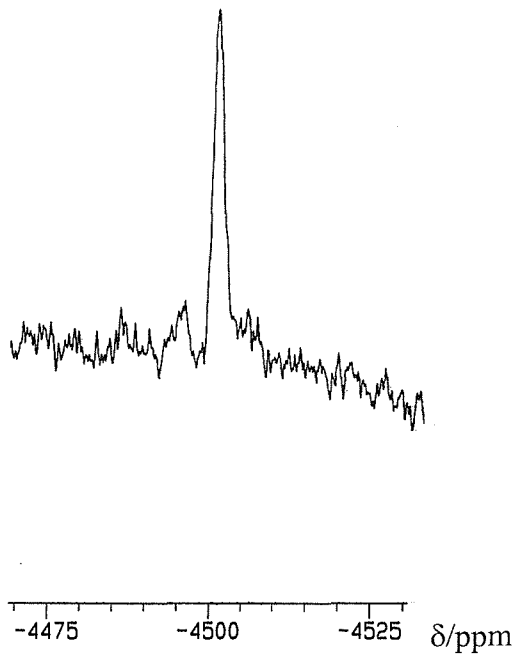

There have been few reported platinum metal complexes of small telluracycles with which to provide comparisons, however the 1-oxa-4-telluracyclohexane complex [PtCl$_2$(TeC$_4$H$_8$O)$_2$] was shown to be *trans* from an X-ray structure of the solid,[24] whilst in complexes of telluracyclopentane (L) the species [MX$_2$L$_2$] (M = Pd and Pt; X = Br or I) are *trans*, whereas [PtCl$_2$L$_2$] was shown to be a mixture of *cis* and *trans* isomers.[25] In addition, the complex [PtCl$_2$L'$_2$], where L' = 1,3-dihydrobenzo[*c*]tellurophene, was shown to be *cis*, whereas the corresponding palladium complex was *trans*.[26] From these examples it can be seen that no clear pattern arises and therefore the differences in stability for the possible *cis* and *trans* isomers are likely to be small.

3.6 [PtCl$_2$([18]aneO$_4$Se$_2$)]

The compound [PtCl$_2$([18]aneO$_4$Se$_2$)] was prepared as for the analogous [PtCl$_2$([18]aneO$_4$Te$_2$)] in order to provide comparisons between the two systems. The UV/visible and IR spectra of the complex were similar to those observed for [PtCl$_2$([18]aneO$_4$Te$_2$)], with two ν(Pt-Cl) bands in the far IR region at 322 and 304 cm^{-1} (as compared with 308 and 291 cm^{-1} for [PtCl$_2$([18]aneO$_4$Te$_2$)]); this being consistent with a *cis* isomer in the solid state. The ^{1}H NMR spectrum of the compound showed a multiplet resonance at δ 3.0 – 4.4 ppm, indicating a high frequency shift for the SeC*H*$_2$ protons compared with those in free [18]aneO$_4$Se$_2$ (δ(SeC*H*$_2$) = 2.78 ppm). The ^{13}C-{^{1}H} NMR spectrum also showed a high frequency shift for the Se*C*H$_2$ resonance, with the *C*H$_2$O resonances being little shifted from those in uncoordinated [18]aneO$_4$Se$_2$. These data suggested that the bonding of [18]aneO$_4$Se$_2$ to Pt(II) occurs through the Se donors only. The ^{77}Se-{^{1}H} NMR spectrum revealed a single resonance at δ 259 ppm, with visible platinum satellites ($^1J_{Se\text{-}Pt}$ = 550 Hz), consistent with a single isomer in solution. The resonance was shifted significantly to high frequency of free [18]aneO$_4$Se$_2$ (δ(^{77}Se) = 144 ppm) therefore confirming that the bonding of the macrocyclic ligand to Pt(II) occurs through both Se donor atoms. The ^{77}Se-{^{1}H} chemical shift and $^1J_{Se\text{-}Pt}$ are similar to those reported for other *cis*-PtCl$_2$Se$_2$ moieties, for example [PtCl$_2$(RSe(CH$_2$)$_3$SeR)] have δ(^{77}Se) = 178 ppm ($^1J_{Se\text{-}Pt}$ = 500 Hz) for R = Me, and δ(^{77}Se) = 314 ppm ($^1J_{Se\text{-}Pt}$ = 625 Hz) for R = Ph.[22]

3.7 Crystal structures of *cis*-[MCl$_2$([18]aneO$_4$Te$_2$)] (M = Pd and Pt) and *cis*-[PtCl$_2$([18]aneO$_4$Se$_2$)]

Crystals of [PdCl$_2$([18]aneO$_4$Te$_2$)] and [PtCl$_2$([18]aneO$_4$Se$_2$)] suitable for X-ray diffraction studies were grown by slow evaporation of solutions of the compounds in CH$_2$Cl$_2$, while crystals of [PtCl$_2$([18]aneO$_4$Te$_2$)] were grown from MeOH solution. The crystal structures ([PdCl$_2$([18]aneO$_4$Te$_2$)] Figure 3.13, Table 3.1), [PtCl$_2$([18]aneO$_4$Te$_2$)] Figure 3.14 , Table 3.2) and [PtCl$_2$([18]aneO$_4$Se$_2$)] Figure 3.15 , Table 3.3) show the expected *cis* square planar complexes, with [18]aneO$_4$Te$_2$ and [18]aneO$_4$Se$_2$ behaving as

chelating bidentate ligands, bonding to Pd(II) and Pt(II) only through the two Te or Se donor atoms. No interaction between the metal centres and the O atoms of the [18]aneO$_4$Te$_2$ and [18]aneO$_4$Se$_2$ rings are evident. The previously reported [PtCl$_2$([18]aneO$_4$S$_2$)] also showed a *cis* square planar arrangement, with the macrocycle coordinating to Pd(II) *via* the S donors only.[9] The angles at the metal are close to 90° in all three compounds, with [PtCl$_2$([18]aneO$_4$Se$_2$) having Se(1)-Pt(1)-Se(2) = 86.57(6), Se(1)-Pt(1)-Cl(1) = 91.59(11), Se(2)-Pt(1)-Cl(2) = 91.74(12) and Cl(1)-Pt(1)-Cl(2) = 90.1(2)°. In [PdCl$_2$([18]aneO$_4$Te$_2$)] the angles around Pd(II) are Te(1)-Pd(1)-Te(2) = 88.29(2), Te(1)-Pd(1)-Cl(1) = 89.98(3), Te(2)-Pd(1)-Cl(2) = 88.84(3) and Cl(1)-Pd(1)-Cl(2) = 93.35(4)°, while the angles around Pt(II) in [PtCl$_2$([18]aneO$_4$Te$_2$)] are Te(1)-Pt(1)-Te(2) = 88.81(2), Te(1)-Pt(1)-Cl(1) = 90.87(6), Te(2)-Pt(1)-Cl(2) = 89.68(5) and Cl(1)-Pt(1)-Cl(2) = 90.97(7)°. From these data, the Cl-M-Cl angles are slightly greater than the E-M-E (E = Se or Te) angles, however there is no significant distortion apparent in the chelate rings.

Figure 3.13 - Crystal structure of [PdCl$_2$([18]aneO$_4$Te$_2$)] with numbering scheme adopted. Ellipsoids are drawn at the 40% probability level and H atoms are omitted for clarity

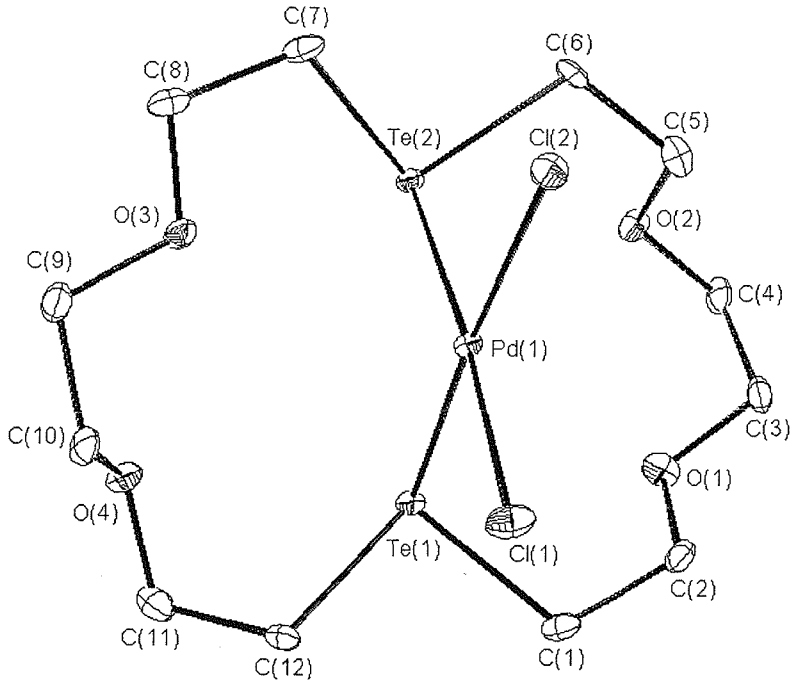

Table 3.1 - Selected bond lengths (Å) and angles (°) for cis-[PdCl$_2$([18]aneO$_4$Te$_2$)]

Bond Lengths			
Pd(1)-Te(1)	2.5567(5)	Te(1)-C(1)	2.157(5)
Pd(1)-Te(2)	2.5398(5)	Te(1)-C(12)	2.156(5)
Pd(1)-Cl(1)	2.3474(13)	Te(2)-C(6)	2.144(5)
Pd(1)-Cl(2)	2.3618(12)	Te(2)-C(7)	2.151(5)
Bond Angles			
Te(1)-Pd(1)-Te(2)	88.29(2)	Pd(1)-Te(1)-C(1)	100.3(1)
Te(1)-Pd(1)-Cl(1)	89.98(3)	Pd(1)-Te(1)-C(12)	105.6(1)
Te(1)-Pd(1)-Cl(2)	173.07(3)	C(1)-Te(1)-C(12)	92.8(2)
Te(2)-Pd(1)-Cl(1)	175.27(4)	Pd(1)-Te(2)-C(6)	100.73(13)
Te(2)-Pd(1)-Cl(2)	88.84(3)	Pd(1)-Te(2)-C(7)	100.09(13)
Cl(1)-Pd(1)-Cl(2)	93.35(4)	C(6)-Te(2)-C(7)	96.4(2)

Figure 3.14 - Crystal structure of [PtCl$_2$([18]aneO$_4$Te$_2$)] with numbering scheme adopted. Ellipsoids are drawn at the 40% probability level and H atoms are omitted for clarity

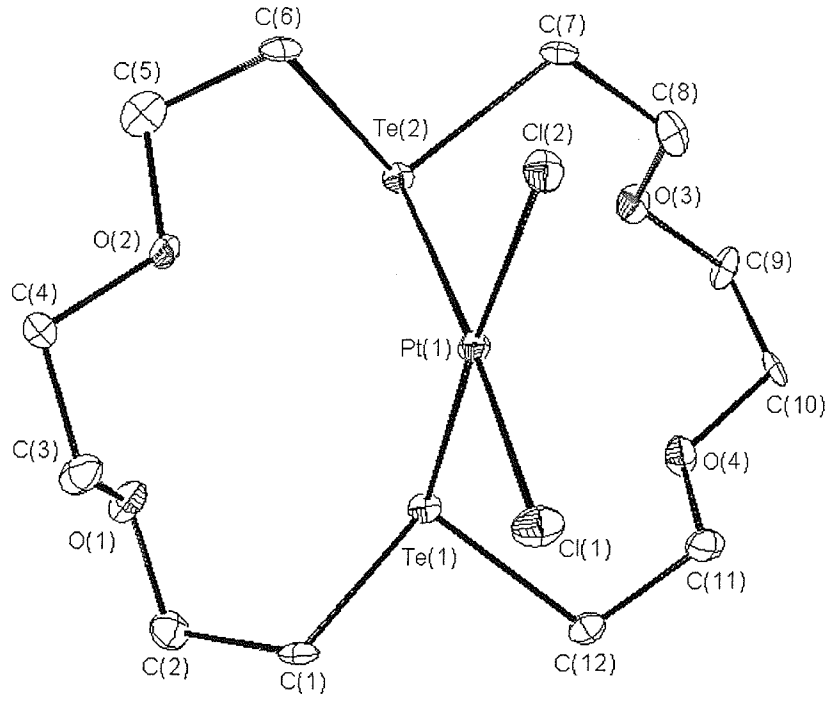

Table 3.2 - Selected bond lengths (Å) and angles (°) for cis-[PtCl$_2$([18]aneO$_4$Te$_2$)]

Bond Lengths			
Pt(1)-Te(1)	2.5357(6)	Te(1)-C(1)	2.164(9)
Pt(1)-Te(2)	2.5322(6)	Te(1)-C(12)	2.159(8)
Pt(1)-Cl(1)	2.344(2)	Te(2)-C(6)	2.156(9)
Pt(1)-Cl(2)	2.356(2)	Te(2)-C(7)	2.161(9)
Bond Angles			
Te(1)-Pt(1)-Te(2)	88.81(2)	Pt(1)-Te(1)-C(1)	105.5(2)
Te(1)-Pt(1)-Cl(1)	90.87(6)	Pt(1)-Te(1)-C(12)	101.7(2)
Te(1)-Pt(1)-Cl(2)	174.96(6)	C(1)-Te(1)-C(12)	93.0(3)
Te(2)-Pt(1)-Cl(1)	176.12(6)	Pt(1)-Te(2)-C(6)	101.2(3)
Te(2)-Pt(1)-Cl(2)	89.68(5)	Pt(1)-Te(2)-C(7)	100.6(2)
Cl(1)-Pt(1)-Cl(2)	90.97(7)	C(6)-Te(2)-C(7)	

Figure 3.15 - Crystal structure of [PtCl$_2$([18]aneO$_4$Se$_2$)] with numbering scheme adopted. Ellipsoids are drawn at the 40% probability level and H atoms are omited for clarity

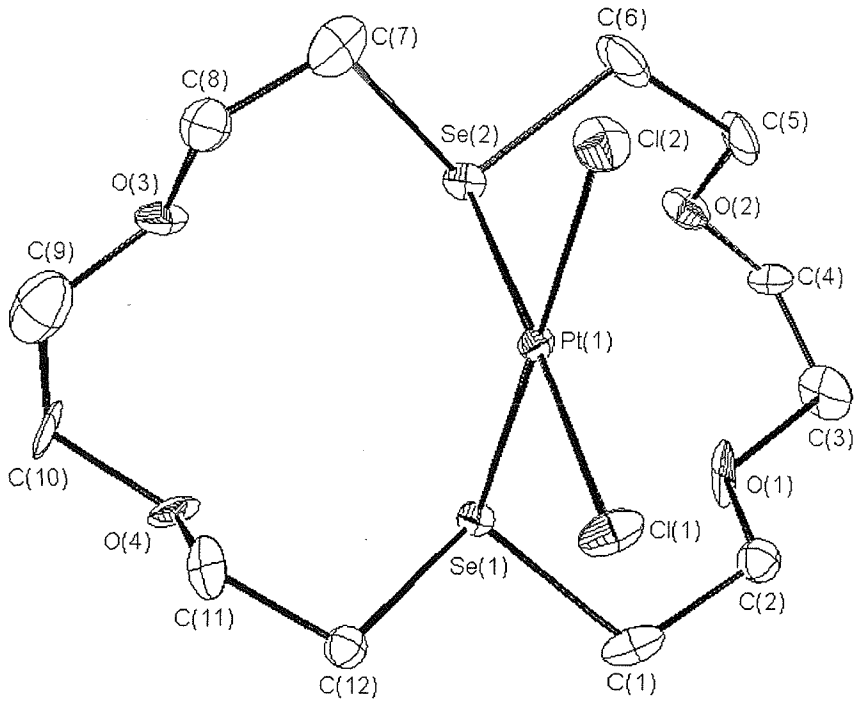

Table 3.3 - Selected bond lengths (Å) and angles (°) for cis-[PtCl$_2$([18]aneO$_4$Se$_2$)]

Bond Lengths			
Pt(1)-Se(1)	2.391(2)	Se(1)-C(1)	1.96(2)
Pt(1)-Se(2)	2.390(2)	Se(1)-C(12)	1.95(2)
Pt(1)-Cl(1)	2.325(4)	Se(2)-C(6)	1.94(2)
Pt(1)-Cl(2)	2.334(4)	Se(2)-C(7)	1.98(2)
Bond Angles			
Se(1)-Pt(1)-Se(2)	86.57(6)	Pt(1)-Se(1)-C(1)	105.2(6)
Se(1)-Pt(1)-Cl(1)	91.59(11)	Pt(1)-Se(1)-C(12)	101.3(5)
Se(1)-Pt(1)-Cl(2)	178.30(12)	C(1)-Se(1)-C(12)	96.1(7)
Se(2)-Pt(1)-Cl(1)	177.91(12)	Pt(1)-Se(2)-C(6)	103.1(6)
Se(2)-Pt(1)-Cl(2)	91.74(12)	Pt(1)-Se(2)-C(7)	102.4(5)
Cl(1)-Pt(1)-Cl(2)	90.1(2)	C(6)-Se(2)-C(7)	98.5(8)

The compounds [MCl_2([18]aneO$_4$Te$_2$)] (M = Pd or Pt) were isomorphous, and both crystallised in the space group $P2_1/n$, however [$PtCl_2$([18]aneO$_4$Se$_2$)] was isomorphous with the related thioether compounds [$PdCl_2$([18]aneO$_4$S$_2$)] and [$PtCl_2$([18]aneO$_4$S$_2$)] which crystallise in the space group $P2_12_12_1$.

The M-Te (*trans* Cl) bond lengths in [MCl_2([18]aneO$_4$Te$_2$)] were 2.3474(13), 2.3618(12) Å and 2.344(2), 2.356(2) Å for M = Pd and Pt, while in [$PtCl_2$([18]aneO$_4$Se$_2$)] the Pt-Se (*trans* Cl) bond lengths were 2.325(4) and 2.334(4) Å. The bond lengths are slightly shorter than those reported for d(Pd-Te) (*trans* Br) in *cis*-[$PdBr_2$(PhTe(CH$_2$)$_3$TePh)] (2.528(1) and 2.525(1) Å)[22] and d(Pt-Te) (*trans* Cl) in [PtCl(MeS(CH$_2$)$_3$Te(CH$_2$)$_3$SMe)][PF_6] (2.5258(11) and 2.5191(12) Å) (Chapter 4). Also of note are the Pd-S bond distances in [$PdCl_2$([18]aneO$_4$S$_2$)] (2.302(2) and 2.305(2) Å).[8] These data show that the E-Pt (E = S, Se or Te) bond lengths increase in the order Te > Se > S, *i.e.* as Group 16 is descended, paralleling the increase in covalent radius of the donor atom. The average Pt-Cl bond lengths in [$PtCl_2$([18]aneO$_4$S$_2$)][9] (2.32 Å), [$PtCl_2$([18]aneO$_4$Se$_2$)] (2.33 Å) and [$PtCl_2$([18]aneO$_4$Te2)] (2.35 Å) show a *trans* influence in the order S < Se < Te. A comparison of the structures [MCl_2([18]aneO$_4$E$_2$)] (M = Pd or Pt, E = S or Te) reveals that the average M-E distance for M = Pt (2.28, 2.53 Å for E = S and Te respectively) is slightly shorter than the corresponding bond length where M = Pd (2.30 and 2.55 Å for E = S and Te). The opposite, although less clear trend is observed for the M-Cl bond lengths; for M = Pt, d(M-Cl) = 2.32 and 2.35 Å for E = S and Te respectively, and for M = Pd, d(M-Cl) for E = S and Te are 2.31 and 2.35 Å respectively.

3.8 [$RhCl_2$([18]aneO$_4$Te$_2$)$_2$]Cl and [$RhCl_2$([18]aneO$_4$Te$_2$)$_2$][PF_6]

The room-temperature reaction of $RhCl_3.3H_2O$ with two equivalents of [18]aneO$_4$Te$_2$ in EtOH-CH_2Cl_2 produced an orange-brown solid. The product was very poorly soluble in common solvents such as CH_2Cl_2, dmso, MeCN and acetone which prevented the acquisition of ^{125}Te-{^{1}H} NMR data, however microanalytical data were consistent with the formulation [$RhCl_2$([18]aneO$_4$Te$_2$)$_2$]Cl. The ^{1}H NMR spectrum, however, showed a broad multiplet resonance in the region δ 3.0 – 4.5 ppm, showing a high frequency shift

upon coordination of [18]aneO$_4$Te$_2$ to the Rh(III) centre. The electrospray mass spectrum showed an ion multiplet at *ca. m/z* = 1154, with the correct isotopic distribution for the cation [RhCl$_2$([18]aneO$_4$^{130}Te$_2$)$_2$]$^+$ (*m/z* = 1158). The UV/visible spectrum showed a d-d band at 28 820 cm^{-1}, which suggested the presence of a *cis* isomer. *Trans* isomers of related complexes typically have much lower first d-d transitions, for example *trans*-[RhCl$_2${MeTe(CH$_2$)$_3$TeMe}$_2$]PF$_6$ has a d-d band at 21 800 cm^{-1}.[27] The presence of a *cis* isomer was supported by the IR spectrum, which showed two ν(Rh-Cl) bands at 335 and 324 cm^{-1}, although the absence of crystallographic or ^{125}Te-{^{1}H} NMR data prevented unambiguous determination of the coordination environment. When the reaction was performed in the presence of one equivalent of NH$_4$PF$_6$, the corresponding PF$_6^-$ salt was isolated, this being confirmed by the presence of PF$_6^-$ absorptions in the IR spectrum at 835 and 560 cm^{-1}. The complex was also very insoluble.

3.9 [Cu([18]aneO$_4$Te$_2$)$_2$][BF$_4$] and [Ag([18]aneO$_4$Te$_2$)$_2$][BF$_4$]

The reaction of [Cu(MeCN)$_4$][BF$_4$][28] or AgBF$_4$ with 2.2 molar equivalents of [18]aneO$_4$Te$_2$ in MeCN produced the compounds [Cu([18]aneO$_4$Te$_2$)$_2$][BF$_4$] and [Ag([18]aneO$_4$Te$_2$)$_2$][BF$_4$] respectively. Microanalytical data were consistent with the proposed formulations, while the electrospray mass spectra showed ion multiplets corresponding to [M([18]aneO$_4$^{130}Te$_2$)$_2$]$^+$ at *ca. m/z* = 1039 and 1085 for M = Cu and Ag respectively. IR spectroscopy of the solids confirmed the presence of BF$_4^-$ anion at *ca.* 1080 and 525 cm^{-1} respectively. ^{1}H NMR spectroscopy of [Cu([18]aneO$_4$Te$_2$)$_2$][BF$_4$] in CDCl$_3$ showed a broad resonance at δ 2.90 ppm, which was assigned to the TeC*H*$_2$ protons of the compound. This showed a high frequency shift from uncoordinated [18]aneO$_4$Te$_2$ (δ(TeC*H*$_2$) = 2.80 ppm). The C*H*$_2$O resonances were essentially unshifted from those in free [18]aneO$_4$Te$_2$ and were observed at δ 3.60 and 3.80 ppm (free [18]aneO$_4$Te$_2$ = 3.57 and 3.85 ppm). The ^{1}H NMR spectrum of [Ag([18]aneO$_4$Te$_2$)$_2$][BF$_4$] was very similar, also showing a high frequency shift for the TeC*H*$_2$ protons (δ = 2.95 ppm, with the C*H*$_2$O environments essentially unshifted (δ = 3.55 and 3.85 ppm). ^{125}Te-{^{1}H} NMR spectra of the complexes in CH$_2$Cl$_2$-CDCl$_3$ showed small low frequency coordination shifts compared to free ligand, with δ(^{125}Te) =

166 and 140 ppm for [Cu([18]aneO$_4$Te$_2$)$_2$][BF$_4$] and [Ag([18]aneO$_4$Te$_2$)$_2$][BF$_4$] respectively. Such low frequency coordination shifts are commonly observed for Cu(I) and Ag(I) telluroether complexes, for example ([Cu(MeS(CH$_2$)$_3$Te(CH$_2$)$_3$SMe)][BF$_4$] had $\delta(^{125}Te)$ = 99 ppm and [Ag(MeS(CH$_2$)$_3$Te(CH$_2$)$_3$SMe)][CF$_3$SO$_3$] had $\delta(^{125}Te)$ = 136 ppm, both to low frequency of MeS(CH$_2$)$_3$Te(CH$_2$)$_3$TeMe ($\delta(^{125}Te)$ = 241 ppm) (Chapter 4). The broad resonances observed for [Ag([18]aneO$_4$Te$_2$)$_2$][BF$_4$] in the ^{1}H and ^{125}Te-{^{1}H} NMR spectra ($w_{½}$ = 1500 Hz) suggested that fast dissociation/exchange processes were occurring in solution. The addition of varying amounts of [18]aneO$_4$Te$_2$ to the NMR solution of [Cu([18]aneO$_4$Te$_2$)$_2$][BF$_4$] produced single ^{125}Te-{^{1}H} resonances with shifts that varied according to the temperature and amount of [18]aneO$_4$Te$_2$ added, which provided evidence for fast exchange processes occurring in solution. The broad ^{1}H NMR spectrum of this compound also suggested a dynamic system. Pure [Cu([18]aneO$_4$Te$_2$)$_2$][BF$_4$] did not show a ^{63}Cu NMR spectrum, however with the addition of excess [18]aneO$_4$Te$_2$, a broad resonance at δ -59 ppm ($w_{½}$ = 11 000 Hz) was observed. This was consistent with the tetrahedral species [Cu([18]aneO$_4$Te$_2$)$_2$]$^+$ in which the quadrupolar relaxation of the ^{63}Cu nucleus (I = 3/2, 69.09%)[29] had been slowed significantly.[30]

When the reactions were carried out using a 2 : 1 ratio of [Cu(MeCN)$_4$][BF$_4$] or AgCF$_3$SO$_3$ to [18]aneO$_4$Te$_2$, compounds having the stoichiometry [Cu$_2$([18]aneO$_4$Te$_2$)][BF$_4$]$_2$ or [Ag$_2$([18]aneO$_4$Te$_2$)][CF$_3$SO$_3$]$_2$ respectively were isolated. The formulations were confirmed by the microanalytical data, however both compounds were very insoluble in common solvents and were not further studied. On the basis of their insolubilities, the compounds were thought likely to be oligomeric in nature, as is common for Ag(I) and Cu(I) Group 16 complexes.[31]

3.10 Conclusions

The new macrocyclic compounds [18]aneO$_4$Te$_2$ and [9]aneO$_2$Te were synthesised *via* the reaction of Cl(CH$_2$)$_2$O(CH$_2$)$_2$O(CH$_2$)$_2$Cl and Na$_2$Te in NH$_{3(l)}$ at -78°C. The separation of the two species present in the crude reaction product was successfully accomplished by recrystallisation and column chromatography on silica using hexane-ethyl acetate 3 : 1 as eluent, and the compounds were isolated as pure solids in *ca.* 55 and 4% yields respectively. The identities of the macrocyclic compounds were confirmed by ^{1}H, ^{13}C-{^{1}H} and ^{125}Te-{^{1}H} NMR spectroscopy, IR spectroscopy and low resolution EI mass spectrometry. The formation of the [1+1] and [2+2] cyclisation products from the reaction is unlike that reported for the formation of the thia-tellura macrocyclic compounds [9]-, [11]- and [12]-aneS$_2$Te, in which the reaction of the appropriate α,ω-dichlorodithioether with Na$_2$Te formed only the [1+1] cyclisation products, with no evidence for higher ring compounds (Chapter 2). A possible reason for the dominance of the [2+2] cyclisation product, [18]aneO$_4$Te$_2$ in the oxa-tellura chemistry may be the templating effect of Na$^+$ in the reaction, which is supported by the presence of the [[18]aneO$_4$Te$_2$Na]$^+$ cation in the electrospray mass spectrum. The formation of [9]aneO$_2$Se and [18]aneO$_4$Se$_2$ *via* a similar route was much less successful, with widely varying yields of the two compounds and large amounts of oligomer formation.

The new compound [18]aneO$_4$Te$_2$ has been shown to react with Cl$_2$ in CH$_2$Cl$_2$ to form the Te(IV) organo-derivative [18]aneO$_4$Te$_2$Cl$_2$, and treatment of [18]aneO$_4$Te$_2$ and [9]aneO$_2$Te with excess MeI in CH$_2$Cl$_2$ formed the methiodide derivatives [18]aneO$_4$Te$_2$MeI and [9]aneO$_2$TeMeI respectively. All of the derivatives had characteristic ^{1}H, ^{13}C-{^{1}H} and ^{125}Te-{^{1}H} NMR spectra, and microanalytical data on [18]aneO$_4$Te$_2$MeI and [9]aneO$_2$TeMeI confirmed their formulations.

The new macrocyclic ligands [9]aneO$_2$Te and [18]aneO$_4$Te$_2$ have been shown to coordinate to a variety of transition metal ions (Pd(II), Pt(II), Rh(III), Cu(I) and Ag(I)) and crystal structures of [MCl$_2$([18]aneO$_4$Te$_2$)] confirm the expected square planar geometry and the identity of the macrocycle.

Table 3.4 - Crystallographic parameters

	[PdCl$_2$([18]aneO$_4$Te$_2$)]	**[PtCl$_2$([18]aneO$_4$Te$_2$)]**	**[PtCl$_2$([18]aneO$_4$Se$_2$)]**
Formula	$C_{12}H_{24}Cl_2O_4PdTe_2$	$C_{12}H_{24}Cl_2O_4PtTe_2$	$C_{12}H_{24}Cl_2O_4PtSe_2$
M	664.83	753.52	656.24
Crystal system	Monoclinic	Monoclinic	Orthorhombic
Space group	$P2_1/n$	$P2_1/n$	$P2_12_12_1$
a/Å	10.5109(3)	10.5179(3)	9.1685(2)
b/Å	15.9002(5)	15.9441(5)	9.5824(2)
c/Å	10.9837(3)	11.0394(3)	20.5134(5)
β/°	96.8439(11)	96.440(2)	90
U/Å^3	1822.58(8)	1839.61(8)	1802.10(6)
Z	4	4	4
μ(Mo-Kα)/mm^{-1}	4.460	11.007	12.102
Unique reflections	4281	4369	3165
Obs. reflections with [I>2σ(I)]	3811	3517	3055
R	0.0370	0.0464	0.0555
R_w	0.0470	0.0500	0.0650

$$R = \Sigma(|F_{obs}|_i - |F_{calc}|_i)/\Sigma|F_{obs}|_i;\ R_w = \sqrt{[\Sigma\ w_i(|F_{obs}|_i - |F_{calc}|_i)^2/\Sigma\ w_i|F_{obs}|_i^2]}$$

3.11 Experimental

The $Cl(CH_2)_2O(CH_2)_2O(CH_2)_2Cl$ was obtained from Aldrich, $[Cu(MeCN)_4][BF_4]$ was synthesised according to the literature method[28] and $[MX_2(MeCN)_2]$ (M = Pd and Pt; X = Cl and Br) were prepared *in situ* according to the literature method.[20]

[18]aneO$_4$Te$_2$

$NH_{3(l)}$ (600 cm^3) was condensed at -78°C in a 1L flask, and Na (1.48g, 64 mmol) added, followed by freshly ground Te powder (3.28g, 26 mmol). The mixture was allowed to warm to -33°C until a white precipitate of Na_2Te was observed, and then re-cooled to -78°C. A solution of $Cl(CH_2)_2O(CH_2)_2O(CH_2)_2Cl$ (4.81g, 26 mmol) in dry thf (*ca.* 100 cm^3) was added dropwise over a period of 30 minutes, and the mixture allowed to slowly warm to room temperature overnight. The resulting yellow-orange mixture was hydrolysed with water (100 cm^3), extracted with CH_2Cl_2 (2 × *ca.* 200 cm^3) and the combined organic extracts dried ($MgSO_4$). The mixture was then filtered to produce a clear orange solution and the solvent removed *in vacuo* to give a pale orange solid. This was recrystallised from CH_2Cl_2-Et_2O at -18°C to produce a yellow solid. Yield 3.39g, 54%. Mpt. 49°C. EIMS: found *m/z* = 488; calculated for $[C_{12}H_{24}O_4{}^{128}Te_2]^+$ and $[C_{12}H_{24}O_4{}^{126}Te^{130}Te]^+$ 488. ^{1}H NMR ($CDCl_3$): δ 2.80 (t, 8H, C*H*$_2$Te), 3.57 (s, 8H, OCH$_2$C*H*$_2$O), 3.85 (t, 8H, TeCH$_2$C*H*$_2$O). ^{13}C-{^{1}H} NMR ($CDCl_3$): δ 2.6 (*C*H$_2$Te), 70.0, 73.4 (*C*H$_2$O). ^{125}Te-{^{1}H} NMR (CH_2Cl_2): δ 176. IR ν/cm^{-1} (CsI disk): 2885w, 1472w, 1419w, 1354m, 1317w, 1263w, 1117vs, 1032w, 964s, 879w, 835w, 738w, 668w, 624w, 555w, 492w.

[9]aneO$_2$Te

The crude reaction mixture, as isolated above, was dissolved in CH_2Cl_2 and absorbed onto a silica column and eluted with hexane: ethyl acetate 3:1. The first fraction to elute was an orange oil having δ(^{125}Te) (CH_2Cl_2) = 288 ppm. The remaining fractions had identical ^{125}Te-{^{1}H} NMR spectra, and were therefore recombined and the solvent removed to give a yellow, microcrystalline solid (0.31g, 4% based on Te). The majority of the crude material ([18]aneO$_4$Te$_2$) did not elute – this, however, could be partly

recovered by stirring the silica in dmf overnight, followed by removal of the solvent by distillation and recrystallisation of the solid from CH_2Cl_2-Et_2O. Mpt. 70-72°C. EIMS: found *m/z* = 246; calculated for $[C_6H_{12}O_2{}^{130}Te]^+$ 246. ^{1}H NMR ($CDCl_3$): δ 2.85 (t, 4H, C*H*$_2$Te), 3.65 (s, 4H, OCH$_2$C*H*$_2$O), 3.80 (t, 4H, TeCH$_2$C*H*$_2$O). ^{13}C-{^{1}H} NMR ($CDCl_3$): δ 2.2 (*C*H$_2$Te), 70.3, 74.0 (*C*H$_2$O). ^{125}Te-{^{1}H} NMR (CH_2Cl_2): δ 200. IR ν/cm^{-1} (CsI disk): 2874w, 1471w, 1433w, 1400w, 1361w, 1344w, 1262m, 1234w, 1184w, 1113br m, 1035m, 991m, 958m, 892s, 875s, 804s, 760s, 726w, 666w, 616m, 555w, 456m, 395m, 351w, 257w.

[9]aneO$_2$Se and [18]aneO$_4$Se$_2$

Method 1. To a solution of Na_2Se, generated as for Na_2Te above, using $NH_{3(l)}$ (600 cm^3), Na(s) (1.72g, 75 mmol) and freshly ground Se powder (2.36g, 30 mmol) was added Cl(CH$_2$)$_2$O(CH$_2$)$_2$O(CH$_2$)$_2$Cl (5.60g, 30 mmol) in dry thf (100 cm^3). The addition was carried out over a period of approximately two hours at the boiling point of ammonia (-33°C). The reaction mixture was allowed to warm to room temperature overnight, then hydrolysed (100 cm^3), extracted with CH_2Cl_2 (2 × *ca.* 200 cm^3) and the combined organic extracts dried ($MgSO_4$). Filtration and removal of the solvent afforded a yellow oil (4.46g). Kugelröhr distillation of the crude product (0.2 mmHg) gave low boiling point non-selenium containing fractions, together with an oil which distilled at 200°C and a residue (which would not distill). The oil was found to contain highly variable quantities of [9]aneO$_2$Se and [18]aneO$_4$Se$_2$ by ^{77}Se-{^{1}H} NMR spectroscopy; in some cases [9]aneO$_2$Se was dominant and in others was present in trace amounts. Separation was achieved by sublimation of the oil *in vacuo* onto a $N_{2(l)}$ cold finger, leaving [9]aneO$_2$Se as a yellow oil and the less volatile [18]aneO$_4$Se$_2$ as the solid residue.

[9]aneO$_2$Se. EIMS: found *m/z* = 196; calculated for $[C_6H_{12}O_2{}^{80}Se]^+$ 196. ^{1}H NMR ($CDCl_3$): δ 2.90 (t, 4H, C*H*$_2$Se), 3.65 (s, 4H, C*H*$_2$O), 4.10 (t, 4H, SeCH$_2$C*H*$_2$O). ^{13}C-{^{1}H} NMR ($CDCl_3$): δ 23.3 (*C*H$_2$Se), 72.5, 75.5 (*C*H$_2$O). ^{77}Se-{^{1}H} NMR (CH_2Cl_2): δ 204.

[18]aneO$_4$Se$_2$. EIMS: found *m/z* = 392; calculated for $[C_{12}H_{24}O_4{}^{80}Se_2]^+$ 392. ^{1}H NMR ($CDCl_3$): δ 2.78 (t, 8H, C*H*$_2$Se), 3.59 (s, 8H, C*H*$_2$O), 3.73 (t, 8H, SeCH$_2$C*H*$_2$O). ^{13}C-{^{1}H} NMR ($CDCl_3$): δ 23.5 (*C*H$_2$Se), 71.3, 71.5 (*C*H2O). ^{77}Se-{^{1}H} NMR (CH_2Cl_2): δ 144.

Method 2. Na_2Se was generated similarly, using $NH_{3(l)}$ (300 cm^3), Na(s) (1.72g, 75 mmol) and freshly ground Se powder (2.36g, 30 mmol), and the mixture left to warm to room temperature overnight. The resulting white solid (Na_2Se) was redissolved in dry EtOH (1000 cm^3) and a solution of $Cl(CH_2)_2O(CH_2)_2O(CH_2)_2Cl$ (5.60g, 30 mmol) in dry EtOH (1000 cm^3) added slowly dropwise over a period of 7 hours. The mixture was then stirred at room temperature overnight, refluxed for 1 hour, allowed to cool and hydrolysed (100 cm^3). The mixture was then filtered and the solvent removed. The residue was extracted with CH_2Cl_2 (2 × *ca.* 60 cm^3) and the combined extracts dried ($MgSO_4$), filtered and the solvent removed *in vacuo* to produce a viscous yellow oil (yield 5.00g). The oil was recrystallised from CH_2Cl_2-hexane to produce impure [18]aneO$_4$Se$_2$ (1g). The mother liquor was reduced to dryness and the residue Kugelröhr distilled to produce four fractions, leaving a residue behind. Fraction 1 distilled at ≤ 125°C (2 mmHg) and was found to be [9]aneO$_2$Se ($\delta(^{77}Se\text{-}\{^1H\})$ = 203), yield 0.25g. Fractions 2 and 3 both distilled at ≤ 200°C (2 mmHg). Fraction 2 was largely diselenide ($\delta(^{77}Se\text{-}\{^1H\})$ = 227) yield 0.09g, while fraction 3 ($\delta(^{77}Se\text{-}\{^1H\})$ = 144) was [18]aneO$_4$Se$_2$, yield 0.050g.

[18]aneO$_4$Te$_2$Me$_2$I$_2$

A solution of [18]aneO$_4$Te$_2$ (0.08g, 0.15 mmol) and excess MeI (*ca.* 1 cm^3) in CH_2Cl_2 (40 cm^3) were stirred at room temperature for 1 hour. The solution was concentrated (10 cm^3) and added to ice-cold Et_2O to produce a precipitate. This was filtered off, washed with Et_2O and dried *in vacuo* to give a pale yellow powdered solid, which quickly turned into a waxy orange solid upon storage. Yield 0.13g, 83%. Calc. for $[C_{14}H_{30}I_2O_4Te_2].CH_2Cl_2$: C, 20.4; H, 3.6%. Found: C, 20.8; H, 3.7%. ESMS: found *m/z* = 645; calculated for $[C_{14}H_{30}O_4{}^{126}Te^{130}TeI]^+$ and $[C_{14}H_{30}O_4{}^{128}Te_2I]^+$ 645. ^1H NMR (d_6-dmso): δ 2.3 (s, 3H, CH_3Te), 3.2 (m, 4H, CH_2Te), 3.6, 3.9 (m, 8H, CH_2O), 5.40 (s, 1H, CH_2Cl_2). $^{13}C\text{-}\{^1H\}$ NMR (d_6-dmso): δ 4.3 (CH_3Te), 25.9 (CH_2Te), 57.0 (CH_2Cl_2), 66.2, 69.9 (CH_2O). $^{125}Te\text{-}\{^1H\}$ NMR (d_6-dmso): δ 506. IR ν/cm^{-1} (CsI disk): 2941w, 2920w, 2875m, 2850w, 1483m, 1400m, 1386m, 1352m, 1345m, 1251m, 1211w, 1128s, 1113s, 1101s, 1053m, 999m, 955w, 899m, 842m, 742w, 610w, 531w, 466w.

[18]aneO$_4$Se$_2$Me$_2$I$_2$

This was prepared similarly, using [18]aneO$_4$Se$_2$ (0.07g, 0.018 mmol) to give a yellow solid. Yield 0.05g, 43%. Calc. for [$C_{14}H_{30}I_2O_4Se_2$]: C, 24.9; H, 4.1%. Found C, 25.3; H, 4.3%. ESMS: found *m/z* = 549, 211; calculated for [$C_{14}H_{30}IO_4{}^{80}Se_2$]$^+$ 549, calculated for [$C_{14}H_{30}O_4{}^{80}Se_2$]$^{2+}$ 211. ^{1}H NMR (d$_6$-dmso): δ 2.90 (s, 6H, C*H*$_3$Se), 3.78 (t, 8H, C*H*$_2$Se), 3.59 (s, 8H, C*H*$_2$O), 3.80 (t, 8H, SeCH$_2$C*H*$_2$O). ^{13}C-{^{1}H} NMR (CH_2Cl_2-$CDCl_3$): δ 19.2 (*C*H$_3$Se), 24.6 (*C*H$_2$Se), 65.5, 70.1 (*C*H$_2$O). ^{77}Se-{^{1}H} NMR (CH_2Cl_2-$CDCl_3$): δ 318.

[9]aneO$_2$TeMeI

This was prepared similarly, using [9]aneO$_2$Te (0.08g, 33 mmol). Yield 0.096g, 75%. Calc. for [$C_7H_{15}IO_2Te$]: C, 21.8; H, 3.9%. Found: C, 21.6; H, 3.7%. ESMS: found *m/z* = 261; calculated for [$C_7H_{15}O_2{}^{130}Te$]$^+$ 261. ^{1}H NMR (d$_6$-dmso): δ 2.3 (s, 3H, C*H*$_3$Te), 3.25 (m, 4H, C*H*$_2$Te), 3.60, 3.85 (m, 8H, C*H*$_2$O). ^{13}C-{^{1}H} NMR (d$_6$-dmso): δ 2.0 (*C*H$_3$Te), 24.9 (*C*H$_2$Te), 64.5, 68.4 (*C*H$_2$O). ^{125}Te-{^{1}H} NMR (d$_6$-dmso): δ 520. IR ν/cm^{-1} (CsI disk): 2944w, 2913w, 2880m, 2855w, 1480m, 1450w, 1397m, 1388m, 1359m, 1347m, 1257m, 1219w, 1173w, 1132s, 1117s, 1103s, 1057m, 997m, 950w, 897m, 845m, 734w, 612w, 534w, 462w.

[9]aneO$_2$SeMeI

This was prepared similarly to give a pale yellow solid. Yield 0.016g, 62%. ESMS: found *m/z* = 211; calculated for [$C_7H_{15}IO_2{}^{80}Se$]$^+$ 211. ^{1}H NMR (d$_6$-dmso): δ 2.90 (s, 3H, C*H*$_3$Se), 3.65 (t, 4H, C*H*$_2$Se), 3.55 (s, 4H, C*H*$_2$O), 3.70 (t, 4H, SeCH$_2$C*H*$_2$O). ^{13}C-{^{1}H} NMR (CH_2Cl_2-$CDCl_3$): δ 22.6 (*C*H$_3$Se), 43.4 (*C*H$_2$Se), 70.8, 71.6 (*C*H$_2$O). ^{77}Se-{^{1}H} NMR (CH_2Cl_2-$CDCl_3$): δ 354.

[18]aneO$_4$Te$_2$Cl$_4$

Cl_2 (generated from HCl + $KMnO_4$) was bubbled through a solution of [18]aneO$_4$Te$_2$ (0.10g, 0.20 mmol) in CH_2Cl_2 (40 cm^3) for 1 minute to produce a colourless solution. The reaction was stirred for a further 30 minutes, concentrated (5 cm^3) and the product precipitated with ice-cold Et_2O. The precipitate was filtered and dried *in vacuo* to give a white solid that darkened on storage to a black gum. Yield 0.13g, 99%. Calc. for

[$C_{12}H_{24}Cl_4O_4Te_2$].CH_2Cl_2: C, 21.8; H, 3.6%. Found C, 21.0; H, 3.4%. ESMS: found *m/z* = 595; calculated for [$C_{12}H_{24}{}^{35}Cl_2{}^{37}ClO_4{}^{126}Te{}^{130}Te$]$^+$ and [$C_{12}H_{24}{}^{35}Cl_2{}^{37}ClO_4{}^{128}Te_2$]$^+$ 595. ^{1}H NMR ($CDCl_3$): δ 4.2 (m, 1H, C*H*$_2$Te), 3.6-3.8 (m, 4H, C*H*$_2$O), 5.40 (s, 1H, C*H*$_2$Cl$_2$). ^{13}C-{^{1}H} NMR (CH_2Cl_2): δ 15.5 (*C*H$_2$Te), 65.4, 66.0 (*C*H$_2$O). ^{125}Te-{^{1}H} NMR (CH_2Cl_2): δ 850.

[PtCl$_2$([18]aneO$_4$Te$_2$)]

$PtCl_2$ (0.04g, 0.15 mmol) was dissolved in refluxing MeCN (40 cm^3) and the solution allowed to cool and filtered. This was then added dropwise to a gently refluxing solution of [18]aneO$_4$Te$_2$ (0.075g, 0.15 mmol) in CH_2Cl_2 (25 cm^3)-MeCN (100cm^3) over *ca.* 30 minutes. The solution was refluxed gently for a further hour, allowed to cool and stirred overnight, before filtering through celite. The solvent volume was reduced (*ca.* 10 cm^3) and the product precipitated by the addition of Et_2O (*ca.* 5 cm^3). The resultant yellow solid was filtered off, washed with Et_2O and dried *in vacuo*. Yield 0.097g, 76%. Calc. for [$C_{12}H_{24}Cl_2O_4PtTe_2$]: C, 19.3; H, 3.2%. Found C, 19.5; H, 3.0. ^{1}H NMR ($CDCl_3$): δ 3.0-4.4 (m). ^{125}Te-{^{1}H} NMR (CH_2Cl_2-$CDCl_3$): δ 393 ($^1J_{Pt\text{-}Te}$ = 862 Hz). ^{125}Pt NMR (CH_2Cl_2-$CDCl_3$ 223K): δ -4257. IR ν/cm^{-1} (CsI disk): 2929w, 2863w, 1472w, 1455w, 1400m, 1357s, 1262m, 1128vs, 1096vs, 981w, 857w, 762w, 614w, 535w, 308m, 291m. UV/vis (CH_2Cl_2) ν_{max}/cm^{-1} (ε_{mol}/dm^3 mol^{-1} cm^{-1}): 34 435 (4770), 25 560 (965).

[PtBr$_2$(18]aneO$_4$Te$_2$)]

This was prepared similarly using $PtBr_2$. Yield 70%. Calc. for [$C_{12}H_{24}Br_2O_4PtTe_2$]: C, 17.1; H, 2.9%. Found: C, 17.3; H, 2.6%. ^{1}H NMR ($CDCl_3$): δ 3.0-4.4 (m). ^{125}Te-{^{1}H} NMR (CH_2Cl_2-$CDCl_3$ 223K): δ 390 ($^1J_{Pt\text{-}Te}$ = 690 Hz). ^{195}Pt NMR (CH_2Cl_2-$CDCl_3$ 223K): δ -4756. IR ν/cm^{-1} (CsI disk): 2926w, 2893w, 2859w, 1472w, 1396m, 1359s, 1287w, 1261m, 1128vs, 1097vs, 981m, 889w, 760w, 613w, 533w, 320w, 312w, 300w, 223w. UV/vis (CH_2Cl_2) ν_{max}/cm^{-1} (ε_{mol}/dm^3 mol^{-1} cm^{-1}): 36 075 (7310), 30 980 (2670).

[PdCl$_2$([18]aneO$_4$Te$_2$)]

This was prepared similarly using $PdCl_2$. Yield 80%. Calc. for $[C_{12}H_{24}Cl_2O_4PdTe_2].½Et_2O$: C, 24.1; H, 4.1%. Found: C, 23.3; H, 3.2. ^{1}H NMR ($CDCl_3$): δ 3.0-4.5 (m). ^{125}Te-{^{1}H} NMR (CH_2Cl_2-$CDCl_3$ 223K): δ 375. IR ν/cm^{-1} (CsI disk): 2938w, 2867w, 1471w, 1360s, 1261w, 1096s, 988w, 834w, 732w, 615w, 542w, 311w, 302w. UV/vis (CH_2Cl_2) ν_{max}/cm^{-1} (ε_{mol}/dm^3 mol^{-1} cm^{-1}): 30 600 (3900), 25 640 (1775).

[PdBr$_2$([18]aneO$_4$Te$_2$)]

This was prepared similarly using $PdBr_2$ to give an orange solid. Yield 36%. Calc. for $[C_{12}H_{24}Br_2O_4PdTe_2].CH_2Cl_2$: C, 18.6; H, 3.1%. Found: C, 18.1; H, 3.4%. ^{1}H NMR ($CDCl_3$): δ 3.2-4.1 (m), 5.4 (s, C*H*$_2$Cl$_2$). ^{125}Te-{^{1}H} NMR (CH_2Cl_2-$CDCl_3$): δ 373. IR ν/cm^{-1} (CsI disk): 3014w, 2907w, 1360s, 1262m, 1128sh, 1095s, 994sh, 803m, 611w, 313w, 243w, 221w. UV/vis (CH_2Cl_2) ν_{max}/cm^{-1} (ε_{mol}/dm^3 mol^{-1} cm^{-1}): 24 630 (4200), 28 900 (7350).

[PtCl$_2$([18]aneO$_4$Se$_2$)]

Procedure as [PtCl$_2$([18]aneO$_4$Te$_2$)] using [18]aneO$_4$Se$_2$ to give a pale yellow powder. Yield 70%. Calc. for $C_{12}H_{24}Cl_2O_4PtSe_2$]: C, 21.9; H, 3.5%. Found: C, 21.3; H, 3.5%. ^{1}H NMR ($CDCl_3$): δ 3.0-4.4 (m). ^{77}Se-{^{1}H} NMR (CH_2Cl_2-$CDCl_3$): δ 259 ($^1J_{Pt\text{-}Se}$ = 550 Hz). ^{195}Pt NMR (CH_2Cl_2-$CDCl_3$): δ -3861. IR ν/cm^{-1} (CsI disk): 2972w, 2923w, 2890w, 2856w, 1477w, 1464w, 1442w, 1408w, 1374m, 1355m, 1291w, 1272w, 1259w, 1135s, 1100s, 1033w, 1002m, 891m, 880m, 834w, 780w, 614w, 565w, 350m, 322m, 304m. UV/vis (CH_2Cl_2) ν_{max}/cm^{-1} (ε_{mol}/dm^3 mol^{-1} cm^{-1}): 30 640 (880).

[PtCl$_2$([9]aneO$_2$Te)$_2$]

$PtCl_2$ (0.05g, 0.17 mmol) was dissolved in refluxing MeCN (100 cm^3) and [9]aneO$_2$Te (0.09g, 0.35 mmol) in CH_2Cl_2 (80 cm^3)-MeCN (20 cm^3) added slowly over *ca.* 30 minutes. The solution was refluxed for a further hour, allowed to cool and stirred overnight before filtering (celite). The solution was then concentrated (*ca.* 10 cm^3) and Et_2O added to produce a greenish-yellow precipitate that was filtered and dried *in vacuo*.

Yield 0.08g, 62%. Calc. for [$C_{12}H_{24}Cl_2O_4PtTe_2$]: C, 19.3; H, 3.2%. Found: C, 19.8; H, 3.0%. ^{1}H NMR ($CDCl_3$): δ 3.0-4.4 (m). ^{125}Te-{^{1}H} NMR (CH_2Cl_2-$CDCl_3$): δ 394 ($^1J_{Pt\text{-}Te}$ = 975 Hz). ^{195}Pt NMR (CH_2Cl_2-$CDCl_3$): δ -4501. IR ν/cm^{-1} (CsI disk): 2967m, 2912m, 1470w, 1398m, 1355s, 1262m, 1131vs, 1097vs, 978m, 891w, 831w, 759w, 612w, 530w, 311m, 290m. UV/vis (CH_2Cl_2) ν_{max}/cm^{-1} (ε_{mol}/dm^3 mol^{-1} cm^{-1}): 37 940 (10 885), 29 205 (368).

[PdCl$_2$([9]aneO$_2$Te)$_2$]

This was prepared similarly using $PdCl_2$. Yield 65%. Calc. for [$C_{12}H_{24}Cl_2O_4PdTe_2$]: C, 21.7; H, 3.6%. Found: C, 21.9; H, 3.3%. ^{1}H NMR ($CDCl_3$): δ 2.9-4.3 (m). ^{125}Te-{^{1}H} NMR (CH_2Cl_2-$CDCl_3$): δ 387. IR ν/cm^{-1} (CsI disk): 2891m, 2851m, 1473m, 1455w, 1403m, 1390m, 1370m, 1355m, 1291m, 1252m, 1182w, 1128s, 1106sh m, 1054m, 978m, 891m, 757m, 536w, 305m, 283m. UV/vis (CH_2Cl_2) ν_{max}/cm^{-1} (ε_{mol}/dm^3 mol^{-1} cm^{-1}): 30 490 (7810), 26 710 (1862).

[RhCl$_2$([18]aneO$_4$Te$_2$)$_2$]Cl

A solution of $RhCl_3.3H_2O$ (0.027g, 0.10 mmol) in EtOH (100 cm^3) was added slowly to a solution of [18]aneO$_4$Te$_2$ (0.10g, 0.20 mmol) in CH_2Cl_2 (20 cm^3) and the mixture stirred at room temperature overnight. Concentration of the reaction mixture (*ca.* 10 cm^3) followed by the dropwise addition of Et_2O formed an orange precipitate that was subsequently filtered, washed with Et_2O and dried *in vacuo*. Yield 0.06g, 48%. Calc. for [$C_{24}H_{48}Cl_3O_8RhTe_4$]: C, 24.3; H, 4.1%. Found: C, 24.5; H, 3.8%. ESMS: found *m/z* = 1154; calculated for [$C_{24}H_{48}{}^{35}Cl_2O_8Rh^{130}Te_4$]$^+$ 1158. ^{1}H NMR ($CDCl_3$): δ 3.0-4.5 (m). IR ν/cm^{-1} (CsI disk): 2995w, 2913w, 1472w, 1356m, 1264w, 1095s, 986w, 882w, 614w, 538w, 335w, 324w. UV/vis (CH_2Cl_2) ν_{max}/cm^{-1} (ε_{mol}/dm^3 mol^{-1} cm^{-1}): 28 820 (880).

[Cu([18]aneO$_4$Te$_2$)][BF$_4$]

[Cu(MeCN)$_4$][BF_4] (0.129g, 0.41 mmol) and [18]aneO$_4$Te$_2$ (0.100g, 0.20 mmol) were stirred in CH_2Cl_2 (30 cm^3) for *ca.* 2 hours. The solution was then concentrated *in vacuo* (*ca.* 5 cm^3) and Et_2O added to form a precipitate that was filtered off, washed with Et_2O and dried *in vacuo* to give a cream-yellow solid. Yield 0.104g, 82%. Calc. for

[$C_{12}H_{24}BCu_2F_8O_4Te_2$]: C, 18.29; H, 3.07%. Found: C, 17.69; H, 3.02%. ESMS: found *m/z* = 553; calculated for [$C_{12}H_{24}{}^{63}CuO_4{}^{130}Te_2$]$^+$ 553. ^{1}H NMR (d_6-dmso): δ 2.95 (br m, 1H, C*H*$_2$Te), 3.55 (br m), 3.75 (br m) (4H, C*H*$_2$O). IR ν/cm^{-1} (CsI disk): 2978w, 2918w, 1481w, 1453w, 1404w, 1355m, 1290w, 1262w, 1093br vs, 891w, 764w, 524m, 470w.

[Ag([18]aneO$_4$Te$_2$)][CF$_3$SO$_3$]

$AgCF_3SO_3$ (0.158g, 0.62 mmol) and [18]aneO$_4$Te$_2$ (0.15g, 0.31 mmol) were stirred in CH_2Cl_2 (40 cm^3) for one hour, then the solution was concentrated to *ca.* 5 cm^3. The product was precipitated by the addition of Et_2O to the concentrate, and then filtered and washed with Et_2O to give a pale yellow solid. Yield 0.198g, 86%. Calc. for [$C_{14}H_{24}Ag_2F_6O_{10}S_2Te_2$]: C, 16.79; H, 2.42%. Found: C, 16.25; H, 2.43. ESMS: found *m/z* = 597; calculated for [$C_{12}H_{24}{}^{109}AgO_4{}^{130}Te_2$]$^+$ 597. ^{1}H NMR (d_6-dmso): δ 3.02 (t, 1H, C*H*$_2$Te), 3.60 (s), 3.72(t) (4H, C*H*$_2$O). IR ν/cm^{-1} (CsI disk): 2932w, 2865w, 1464w, 1404w, 1352m, 1262s, 1229s, 1164s, 1106s, 1038s, 890w, 759m, 639s, 580m, 514m.

[Cu([18]aneO$_4$Te$_2$)$_2$][BF$_4$]

[Cu(MeCN)$_4$][BF_4] (0.043g, 0.14 mmol) was added to a solution of [18]aneO$_4$Te$_2$ (0.15g, 0.31 mmol) in CH_2Cl_2 (10 cm^3) and the mixture stirred at room temperature overnight. The mixture was then concentrated (*ca.* 5 cm^3) and the product precipitated by the addition of Et_2O. The precipitate was filtered off and dried *in vacuo* to give an orange-brown waxy solid. Yield 0.130g, 85%. Calc. for [$C_{24}H_{48}BCuF_4O_8Te_4$]: C, 25.6; H, 4.3%. Found: C, 25.3; H, 4.3%. ESMS: found *m/z* = 1039; calculated for [$C_{24}H_{48}{}^{63}CuO_8{}^{130}Te_4$]$^+$ 1047. ^{1}H NMR ($CDCl_3$): δ 2.9 (t, 1H, C*H*$_2$Te), 3.6 (s), 3.8 (t) (4H, C*H*$_2$O). ^{63}Cu NMR (CH_2Cl_2-$CDCl_3$ + excess [18]aneO$_4$Te$_2$): δ -59 ($w_{1/2}$ = 11 000 Hz). ^{125}Te-{^{1}H} NMR (CH_2Cl_2-$CDCl_3$): δ 166. IR ν/cm^{-1} (CsI disk): 3014w, 2947w, 1411m, 1359m, 1292w, 1255w, 1080vs br, 830m, 524m.

[Ag([18]aneO$_4$Te$_2$)$_2$][BF$_4$]

$AgBF_4$ (0.027g, 0.15 mmol) in CH_2Cl_2 (*ca.* 10 cm^3) was added to a solution of [18]aneO$_4$Te$_2$ (0.15g, 0.31 mmol) in CH_2Cl_2 (*ca.* 10 cm^3) and the mixture stirred at room temperature in a foil-wrapped vessel for 2 hours. The solution was concentrated (*ca.* 5

cm^3) and pipetted into Et_2O to give a pale orange solid. Yield 0.115g, 72%. Calc. for $[C_{24}H_{48}AgBF_4O_8Te_4]$: C, 24.6; H, 4.1%. Found C, 25.3; H, 4.3%. ESMS: found *m/z* = 1085; calculated for $[C_{24}H_{48}{}^{109}AgO_8{}^{130}Te_4]^+$ 1093. ^{1}H NMR ($CDCl_3$): δ 2.95 (m, 1H, C*H*$_2$Te), 3.55 (m), 3.85 (m) (4H, C*H*$_2$O). ^{125}Te-{^{1}H} NMR (CH_2Cl_2-$CDCl_3$): δ 140 ($w_{1/2}$ = 1500 Hz). IR ν/cm^{-1} (CsI disk): 2962w, 2932w, 2857w, 1358s, 1086vs, 987m, 526m.

X-ray crystallography

Details of the crystallographic data parameters are given in Table 3.4. Crystals of $[PdCl_2([18]aneO_4Te_2)]$ and $[PtCl_2([18]aneO_4Te_2)]$ were grown from solutions of the complexes in CH_2Cl_2, while crystals of $[PtCl_2([18]aneO_4Se_2)]$ were obtained by slow evaporation of a MeOH solution of the compound. Data collection used a Nonius Kappa CCD diffractometer equipped with an Oxford Systems open-flow crysostat operating at 120K, using graphite-monochromated Mo-K_α X-radiation (λ = 0.71073 Å) and was collected by Melissa Matthews. Structure solution and refinement were routine.[32-35]

3.12 References

1. A. Lüttringhaus and K. Ziegler, *Ann. Chem.*, 1937, **528**, 155.
2. C. J. Pedersen, *J. Am. Chem. Soc.*, 1967, **89**, 2495 and 7017.
3. H. K. Frensdorff, *J. Am. Chem. Soc.*, 1971, **93**, 600.
4. E. Weber and F. Vögtle, *Crown Ethers and Analogs*, S. Patai and Z. Rappoport (eds.), Wiley, New York, 1989, 207.
5. V. K. Belsky and B. M. Bulychev, *Russ. Chem. Rev.*, 1999, **68**, 119.
6. J. R. Dann, P. P. Chiesa and J. W. Gates Jr., *J. Org. Chem.*, 1961, **26**, 1991.
7. R. M. Izatt, G. Wu, W. Jiang and N. K. Dalley, *Inorg. Chem.*, 1990, **29**, 3828.
8. B. Metz, D. Moras and R. Weiss, *J. Inorg. Nucl. Chem.*, 1974, **36**, 785.
9. A. A. Dvorkin, Y. A. Simonov, T. I. Malinovskii, S. V. Pavlova and L. I. Budarin, *Russ. J. Inorg. Chem.*, 1989, **34**, 1481.
10. J. S. Bradshaw, J. Y. Hui, B. L. Haymore, J. J. Christensen and R. M. Izatt, *J. Heterocycl. Chem.*, 1973, **10**, 1.
11. H. Higuchi, K. Tani, T. Otsubo, Y. Sakata and S. Misumi, *Bull. Chem. Soc. Jpn.*, 1987, **60**, 4027.
12. W. Levason, S. D. Orchard and G. Reid, *Coord. Chem. Rev.*, 2002, **225**, 159.
13. X. Liu, W. Li, X. Lu and H. Xu, *Chin. Chem. Lett.*, 1992, **3**, 589. (*Chem. Abs.*, 1993, **118**, 39140a).
14. W-P. Li, S-L. Gong, X-F. Liu, X-R. Lu and H-S. Xu, *Gaodeng Xuexiao Huaxue Xuebao*, 1996, **17**, 501.
15. H. Xu, W. Li, X. Liu, L. Shen, X. Mao and M. Li, *Huaxue Xuebao*, 1994, **52**, 386. (*Chem. Abs.*, 1994, **121**, 25539n).
16. V. W-W. Yam, Y-L. Pui, W-P. Li, K. K-W. Lo and K-K. Cheung, *J. Chem. Soc., Dalton Trans.*, 1998, 3615.
17. E. G. Hope, T. Kemmitt and W. Levason, *Organometallics*, 1988, **7**, 78.
18. W. V. Farrar and J. M. Mulland, *J. Chem. Soc.*, 1945, 11.
19. N. P. Luthra and J. D. Odom, in *The Chemistry of Organic Selenium and Tellurium Compounds*, S. Patai and Z. Rappoport (eds.), Wiley, NY, 1986, vol. 1, ch. 6.

20. F. R. Hartley, S. Murray and C. A. McAuliffe, *Inorg. Chem.*, 1979, **18**, 1394.

21. T. Kemmitt and W. Levason, *Inorg. Chem.*, 1990, **29**, 731.

22. T. Kemmitt, W. Levason and M. Webster, *Inorg. Chem.*, 1989, **28**, 692.

23. D. H. O'Brien, N. Dereu, C-K. Huang, K. J. Irgolic and F. F. Knapp Jr., *Organometallics*, 1983, **2**, 305.

24. A. K. Singh, M. Kadarkaraisamy, S. Husebye and K. W. Tornroos, *J. Chem. Res. (S)*, 2000, 64.

25. T. Kemmitt, W. Levason, R. D. Oldroyd and M. Webster, *Polyhedron*, 1992, **11**, 2165.

26. W. Levason, G. Reid and V-A. Tolhurst, *J. Chem. Soc., Dalton Trans.*, 1998, 3411.

27. W. Levason, S. D. Orchard, G. Reid and V-A. Tolhurst, *J. Chem. Soc., Dalton Trans.*, 1999, 2071.

28. G. Kubas, *Inorg. Synth.*, 1990, **28**, 68.

29. R. J. Goodfellow, in *Multinuclear NMR*, J. Mason (ed.), Plenum, New York, 1987, Ch. 21.

30. J. R. Black and W. Levason, *J. Chem. Soc., Dalton Trans.*, 1994, 3225.

31. J. R. Black, N. R. Champness, W. Levason and G. Reid, *J. Chem. Soc., Dalton Trans.*, 1995, 3439.

32. PATTY, The DIRDIF Program System, P. T. Beurskens, G. Admiraal, G. Beurskens, W. P. Bosman, S. Garcia-Granda, R. O. Gould, J. M. M. Smits and C. Smykalla, Technical Report of the Crystallography Laboratory, University of Nijmegen, The Netherlands, 1992.

33. TeXsan: Crystal Structure Analysis Package, Molecular Structure Corporation, Texas, 1995.

34. SHELXL-97: Programme for crystal structure refinement: G. M. Sheldrick, University of Göttingen, 1997.

35. H. D. Flack, *Acta Crystallogr., Sect. A*, 1983, **39**, 876.

Chapter 4:

Transition metal complexes of $MeS(CH_2)_3Te(CH_2)_3SMe$

4.0 Introduction - open-chain tridentate Group 16 ligands

A series of linear tridentate group 16 ligands, all with the general formula $MeE(CH_2)_nE(CH_2)_nEMe$, where n = 2 (E = S or Se) or 3 (E = S, Se or Te) have been reported. The first to be synthesised in 1972 was the homoleptic ligand bis(3-methylthiopropyl)sulfide, $MeS(CH_2)_3S(CH_2)_3SMe$ (L_1). Its reported complexes include $[PtMe_3(L_1)][BF_4]$,[1] in which the tridentate ligand bonds *fac* through all three S donors to the Pt(IV) centre, and $[RuCl_3(L_1)]$, where the ligand also bonds through all three donors to the Ru(III) centre, but this time forming the *mer* isomer, which was identified by three ν(Ru-Cl) absorptions in the far IR spectrum.[2] The Os(III) and Os(IV) complexes $[OsX_3(L_1)]$ (X = Cl, Br) and $[OsX_4(L_1)]$ (X = Cl, Br) have also been reported from the reaction of the ligand with Na_2OsX_6 (X = Cl or Br) with the Os(III) complexes being the major products isolated from the reactions, in typically *ca.* 55% yield. The Os(IV) complexes were isolated as far less soluble species from the same reactions in much lower yields (*ca.* 6%).[2]

Other variants of the trithioether are also known, with the ligands $EtS(CH_2)_3S(CH_2)_3SEt$, $PhS(CH_2)_3S(CH_2)_3SPh$ and $^iPrS(CH_2)_3S(CH_2)_3S^iPr$ having been reported.[3] Of their various Pt complexes, crystal structures of $[PtCl(^iPrS(CH_2)_2S(CH_2)_2S^iPr)][BF_4]$ (Figure 4.0) and $[PtI(PhS(CH_2)_2S(CH_2)_2SPh)][BF_4]$ display distorted square planar geometries about Pt(II), with the ligands adopting the *meso*-B conformation (Figure 4.1), whereby the S-isopropyl and S-phenyl groups are positioned on the same side of the square plane in a *syn* arrangement.[3] The Pt-$S_{transCl}$ and Pt-S_{transI} distances (2.256(4) and 2.280(5) Å) are considerably shorter than the terminal Pt-S bond lengths (2.302(3), 2.306(4) Å for $[PtCl(^iPrS(CH_2)_2S(CH_2)_2S^iPr)][BF_4]$ and 2.293(4), 2.289(4) Å for $[PtI(PhS(CH_2)_2S(CH_2)_2SPh)][BF_4]$) due to the *trans* influence of the Cl and I co-ligands respectively, which is stronger for I than for Cl. The possible invertomers for the Pt(II) complexes (*meso*-A, *meso*-B and *racemic* (DL) forms are shown in Figure 4.1).

Figure 4.0 - Crystal structure of $[PtCl(^iPrS(CH_2)_2S(CH_2)_2S^iPr)]^{+3}$

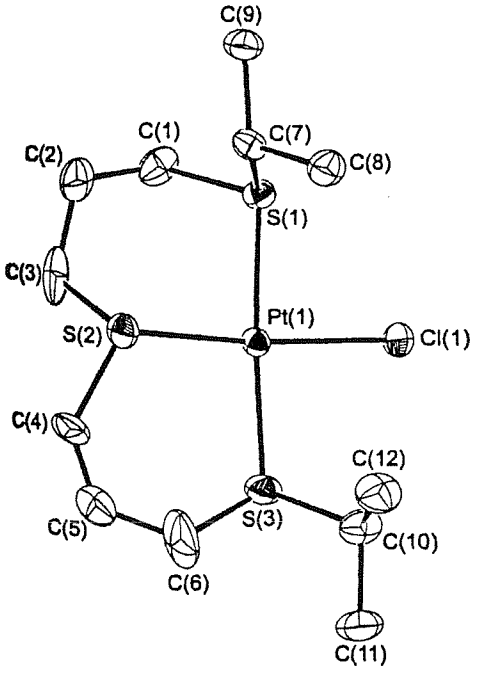

Figure 4.1 - The possible invertomers for the $[PtCl(RS(CH_2)_2S(CH_2)_2SR)]^+$ cations

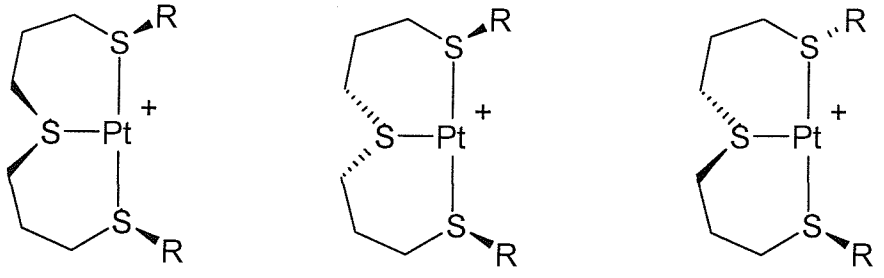

meso-A *meso*-B DL

The analogous homoleptic selenium ligand, 2,6,10-triselenaundecane, $MeSe(CH_2)_3Se(CH_2)_3SeMe$ (L_2) was first reported in 1984 by Levason and co-workers.[4] The ligand was originally prepared from $MeSe(CH_2)_3OTs$, but has also more recently been prepared from $MeSe(CH_2)_3Cl$[5] (Figure 4.2) and forms a *fac*-Mn(I) complex, $[Mn(CO)_3(MeSe(CH_2)_3Se(CH_2)_3SeMe)][CF_3SO_3]$[6] in which the cation adopts a distorted octahedral arrangement, and two Cr(III) complexes, $[CrX_3(L_2)]$ (X = Cl, Br) which were formed *via* the reaction of the ligand with $[CrX_3(thf)_3]$ in anhydrous CH_2Cl_2 solution.[7]

The Cr(III) compounds were tentatively assigned as *mer* isomers on the basis of IR spectroscopy, with UV-visible spectra confirming the presence of *pseudo*-octahedral Cr(III). They were also found to hydrolyse rapidly on exposure to air, and were decomposed by O or N donor solvents. This study demonstrated the weak binding of the soft Se donors to the hard Cr(III) centre.

Figure 4.2 - Synthesis of $MeSe(CH_2)_3Se(CH_2)_3SeMe$[4,5]

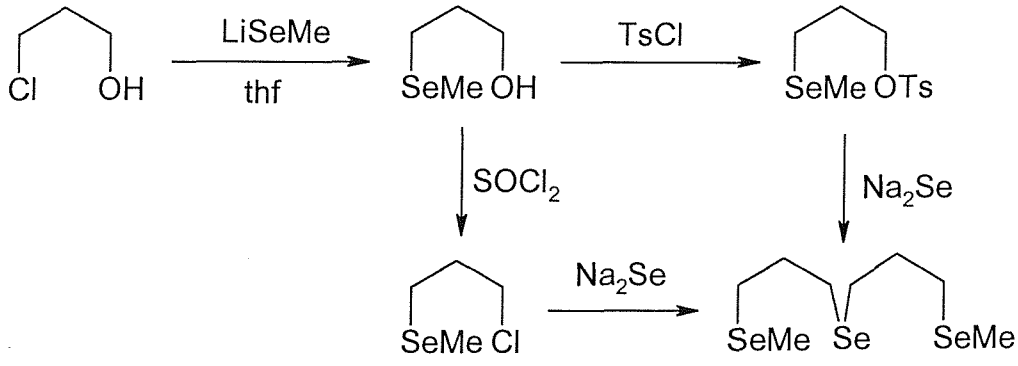

Other reported ligands in the series include the dimethylene linked $MeS(CH_2)_2S(CH_2)_2SMe$ (L_3),[1] for which the known complexes include $[PtMe_3(L_3)][X]$ ($X = BPh_4$, I)[1] $[Mn(CO)_3(L_3)][CF_3SO_3]$[6] and $[WI_2(CO)_3(L_3)_2]$.[8] A crystal structure of the Mn(I) complex displayed the trithioether binding facially to the metal centre, with three CO co-ligands completing the distorted octahedral geometry.[6] The tridentate selenoether $MeSe(CH_2)_2Se(CH_2)_2SeMe$ (L_4)[1] is also known, and forms a Pt(IV) complex of the type $[PtMe_3(L_4)][BF_4]$.[1]

Related mixed donor ligands include $MeS(CH_2)_2Se(CH_2)_2SMe$[1] and the analogous $MeSe(CH_2)_2S(CH_2)_2SeMe$,[1] which have been shown to form complexes of the type $[PtMe_3(L)]^+$.[1] Another mixed donor group 16 tridentate ligand, $MeS(CH_2)_2Te(CH_2)_2SMe$ has also been reported,[9] and it has been shown to coordinate to Pd(II), Hg(II) and Cd(II) centres, although the ligand is believed to be fairly unstable, probably as a result of the $Te(CH_2)S$ linkages.

The first facultative tridentate telluroether ligands, $RTe(CH_2)_3Te(CH_2)_3TeR$ (L_5) (R = Me or Ph) were recently prepared by the Southampton group in good yield (R = Me,

56%; R = Ph, 62%) *via* the reaction of $RTe(CH_2)_3Cl$ and Na_2Te[5] (Figure 4.3) and a number of transition metal complexes, including $[Rh(cp^*)(L_5)][PF_6]_2$ ($cp^* = C_5Me_5$), *fac*-$[Mn(CO)_3(L_5)][CF_3SO_3]$ and $[PtCl(L_5)][PF_6]$[5] demonstrate their coordination chemistry.

Figure 4.3 - Synthesis of $RTe(CH_2)_3Te(CH_2)_3TeR$ (R = Me or Ph)[5]

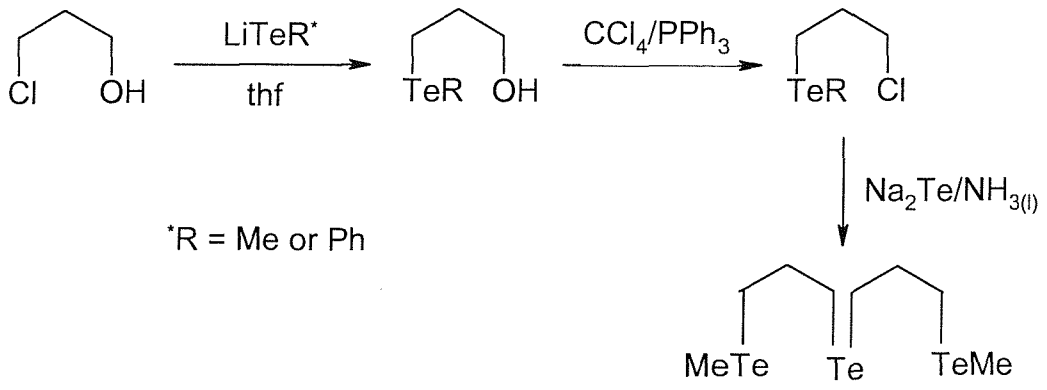

The crystal structure of $[Rh(cp^*)\{PhTe(CH_2)_3Te(CH_2)_3TePh\}][PF_6]_2$ (Figure 4.4) showed the cation adopting a *pseudo*-octahedral geometry with the ligand acting as a facially coordinating tridentate ligand in a DL conformation, whereby one Ph group was observed to point towards the cp^* ring and the other away.[5] The Te-Rh bond distances were in the range 2.6015(7) – 2.6177(7) Å, with d(Te-C) 2.110(6) – 2.155(7) Å.

Figure 4.4 - Crystal structure of $[Rh(cp^*)\{PhTe(CH_2)_3Te(CH_2)_3TePh\}][PF_6]_2$[5]

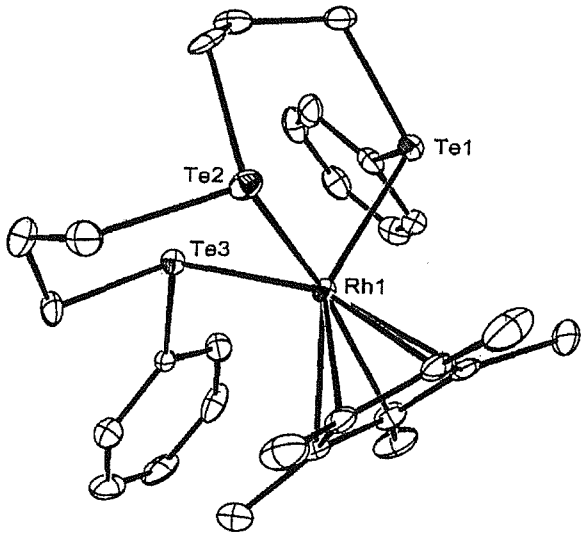

The complexes *fac*-$[Mn(CO)_3(L_5)][CF_3SO_3]$ were confirmed as *fac* isomers from the presence of two ν(CO) stretches in their solution IR spectra (for R = Me, ν(CO) = 2014 and 1936 cm^{-1}; R = Ph, ν(CO) = 2017 and 1940 cm^{-1}). The invertomers were not resolvable from the IR data, but they were clearly identified in the ^{55}Mn and ^{125}Te-{^1H} NMR spectra. The ^{55}Mn NMR spectrum of *fac*-$[Mn(CO)_3\{MeTe(CH_2)_3Te(CH_2)_3TeMe\}][CF_3SO_3]$ showed a strong resonance at δ -1338 ppm, together with a weaker resonance at –1362 ppm in an approximately 10 : 1 ratio. From the ^{125}Te-{^1H} NMR spectrum, it was concluded that two isomers were present in solution, these being the DL (as a minor species) and one *meso* invertomer as the major species. The latter was believed to be the *meso*-1 isomer, since the *meso*-2 isomer would have placed the TeR groups unfavourably close to the CO co-ligands.[5]

For a *fac*-coordinated open-chain tridentate Group 16 ligand complex of the form $MX_3(L^3)$, three different invertomers are possible by symmetry (Figure 4.5). These are the *meso-1*, *meso-2* and DL forms for each of the two orientations of the lone pair on the central Te atom. It must be noted, however, that for any given complex, some invertomers may not be present in significant amounts. A detailed discussion of pyramidal inversion in Group 16 metal complexes is given in chapter 1, with the barrier to pyramidal inversion being much greater for Te than S.[6] The invertomers may be distinguished by NMR spectroscopy providing that they are not interconverting *via* rapid pyramidal inversion (on the NMR timescale) at the S or Te donors.

Figure 4.5 - The possible invertomers for a fac-coordinated tridentate group 16 ligand complex

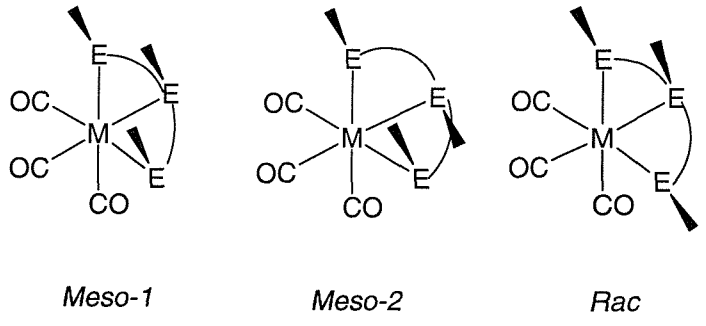

The complexes $[PtCl(L_5)][PF_6]$ showed two broad resonances in their ^{195}Pt NMR spectra in the range δ -3600 to -4000 ppm, which is between the values previously reported for compounds having $Pt(II)Cl_2Te_2$ (*ca.* -3000 to -3300 ppm) and $Pt(II)Te_4$ (*ca.* -4700 to -5000 ppm) donor sets. The complexes were therefore identified as planar $Pt(II)Te_3Cl$ species, with the lack of ^{125}Te-^{195}Pt couplings and the broadness of the resonances being attributed to the onset of pyramidal inversion processes. Such behaviour has also been observed in $[Pt(ditelluroether)_2]^{2+}$ complexes[10] where the high *trans* effect of Te-Pt-Te was observed to lower the pyramidal inversion barrier. Two *meso* forms of the $[PtCl(L_5)][PF_6]$ complexes were evident in solution from the presence of two sharp RTe resonances in their respective ^{125}Te-$\{^1H\}$ NMR spectra. Additional very weak features in the ^{125}Te-$\{^1H\}$ NMR spectrum of $[PtCl\{MeTe(CH_2)_3Te(CH_2)_3TeMe\}][PF_6]$ were thought either to be due the presence of a minor DL form of the complex, or due to impurities.

The mixed thia-tellura ligand $MeS(CH_2)_3Te(CH_2)_3SMe$ was recently prepared in the Southampton laboratory[11] and, apart from the unstable $MeS(CH_2)_2Te(CH_2)_2SMe$, it represents the only example of a mixed-donor Te-containing open-chain ligand. Synthesis was accomplished in good yield and the ligand isolated as a yellow oil from the reaction of $Cl(CH_2)_3SMe$ with Na_2Te[10] (Figure 4.6). No studies into the complexation behaviour of the ligand had been reported prior to this study, and therefore complexes with a variety of low and medium oxidation state transition metal ions (Mn(I), Pd(II), Pt(II), Pd(III), Cu(I) and Ag(I)) have been prepared in order to investigate its coordination behaviour. Particularly interesting will be the comparisons to be made between the S and the (softer) Te donors' ability to coordinate to a variety of metal centres, and between the reported complexes of the other related group 16 acyclic tridentate ligands and the mixed donor macrocyclic ligands [9]aneS_2Te, [11]aneS_2Te and [12]aneS_2Te[12] (Chapter 2).

4.1 Results and discussion

4.2 Synthesis of $MeS(CH_2)_3Te(CH_2)_3SMe$

The ligand was prepared according to a previously described method[11] (Figure 4.6). Freshly ground tellurium powder, sodium hydroxide and rongalite were refluxed in degassed water to form Na_2Te, to which a solution of the previously synthesised $Cl(CH_2)_3SMe$[13] in ethanol was added. Reflux of the mixture for 90 minutes, followed by stirring overnight at room temperature, yielded, after work-up, a clear yellow oil in high yield (81%). The synthetic route employed was similar to that used to prepare the homoleptic compounds $RTe(CH_2)_3Te(CH_2)_3TeR$ (R = Me or Ph) which were prepared *via* the reactions of $Na_2Te/NH_{3(l)}$ with $RTe(CH_2)_3Cl$ (Introduction, Figure 4.3).

Figure 4.6 - Synthesis of $MeS(CH_2)_3Te(CH_2)_3SMe$[11]

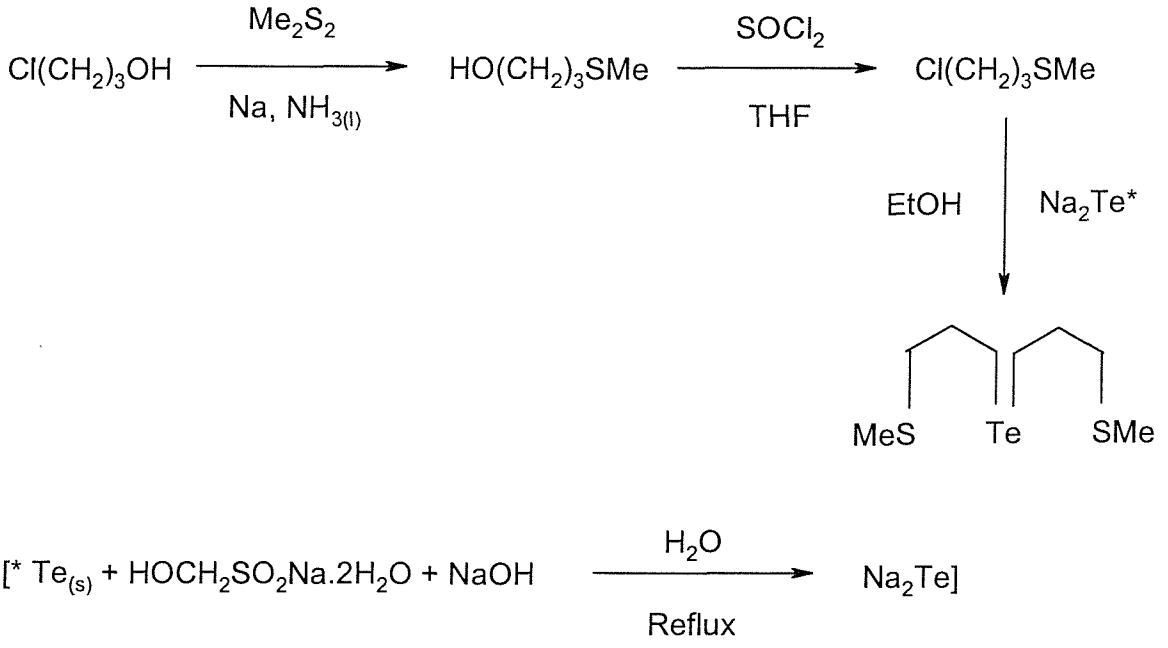

^1H, ^{13}C-{^1H} and ^{125}Te-{^1H} NMR spectra of the compound were all consistent with the previously reported values.[11] The ^1H NMR spectrum displayed a quintet at δ 1.98 ppm which was assigned as the $CH_2CH_2CH_2$ proton resonances, whilst the SCH_3 and SCH_2

signals were observed at δ 2.53 and 2.69 ppm respectively (both triplet resonances). The CH_2 resonance was observed at 2.69 ppm. ^{13}C-{^1H} NMR spectoscopy displayed a resonance at δ 1.5 ppm, with visible ^{125}Te couplings ($^1J_{Te\text{-}C}$ = 155 Hz) and was therefore assigned as the $TeCH_2$ carbon resonance. Additional resonances at 15.7, 31.6 and 36.2 ppm were assigned to the SCH_3, SCH_2 and $CH_2CH_2CH_2$ environments respectively. ^{125}Te-{^1H} NMR spectroscopy of the neat oil revealed a single resonance at 241 ppm, which was also consistent with the previously reported value (δ 238 ppm).[11] The chemical shift was similar to those of the macrocyclic ligands [11]- and [12]-aneS_2Te (234 and 217 ppm respectively), which conforms to the observation that substituents more remote than the γ-carbon have little effect on the ^{125}Te-{^1H} NMR shift.[14] The values also suggest that the presence of the macrocyclic ring in the compounds [11]- and [12]-aneS_2Te do not significantly affect the ^{125}Te-{^1H} NMR shift.

4.3 *Fac*-[$Mn(CO)_3(MeS(CH_2)_3Te(CH_2)_3SMe)][CF_3SO_3]$

We wished to prepare the compound *fac*-$[Mn(CO)_3(MeS(CH_2)_3Te(CH_2)_3SMe)][CF_3SO_3]$, since displacement of acetone from the *in-situ* intermediate $[Mn(CO)_3(Me_2CO)_3][CF_3SO_3]$ was expected to form a complex in which $MeS(CH_2)_3Te(CH_2)_3SMe$ coordinates *fac* to the Mn(I) centre through all three donor atoms. This would allow for comparisons to be made with the analogous *fac*-$[Mn(CO)_3(MeSe(CH_2)_3Se(CH_2)_3SeMe)][CF_3SO_3]$[6] and *fac*-$[Mn(CO)_3(RTe(CH_2)_3Te(CH_2)_3TeR)][CF_3SO_3]$ (R = Me or Ph) together with the complexes *fac*-$[Mn(CO)_3([n]aneS_2Te)][CF_3SO_3]$ (n = 9, 11 and 12 – see Chapter 2).

The reaction of $AgCF_3SO_3$ and $[Mn(CO)_5Cl]$ in refluxing acetone afforded $[Mn(CO)_3(Me_2CO)_3][CF_3SO_3]$[15] after one hour. The reaction was undertaken in a foil wrapped vessel and monitored by solution IR spectroscopy to ensure reaction completeness. This was determined by the observation of two (C_{3V} theory A_1 + E) carbonyl absorptions at 2054 cm^{-1} and 1974 cm^{-1}, which confirmed the presence of a *fac*-tricarbonyl unit, as observed for other tricarbonyl manganese cations.[5,6] This was in contrast to the IR spectrum of $[Mn(CO)_5Cl]$ which displayed three carbonyl absorptions at 2056 cm^{-1}, 2006 cm^{-1} and 1976 cm^{-1}. The AgCl precipitate was allowed to settle and

the supernatant syringed into a vessel containing the ligand. The mixture was refluxed for 20 minutes, and then stirred at room temperature for a further 18 hours. The reaction was monitored by solution IR spectroscopy in order to ensure completeness. Concentration of the reaction mixture, followed by addition to ice-cold Et_2O, yielded a brown-orange gum that could not be obtained in solid form despite many attempts at recrystallisation using different solvent systems, for example CH_2Cl_2-Et_2O, CH_2Cl_2-hexane and Me_2CO-Et_2O. It should be noted that the analogous complex $[Mn(CO)_3(MeSe(CH_2)_3Se(CH_2)_3SeMe)][CF_3SO_3]$ was isolated as a yellow-orange oil.[6]

Reaction of the highly symmetrical [9]aneS_3 ligand with $[Mn(CO)_3(Me_2CO)_3][CF_3SO_3]$ forms $[Mn(CO)_3([9]aneS_3)][CF_3SO_3]$, which has C_{3V} symmetry. The $[Mn(CO)_3(MeS(CH_2)_3Te(CH_2)_3SMe)][CF_3SO_3]$, however, has lower ($C_s$) symmetry due to the coordination of the less symmetric $MeS(CH_2)_3Te(CH_2)_3SMe$. A C_s *fac*-tricarbonyl unit is expected to show three bands (2A' + A"). Solution IR spectroscopy of the product in CH_2Cl_2, however, showed two ν(CO) bands at 2035 cm^{-1} and 1950 cm^{-1}, the latter of which was very broad. Therefore the complex appeared to be *psuedo-*C_{3V}, despite the formal C_s symmetry. The values for ν(CO) may be compared with the previously reported $[Mn(CO)_3(MeE(CH_2)_3E(CH_2)_3EMe][CF_3SO_3]$ (E = Te, ν(CO) = 2014, 1936 cm^{-1};[5] E = Se, ν(CO) = 2029, 1945 cm^{-1}).[6] The analogous complex where E = S has not been described, however the complex of the dimethylene linked $MeS(CH_2)_2S(CH_2)_2SMe$ has, with ν(CO) at 2047 and 1957 cm^{-1}.[6] The fall in ν(CO) along the series $MeS(CH_2)_2S(CH_2)_2SMe$ > $MeS(CH_2)_3Te(CH_2)_3SMe$ ≥ $MeSe(CH_2)_3Te(CH_2)_3SeMe$ > $MeTe(CH_2)_3Te(CH_2)_3TeMe$ illustrates the previously observed trend[5,16] of increasing ligand → Mn σ-donation as one descends Group 16. Increased σ-donation from the ligand to Mn(I) raises the electron density on the metal centre, which in turn increases the Mn → π*(CO) backbonding, resulting in weakened C-O bonds and therefore lower values for ν(CO).

A positive ion electrospray mass spectrum of the product displayed one cluster of peaks centered at *m/z* = 447, with an isotopic distribution consistent with the cation $[Mn(CO)_3(L)]^+$, *m/z* = 447 (Figure 4.7).

The ^1H NMR spectrum of the product revealed a very broad, unresolved multiplet at δ 2.3 - 4.0 as a result of quadrupolar broadening by the ^{55}Mn nucleus. The ^{13}C-{^1H}

NMR spectrum was more simple, however, and displayed a total of four resonances in addition to a single, broad δ(CO) in the range 213 – 217 ppm. The broadness prevented the expected two resonances (as predicted by Group Theory for the *effectively* C_{3V} molecule) from being resolved. A resonance at δ 15.5 was assigned to the $TeCH_2$ carbon, whilst the signal at δ 25.9 was attributed to the CH_3S resonance of the coordinated ligand. The latter signal was broader than the others, this almost certainly being caused by fast pyramidal inversion at coordinated sulfur, resulting in the interconversion of the possible DL and two *meso* forms of the complex. Two additional resonances at δ 25.4 and δ 39.2 were assigned as the CH_2S and $CH_2CH_2CH_2$ protons. All of the resonances apart from the CH_2S resonance were observed to be shifted to higher frequency of their respective values in the free ligand, as was expected upon coordination of the ligand to the Mn(I) centre.

Figure 4.7 - Electrospray mass spectrum of fac-$[Mn(CO)_3(MeS(CH_2)_3Te(CH_2)_3SMe)]^+$ (MeCN)

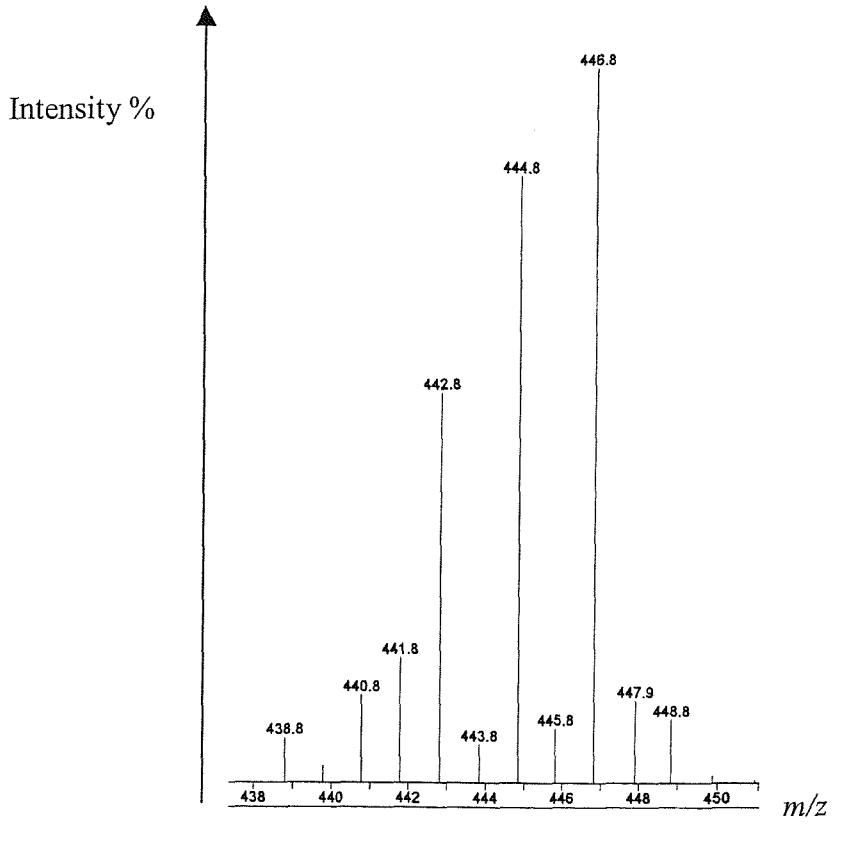

The ^{125}Te-{^1H} NMR spectrum of the product revealed a single resonance at δ 81 ppm. This represents a low frequency shift upon coordination of the ligand to Mn(I). The value may be compared with the analogous $MeTe(CH_2)_3Te(CH_2)_3TeMe$ complex,[5] which had δ 120 and 129 for the central tellurium donor (free ligand δ 116.8, 154.4 ppm) and $[Mn(CO)_3([n]aneS_2Te)][CF_3SO_3]$, where $\delta(^{55}Mn)$ = 214 and 110 ppm for n = 9 and 11 respectively (free [9]$aneS_2Te$ = δ 345 ppm and free [11]$aneS_2Te$ = δ 234 ppm – see Chapter 2) which also display low frequency ^{125}Te-{^1H} NMR shifts upon coordination to Mn(I).

The ^{55}Mn NMR spectrum showed a single, very broad resonance ($w_{½}$ = 1850 Hz) at δ -645 ppm. The ^{55}Mn NMR chemical shift displayed a slightly different order to those observed for ν(CO), where $MeSe(CH_2)_3Se(CH_2)_3SeMe$ (δ -560)[6] > $MeS(CH_2)_3Te(CH_2)_3SMe$ (δ -645) > $MeTe(CH_2)_3Te(CH_2)_3TeMe$ (δ -1338 ppm).[5] Comparisons with the complex of the dimethylene linked $MeS(CH_2)_2S(CH_2)_2SMe$ ligand cannot be made, however, due to the sensitivity of the ^{55}Mn chemical shift to chelate ring size as well as donor atom type.[6,16]

The chiral centres in the coordinated tridentate ligands generate several NMR distinguishable invertomers for $[Mn(CO)_3(MeE(CH_2)_3E(CH_2)_3EMe)]^+$ (Figure 4.5). In the case of the manganese complex of $MeTe(CH_2)_3Te(CH_2)_3TeMe$, two invertomers were observed,[5] but for the $MeS(CH_2)_3Te(CH_2)_3SMe$ complex only single ^{55}Mn and ^{125}Te-{^1H} resonances were detected. This may be due to a single, predominant isomer in solution, although since barriers to inversion are much lower at coordinated sulfur than for tellurium,[6] fast pyramidal inversion on the NMR timescale is likely.

4.4 $[MCl(MeS(CH_2)_3Te(CH_2)_3SMe)][PF_6]$; M = Pd or Pt

MCl_2 (M = Pd or Pt) were refluxed in MeCN for one hour to form $[MCl_2(NCMe)_2]$,[17] to each of which was added one equivalent of $TlPF_6$. Addition of the ligand, followed by stirring for 18 hours at room temperature yielded the products, after the removal of TlCl precipitate and work up, as yellow powders of stoichiometry $[MCl(MeS(CH_2)_3Te(CH_2)_3SMe)][PF_6]$, with yields of 43% and 38% for the Pd and Pt complexes respectively.

Electrospray mass spectra of the products revealed clusters of peaks centred at *m/z* = 449 and *m/z* = 537 for the Pd and Pt complexes respectively, which were consistent with the parent monocations $[^{106}Pd^{35}Cl(MeS(CH_2)_3{}^{130}Te(CH_2)_3SMe)]^+$ and $[^{195}Pt^{35}Cl(MeS(CH_2)_3{}^{130}Te(CH_2)_3SMe)]^+$ (Figure 4.8). The IR spectra of both complexes displayed the presence of coordinated ligand absorbances, together with those for the PF_6^- anion at *ca.* 834 and 559 cm^{-1}.

Figure 4.8 - Electrospray mass spectrum of $[PtCl(MeS(CH_2)_3Te(CH_2)_3SMe)]^+$ (MeCN)

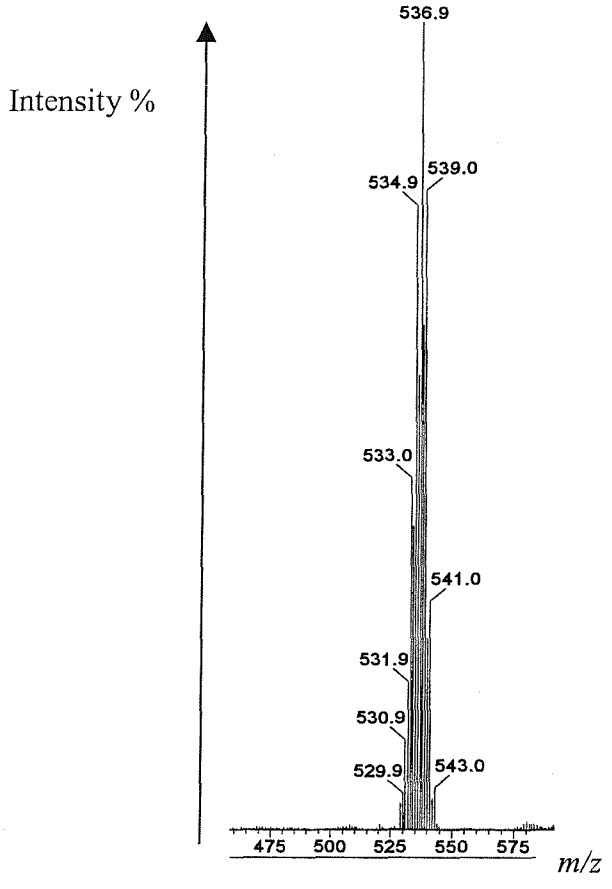

^1H NMR spectra of the products displayed fairly broad resonances, probably due to the occurrence of pyramidal inversion. For $[PtCl(MeS(CH_2)_3Te(CH_2)_3SMe)][PF_6]$, a complex, unresolved resonance at δ 2.6 ppm was assigned to the $CH_2CH_2CH_2$ protons of the ligand, whilst three singlets at δ 2.7, 2.85 and 2.9 ppm were assigned to three different SCH_3 environments. The CH_2S protons were observed as a multiplet centred at δ 3.0 ppm, whilst the $TeCH_2$ protons were assigned to the multiplet resonance observed

at δ 3.4 ppm, these having ill-defined ^{195}Pt satellites, suggesting a system approaching coalescence. All of the resonances were observed to be shifted to high frequency of those in the free ligand, which is consistent with its coordination to the Pt(II) centre. Pyramidal inversion at thioethers coordinated to Pd(II) is usually rapid on the NMR timescale at room temperature,[18] and the complex with $MeS(CH_2)_3Te(CH_2)_3SMe$ is no exception. Broader resonances than those observed for the Pt(II) complex meant that the SCH_3 protons were not resolved into separate signals, and a single resonance was observed for these at δ 2.6 ppm. This was attributed to faster inversion on the NMR timescale than in the Pt(II) complex. A multiplet resonance observed at δ 3.4 ppm was assigned to the $TeCH_2$ protons of the coordinated $MeS(CH_2)_3Te(CH_2)_3SMe$ ligand, whilst the SCH_2 and $CH_2CH_2CH_2$ resonances were observed at 2.90 and 1.98 ppm respectively. All of the resonances were observed at slightly higher frequency than their counterparts in the Pt(II) complex as a result of the greater electronegativity of Pd(II) over Pt(II), thereby causing greater deshielding of the ligand protons.

A ^{195}Pt-{^1H} NMR spectrum of $[PtCl(MeS(CH_2)_3Te(CH_2)_3SMe)][PF_6]$ at room temperature failed to display any resonances. On cooling the solution to -80°C, however, two resonances at δ -3079 and δ -3140 ppm were observed. This is consistent with the presence of the expected *meso* and DL invertomers in solution (Figure 4.9).

Figure 4.9 - The invertomers possible for $[PtCl\{MeS(CH_2)_3Te(CH_2)_3SMe\}]^+$

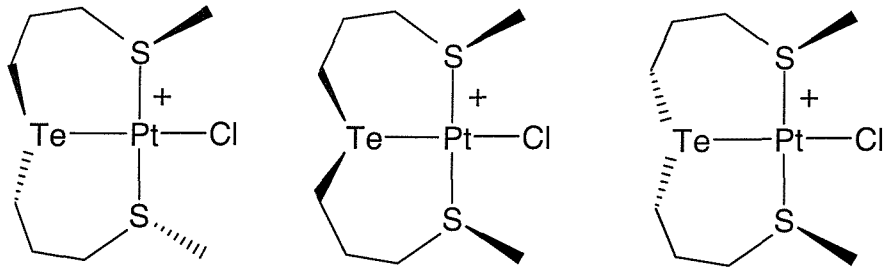

Rac *Meso-A* *Meso-B*

The chemical shifts for the complex (TeS_2Cl donor set) are reasonable in comparison to the reported values for $PtSe_3Cl$ (*ca.* -3700)[19] and $PtTe_3Cl$ (*ca.* -3900 ppm).[5] The

macrocyclic complexes $[(PtCl_2([n]aneS_2Te)][PF_6]_2$ had $\delta(^{195}Pt)$ = -3834 and -3890 ppm for n = 11 and 12 respectively, which are comparable despite the differing donor set at Pt(II) ($STeCl_2$ system).

A ^{125}Te-{^1H} NMR spectrum of the Pt complex displayed two, broad resonances at δ 348 and δ 356 ppm, as compared with δ 229 ppm in the free ligand. The value represented a high frequency Te shift upon coordination to the Pt(II) centre, which is consistent with σ-donation from Te → Pt, thereby deshielding the tellurium donor. The related $[PtCl(RTe(CH_2)_3Te(CH_2)_3TeR)][PF_6]$ had $\delta(^{125}Te)$ = 183.5 ($^1J_{Te\text{-}Pt}$ = 296 Hz), 194 ($^1J_{Te\text{-}Pt}$ = 308 Hz), 355.5 ($^1J_{Te\text{-}Pt}$ = 1400 Hz) and 355 ppm ($^1J_{Te\text{-}Pt}$ = 1550 Hz) for R = Me, and 374 ($^1J_{Te\text{-}Pt}$ = 1225 Hz), 373 ($^1J_{Te\text{-}Pt}$ = 1200 Hz), 415.5 ($^1J_{Te\text{-}Pt}$ = 485 Hz) and 433 ppm ($^1J_{Te\text{-}Pt}$ = 486 Hz) for R = Ph. The two RTe resonances in each case were attributed to two *meso* invertomers, consistent with the ^{195}Pt NMR spectra. The compounds $[PtCl_2([n]aneS_2Te)][PF_6]_2$ had $\delta(^{125}Te)$ = 299 and 374 ppm for n = 11 and 12 respectively (Chapter 2), the values being very similar to the S_2TeCl system. The two resonances observed in the ^{125}Te-{^1H} NMR spectrum of $[PtCl(MeS(CH_2)_3Te(CH_2)_3SMe)][PF_6]$ (as in the ^{195}Pt NMR spectrum) were consistent with the presence of one *meso* and the DL invertomer in solution. No ^{195}Pt satellites were resolved in the spectrum due to the broadness of the signals. The Te donor was therefore slightly more deshielded when coordinated to the more electronegative Pd(II) centre as a result of the greater transferral of electron density from Te to Pd *via* σ-bonding. No resolution of individual invertomers was observed due to the broadness of the signal. In comparison, the compounds $[PdCl_2([n]aneS_2Te)][PF_6]_2$ had $\delta(^{125}Te)$ = 330 and 387 ppm for n = 11 and 12 respectively, again showing high frequency shifts upon coordination to Pd(II). The values were similar to that observed for the $[PdCl(MeS(CH_2)_3Te(CH_2)_3SMe)][PF_6]$ complex (TeS_2Cl system) despite the differing donor set in the macrocyclic complexes ($STeCl_2$ systems).

A crystal structure of the platinum complex was obtained from crystals grown by the vapour diffusion of Et_2O into an acetone solution of the product (Figure 4.10 and Table 4.0).

Figure 4.10 - Crystal structure of $[PtCl(MeS(CH_2)_3Te(CH_2)_3SMe)]^+$ with numbering scheme adopted. Ellipsoids are drawn at the 40% probability level and H atoms are omitted for clarity

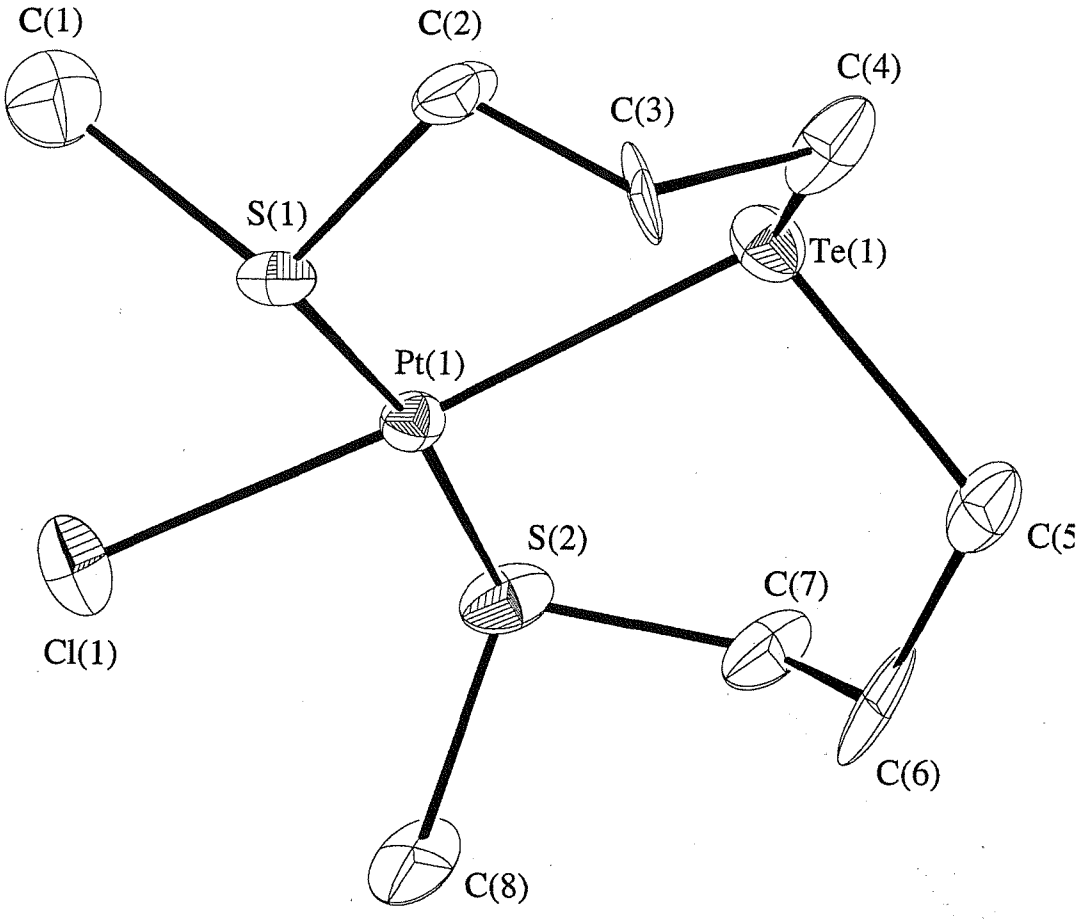

Two independent anions and cations were identified in the asymmetric unit, although a higher symmetry cell could not be identified. The small differences between the two cations were not significant in chemical terms (Table 4.0), and only one is depicted in Figure 4.10. The structure reveals the expected square planar coordination of the ligand to the Pt(II) centre through all 3 donor atoms. Te-Pt-S bond angles were between 90.57(12) – 97.69(10)°, whilst S-Pt-Cl bond angles were in the range 83.9(1) – 87.9(2)° and Cl-Pt-Te angles were 174.39(11)° and 175.73(12)°, therefore confirming the near-square planar geometry around Pt(II). Pt-Te bond lengths were 2.5191(12) and

2.5258(11) Å, whilst Pt-S bond lengths were in the range 2.288(4) – 2.310(4) Å. The methyl groups were observed to point in opposite directions (an *anti* arrangement) and hence the cation adopts a DL conformation.

Table 4.0 - Selected bond lengths (Å) and angles (°) for [PtCl(MeS(CH$_2$)$_3$Te(CH$_2$)$_3$SMe)][PF$_6$]

Bond lengths			
Pt(1)-Te(1)	2.5258(11)	Pt(2)-Te(2)	2.5191(12)
Pt(1)-S(1)	2.310(4)	Pt(2)-S(3)	2.304(4)
Pt(1)-S(2)	2.288(4)	Pt(2)-S(4)	2.291(4)
Pt(1)-Cl(1)	2.358(4)	Pt(2)-Cl(2)	2.351(4)
Bond angles			
Te(1)-Pt(1)-Cl(1)	174.39(11)	Te(2)-Pt(2)-Cl(2)	175.73(12)
Te(1)-Pt(1)-S(1)	90.57(12)	Te(2)-Pt(2)-S(4)	91.26(11)
Te(1)-Pt(1)-S(2)	97.69(10)	Te(2)-Pt(2)-S(3)	97.39(11)
Cl(1)-Pt(1)-S(1)	87.9(2)	Cl(2)-Pt(2)-S(3)	86.3(2)
Cl(1)-Pt(1)-S(2)	83.9(1)	Cl(2)-Pt(2)-S(4)	84.9(2)
S(1)-Pt(1)-S(2)	171.7(1)	S(3)-Pt(2)-S(4)	170.2(2)

The structure is similar to that reported for $[PtCl(^iPrS(CH_2)_3S(CH_2)_3S^iPr)][BF_4]$,[3] which also displayed a slightly distorted square planar geometry. Unlike in the present example, however, the coordinated ligand adopts the *meso*-B conformation, which places the S^iPr groups on the same side of the square plane in a *syn* arrangement. The two, terminal S atoms are chemically equivalent and the Pt-S_{transS} distances equal within experimental error (2.302(3) and 2.306(4) Å). This is almost identical to $[PtCl(MeS(CH_2)_3Te(CH_2)_3SMe)][PF_6]$ where Pt-S_{transS} for the two independent cations were 2.310(4), 2.288(4), 2.304(4) and 2.291(4) Å. Likewise, Pt-$Cl_{transTe}$ (2.358(4) and

2.351(4) Å) and Pt-$Te_{transCl}$ (2.5258(11) and 2.5191(12) Å) are similar to those reported for Pt-$Cl_{transTe}$ and Pt-$Te_{transCl}$ in *cis*-$[PtCl_2(EtOC_6H_4TeCH_2CH_2SMe)]$ (2.336(3) Å and 2.514(1) Å respectively). The Pt-S_{transS} bond lengths in $[PtCl(MeS(CH_2)_3Te(CH_2)_3SMe)][PF_6]$ (2.310(4), 2.304(4), 2.288(4) and 2.291(4) Å) may also be compared with Pt-S_{transS} in $[PtCl(^iPrS(CH_2)_3S(CH_2)_3S^iPr)][BF_4]$ (2.302(3), 2.256(4) and 2.306(4) Å).

4.5 $[Rh(cp^*)(MeS(CH_2)_3Te(CH_2)_3SMe)][PF_6]_2$

The compound $[Rh(cp^*)(MeS(CH_2)_3Te(CH_2)_3SMe)][PF_6]_2$ was synthesised from a solution of the ligand and $[Rh(cp^*)Cl_2]_2$ (which had previously been prepared according to a literature procedure[20]) in MeOH, to which was added $TlPF_6$. The mixture was refluxed for two hours, concentrated to *ca.* 5 cm^3 and injected into ice-cold Et_2O to give the product in 29% yield as a bright yellow powder. The $Rh(cp^*)$ fragment was chosen, since the cp^* co-ligand would block one face of the Rh(III) centre, thereby promoting *fac*-coordination of the tridentate open-chain ligand. Comparisons may also be made with the previously reported $[Rh(cp^*)(MeTe(CH_2)_3Te(CH_2)_3TeMe)][PF_6]_2$, and with $[Rh(cp^*)([n]aneS_2Te)][PF_6]_2$.

An electrospray mass spectrum of the product displayed two clusters of peaks at *m/z* = 273 and 294, which were consistent with the monocationic species $[Rh(cp^*)(MeS(CH_2)_3Te(CH_2)_3SMe)]^{2+}$ and $[Rh(cp^*)(MeS(CH_2)_3Te(CH_2)_3SMe).MeCN]^{2+}$ respectively. The latter arose from the association of the parent monocation with a molecule of acetonitrile solvent in solution. Microanalytical data were consistent with the proposed formulation, and an IR spectrum of the solid showed evidence for coordinated ligand and PF_6^- anion at 840 and 560 cm^{-1}.

The ^1H NMR spectrum of the product in d_6-acetone displayed a singlet at δ 2.6, which was attributed to the resonance of the cp^* methyl protons in the complex. A singlet at δ 2.73 was assigned to the S*CH*$_3$ protons; the presence of only one resonance being indicative of fast inversion at coordinated sulfur in solution. This is in contrast to $[Rh(cp^*)(MeTe(CH_2)_3Te(CH_2)_3TeMe)][PF_6]_2$,[5] where three δ(Te*CH*$_3$) doublets of approximately equal intensity, together with a fourth, much weaker doublet were

observed. These were due to the presence of one *meso* and the DL forms of the complex as the major species in solution, together with a minor, second *meso* form. In $[Rh(cp^*)(MeS(CH_2)_3Te(CH_2)_3SMe)][PF_6]_2$, two unresolved multiplets were observed between δ 2.20 – 2.48 ppm and δ 2.93 – 3.25 ppm, which were assigned to the (SCH_2 and $-CH_2$-) and the CH_2Te protons respectively. All of the proton resonances in the complex were shifted to high frequency of those in the free ligand, which is expected upon coordination to the Rh(III) centre. The $^{13}C-\{^1H\}$ NMR spectrum showed a resonance at δ 14.0 which was assigned to the CH_2Te carbon, with CH_2S and $CH_2CH_2CH_2$ resonances observed at δ 22.0 and 36.8 ppm respectively. The cp^* protons were identified by resonances at δ 9.1 (CCH_3) and 106.0 (CCH_3) ppm. The SCH_3 resonance was observed at δ 25.0, and once again the presence of a single signal for the methyl group was indicative of fast inversion at coordinated sulfur.

A $^{125}Te-\{^1H\}$ NMR spectrum of the product (Figure 4.11) revealed a doublet resonance to low frequency of free ligand (δ 241) at δ 191, with $^1J_{Rh\text{-}Te}$ = 94 Hz. The coupling constants are comparable with those reported for other Rh(III)-Te systems, for example $[Rh(cp^*)(MeC(CH_2TeR)_3)]^{2+}$ (R = Me or Ph) where $^1J_{Rh\text{-}Te}$ = 91 Hz[21] and $[Rh(cp^*)(MeTe(CH_2)_3Te(CH_2)_3TeMe)][PF_6]_2$[5] where $^1J_{Rh\text{-}Te}$ = 88 Hz (av.). The related macrocyclic complexes $[Rh(cp^*)([n]aneS_2Te)][PF_6]_2$ (n = 9, 11 or 12) (see Chapter 2) also displayed doublet resonances in their respective $^{125}Te-\{^1H\}$ NMR spectra, which again, unlike that observed for the $MeS(CH_2)_3Te(CH_2)_3SMe$ complex, were to high frequency of free ligand. Coupling constants were similar to those found here for the $MeS(CH_2)_3Te(CH_2)_3SMe$ complex: $[Rh(cp^*)([9]aneS_2Te)]^{2+}$ δ = 397, $^1J_{Rh\text{-}Te}$ = 75 Hz; $[Rh(cp^*)([11]aneS_2Te)]^{2+}$ δ = 282, $^1J_{Rh\text{-}Te}$ = 106 Hz and $[Rh(cp^*)([12]aneS_2Te)]^{2+}$ δ = 275, $^1J_{Rh\text{-}Te}$ = 102 Hz.

Figure 4.11 - ^{125}Te-{^1H} NMR spectrum of $[Rh(cp^*)(MeS(CH_2)_3Te(CH_2)_3SMe)][PF_6]_2$ in d_6-Me_2CO

A crystal structure was obtained from crystals grown by the vapour diffusion of Et_2O into an acetone solution of the product. (Figure 4.12 and Table 4.1).

Figure 4.12 - Crystal structure of $[Rh(cp^*)(MeS(CH_2)_3Te(CH_2)_3SMe)]^{2+}$ with numbering scheme adopted. Ellipsoids are drawn at the 40% probability level and H atoms are omitted for clarity

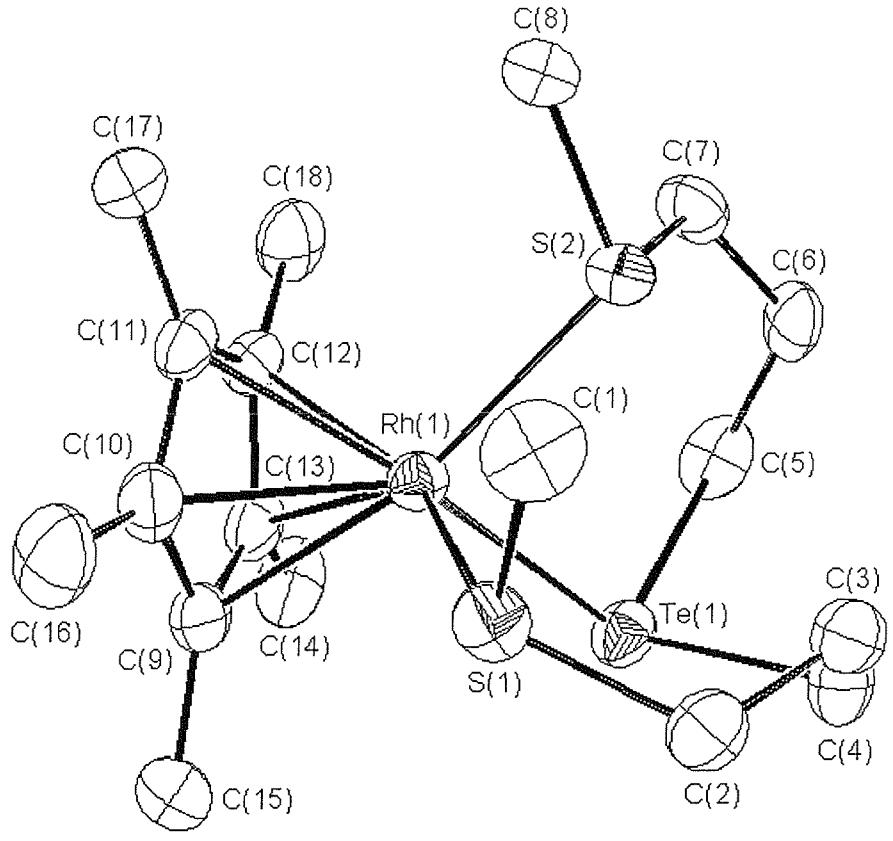

The structure (Figure 4.12) showed the expected *pseudo*-octahedral Rh(III) centre bonding *fac* to all three donor atoms of the open-chain $MeS(CH_2)_3Te(CH_2)_3SMe$ ligand, and η^5 to the cp^* co-ligand. The methyl groups of the tridentate ligand were observed to adopt the DL configuration, being directed in opposite directions to the cp^* plane. The bond lengths and angles may be compared with the analogous $[Rh(cp^*)(PhTe(CH_2)_3Te(CH_2)_3TePh)][PF_6]_2$,[5] which also adopts the DL conformation in the solid state. The Rh-Te bond distances are identical in both cases (2.6106(8) and 2.6016(7) Å for the $[Rh(cp^*)(MeS(CH_2)_3Te(CH_2)_3SMe)][PF_6]_2$ and $[Rh(cp^*)(PhTe(CH_2)_3Te(CH_2)_3TePh)][PF_6]_2$ complexes respectively), whilst d(Rh-S) in $[Rh(cp^*)(MeS(CH_2)_3Te(CH_2)_3SMe)][PF_6]_2$ (2.364(2) and 2.368(2) Å) were fairly typical. For example $[Rh_2(cp^*)_2Cl_2(L)][BPh_4]_2$ (L = 1,4,7,10,13,16-hexathiacyclooctadecane) has d(Rh-S) = 2.3766(9) and 2.3645(9) Å.[22]

Table 4.1 - Selected bond lengths (Å) and angles (°) for $[Rh(cp^*)(MeS(CH_2)_3Te(CH_2)_3SMe)]^{2+}$

Bond lengths			
Rh(1)-Te(1)	2.6106(7)	Rh(1)-S(1)	2.364(2)
Rh(1)-S(2)	2.368(2)	Rh(1)-C(Me)	2.178(7)-2.232(8)
Te(1)-C(4)	2.157(8)	Te(1)-C(5)	2.140(8)
Bond angles			
Te(1)-Rh(1)-S(1)	93.14(5)	Te(1)-Rh(1)-S(2)	88.23(5)
S(1)-Rh(1)-S(2)	90.78(6)		

4.6 $[M(MeS(CH_2)_3Te(CH_2)_3SMe)]^+$; M = Cu, Ag

The complexes $[Cu(MeS(CH_2)_3Te(CH_2)_3SMe)][BF_4]$ and $[Ag(MeS(CH_2)_3Te(CH_2)_3SMe)][CF_3SO_3]$ were synthesised *via* the room temperature reaction of the ligand with one equivalent of either $[Cu(MeCN)_4][BF_4]$[23] or $AgCF_3SO_3$ in dichloromethane. The compounds were isolated by addition of the concentrated reaction mixture into ice cold Et_2O as white solids, in yields of 79% and 64% respectively. Microanalysis of the solids identified their stoichiometries as 1:1 complexes, and it is possible that under different reaction conditions or using different ratios of $MeS(CH_2)_3Te(CH_2)_3SMe$ to Cu(I) or Ag(I) that compounds of differing stoichiometry would have been obtained.

Electrospray mass spectra of the products revealed clusters of peaks at *m/z* = 371 and 412 for the Cu complex, which were consistent with the cations $[Cu\{MeS(CH_2)_3Te(CH_2)_3SMe\}]^+$ and $[Cu\{MeS(CH_2)_3Te(CH_2)_3SMe\}.MeCN]^+$ respectively, whilst the Ag complex showed a single cluster of peaks at *m/z* = 415, which was consistent with the parent monocation. ^1H NMR spectra of the complexes showed that the shifts and resonance multiplicities the proton environments were similar to those

in the free ligand, with a small shift to high frequency upon coordination to the M(I) centre.

The $^{125}Te-\{^1H\}$ NMR spectra of both complexes showed singlet resonances to low frequency of free ligand ($[Cu\{MeS(CH_2)_3Te(CH_2)_3SMe\}][BF_4]$ δ = 99 ppm ($w_{1/2}$ = 700 Hz) and $[Ag\{MeS(CH_2)_3Te(CH_2)_3SMe\}][CF_3SO_3]$ δ = 136 ppm). Such low frequency $^{125}Te-\{^1H\}$ (and ^1H) NMR shifts are typical of group 16 complexes of Ag(I) and Cu(I).[24,25] Neither complex provided crystals suitable for single crystal X-ray diffraction studies, and therefore the structures are not clear, however they are likely to be oligomeric in nature.[12] Examples of oligomeric Ag(I) complexes include $[Ag([11]aneS_2Te)][BF_4]$, in which the cation adopts a one-dimensional polymeric structure, where the Ag(I) centres are bridged by $[11]aneS_2Te$ ligands, and a Ag(I) ion is coordinated to each macrocyclic donor in a distorted trigonal planar coordination geometry.[12] The Ag-Te bond length reported for this structure was 2.674(1) Å, whilst $[Ag(MeTe(CH_2)_3TeMe)_2][BF_4]$ has a slightly longer Ag-Te distance (d(Ag-Te) = 2.785(2) – 2.837(2) Å).[26] The Ag-S distances observed in $[Ag([11]aneS_2Te)][BF_4]$ (2.521(3) and 2.634(3) Å) were similar to those reported for $[Ag(PhS(CH_2)_3SPh)][BF_4]$ (d(Ag-S) = 2.573(3) – 2.623(3) Å).[25]

4.7 Conclusions

A range of low and medium oxidation state transition metal complexes of the open-chain mixed donor ligand $MeS(CH_2)_3Te(CH_2)_3SMe$ (L) have been prepared in order to explore its coordination behaviour and to provide some comparisons with the related macrocyclic species [9]-, [11]- and [12]-aneS_2Te (Chapter 2) and the group 16 open-chain ligands including $RTe(CH_2)_3Te(CH_2)_3TeR$ (R = Me or Ph).

The complex *fac*-$[Mn(CO)_3(L)][CF_3SO_3]$ displayed a low frequency $^{125}Te-\{^1H\}$ NMR shift upon coordination of the Te donor to the Mn(I) centre, as was also observed for the related $MeTe(CH_2)_3Te(CH_2)_3TeMe$[5] and [n]ane$S_2$Te (n = 9 or 11) complexes (Chapter 2).

L has also been shown to form square planar complexes of the type $[MCl(L)][PF_6]_2$ (M = Pd or Pt). The crystal structure of $[Pt(L)][PF_6]_2$ revealed a *pseudo* square planar geometry about Pt(II), with coordination of the ligand to the metal centre in the DL conformation through an S_2Te donor set.

The Rh(III) complex $[Rh(cp^*)(L)][PF_6]$ was also prepared, and the structure showed the expected *pseudo*-octahedral Rh(III) centre bonding *fac* to all three donor atoms in the linear S_2Te ligand, and η^5 to the cp^* co-ligand in the DL conformation. The bond lengths and angles were almost identical to the analogous $[Rh(cp^*)(PhTe(CH_2)_3Te(CH_2)_3TePh)][PF_6]_2$.[5]

The complexes [M(L)][X] (M = Cu, X = BF_4; M = Ag, X = CF_3SO_3) displayed $^{125}Te-\{^1H\}$ NMR resonances to low frequency of free ligand, this being typical for Group 16 donor complexes of Ag(I) and Cu(I).[24,25] Although neither complex yielded crystals suitable for X-ray crystallographic studies, the structures are likely to be oligomeric.

Table 4.2 - Crystallographic parameters

	[PtCl(MeS(CH$_2$)$_3$Te(CH$_2$)$_3$SMe)][PF$_6$]	**[Rh(cp*)(MeS(CH$_2$)$_3$Te(CH$_2$)$_3$SMe)][PF$_6$]$_2$**
Formula	$C_8H_{18}ClF_6PPtS_2Te$	$C_{18}H_{33}F_{12}P_2RhS_2Te$
M	681.46	834.01
Crystal system	monoclinic	monoclinic
Space group	$P2_1/a$	$P2_1/n$
a/Å	9.80280(10)	10.46020(10)
b/Å	27.4365(5)	19.5063(3)
c/Å	13.5436(2)	13.5739(2)
β/°	109.0449	93.6329(9)
U/Å^3	3443.23(7)	2764.05(6)
Z	8	4
μ(Mo-Kα)/mm^{-1}	103.12	20.07
Unique reflections	7928	6476
Obs. reflections with [I>2σ(I)]	5159	4196
R	0.061	0.047
R_w	0.064	0.056

$$R = \Sigma(|F_{obs}|_i - |F_{calc}|_i)/\Sigma|F_{obs}|_i;\ R_w = \sqrt{[\Sigma\ w_i(|F_{obs}|_i - |F_{calc}|_i)^2/\Sigma\ w_i|F_{obs}|_i^2]}$$

4.8 Experimental

$[Rh(cp^*)Cl_2]_2$,[20] $[Cu(MeCN)_4][BF_4]$,[23] and $[MCl_2(MeCN)_2]$ (M = Pd and Pt)[17] were synthesised according to the literature procedures.

$MeS(CH_2)_3OH$[13]

$NH_{3(l)}$ (100 cm^3) was condensed onto dry THF (*ca.* 75 cm^3) and Na (1.84g, 80 mmol) added. Me_2S_2 (3.77 g, 40 mmol) was added dropwise to the solution and the ammonia left to boil off overnight, after which time a solution of $Cl(CH_2)_3OH$ (7.57g, 80 mmol) in dry THF (*ca.* 30 cm^3) was added over a period of 5 minutes. The mixture was then refluxed for 3 hours, allowed to cool and filtered (celite). The thf was removed *in vacuo* to leave a yellow/beige oil, yield 5.7g, 64%. $^{13}C-\{^1H\}$ NMR ($CH_2Cl_2/CDCl_3$): δ 15.5 (CH_3S), 30.9, 31.6 (CH_2CH_2SMe and CH_2CH_2SMe), 61.3 (CH_2OH).

$MeS(CH_2)_3Cl$[13]

To a solution of $MeS(CH_2)_3OH$ (8.8g, 83 mmol) in dry $CHCl_3$ (*ca.* 100 cm^3) was added to a solution of $SOCl_2$ (11.9g, 99 mmol) in dry $CHCl_3$ (*ca.* 100 cm^3) dropwise over a period of 2 hours. The mixture was heated gently to maintain reflux. After the addition, stirring was continued at room temperature overnight. The product was collected by distillation (10 mmHg, 45°C) as a clear, colourless liquid. Yield 5.2g, 67%. ^1H NMR ($CDCl_3$): δ 1.98, q, 2H ($CH_2CH_2CH_2$), 2.02, s, 3H (CH_3S), 2.55, t, 2H (SCH_2), 3.58, t, 2H (CH_2CH_2Cl).

$MeS(CH_2)_3Te(CH_2)_3SMe$

Freshly ground Te powder (3.19g, 25.0 mmol) was added to a solution of NaOH (13g, 250 mmol) and $HOCH_2SO_2Na.2H_2O$ (10g, 65 mmol) in H_2O (50 cm^3) and the mixture refluxed for 30 minutes to form a white precipitate. A solution of $Cl(CH_2)_3SMe$ (6.10g, 50 mmol) in EtOH (*ca.* 25 cm^3) was then added and reflux resumed for 1.5 hours, after which time the reaction was allowed to cool and stir at room temperature overnight. The reaction mixture was extracted with Et_2O (25 cm^3) and the organic layer separated. The aqueous layer was then washed with Et_2O (2 × *ca.* 50 cm^3) and the combined organic

extracts dried over anhydrous $MgSO_4$. Filtration *in vacuo* and removal of the solvent afforded the product as a pale yellow oil. Yield 6.2g, 81%. FABMS (3-NOBA): found *m/z* = 308, 219; calculated for $[C_8H_{18}S_2{}^{130}Te]^+$ 308, calculated for $[C_4H_9S^{130}Te]^+$ 219. ^1H NMR ($CDCl_3$): δ 1.98, (quin., 2H, $CH_2CH_2CH_2$), 2.06 (s, 3H, SCH_3), 2.53 (t, 2H, SCH_2), 2.69 (t, 2H, CH_2Te). ^{13}C-{^1H} NMR ($CDCl_3$): δ 1.5 ($^1J_{Te\text{-}C}$ = 155 Hz, CH_2Te), 15.7 (SCH_3), 31.6 (CH_2S), 36.2 ($CH_2CH_2CH_2$). ^{125}Te-{^1H} NMR (neat): δ 241.

[Mn(CO)$_3$(MeS(CH$_2$)$_3$Te(CH$_2$)$_3$SMe)][CF$_3$SO$_3$]

$AgCF_3SO_3$ (0.11g, 0.44 mmol) was refluxed with $Mn(CO)_5Cl$ (0.10g, 0.44 mmol) in degassed acetone (*ca.* 30 cm^3) for one hour to produce the yellow *in-situ* intermediate $[Mn(CO)_3(Me_2CO)_3][CF_3SO_3]$ with a precipitate of AgCl. The formation of the intermediate was monitored by solution IR spectroscopy to ensure reaction completeness. The clear yellow solution was transferred *via* cannula into a vessel containing $MeS(CH_2)_3Te(CH_2)_3SMe$ (0.13g, 0.44 mmol). The solution was refluxed for 30 minutes and then stirred at room temperature for 20 hours, after which time solution IR spectroscopy indicated that the reaction was complete. Reduction of the solvent volume to *ca.* 5 cm^3, followed by addition to ice-cold Et_2O, produced a yellow-brown gum that was dried *in vacuo*. Repeated attempts at recrystallisation from different solvent systems (see text) failed to produce a solid product. Yield 0.22g, 86%. ESMS (MeCN): found *m/z* = 447; calculated for $[C_{11}H_{18}O_3S_2{}^{130}Te^{55}Mn]^+$ 447. ^1H NMR ($CDCl_3$): δ 2.30 – 4.0 (br m). ^{13}C-{^1H} NMR ($CH_2Cl_2/CDCl_3$): δ 15.5 (CH_2Te), 25.4 (CH_2S), 25.9 (CH_3S), 39.2 ($CH_2CH_2CH_2$), 217 (br, *C*O). ^{55}Mn NMR ($CH_2Cl_2/CDCl_3$): δ -645 ($w_{½}$ = 1850 Hz). ^{125}Te-{^1H} NMR ($CH_2Cl_2/CDCl_3$): δ 81. IR ν(CO)/cm^{-1} (CH_2Cl_2): 2035m, 1950 br m.

[PdCl(MeS(CH$_2$)$_3$Te(CH$_2$)$_3$SMe)][PF$_6$]

$[PdCl_2(MeCN)_2]$ (0.08g, 0.32 mmol) in MeCN (*ca.* 5 cm^3) was added to a solution of $MeS(CH_2)_3Te(CH_2)_3SMe$ (0.10g, 0.34 mmol) in CH_2Cl_2 (*ca.* 20 cm^3), followed by the addition of $TlPF_6$ (0.13g, 0.36 mmol). The mixture was stirred at room temperature overnight, filtered through celite and the solvent volume reduced to *ca.* 10 cm^3 *in vacuo*. The concentrate was added to ice-cold Et_2O to form a gum, which was recrystallised from Me_2CO/Et_2O to produce a yellow solid. Yield 0.09g, 43%. Calc. for

$[C_8H_{18}S_2TeClPd].¼Et_2O$: C, 17.7; H, 3.3%. Found C, 17.4; H, 3.0%. ESMS (MeCN): found *m/z* = 449; calculated for $[C_8H_{18}S_2{}^{130}Te^{35}Cl^{106}Pd]^+$ 449. ^1H NMR ($(CD_3)_2CO$): δ 1.98 (m, $CH_2CH_2CH_2$), 2.6 (s, SCH_3), 2.9 (m, SCH_2), 3.4 (m, CH_2Te). ^{125}Te-{^1H} NMR ($CH_2Cl_2/CDCl_3$): δ 379. IR ν/cm^{-1} (CsI disk): 3025vw, 2962w, 2899vw, 1429m, 1357m, 1249m, 1212w, 1156w, 1002w, 977w, 829vs, 739vw, 713vw, 559vs, 313w.

[PtCl(MeS(CH$_2$)$_3$Te(CH$_2$)$_3$SMe)][PF$_6$]

$PtCl_2$ (0.05g, 0.20 mmol) was refluxed in MeCN (*ca.* 30 cm^3) for 1 hour to produce a clear, pale yellow solution. $TlPF_6$ (0.08g, 0.22 mmol) was added and the mixture stirred at room temperature for 15 minutes. A solution of the $MeS(CH_2)_3Te(CH_2)_3SMe$ (0.06g, 0.20 mmol) in MeCN (*ca.* 5 cm^3) was added and the solution stirred at room temperature for a further 18 hours. Removal of the solvent *in vacuo*, followed by dissolution of the residue in acetone and filtration (celite) afforded a clear pale yellow solution. Reduction of the solvent volume to *ca.* 5 cm^3 and addition to ice-cold Et_2O produced a yellow solid, which was filtered, washed with Et_2O and dried *in vacuo*. Yield 0.05g, 38%. Calc. for $[C_8H_{18}S_2TeClPt]$: C, 14.1; H, 2.7%. Found C, 14.6; H, 2.6%. ESMS (MeCN): found *m/z* = 537; calculated for $[C_8H_{18}S_2{}^{130}Te^{195}Pt^{35}Cl]^+$ 537. ^1H NMR ($(CD_3)_2CO$): δ 2.6 (br m, 4H, $CH_2CH_2CH_2$), 2.7, 2.85, 2.9 (s, 6H, SCH_3), 3.0 (m, SCH_2), 3.40 (m, $TeCH_2$). ^{125}Te-{^1H} NMR ($(CD_3)_2CO$): δ 348, 356 (*ca.* 3 : 2). ^{195}Pt-{^1H} NMR ($(CD_3)_2CO$), -80°C: δ -3079, -3140 (*ca.* 1 : 1). IR ν/cm^{-1} (CsI disk): 2925vw, 1708m, 1435m, 1362m, 1093m, 838vs, 559vs, 306s.

[Rh(cp*)(MeS(CH$_2$)$_3$Te(CH$_2$)$_3$SMe)][PF$_6$]$_2$

To a vessel containing $MeS(CH_2)_3Te(CH_2)_3SMe$ (0.08g, 0.26 mmol) was added a solution of $[Rh(cp^*)Cl_2]_2$ (0.08g, 0.13 mmol) and $TlPF_6$ (0.20g, 0.58 mmol) in MeOH (*ca.* 30 cm^3). The mixture was refluxed for 2 hours before being allowed to cool. The TlCl precipitate was removed by filtration (celite) and the solvent volume reduced *in vacuo* to *ca.* 5 cm^3 before addition to ice-cold Et_2O. The resulting bright yellow solid was filtered, washed with Et_2O and dried *in vacuo*. Yield 0.03g, 29%. Calc. for $[C_{18}H_{33}S_2TeRhP_2F_{12}]$: C, 25.9; H, 4.0%. Found: C, 25.8; H, 3.8. ESMS (MeCN): found *m/z* = 273, 294; calculated for $[C_{18}H_{33}S_2{}^{103}Rh^{130}Te]^{2+}$ 273, calculated for

$[C_{18}H_{33}S_2{}^{103}Rh^{130}Te.MeCN]^{2+}$ 294). ^1H NMR ($(CD_3)_2CO$): δ 2.2 (m, $CH_2CH_2CH_2$), 2.6 (s, CCH_3), 2.73 (s, SCH_3), 2.80 – 3.40 (SCH_2 and $TeCH_2$). ^{13}C-{^1H} NMR ($(CD_3)_2CO$): δ 106 (CCH_3), 36.8, 22.0 ($CH_2CH_2CH_2$), 25.0 (SCH_3), 22.0 (SCH_2), 14.0 ($TeCH_2$), 9.1 (CCH_3). ^{125}Te-{^1H} NMR ($(CD_3)_2CO$): δ 191 d, $^1J_{Rh\text{-}Te}$ = 94Hz. IR ν/cm^{-1} (CsI disk): 2972s, 1621m, 1583w, 1559w, 1479s, 1428s, 1381s, 1365m, 1327m, 1260s, 1232m, 1215w, 1171sh, 1159m, 1078m, 1059w, 1023m, 973w, 840vs, 613w, 560vs, 403w, 374w, 320w, 295w.

[Cu(MeS(CH$_2$)$_3$Te(CH$_2$)$_3$SMe)][BF$_4$]

A solution of $MeS(CH_2)_3Te(CH_2)_3SMe$ (0.08g, 0.25 mmol) and $[Cu(MeCN)_4][BF_4]$ (0.08g, 0.25 mmol) were stirred in CH_2Cl_2 (*ca.* 40 cm^3) for 1 hour. The solvent volume was reduced *in vacuo* to *ca.* 5 cm^3 and added to ice-cold Et_2O (*ca.* 30 cm^3) to produce a white solid, which was filtered, washed with Et_2O and dried *in vacuo*. Yield 0.09g, 79%. Calc. for $[C_8H_{18}S_2TeCu].½MeCN$: C, 22.7; H, 4.0%. Found: C, 23.2; H, 4.3%. ESMS (MeCN): found *m/z* = 371, 412; calculated for $[C_8H_{18}S_2{}^{130}Te^{63}Cu]^+$ 371, calculated for $[C_8H_{18}S_2{}^{130}Te^{63}Cu.MeCN]^+$ 412). ^1H NMR ($(CH_3)_2CO$): δ 1.98 (CH_3CN), 2.20 (m, 4H, $CH_2CH_2CH_2$), 2.32 (s, SCH_3), 2.76 (m, SCH_2), 2.88 (m, $TeCH_2$). ^{125}Te-{^1H} NMR ($(CD_3)_2CO$): δ 99 ($w_{1/2}$ = 700 Hz). IR ν/cm^{-1} (CsI disk): 2962s, 2925m, 2859m, 2270w, 1817vw, 1629m, 1553m, 1424s, 1379sh, 1825w, 1261s, 1211w, 1080br s, 865m, 807s, 704m, 567w, 519m, 473w, 444vw, 397s, 286m, 275m, 271m, 257m, 253s, 244s, 231s, 227vs.

[Ag(MeS(CH$_2$)$_3$Te(CH$_2$)$_3$SMe)][CF$_3$SO$_3$]

$AgCF_3SO_3$ (0.09g, 0.34 mmol) and $MeS(CH_2)_3Te(CH_2)_3SMe$ (0.10g, 0.34 mmol) were stirred in CH_2Cl_2 (*ca.* 30 cm^3) in a foil-wrapped vessel for 30 minutes. The solvent volume was reduced *in vacuo* to *ca.* 10 cm^3 and hexane (*ca.* 20 cm^3) added. After chilling overnight (-18°C) the resultant precipitate was filtered off, washed with Et_2O and dried *in vacuo* to give a white solid. Yield 0.10g, 64%. Calc. for $[C_9H_{18}S_3TeAgF_3O_3]$: C, 19.2; H, 3.2%. Found: C, 19.7; H, 2.6%. ESMS (MeCN): found *m/z* = 415; calculated for $[C_8H_{18}S_2{}^{130}Te^{106}Ag]^+$ 415. ^1H NMR (CD_2Cl_2): δ 1.90 (m, 4H, $CH_2CH_2CH_2$), 2.00 (s, 6H, SCH_3), 2.40 (m, 4H, SCH_2), 2.60 (m, 4H, $TeCH_2$). IR ν/cm^{-1} (CsI disk): 2915w,

2852vw, 2363vw, 1653w, 1424sh., 1358sh., 1283s, 1232s, 1163s, 1094sh., 1038s, 991sh., 834w, 760m, 643s, 580m, 514m, 351w, 319vw, 290vw, 283vw, 267vw, 262vw.

X-ray crystallography

Details of the crystallographic parameters are given in Table 4.2. Data collection was performed by Melissa Matthews using an Enraf-Nonius Kappa CCD diffractometer operating at 120K for $[PtCl(MeS(CH_2)_3Te(CH_2)_3SMe)][PF_6]$ and 150K for $[Rh(cp^*)(MeS(CH_2)_3Te(CH_2)_3SMe)][PF_6]_2$. The data were corrected for absorption by SORTAV.[27,28] Structure solution and refinement were routine for both structures.[29,30] In $[PtCl(MeS(CH_2)_3Te(CH_2)_3SMe)][PF_6]$, two independent cations and anions were identified in the asymmetric unit, although no higher symmetry cell could be identified. One PF_6^- anion was disordered; this being modeled reasonably successfully using a 65:35 split occupancy.

4.9 References

1. E. W. Abel, K. Kite and P. S. Perkins, *Polyhedron*, 1986, **5**, 1459.
2. R. Ali, S. J. Higgins and W. Levason, *Inorg. Chim. Acta.*, 1984, **84**, 65.
3. S. J. Loeb and J. R. Mansfield, *Can. J. Chem.*, 1996, **74**, 1377.
4. D. J. Gulliver, E. G. Hope and W. Levason, *J. Chem. Soc., Perkin Trans. II*, 1984, 429.
5. A. J. Barton, W. Levason, G. Reid and A. J. Ward, *Organometallics*, 2001, **20**, 3644.
6. J. Connolly, A. R. J. Genge, W. Levason, S. D. Orchard, S. J. A. Pope and G. Reid, *J. Chem. Soc., Dalton Trans.*, 1999, 2343.
7. W. Levason, G. Reid and S. M. Smith, *Polyhedron*, 1997, **16**, 4253.
8. P. K. Baker, A. I. Clark, S. J. Coles, M. B. Hursthouse and R. L. Richards, *J. Organomet. Chem.*, 1996, **518**, 235.
9. M. Misra, and A. K. Singh, *Phosphorus, Sulfur, Silicon, Relat. Elem.*, 1998, **134-135**, 537.
10. W. Levason, S. D. Orchard, G. Reid and V.-A. Tolhurst, *J. Chem. Soc., Dalton Trans.*, 1999, 2071.
11. S. D. Orchard, Ph. D. thesis, University of Southampton, 2000.
12. W. Levason, S. D. Orchard and G. Reid, *J. Chem. Soc., Chem. Commun.*, 2001, **5**, 427.
13. W. Levason, C. A. McAuliffe and S. G. Murray, *Inorg. Chim. Acta*, 1976, **17**, 247.
14. D. H. O'Brien, N. Dereu, C. K. Huang, K. J. Irgolic and F. F. Knapp Jr., *Organometallics*, 1983, **2**, 305.
15. R. Usón, V. Riera, J. Gimeno, M. Laguna and M. P. Gamasa, *J. Chem. Soc., Dalton Trans.*, 1979, 996.
16. W. Levason, S. D. Orchard and G. Reid, *Organometallics*, 1999, **18**, 1275.
17. F. R. Hartley, S. Murray and C. A. McAuliffe, *Inorg. Chem.*, 1979, **18**, 1394.
18. E. W. Abel, S. K. Bhargava, K. G. Orrel, *Prog. Inorg. Chem.*, 1984, **32**, 1.

19. E. G. Hope, W. Levason, S. G. Murray, G. L. Marshall, *J. Chem. Soc., Dalton Trans.*, 1985, 2185.
20. J. W. Kang, K. Mosely and P. M. Maitlis, *J. Am. Chem. Soc.*, 1969, **91**, 5970.
21. W. Levason, S. D. Orchard, G. Reid and J. M. Street, *J. Chem. Soc., Dalton Trans.*, 2000, 2537.
22. M. N. Bell, A. J. Blake, M. Schröder and T. A. Stephenson, *J. Chem. Soc., Chem. Commun.*, 1986, 471.
23. G. Kubas, *Inorg. Synth.*, 1990, **28**, 68.
24. J. R. Black and W. Levason, *J. Chem. Soc., Dalton Trans.*, 1994, 3225.
25. J. R. Black, N. R. Champness, W. Levason and G. Reid, *J. Chem. Soc., Dalton. Trans.*, 1995, 3439.
26. W–F. Liaw, C–H. Lai, S–J. Chiou, Y–C. Horng, C–C. Chou, M–C. Liaw, G–S. Lee and S–M. Peng, *Inorg. Chem.*, 1995, **34**, 3755.
27. R. H. Blessing, *Acta Crystallogr. Sect. A*, 1995, **51**, 33.
28. R. H. Blessing, *J. Appl. Crystallogr.*, 1997, **30**, 421.
29. PATTY, the DIRDIF Program System, P. T. Beurskens, G. Admiraal, G. Beurskens, W. P. Bosman, S. Garcia-Granda, R. O. Gould, J. M. M. Smits and C. Smykalla, *Technical Report of the Crystallography Laboratory*, University of Nijmegen, The Netherlands, 1992.
30. TeXsan: Crystal Structure Analysis Package, Molecular Structure Corporation, Texas, 1995.

Chapter 5:

Synthesis and Te(IV) derivatives of xylyl-based telluroether ligands

5.0 Introduction

Our group has been interested in the synthesis and coordination chemistry of polydentate and macrocyclic telluroether ligands with transition metal ions. Unlike in thioether chemistry where the ligand synthesis is not greatly affected by the nature of the inter-donor linkage, for telluroethers the choice of inter-donor linkage can play an important role in determining the outcome of the organotellurium reaction chemistry and therefore only a restricted range of linking units have been reported to date.[1,2] The nature of the inter-donor unit can also significantly influence the metal binding properties of the ligands, and therefore we wished to extend the range of di- and poly-telluroether compounds to investigate these factors in more detail.

During studies into the incorporation of *o*-xylyl linkages into tellurium compounds, our laboratory reported the synthesis of 1,2-bis(methyltelluromethyl)benzene, *o*-$C_6H_4(CH_2TeMe)_2$, *via* the reaction of α,α'-dibromo-*o*-xylene with MeTeLi in thf solution[3] (Figure 5.0).

Figure 5.0 - Synthesis of o-$C_6H_4(CH_2TeMe)_2$[3]

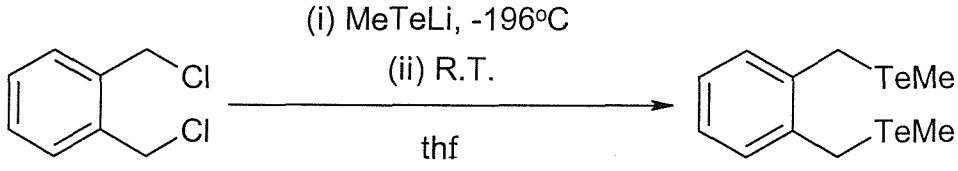

The ligand was reported to form the white Te(IV) derivative *o*-$C_6H_4(CH_2TeMe_2I)_2$ upon reaction with MeI in acetone solution.[4] The crystal structure of the compound (Figure 5.1) showed a weakly associated dimer, assembled through a series of secondary Te···I interactions to give a *pseudo*-cubane Te_4I_4 core involving 3-coordinate (*i.e.* pyramidal) iodine and 6-coordinate (distorted octahedral) tellurium. The *o*-xylyl backbone units were oriented across the diagonal of two opposite faces of the cubane.[4]

Figure 5.1 - Crystal structure of o-$C_6H_4(CH_2TeMe_2I)_2$[4]

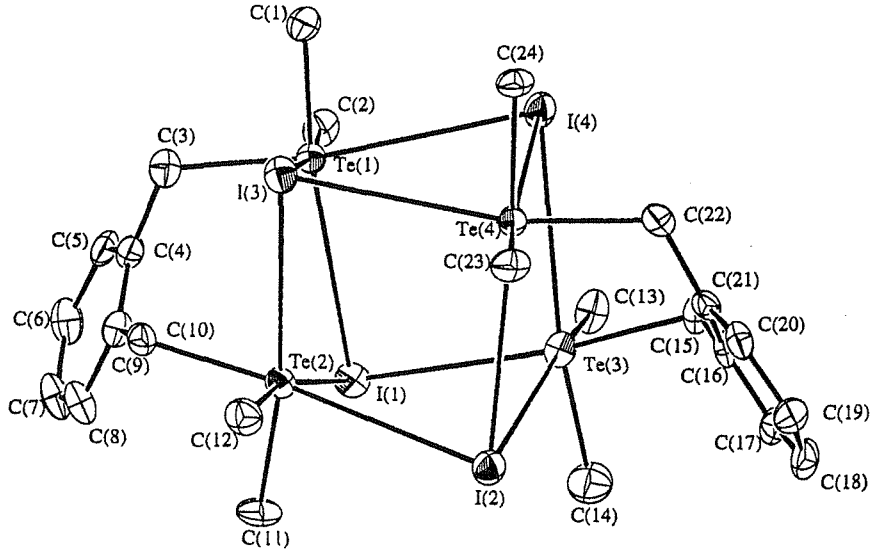

Upon chelation of *o*-$C_6H_4(CH_2TeMe)_2$ to a metal centre, seven membered rings are produced and a selected range of metal complexes have been reported. The reaction of $[Cu(MeCN)_4][PF_6]$ or $Ag(CF_3SO_3)$ with 2 molar equivalents of the ligand in MeCN solution formed the yellow $[Cu\{o\text{-}C_6H_4(CH_2TeMe)_2\}_2][PF_6]$ and off-white $[Ag\{o\text{-}C_6H_4(CH_2TeMe)_2\}_2][CF_3SO_3]$ respectively.[3] Both complexes displayed small, negative coordination shifts in their respective $^{125}Te\text{-}\{^1H\}$ NMR spectra, with $[Ag\{o\text{-}C_6H_4(CH_2TeMe)_2\}_2][CF_3SO_3]$ being unstable in solution, as has been observed for other Ag-telluroether complexes.[5] The ligand also reacts with $[MCl_2(MeCN)_2]$ and $TlPF_6$ in MeCN solution to form the complexes $[M\{o\text{-}C_6H_4(CH_2TeMe)_2\}_2][PF_6]_2$ (M = Pd or Pt).[3] The ^1H NMR spectra of the compounds showed broad features due to the occurrence of inversion processes at room temperature, while the poor solubility of the compounds prevented low temperature $^{125}Te\text{-}\{^1H\}$ NMR studies (no resonances were observed at ambient temperatures). The $[MCl_2\{o\text{-}C_6H_4(CH_2TeMe)_2\}]$ have also been reported *via* the reactions of $[MCl_2(MeCN)_2]$ (M = Pd or Pt) with one molar equivalent of *o*-$C_6H_4(CH_2TeMe)_2$ in MeCN.[3] The $[PtCl_2\{o\text{-}C_6H_4(CH_2TeMe)_2\}]$ complex showed two resonances in its $^{125}Te\text{-}\{^1H\}$ and ^{195}Pt NMR spectra, which were attributed to the resolution of the two invertomers due to slow pyramidal inversion in the *trans*-Cl-Pt-Te system.[3] The corresponding Pd complex only displayed one resonance in its $^{125}Te\text{-}\{^1H\}$

NMR spectrum; the inability to detect the second invertomer being attributed to the low solubility of the compound.

The $[RuCl_2\{o\text{-}C_6H_4(CH_2TeMe)_2\}_2]$ has been reported from the reaction of $[Ru(dmf)_6][CF_3SO_3]_3$ with $o\text{-}C_6H_4(CH_2TeMe)_2$ and LiCl in EtOH and $[OsCl_2\{o\text{-}C_6H_4(CH_2TeMe)_2\}_2]$ from $o\text{-}C_6H_4(CH_2TeMe)_2$ and $[OsCl_2(dmso)_4]$ in MeCN.[3] The compounds were characterised by analysis, electrospray mass spectrometry and IR spectroscopy and were identified as *trans* isomers from their characteristic UV-visible spectra. The poor solubility of the compounds in common solvents prevented NMR studies from being undertaken, however.

The $o\text{-}C_6H_4(CH_2TeMe)_2$ reacts with $[Mn(CO)_5Cl]$ to form *fac*-$[Mn(CO)_3Cl\{o\text{-}C_6H_4(CH_2TeMe)_2\}]$.[3] The complex exhibited three ν(CO) bands in its IR spectrum, consistent with the expected C_s structure. The ^{55}Mn NMR spectrum showed three resonances that were indicative of slow pyramidal inversion and the presence of three invertomers (Figure 5.2). The $^{125}Te\text{-}\{^1H\}$ NMR spectrum showed a total of four resonances, since by symmetry the two *meso* forms each have one tellurium environment and the DL has two. The X-ray structure (Figure 5.3) confirmed the *meso*-2 geometry in the solid state (as was observed for the analogous *fac*-$[Mn(CO)_3Cl\{o\text{-}C_6H_4(TeMe)_2\}]$[6]) and revealed that the Mn-Te bonds were significantly longer than those found in complexes involving smaller chelate rings.[3]

Figure 5.2 - The NMR distinguishable isomers possible for fac-[Mn(CO)$_3$Cl{o-C$_6$H$_4$(CH$_2$TeMe)$_2$}]

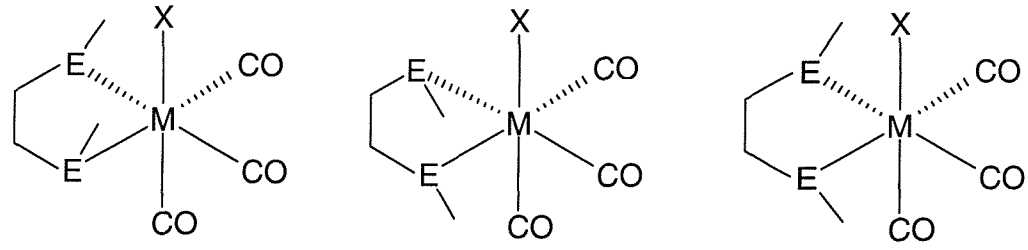

meso-1 *meso-2* *Rac*

Figure 5.3 - Crystal structure of [Mn(CO)$_3$Cl{meso-2-o-C$_6$H$_4$(CH$_2$TeMe)$_2$}][3]

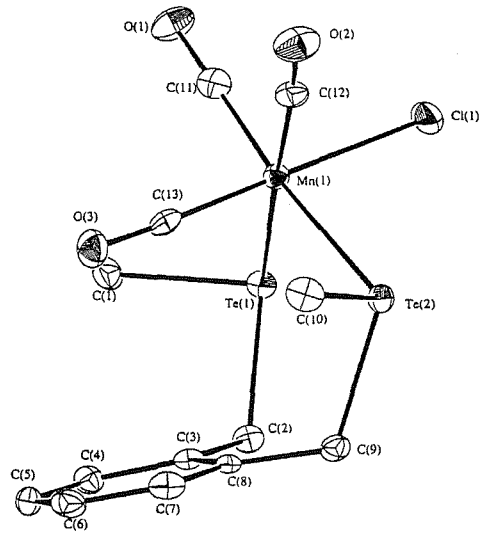

The [W(CO)$_4${*o*-C$_6$H$_4$(CH$_2$TeMe)$_2$}] and [Mo(CO)$_4${*o*-C$_6$H$_4$(CH$_2$TeMe)$_2$}] were also prepared from the reaction of *o*-C$_6$H$_4$(CH$_2$TeMe)$_2$ with the appropriate [M(CO)$_4$(piperidine)$_2$] (M = W or Mo) in thf or CH_2Cl_2 solution respectively.[3] The *cis*-tetracarbonyl geometries were confirmed by the presence of four IR active CO stretches (theory $2A_1 + B_1 + B_2$). Pyramidal inversion for both complexes was slow at room temperature, and therefore the *meso* and DL invertomers were identified in the ^{1}H, ^{13}C-{^{1}H} and ^{125}Te-{^{1}H} NMR spectra. The crystal structure of [W(CO)$_4${*o*-C$_6$H$_4$(CH$_2$TeMe)$_2$}] confirmed the expected *cis* geometry, with the *o*-C$_6$H$_4$(CH$_2$TeMe)$_2$ ligand present as the *meso* invertomer (Figure 5.4).[3]

Figure 5.4 - Crystal structure of [W(CO)$_4${o-C$_6$H$_4$(CH$_2$TeMe)$_2$}][3]

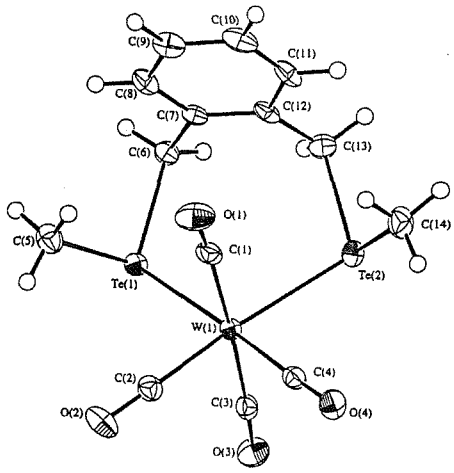

The Te···Te distances within the *o*-xylyl bridged units were 3.943 and 3.995 Å in *o*-$C_6H_4(CH_2TeMe_2I)_2$, similar to the corresponding distances in *fac*-$[M(CO)_3Cl(xyte)]$ and $[W(CO)_4(xyte)]$, which suggested that the *o*-xylyl unit provides a fairly rigid inter-tellurium linkage.[3,4]

The xylyl based telluroether ligands *m*-$C_6H_4(CH_2TePh)_2$ and *o*-$C_6H_4(CH_2TePh)_2$[7] have also been reported, although no studies into their coordination chemistry have been undertaken. There have also been reports of other related telluroether ligands incorporating a single tellurium donor atom, including the benzyl ligand $C_6H_4(CH_2TePh)$ and *p*-$C_6H_4(R)(TePh)$ (R = MeO or NO_2) although their coordination chemistry has not been investigated.[7]

We wished to investigate the synthesis of the direct analogues of *o*-$C_6H_4(CH_2TeMe)_2$, *m*- and *p*-$C_6H_4(CH_2TeMe)_2$, and to probe the occurrence of secondary bonding interactions in their Te(IV) iodide derivatives in order to compare their structural motifs with that of the previously reported *o*-$C_6H_4(CH_2TeMe_2I)_2$,[4] since the change in substitution around the aromatic unit was expected to give interesting and differing morphologies. Also described in this chapter are the reactions of the ligands with $[Cu(MeCN)_4][BF_4]$ in order to probe their coordination chemistry.

We are also interested in the incorporation of more than one tellurium donor within a rigid macrocyclic environment, following our studies into the synthesis and complexation behaviour of the mixed donor ligands [9]-, [11]- and [12]-aneS_2Te (Chapter 2) and [9]aneO_2Te and [18]aneO_4Te_2 (Chapter 3). The cyclic analogues of the *o*- and *m*-xylyl ligands, 2,11-ditellura[3.3]orthocyclophane and 2,11-ditellura[3.3]metacyclophane (Figure 5.5) are of interest since they would incorporate two tellurium atoms within a rigid, macrocyclic framework and would allow for comparisons with the *o*- and *m*-$C_6H_4(CH_2TeMe)_2$.

There are many known sulfur and selenium-containing cyclophanes, including the sulfur and selenium analogues of 2,11-ditellura[3.3]orthocyclophane,[7] together with numerous other examples.[9,10]

Figure 5.5 - 2,11-ditellura[3.3]orthocyclophane (i) and 2,11-ditellura[3.3]metacyclophane (ii)

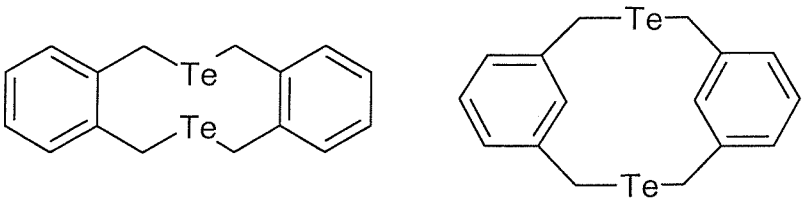

(i) (ii)

The crystal structures of 2,11-dithia[3.3]orthocyclophane and 2,11-diselena[3.3]orthocyclophane are very similar, showing the molecules adopting *anti* conformations with the benzene ring units staggered (Figure 5.6).[7] There have been no reports of any tellurium-containing cyclophanes, however, so this chapter will describe the attempted syntheses of 2,11-ditellura[3.3]orthocyclophane and 2,11-ditellura[3.3]metacyclophane.

Figure 5.6 – Crystal structures of 2,11-dithia[3.3]orthocyclophane (i) and 2,11-diselena[3.3]orthocyclophane (ii)[7]

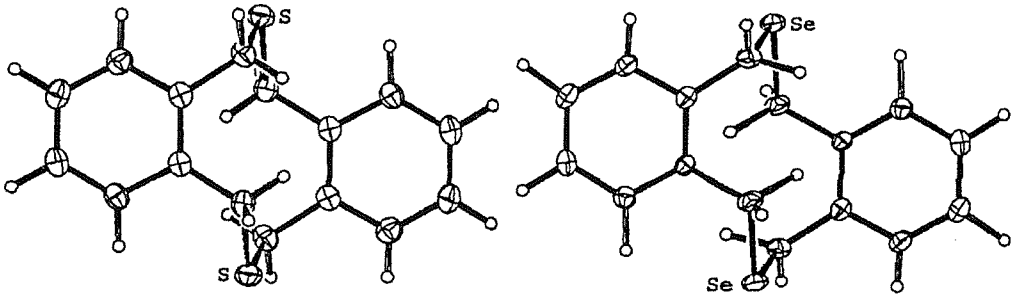

(i) (ii)

5.1 Results and discussion

5.1.1 Ligand synthesis

The new ditelluroether ligands *m*-$C_6H_4(CH_2TeMe)_2$ and *p*-$C_6H_4(CH_2TeMe)_2$ (Figure 5.7) were prepared similarly to the method previously described for the preparation of the analogous *o*-$C_6H_4(CH_2TeMe)_2$.[3]

Figure 5.7 - m-$C_6H_4(CH_2TeMe)_2$ and p-$C_6H_4(CH_2TeMe)_2$

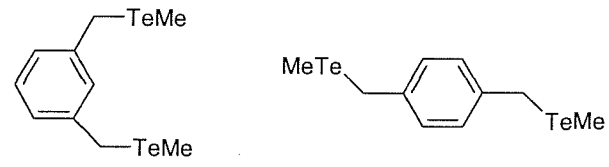

m-$C_6H_4(CH_2TeMe)_2$ *p*-$C_6H_4(CH_2TeMe)_2$

Freshly ground Te powder was frozen (-196°C) in dry thf and MeLi added, which, upon warming to room temperature formed clear yellow solutions of MeTeLi. These were refrozen (-196°C) and solutions of *m*-$C_6H_4(CH_2Br)_2$ or *p*-$C_6H_4(CH_2Br)_2$ in thf added, before allowing the mixtures to warm to room temperature and stir for approximately 20 hours. The resulting orange mixtures were hydrolysed and extracted with CH_2Cl_2, and the combined organic extracts dried over $MgSO_4$. Filtration and removal of the solvent *in vacuo* afforded the compounds *m*-$C_6H_4(CH_2TeMe)_2$ and *p*-$C_6H_4(CH_2TeMe)_2$ as air sensitive yellow-orange solids, yields 69% and 82% respectively. The preparation of the *o*-$C_6H_4(CH_2TeMe)_2$ was undertaken similarly to give a red gum in 83% yield.

The ^1H, ^{13}C-{^1H} and ^{125}Te-{^1H} NMR spectra of the compounds (Table 5.0) were consistent with the proposed formulations, while the data for *o*-$C_6H_4(CH_2TeMe)_2$ were consistent with previously obtained values.[7] The single resonance at δ 264 ppm in the ^{125}Te-{^1H} NMR spectrum was identical to the literature value, whilst the characteristic δ(TeMe) resonance in the ^{13}C-{^1H} NMR spectrum was observed at –18.9 ppm. The NMR spectra of *m*-$C_6H_4(CH_2TeMe)_2$ and *p*-$C_6H_4(CH_2TeMe)_2$ were similar to each other and *o*-$C_6H_4(CH_2TeMe)_2$, with the most notable difference being in their ^{125}Te-{^1H} NMR spectra (δ(^{125}Te) = 311 ppm for both *m*- and *p*-$C_6H_4(CH_2TeMe)_2$, compared

with δ 264 ppm for *o*-$C_6H_4(CH_2TeMe)_2$). The *m*- and *p*-$C_6H_4(CH_2TeMe)_2$ both showed δ(TeMe) resonances at -20.1 ppm in their respective ^{13}C-{^1H} NMR spectra, which were very similar to the value for the analogous *o*-$C_6H_4(CH_2TeMe)_2$ (-18.9 ppm). The $TeCH_2$ resonances were observed at 3.5, 5.7 and 5.3 ppm for *o*-, *m*- and *p*-$C_6H_4(CH_2TeMe)_2$ respectively, with the aromatic resonances observed between 126.4 and 141.4 ppm. Of these, the *ipso*-carbons resonated at the highest frequency. ^1H NMR spectra of the compounds were also very similar, showing $TeCH_3$ resonances at 1.79, 1.95 and 1.75 ppm and $TeCH_2$ resonances at 4.0, 4.0 and 3.9 ppm for *o*-, *m*- and *p*-$C_6H_4(CH_2TeMe)_2$ respectively.

Table 5.0 - ^1H, ^{13}C-{^1H} and ^{125}Te-{^1H} NMR data for o-, m- and p-$C_6H_4(CH_2TeMe)_2$ (o, m and p respectively)

	^1H δ (ppm)[a]	Assignment	^{13}C-{^1H} δ (ppm)[a]	Assignment	^{125}Te-{^1H} δ (ppm)[b]
o	7.0 – 7.03, m, 4H	*o*-C_6H_4	138.3	*ipso-C*, *o*-C_6H_4	264
	3.97, s, 4H	CH_2	130.6	*o*-C_6H_4	
	1.79, s, 6H	CH_3	126.9	*o*-C_6H_4	
			3.5	CH_2	
			-18.9	CH_3	
m	7.0 – 7.2, m, 4H	*m*-C_6H_4	141.4	*ipso-C*, *m*-C_6H_4	311
	4.0, s, 4H	CH_2	128.8	1C, *m*-C_6H_4	
	1.95, s, 6H	CH_3	128.6	1C, *m*-C_6H_4	
			126.4	2C, *m*-C_6H_4	
			5.7	CH_2	
			-20.1	CH_3	
p	7.05, s, 4H	*p*-C_6H_4	138.8	*ipso-C*, *p*-C_6H_4	311
	3.9, s, 4H	CH_2	129.0	*p*-C_6H_4	
	1.75, s, 6H	CH_3	5.3	CH_2	
			-20.1	CH_3	

([a]: $CDCl_3$ solution; [b]: CH_2Cl_2 solution). *o*-$C_6H_4(CH_2TeMe)_2$ lit.[7]: ^1H NMR ($CDCl_3$): δ 7.09 (m, 4H), 4.05 (s, 4H), 1.78 (s, 6H). ^{13}C-{^1H} NMR ($CDCl_3$): δ 138.1, 130.6, 126.6, 3.7, -15.5. ^{125}Te-{^1H} NMR ($CDCl_3$): δ 264.

EI mass spectrometry of both *m*- and *p*-$C_6H_4(CH_2TeMe)_2$ showed clusters of peaks centred at *m/z* = 390 for both compounds, consistent with the monocationic [*m*-/*p*-$C_6H_4(CH_2TeMe)_2]^+$.

5.2 Organo-derivatives

Several Te(IV) organo-derivatives of the xylyl ligands have been synthesised in order to confirm the identities of the parent telluroether compounds (since the Te(IV) species are air-stable solids and are therefore easy to handle and characterise) and to probe the occurrence of secondary Te···I interactions and lone pair effects in the systems.

Reaction of *m*- or *p*-$C_6H_4(CH_2TeMe)_2$ with excess MeI in CH_2Cl_2 solution produced the telluronium salts *m*- or *p*-$C_6H_4(CH_2TeMe_2I)_2$ respectively as cream coloured powdered solids in good yield (both 72%). The formulations were confirmed by the microanalytical data, whilst the electrospray mass spectra displayed the dicationic [*m*-/*p*-$C_6H_4(CH_2TeMe)_2]^{2+}$ as the major species, with minor fragments consistent with the loss of Me groups also present. The compounds were poorly soluble in chlorinated solvents, unlike the analogous *o*-$C_6H_4(CH_2TeMe_2I)_2$, which was reasonably soluble in $CHCl_3$.[4] All NMR measurements were therefore undertaken using solutions of the compounds in d_6-dmso. The ^1H NMR spectra of the compounds displayed essentially unshifted aromatic resonances, with the TeCH_2 resonances being observed at δ 4.1 and 4.05 ppm for *m*- and *p*-$C_6H_4(CH_2TeMe_2I)_2$ (compared with δ 4.0 and 3.9 ppm in *m*- and *p*-$C_6H_4(CH_2TeMe)_2$ respectively). The TeCH_3 resonances were observed at δ 1.9 and 1.8 ppm for the *m*- and *p*-derivatives, which were similar to the values observed for *m*- and *p*-$C_6H_4(CH_2TeMe)_2$ (δ 1.95 and 1.75 ppm respectively). The ^{13}C-{^1H} NMR spectra of the compounds displayed characteristic high frequency shifts for the TeCH_3 and TeCH_2 resonances (δ(^{125}Te(TeCH_3)) = δ 7.1 and 6.9 ppm for *m*- and *p*-$C_6H_4(CH_2TeMe)_2$ compared with δ -20.1 and -20.1 ppm for *m*- and *p*-$C_6H_4(CH_2TeMe)_2$ respectively, whilst

the $TeCH_2$ resonances were observed at δ 29.1 and 28.2 ppm for *m*- and *p*-$C_6H_4(CH_2TeMe)_2$ (δ 5.7 and 3.9 ppm in *m*- and *p*-$C_6H_4(CH_2TeMe)_2$ respectively). The ^{125}Te-{^1H} NMR spectra of the compounds displayed noticeable high frequency shifts to δ 531 and 537 ppm for the *m*- and *p*-derivatives respectively, compared with δ 311 in *m*- and *p*-$C_6H_4(CH_2TeMe)_2$. The values were similar to the previously reported ^{125}Te-{^1H} NMR shift for *o*-$C_6H_4(CH_2TeMe_2I)_2$ (δ 526 ppm)[4] and were consistent with other known Te(IV)Me_2I derivatives, for example *o*-$C_6H_4(TeMe_2I)_2$ has δ(^{125}Te) = 588 ppm.[11] These data were consistent with the oxidation of the formally Te(II) centers in *m*- and *p*-$C_6H_4(CH_2TeMe)_2$ to Te(IV) in the compounds *m*- and *p*-$C_6H_4(CH_2TeMe_2I)_2$.

The compounds *o*-, *m*- and *p*-$C_6H_4(CH_2TeMe)_2$ also react with two equivalents of diiodine in thf solution to produce the air-stable, formally Te(IV) derivatives *o*-, *m*- or *p*-$C_6H_4(CH_2TeI_2Me)_2$ (Figure 5.8) as brick-red solids in moderate yield (30 – 47%).

Figure 5.8 - o-, m- and p-$C_6H_4(CH_2TeI_2Me)_2$ ((i), (ii) and (iii) respectively)

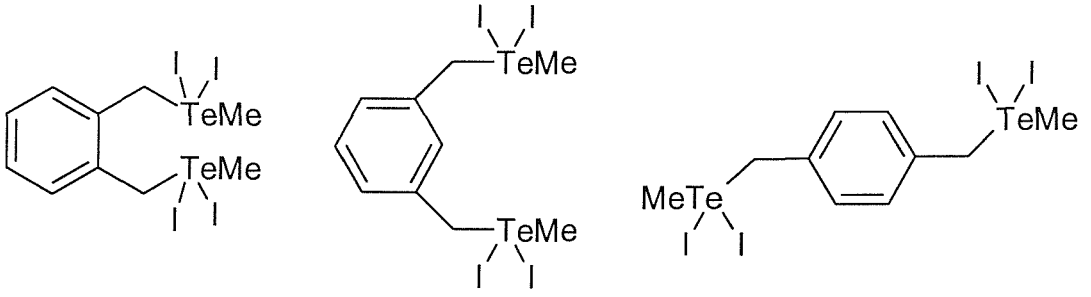

(i) (ii) (iii)

Microanalytical data for all three compounds confirmed the proposed formulations, whilst the ^1H NMR spectra in d_6-dmso showed resonances consistent with the formation of Te(IV) diiodide species. The $TeCH_3$ resonances were observed at δ 2.95, 2.4 and 2.35 ppm for *o*-, *m*- and *p*-$C_6H_4(CH_2TeI_2Me)_2$ respectively, showing a high frequency shift upon conversion of the formally Te(II) centres to Te(IV). (The δ($TeCH_3$) are δ 1.79, 1.95 and 1.75 ppm for *o*-, *m*- and *p*-$C_6H_4(CH_2TeMe)_2$ respectively. The $TeCH_2$ resonances were also observed to shift to high frequency compared with the free ligand values,

showing resonances at δ 4.30, 4.6 and 4.65 ppm for *o*-, *m*- and *p*-$C_6H_4(CH_2TeI_2Me)_2$ (compared with δ 3.97, 4.0 and 3.9 ppm for *o*-, *m*- and *p*-$C_6H_4(CH_2TeMe)_2$ respectively. For all three compounds, resonances assigned to the aromatic ring were essentially unshifted from those in the free ligands at *ca.* 7.1 – 7.7 ppm. The ^{13}C-{^1H} NMR spectra of *m*- and *p*-$C_6H_4(CH_2TeI_2Me)_2$ showed considerable high frequency shifts for the TeCH_3 resonances at δ 10.8 and 20.9 ppm for *m*- and *p*-$C_6H_4(CH_2TeI_2Me)_2$ respectively (compared with δ -20.1 for both *m*- and *p*-$C_6H_4(CH_2TeMe)_2$). The TeCH_2 resonances also displayed significant shifts upon quaternisation (δ 41.3 and 41.4 ppm for *m*- and *p*-$C_6H_4(CH_2TeI_2Me)_2$ compared with δ 5.7 and 5.3 ppm for *m*- and *p*-$C_6H_4(CH_2TeI_2Me)_2$ respectively). The aromatic carbon resonances were observed to be essentially unshifted from those in *m*- and *p*-$C_6H_4(CH_2TeMe)_2$. The *o*-$C_6H_4(CH_2TeI_2Me)_2$ was observed to decompose appreciably over the course of about one hour in solution, and therefore ^{13}C-{^1H} NMR data were not recorded for this compound. The ^{125}Te-{^1H} NMR spectra of *m*- and *p*-$C_6H_4(CH_2TeI_2Me)$ (Figure 5.9) showed resonances at δ 738 and 739 ppm respectively, these being shifted significantly to high frequency of the values for the respective *m*- and *p*-$C_6H_4(CH_2TeMe)_2$, which both had δ(^{125}Te) = 311 ppm.

Figure 5.9 - ^{125}Te-{^1H} NMR spectrum of p-$C_6H_4(CH_2TeI_2Me)_2$ in thf-$CDCl_3$

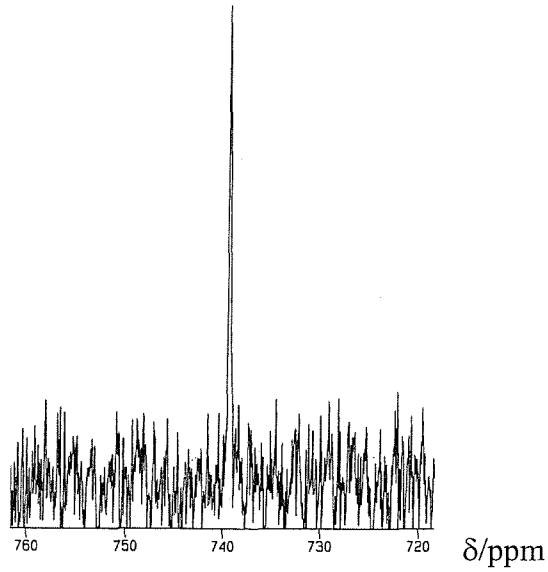

The ^{125}Te-{^{1}H} NMR spectrum of *o*-$C_6H_4(CH_2TeI_2Me)_2$ displayed 3 resonances at δ 791, 778 and 770 ppm in an approximately 3 : 2 : 1 ratio, with only the resonance at δ 778 ppm remaining after allowing the sealed NMR solution to stand at room temperature for one week. After this time, decomposition was clearly evident in the sample, with the precipitation of black material. A crystal of I_2 was added to a solution of *o*-$C_6H_4(CH_2TeMe)_2$ in thf/$CDCl_3$ and a ^{125}Te-{^{1}H} NMR spectrum of the mixture recorded, this time two resonances at δ 793 and 780 ppm were observed in an approximately 1 : 1 ratio. From these data it was concluded that the *o*-$C_6H_4(CH_2TeI_2Me)_2$ compound is unstable in solution.

5.3 Crystal structures of *m*- and *p*-$C_6H_4(CH_2TeI_2Me)_2$

Crystals of *m*- and *p*-$C_6H_4(CH_2TeI_2Me)_2$ were grown by slow evaporation of solutions of the compounds in CH_2Cl_2-$CDCl_3$. The structures (*m*-$C_6H_4(CH_2TeI_2Me)_2$ Figure 5.10, Table 5.1, and *p*-$C_6H_4(CH_2TeI_2Me)_2$ Figure 5.11, Table 5.2) showed essentially *pseudo*-trigonal bipyramidal geometries about the Te(IV) centres, with the Te-based lone pair assumed to occupy the vacant equatorial vertex in each case. The *m*-$C_6H_4(CH_2TeI_2Me)_2$ was observed to be an essentially covalent compound, with two iodine atoms coordinated to each Te atom in an axial (*trans*) arrangement, hence the formally Te(IV) centres, with the CH_2TeI_2Me units lying directed on opposite sides of the arene unit. The primary Te-I bonds were observed to lie in the range 2.870(2) – 2.997(2) Å. The values are similar to the Te-I bond lengths in other Te(IV) iodide compounds, for example [12]aneS_2TeI_2 had d(Te-I) = 2.8990(9) and 2.9179(9) Å (Chapter 2), whilst 1,1-diiodo-3,4-benzo-1-telluracyclopentane had d(Te-I) = 2.928 and 2.900 Å).[12] An examination of the crystal packing in *m*-$C_6H_4(CH_2TeI_2Me)_2$ also showed significant, longer range (secondary) Te···I interactions (Te(1)···I(4)' = 3.760(2), Te(2)···I(2)'' = 3.686 Å) between adjacent molecules which link them into an infinite array. There is also a long intermolecular Te···I contact to each Te atom (Te(1)-I(2)''' = 4.110(2), Te(2)-I(3)'''' = 4.059(2) Å). The van der Waals radii for Te and I are 2.20 and 2.15 Å respectively,[13] so these may be considered as weak contacts. Therefore a distorted octahedral environment is produced

at Te, with four primary bonds at each Te(IV) centre (2 C and 2 I) and two secondary interactions.

Figure 5.10 - Crystal structure of m-$C_6H_4(CH_2TeI_2Me)_2$ with numbering scheme adopted. Ellipsoids are drawn at the 40% probability level and H atoms are omitted for clarity. Intermolecular secondary Te···I contacts are indicated by thin bonds

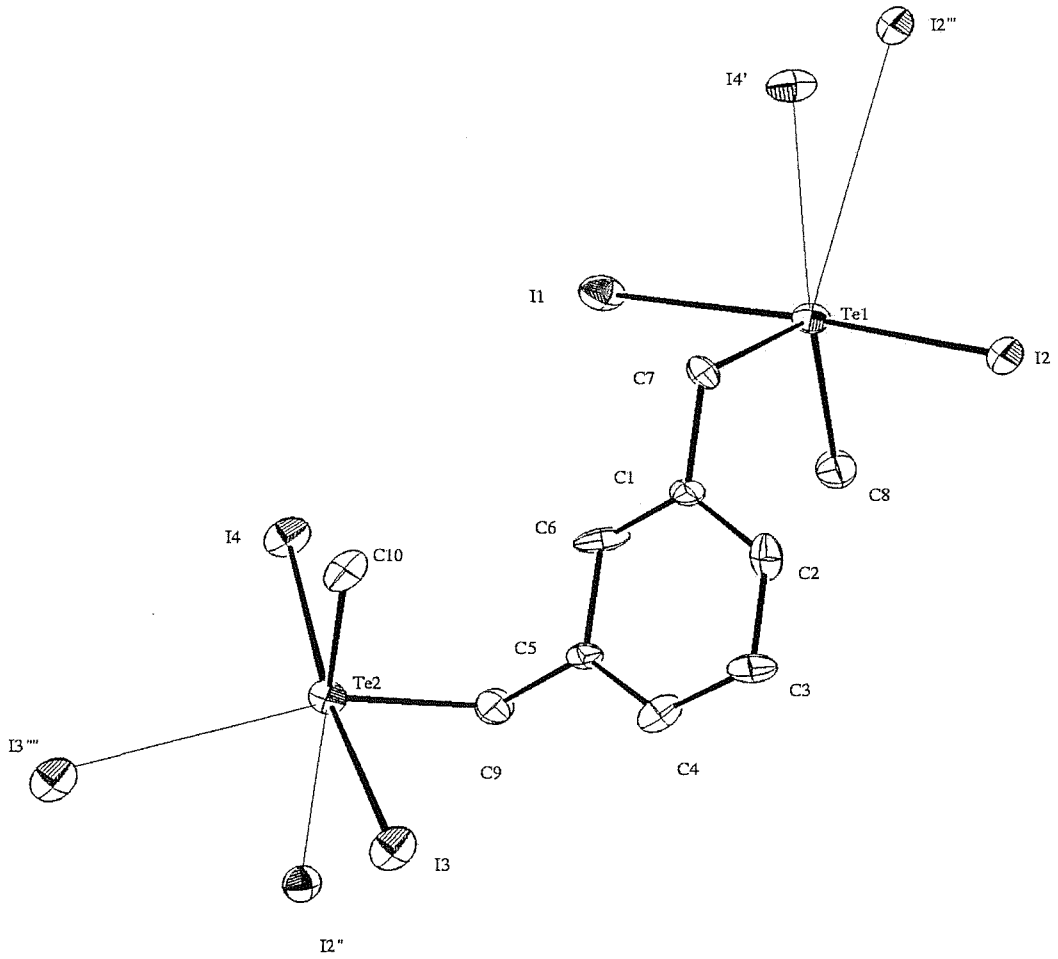

Table 5.1 - Selected bond lengths (Å) and angles (°) for m-$C_6H_4(CH_2TeI_2Me)_2$

Bond lengths			
Te(1)-C(8)	2.12(2)	Te(1)-C(7)	2.20(2)
Te(1)-I(1)	2.892(2)	Te(1)-I(2)	2.938(2)
Te(1)-C(1)	3.10(2)	Te(1)-I(4)'	3.760(2)
Te(2)-C(10)	2.08(2)	Te(2)-C(9)	2.18(3)
Te(2)-I(3)	2.870(2)	Te(2)-I(4)	2.997(2)
Te(2)-C(5)	3.11(2)	Te(2)-I(2)''	3.686(2)
Te(1)-I(2)'''	4.110(2)	Te(2)-I(3)''''	4.059(2)
Bond angles			
C(8)-Te(1)-C(7)	99.0(9)	C(8)-Te(1)-I(1)	89.4(7)
C(7)-Te(1)-I(1)	87.3(6)	C(8)-Te(1)-I(2)	90.1(7)
C(7)-Te(1)-I(2)	87.1(6)	I(1)-Te(1)-I(2)	174.20(7)
C(8)-Te(1)-I(4)'	166.0(7)	C(7)-Te(1)-I(4)'	72.8(6)
I(1)-Te(1)-I(4)'	101.24(6)	I(2)-Te(1)-I(4)'	78.41(5)
C(10)-Te(2)-C(9)	102.0(9)	C(10)-Te(2)-I(3)	90.1(7)
C(9)-Te(2)-I(3)	89.4(7)	C(10)-Te(2)-I(4)	89.7(7)
C(9)-Te(2)-I(4)	84.2(7)	I(3)-Te(2)-I(4)	173.41(8)
C(10)-Te(2)-I(2)''	170.0(7)	C(9)-Te(2)-I(2)''	74.6(6)
I(3)-Te(2)-I(2)''	99.15(6)	I(4)-Te(2)-I(2)''	80.62(5)

Symmetry operations: ' = 1-x, y-½, -z+½; '' = x, 1½-y, z+½;, ''' = 1-x, 1-y, -z; '''' = -x, 1-y, 1-z.

The crystal structure of *p*-$C_6H_4(CH_2TeI_2Me)_2$ was also determined in order to investigate the effects of the substitution patterns on the gross structure produced. The structure (Figure 5.11, Table 5.2) was found to be centrosymmetric, with an inversion centre at the mid-point of the aromatic ring and *trans*, axial iodines bound to each formally Te(IV) centre. As a result of the centre of symmetry, the CH_2TeI_2Me units lie on opposite sides of the arene ring, and the primary Te-I bond distances (2.8967(8) and 2.9309(7) Å) are similar to those in *m*-$C_6H_4(CH_2TeI_2Me)_2$ (2.870(2) – 2.997(2) Å). The *p*-$C_6H_4(CH_2TeI_2Me)_2$ was observed to have two significant secondary intermolecular bonding interactions to each Te centre; Te(1)···I(2)''' = 3.6519(8) and Te(1)···I(1)'' = 3.7979(7) Å, which resulted in a complicated infinite array. Therefore each Te(IV) centre is again in a very distorted octahedral environment consisting of two Te-C bonds, two primary Te-I bonds and two secondary Te···I interactions (Figure 5.12).

Figure 5.11 - Crystal structure of p-$C_6H_4(CH_2TeI_2Me)_2$ with numbering scheme adopted. Ellipsoids are drawn at the 40% probability level

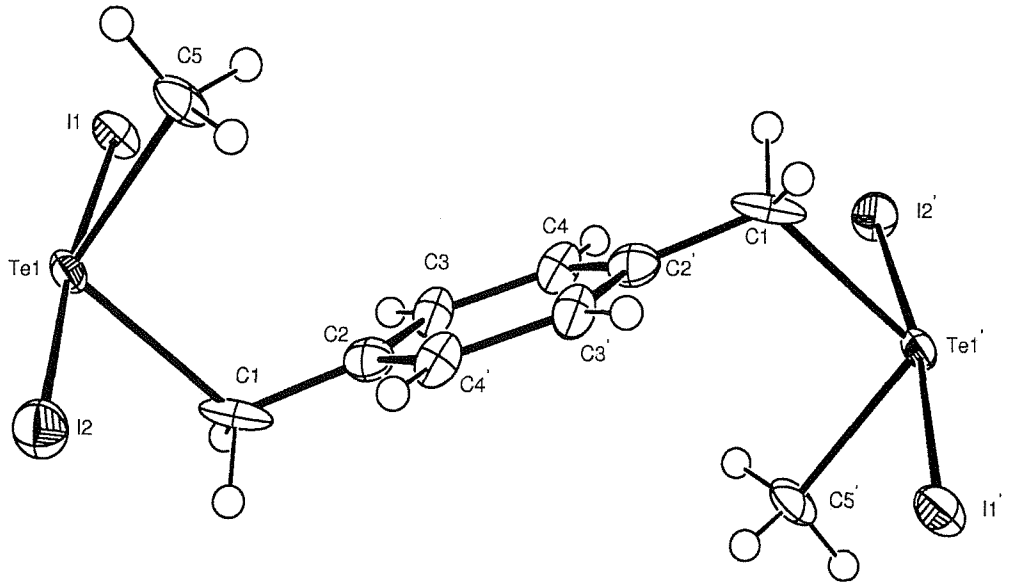

Table 5.2 - Selected bond lengths (Å) and angles (°) for p-$C_6H_4(CH_2TeI_2Me)_2$

Bond lengths			
C(1)-Te(1)	2.241(10)	C(5)-Te(1)	2.137(8)
Te(1)-I(1)	2.8967(8)	Te(1)-I(2)	2.9309(7)
Te(1)-I(2)'''	3.6519(8)	Te(1)-I(1)''	3.7979(7)
Bond angles			
C(5)-Te(1)-C(1)	100.7(3)	C(5)-Te(1)-I(1)	87.8(3)
C(1)-Te(1)-I(1)	89.0(2)	C(5)-Te(1)-I(2)	88.1(3)
C(1)-Te(1)-I(2)	88.1(2)	I(1)-Te(1)-I(2)	174.48(2)
C(5)-Te(1)-I(2)'''	85.3(3)	C(1)-Te(1)-I(2)'''	173.6(2)
I(1)-Te(1)-I(2)'''	93.38(2)	I(2)-Te(1)-I(2)'''	89.914(19)
C(5)-Te(1)-I(1)''	162.7(3)	C(1)-Te(1)-I(1)''	84.0(2)
I(1)-Te(1)-I(1)''	109.138(18)	I(2)-Te(1)-I(1)''	75.272(18)

Symmetry operations: '' = 2-x, -y, 2-z; ''' = x, ½-y, z+½.

Figure 5.12 - The environment about Te(IV) in p-$C_6H_4(CH_2TeI_2Me)_2$ with numbering scheme adopted. Ellipsoids are drawn at the 40% probability level. Secondary Te···I contacts are indicated by thin bonds

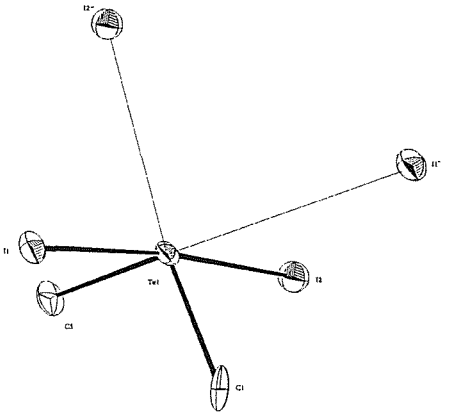

Although the secondary Te···I contacts are at similar distances to those in *o*-$C_6H_4(CH_2TeMe_2I)_2$, the extended structures are quite different from the weakly associated dimeric assembly observed in the latter compound. This is almost certainly in part due to the different substitution patterns of the arene rings which prevent simple dimer formation in the cases of *m*- and *p*-$C_6H_4(CH_2TeI_2Me)_2$.

The structures of *m*- and *p*-$C_6H_4(CH_2TeI_2Me)_2$ may be compared with the related $PhTeI_2(CH_2)_3TeI_2Ph$, formed from the reaction of $PhTe(CH_2)_3TePh$ with excess I_2 in thf solution.[14] The crystal structure of this species, as for the *m*- and *p*-$C_6H_4(CH_2TeI_2Me)_2$, has axial (*trans*) iodines bonded to the Te(IV) centres with the Te-C bonds equatorial (Figure 5.13). The primary Te-I bonds are in the range 2.883(4) – 2.938(3) Å, which was similar to the values observed for *m*-$C_6H_4(CH_2TeI_2Me)_2$ (2.870(2) – 2.997(2) Å) and *p*-$C_6H_4(CH_2TeI_2Me)_2$ (2.8967(8) and 2.9309(7) Å). An examination of the packing of the $PhTeI_2(CH_2)_3TeI_2Ph$ units also reveals an extended network formed as a result of secondary Te(1)···I(1)'' interactions (3.702(4) Å), producing weakly bound chains with the linear I-Te-I units in adjacent molecules aligned parallel and Te_2I_2 rhomboid units. In addition, weaker Te(1)···I(1)''' contacts (4.0712(6) Å) occur between a Te atom within each Te_2I_2 rhomboid unit and an I atom diagonally opposite, giving an 'up-down' chain arrangement. As for *m*- and *p*-$C_6H_4(CH_2TeI_2Me)_2$, the environment at each Te centre is *pseudo*-six coordinate, with severely distorted bond angles from those of a regular octahedral environment.[14]

A number of other Te(IV) diiodide compounds containing one Te atom have been structurally characterised, for example Me_2TeI_2. The environment at Te in the α-form of the compound was found to be *pseudo*-six coordinate, as for the *m*- and *p*-$C_6H_4(CH_2TeI_2Me)_2$, with two axial iodines having d(Te-I) = 2.885(3) and 2.965(3) Å, two *cis* Me groups and two weak intermolecular Te···I contacts (3.659(3) and 3.919(3) Å) giving an extended array.[15] The d(Te-I) and Te···I distances were similar to the values observed for the compounds *m*- and *p*-$C_6H_4(CH_2TeI_2Me)_2$. The β-form of Me_2TeI_2 was found to be the ionic species $[TeMe_3][TeMeI_4]$.[16]

Figure 5.13 - Crystal structure of $PhTeI_2(CH_2)_3TeI_2Ph$. Intermolecular secondary Te···I contacts are indicated by thin bonds[14]

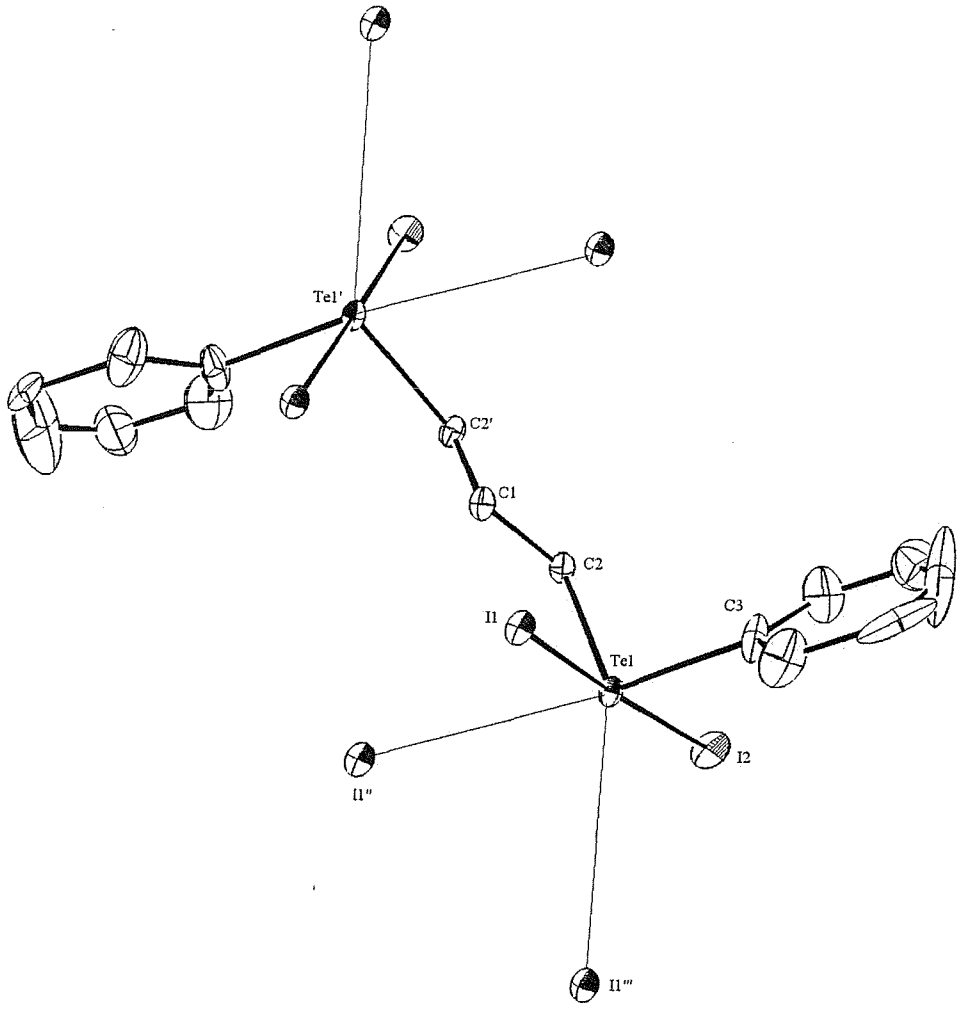

5.4 $[Cu(MeCN)_4][BF_4]$ + 2 L-L (L-L = *m*- or *p*-$C_6H_4(CH_2TeMe)_2$

The reaction of $[Cu(MeCN)_4]BF_4$[17] with two molar equivalents of *m*- or *p*-$C_6H_4(CH_2TeMe)_2$ in CH_2Cl_2 solution formed cream-coloured precipitates, which were subsequently filtered off and washed with Et_2O. The compounds were found to be poorly soluble in non-coordinating solvents (*e.g.* CH_2Cl_2, $CHCl_3$) but dissolved readily in MeCN. Electrospray mass spectra of the *m*-$C_6H_4(CH_2TeMe)_2$ Cu(I) complex showed

clusters of peaks with the correct *m/z* and isotopic distributions for the species $[Cu\{m\text{-}C_6H_4(CH_2TeMe)_2\}_2]^+$, as well as $[Cu\{m\text{-}C_6H_4(CH_2TeMe)_2\}_2 - 2\ TeMe]^+$ and $[Cu\{m\text{-}C_6H_4(CH_2TeMe)_2\}]^+$. The electrospray mass spectrum of the analogous *para*-xylyl complex showed evidence for $[Cu\{p\text{-}C_6H_4(CH_2TeMe)_2\}_2 - 2\ TeMe]^+$. The dominant species in both spectra, however, were $[Cu(MeCN)_3]^+$ and $[Cu(MeCN)_2]^+$ which showed that substantial dissociation of the complexes was occurring in MeCN solution. IR spectra of both compounds confirmed the presence of coordinated telluroether ligand, plus the presence of uncoordinated BF_4^- anion at *ca.* 1055 cm^{-1}, with no evidence of any residual MeCN in the solid compounds. ^1H NMR spectra of the Cu(I) complexes in CD_3CN solution were almost identical to those of the *m*- and *p*-$C_6H_4(CH_2TeMe)_2$ ligands, for example $\delta(TeCH_3)$ were 1.85 and 1.80 ppm for the *m*- and *p*- complexes respectively. (Compare with *m*-$C_6H_4(CH_2TeMe)_2$, $\delta(TeCH_3)$ = 1.95 ppm and *p*-$C_6H_4(CH_2TeMe)_2$, $\delta(TeCH_3)$ = 1.75 ppm). $^{125}Te\text{-}\{^1H\}$ NMR spectra of both complexes in MeCN-CD_3CN solution displayed a single resonance at δ 292 ppm, *i.e.* small low frequency coordination shifts with respect to the uncoordinated ligands ($\delta(^{125}Te)$ for *m*-and *p*-$C_6H_4(CH_2TeMe)_2$ = 311 ppm, Figure 5.14). Low frequency coordination shifts in $^{125}Te\text{-}\{^1H\}$ NMR spectroscopy are fairly unusual, but have been reported for certain complexes, for example $[Cu(MeTeCH_2TeMe)_2][BF_4]$ and $[Ag(RTe(CH_2)_3TeR)_2][BF_4]$ (R = Me or Ph).[18,19] The complexes $[Cu([18]aneO_4Te_2)_2][BF_4]$ and $[Ag([18]aneO_4Te_2)_2][BF_4]$ (Chapter 3) also displayed low frequency $^{125}Te\text{-}\{^1H\}$ coordination shifts.

The structures of the *m*- and *p*-$C_6H_4(CH_2TeMe)_2$ Cu(I) complexes are unclear since suitable crystals for X-ray structure determination were not obtainable. Microanalytical data for the *meta* complex were consistent with a 2 : 1 ligand to Cu ratio, *i.e.* $[Cu\{m\text{-}C_6H_4(CH_2TeMe)_2\}_2][BF_4]$, however the microanalytical data for the *para* complex were close to the calculated values for a 1.5 : 1 ligand : Cu ratio. EDX analysis of both compounds were very similar, and revealed an approximately 3 : 1 ratio of Te to Cu. These data supported the microanalytical data for the *para*-xylyl complex, but were in contrast to the microanalytical data for the *meta*-xylyl complex which suggested a 2 : 1 ligand : Cu (*i.e.* 4Te : 1 Cu) stoichiometry. The *m*- and *p*-substitution in the xylyl ditelluroethers, combined with the insolubility of the complexes in non-coordinating

solvents suggests that they may adopt polymeric structures, although these are unclear in the absence of X-ray crystallographic data.

Figure 5.14 - ^{125}Te-{^{1}H} NMR spectrum of "[Cu{p-$C_6H_4(CH_2TeMe)_2$}][BF_4]" in MeCN-$CDCl_3$

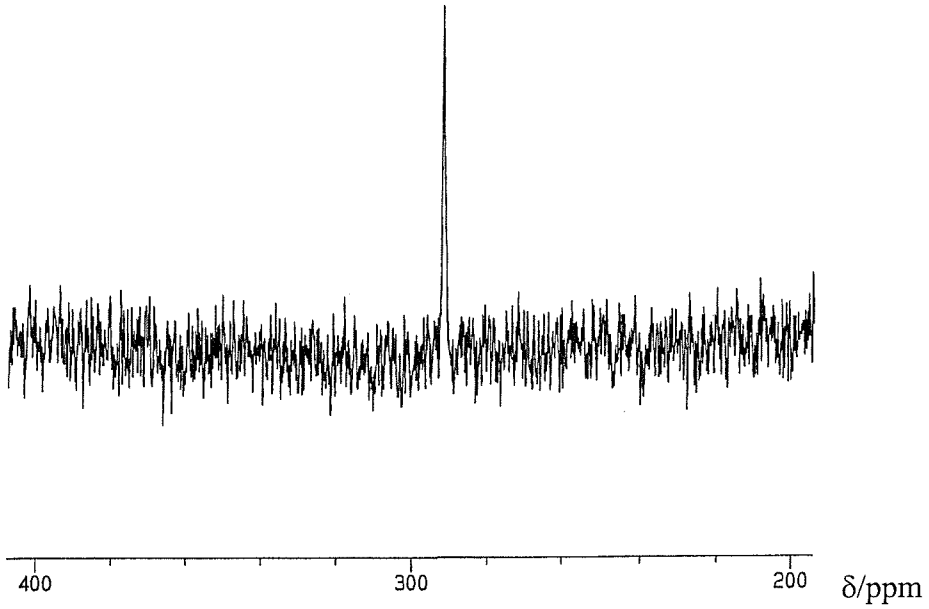

5.5 Attempted preparation of 2,11-ditellura[3.3]orthocyclophane

The preparation of 2,11-ditellura[3.3]orthocyclophane ((i), Figure 5.15) was attempted by the modification of a previously detailed procedure.[20] The original procedure involved the treatment of α,α'-dichloro-*o*-xylene with two molar equivalents of KTeCN in dmso solution. The product isolated from that reaction was dissolved in thf-EtOH and simultaneously added with a solution of α,α'-dichloro-*o*-xylene in thf-EtOH to a suspension of $NaBH_4$ in thf-EtOH over a period of *ca.* 20 hours. Following work up, the crude solid was purified by flash chromatography on silica using light petroleum as eluent to give a small amount of a yellow solid. ^{1}H, ^{13}C-{^{1}H} and ^{125}Te-{^{1}H} NMR spectroscopy of the product were all consistent with the formation of the [1+1]

cyclisation product, 1,3-dihydrobenzo[*c*]tellurophene ((ii), Figure 5.15) instead of the [2+2] cyclisation product 2,11-ditellura[3.3]orthocyclophane. The latter was observed, however, in the FAB mass spectrum of the crude product as a cluster of low intensity peaks at *m/z* = 462.[20] The selenium-containing cyclophane compound 2,11-diselena[3.3]orthocyclophane is known to convert into 1,3-dihydrobenzo[*c*]selenophene when heated to 600°C,[21] and since telluroether compounds are known to be susceptible to elimination reactions even at room temperature, it was concluded that a similar process may have occurred during the attempted preparation of 2,11-ditellura[3.3]orthocyclophane. It was noted, however, that it was not clear whether 1,3-dihydrobenzo[*c*]tellurophene was formed directly from the reactants or by an elimination reaction from the [2+2] species 2,11-ditellura[3.3]orthocyclophane.[20]

Figure 5.15 - 2,11-ditellura[3.3]orthocyclophane (i) and 1,3-dihydrobenzo[c]tellurophene (ii)

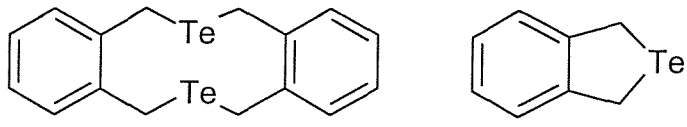

(i) (ii)

Since the preparation of the *o*-, *m*- and *p*-$C_6H_4(CH_2TeMe)_2$ compounds from the reactions of MeTeLi with either *o*-, *m*- or *p*-$C_6H_4(CH_2Br)_2$ were fairly straightforward and reproducible,[3] (Section 5.2) we decided to attempt the synthesis of 2,11-ditellura[3.3]orthocyclophane *via* a similar method, in the hope that the different reaction conditions might favour the production of the [2+2] cyclisation product.

A solution of α-α'-dibromo-*o*-xylene in dry thf was added over the course of two hours to Na_2Te in $NH_{3(l)}$ at -78°C. The mixture was allowed to warm to room temperature overnight, hydrolysed and extracted with Et_2O. The organic extracts were dried ($MgSO_4$), filtered and the solvent removed *in vacuo* to give a waxy yellow solid that darkened to a green colour whilst under vacuum. The EI mass spectrum of the product showed a minor cluster of peaks (5% relative intensity) at *m/z* = 464, consistent with the monocationic $[C_{16}H_{16}Te_2]^+$, together with a more intense cluster (17% relative

intensity) at *m/z* = 360 consistent with the loss of C_8H_8 from $[C_{16}H_{16}Te_2]^+$, *i.e.* $[C_8H_8Te_2]^+$. The most intense cluster of peaks (100% relative intensity) were centred at *m/z* = 234 with the correct isotopic distribution for $[C_8H_8Te]^+$. From these data it was unclear whether the peaks centred at *m/z* = 360 and 234 were arising from the fragmentation of the species at *m/z* = 464 ([2,11-ditellura[3.3]orthocyclophane]$^+$) or whether the $[C_8H_8Te]^+$ ([1,3-dihydrobenzo[*c*]tellurophene]$^+$) was the major product of the reaction. ^{1}H NMR spectroscopy of the product showed a singlet resonance at δ 4.52 ppm with visible tellurium satellites ($^1J_{Te\text{-}H}$ = 22.8 Hz) that was assigned to the Te*C*H_2 protons. The *m*-C_6H_4 proton resonances were observed as a multiplet between δ 6.9 – 7.2 ppm. These data were similar to those reported by McWhinnie and co-workers for 1,3-dihydrobenzo[*c*]tellurophene which had a Te*C*H_2 resonance at δ 4.65 ppm ($^1J_{H\text{-}Te}$ = 22.26 Hz) while the aromatic resonances were observed as a multiplet in the range δ 7.15 – 7.3 ppm.[22] The ^{13}C-{^{1}H} NMR spectrum of the compound showed a resonance at δ 9.7 ppm, consistent with a Te*C*H_2 resonance. The *o*-C_6H_4 carbon environments were observed at δ 126.3, 128.1 and 144.2 ppm, with the latter being assigned to the *ipso*-carbon environment. The ^{125}Te-{^{1}H} NMR spectrum of the compound showed a single resonance at δ 277 ppm, which was similar to the value reported by McWhinnie for 1,3-dihydrobenzo[*c*]tellurophene (Figure 5.15, (ii)) in $CDCl_3$, which had δ(^{125}Te) = 268 ppm.[22] From the inconclusive EI mass spectrum and since 2,11-ditellura[3.3]orthocyclophane would likely have very similar ^{1}H, ^{13}C-{^{1}H} and ^{125}Te-{^{1}H} NMR spectra to those of 1,3-dihydrobenzo[*c*]tellurophene, we decided to quaternise the compound by reaction with MeI, since the resulting Te(IV) derivative would be air-stable and therefore easier to characterise, and would allow for comparisons with the previously reported 1-methyl-1-iodo-3,4-benzo-1-telluracyclopentane[22] (Figure 5.16).

Figure 5.16 - 1-methyl-1-iodo-3,4-benzo-1-telluracyclopentane

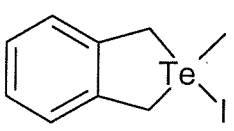

Reaction of the compound with excess MeI in CH_2Cl_2 solution yielded a pale cream-coloured powdered solid in 84% yield. Electrospray mass spectrometry of the product revealed only a very minor cluster of peaks centred at m/z = 249, but this had the correct isotopic distribution for the monocationic $[C_9H_{11}Te]^+$ with no evidence for the dicationic species $[C_{18}H_{22}Te_2]^{2+}$. ^{1}H NMR spectroscopy of the compound showed a resonance at δ 2.38 ppm, consistent with a TeCH_3 resonance. The TeCH_2 resonances were observed as two doublets at δ 4.21 and 4.92 ppm ($^1J_{H\text{-}Te}$ = 14.3 Hz) while the aromatic protons were observed as a multiplet resonance in the range δ 7.05 – 7.20 ppm. These data were very similar to those reported by McWhinnie, who reported δ 2.42 ppm for the TeCH_3 resonance, δ 4.28, 5.00 ppm ($^1J_{H\text{-}Te}$ = 15 Hz) for the TeCH_2 resonances and δ 6.9 – 7.3 ppm for the aromatic protons.[22] The ^{13}C-{^{1}H} NMR spectrum of the compound displayed a resonance at δ 7.69 ppm, consistent with the TeCH_3 carbon environment, while the TeCH_2 resonance was observed at δ 37.3 ppm. The aromatic resonances were observed at δ 126.5, 130.3 and 138.7 ppm. These data were also very similar to those published by McWhinnie, who reported δ 7.1 (TeCH_3), δ 36.7 (TeCH_2) and δ 127.9, 130.1 and 138.4 ppm (*o*-C_6H_4).[22] The ^{125}Te-{^{1}H} NMR spectrum of the compound in CH_2Cl_2-$CDCl_3$ displayed a single resonance at δ 634 ppm, which was similar to the value reported by McWhinnie in $CDCl_3$ solution (δ 652 ppm).[22] Although the data on the methiodide derivative suggested that the product was 1-methyl-1-iodo-3,4-benzo-1-telluracyclopentane, the data would not be expected to be significantly different for 2,11-ditellura[3.3]orthocyclophanemethiodide. Therefore the compound was also reacted with I_2 in thf solution to obtain further spectroscopic data on the previously synthesised[22] Te(IV) derivative, including the possibility of obtaining crystals suitable for X-ray studies. The Te(IV) derivative was isolated as a brick red solid in 73% yield, and ^{1}H NMR spectroscopy of the product in $CDCl_3$ displayed a resonance at δ 5.35 ppm, consistent with an I_2TeCH_2 resonance ($^1J_{H\text{-}Te}$ = 40 Hz). The aromatic protons were observed as a multiplet in the range δ 7.15 – 7.3 ppm. These data are in contrast to those reported by McWhinnie for the compound in dmso solution, which had δ 4.75 ppm for the TeCH_2 resonance ($^1J_{H\text{-}Te}$ = 24Hz) and δ 7.2 – 7.4 ppm for the aromatic protons. The ^{13}C-{^{1}H} NMR spectrum of the compound showed a resonance at δ 25.9 ppm, consistent

with the I_2TeCH_2 resonance, this being shifted significantly to high frequency of the $TeCH_2$ resonance in the starting compound (δ 9.7 ppm). The ^{125}Te-{^{1}H} NMR spectrum of the compound in CH_2Cl_2-$CDCl_3$ solution displayed a single resonance at δ 699 ppm, in contrast to the value of δ 829 ppm for the compound in dmf reported by McWhinnie,[22] and δ *ca.* 739 ppm for the compound in $CDCl_3$ reported by Gysling.[23] These data suggest a large solvent dependence upon the ^{125}Te-{^{1}H} NMR spectrum of 1,1-diiodo-3,4-benzo-1-telluracyclopentane.

Crystals suitable for X-ray diffraction studies were grown from a solution of the compound in $CDCl_3$-CH_2Cl_2, and the unit cell data and crystal system (monoclinic, $P2_1/c$) were very similar to those reported by Ziolo and Günther for the α-form of 1,1-diiodo-3,4-benzo-1-telluracyclopentane, $C_8H_8TeI_2$[24] (Table 5.3). The structure (Figure 5.17) shows the Te(IV) atom in a *pseudo*-trigonal bipyramidal environment, with axial iodines.

Table 5.3 - Unit cell data for $C_8H_8TeI_2$

Compound	*a*/Å	*b*/Å	*c*/Å	*α*/°	*β*/°	*γ*/°	*V*/Å^3	*Z*
$C_4H_8TeI_2$	9.2871(3)	9.7963(4)	12.3872(6)	90	104.814(1)	90	1089.52(7)	4
$C_4H_8TeI_2$*	12.573(5)	9.881(2)	9.271(7)	90	104.96(4)	90	1112.7(5)	4

(* = Ziolo and Günther $C_8H_8TeI_2$[24])

It was therefore established that the [1+1] cyclisation product, 1,3-dihydrobenzo[*c*]tellurophene, had been isolated from the reaction of Na_2Te with α-α'-dibromo-*o*-xylene. It is not certain, however, at which point in the reaction the product was formed; it may have formed from the direct reaction of Na_2Te with α-α'-dibromo-*o*-xylene or it may have resulted from an elimination reaction from initially formed 2,11-ditellura[3.3]orthocyclophane. The latter is a possibility, since the low resolution EI mass spectrum showed a cluster of low intensity peaks at the correct *m/z* for the cationic species $[C_{16}H_{16}Te_2]^+$, and the darkening of the isolated compound from a bright yellow waxy solid to a dark green colour whilst drying *in vacuo* may have been evidence that an unstable product (possibly 2,11-ditellura[3.3]orthocyclophane) was undergoing a rapid

elimination reaction at room temperature in the solid state. This problem might be solved in a future study by monitoring the reaction mixture by ^{125}Te-{^{1}H} NMR spectroscopy.

Figure 5.17 - Crystal structure of 1,1-diiodo-3,4-benzo-1-telluracyclopentane with numbering scheme adopted. Ellipsoids are drawn at the 40% probability level and H atoms are omitted for clarity.

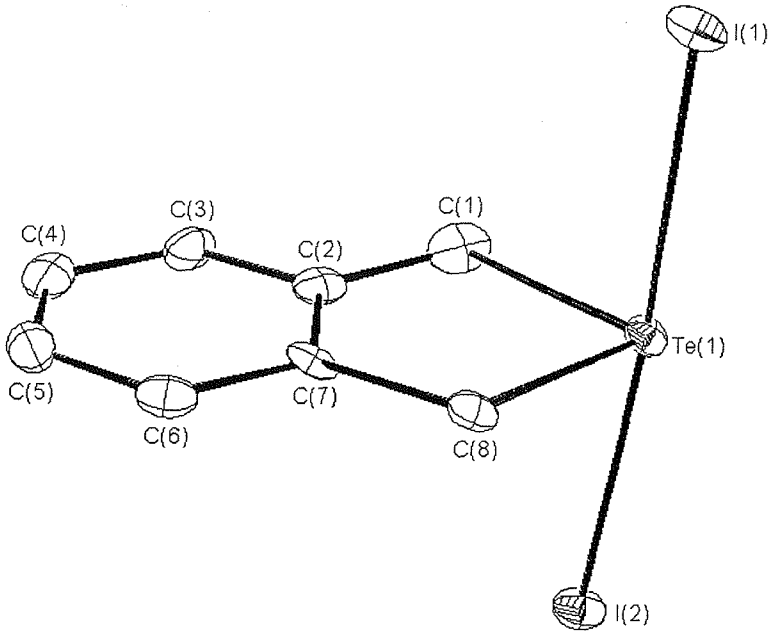

$R = 0.0515$, $R_w = 0.0685$

5.6 Attempted preparation of 2,11-ditellura[3.3]metacyclophane

Unlike 1,3-dihydrobenzo[*c*]tellurophene, the *meta* analogue (Figure 5.18) is unknown, probably due to greater ring strain.

Figure 5.18 - The meta analogue of 1,3-dihydrobenzo[c]tellurophene

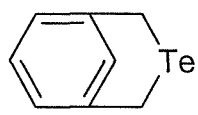

Since the formation of the *meta* tellurophene was thought to be unlikely, we decided to attempt the preparation of 2,11-ditellura[3.3]metacyclophane (Figure 5.19) from the reaction of Na_2Te with α-α'-dibromo-*m*-xylene.

Figure 5.19 - 2,11-ditellura[3.3]metacyclophane

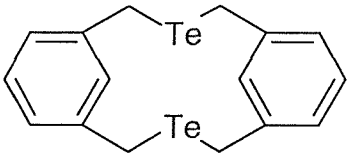

The reaction and work-up were carried out using the same molar quantities and conditions as for the attempted preparation of 2,11-ditellura[3.3]orthocyclophane, using α-α'-dibromo-*m*-xylene instead of α-α'-dibromo-*o*-xylene to give an orange solid. This was recrystallised from CH_2Cl_2-hexane at -18°C to give a fairly insoluble yellow-beige coloured solid that was filtered off and dried *in vacuo* (crop 1 yield 0.309g). The mother liquor was concentrated *in vacuo* and further hexane added to give an orange gum that was separated and dried *in vacuo* (crop 2 yield 0.892g). The remaining mother liquor was evaporated *in vacuo* to produce a small quantity of a yellow wax (crop 3 yield 0.272g). The ^{125}Te-{^{1}H} NMR spectrum of crop 1 showed only a very weak resonance at δ 362 ppm due to the low solubility of the solid, whilst crop 2 showed two resonances at δ 362 and 341 ppm in an approximately 3 : 1 ratio. Crop 3 was found to contain little tellurium, however weak resonances at δ 362 and 341 ppm were observed as in crop 2. It was therefore concluded that crop 1 was probably oligomeric/polymeric material (based on its high insolubility in common solvents such as CH_2Cl_2, MeCN and dmso) and that crop 3 was largely non-tellurium containing, and these were not pursued any further. The ^{1}H NMR spectrum of crop 2 showed a complex multiplet in the range δ 3.75 – 4.10 ppm, together with another complex multiplet between δ 6.75 and 7.65 ppm which integrated in a 1 : 1 ratio. The former was consistent with TeCH_2 resonances (for example in *m*-$C_6H_4(CH_2TeMe)_2$, δ(TeCH_2) = 4.0 ppm). The compound 2,11-ditellura[3.3]metacyclophane would be expected to have up to four different TeCH_2

environments due to the fairly rigid *m*-xylyl linkages. The multiplet resonance between δ 6.75 and 7.65 ppm was assigned to the *m*-C_6H_4 proton environments. The ^{13}C-{^1H} NMR spectrum of the product showed four resonances at δ 5.8, 6.7, 7.7 and 8.0 ppm, consistent with four different Te*C*H_2 environments (*m*-$C_6H_4(CH_2TeMe)_2$ has δ(Te*C*H_2) = 5.7 ppm). The aromatic region was more complex, however, and displayed a total of 17 resonances between δ 125.1 and 142.7 ppm, possibly indicating the presence of some aromatic impurities in the compound. The identity of crop 2 is therefore not clear from the ^1H, ^{13}C-{^1H} and ^{125}Te-{^1H} NMR data, but the presence of resonances attributed to $TeCH_2$ and C_6H_4 groups is not inconsistent with the formation of 2,11-ditellura[3.3]metacyclophane. The ^{125}Te-{^1H} NMR spectrum (δ(^{125}Te) = 362 and 341 ppm) is significantly different to those for *m*-$C_6H_4(CH_2TeMe)_2$ (δ(^{125}Te) = 311 ppm) and 1,3-dihydrobenzo[c]tellurophene (δ(^{125}Te) = 277 ppm) and assuming that the production of the *meta* analogue of 1,3-dihydrobenzo[c]tellurophene was unlikely due to ring strain, the identity of the product as 2,11-ditellura[3.3]metacyclophane is possible. This is supported by the good solubility of the compound in chlorinated solvents, which would be unlikely in the case of an oligomeric or polymeric product. It is possible, however, that other products may have formed from the reaction, for example the [3+3] cyclisation product depicted in Figure 5.20, which would form from the reaction of three molecules of Na_2Te with three α,α'-dibromo-*m*-xylene molecules. The formation of the [3+3] product may be less likely than that of the [2+2] cyclisation product, however, due to the larger amount of preorganisation required of the reactants.

In an attempt to confirm the identity of crop 2 from the reaction of Na_2Te and α-α'-dibromo-*m*-xylene, the product was quaternised by reaction with MeI. A solution of the product and excess MeI were stirred in CH_2Cl_2 for two hours at room temperature. The solution was then concentrated and the product precipitated by the addition of Et_2O. The resultant precipitate was filtered off, washed with Et_2O and dried *in vacuo* to give a pale cream-coloured solid in good yield (0.126g, 78%). Electrospray mass spectrometry of the solid displayed two identifiable clusters of peaks at *m/z* = 247 and 175, the first of which was of low intensity (*ca.* 5%) and consistent with the dicationic [2,11-

ditellura[3.3]metacyclophane-$Me_2]^{2+}$ (*i.e.* $[C_{18}H_{22}Te_2]^{2+}$) and possessed an isotopic distribution that was correct for a species containing two tellurium atoms (Chapter 1).

Figure 5.20 - Possible [3+3] cyclisation product from the reaction of Na_2Te with α-α'-dibromo-m-xylene

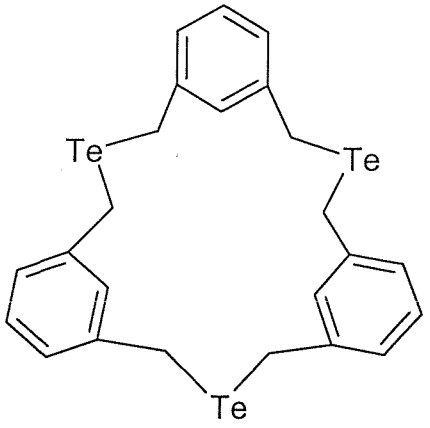

The latter, much more intense (100%) cluster of peaks was consistent with $[Te(CH_3)_3]^+$, possibly indicating that a substantial amount of fragmentation had occurred. The ^1H NMR spectrum of the product showed resonances consistent with *m*-C_6H_4 and TeCH_2 groups between δ 7.0 – 7.5 ppm and δ 3.75 – 4.2 ppm respectively, together with a singlet at δ 1.85 ppm, which was assigned as a TeCH_3 resonance. The ^{125}Te-{^{1}H} NMR spectrum of the product showed a single resonance at δ 521, which was shifted significantly to high frequency of the starting material (δ 362, 341 ppm) and is similar to the value obtained for *m*-$C_6H_4(CH_2TeMe_2I)_2$ (δ(^{125}Te) = 531 ppm. From these data and the data obtained for crop 2 from the reaction of Na_2Te with *m*-$C_6H_4(CH_2Br)_2$ the identity of the product is unclear, however the solubility of the compound, its reaction with MeI and the spectroscopic data suggest that the [2+2] and [3+3] cyclisation products are both possible structures.

5.7 Attempted preparation of *o*-$C_6H_4(CH_2TeMe)_2$ *via* a Grignard intermediate

We wished to establish whether the intermediate *o*-$C_6H_4(CH_2TeMgCl)_2$ (Figure 5.21) could be successfully synthesised and used as a precursor for new tellurium-containing compounds, for example its reaction with α,α'-dichloro-*o*-xylene may potentially form the new compound 2,11-ditellura[3.3]orthocyclophane (Figure 5.22) which was unsuccessfully prepared from the reaction of Na_2Te with α,α'-dichloro-*o*-xylene.

Figure 5.21 - The in-situ 'TeMgCl' reagent

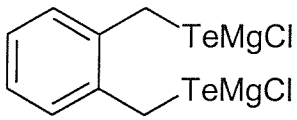

Figure 5.22 - Possible synthetic route to 2,11-ditellura[3.3]orthocyclophane

Similar telluroether reagents incorporating one Te atom have been successfully prepared, for example *o*-$C_6H_4Cl(TeMgBr)$ which was used in the synthesis of *o*-$C_6H_4Cl(TeMe)$.[11] The preparation of the potentially useful intermediate shown in Figure 5.21 has not been reported, however, although Engman and Hellberg reported the synthesis of *p*-$C_6H_4(TeMe)_2$ from *p*-$C_6H_4(TeLi)_2$ (Figure 5.23).[25]

Figure 5.23 - Synthesis of p-$C_6H_4(TeMe)_2$[25]

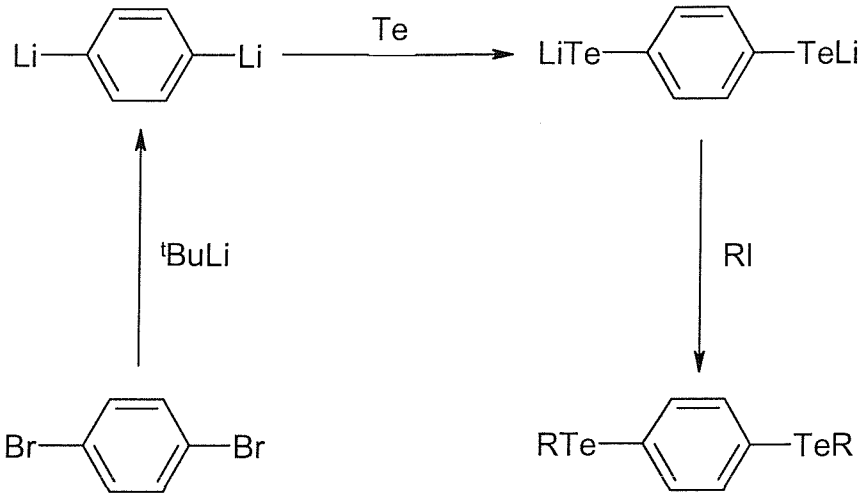

We decided to attempt the preparation of the previously characterised *o*-$C_6H_4(CH_2TeMe)_2$ *via* the *in-situ* intermediate *o*-$C_6H_4(CH_2TeMgCl)_2$. The successful isolation of *o*-$C_6H_4(CH_2TeMe)_2$ from the reaction would verify the preparation of the precursor which may then be used as a potentially useful synthon for new tellurium-containing ring compounds. Magnesium powder and a few drops of 1,2-dibromoethane in dry thf (*ca.* 10 cm^3) were warmed gently to activate the mixture, and then a solution of *o*-$C_6H_4(CH_2Cl)_2$ in thf was added slowly over the course of four hours and stirred for a further 18 hours at room temperature. The mixture was then transferred *via* a cannula onto a frozen (-196°C) suspension of freshly ground Te powder in thf and allowed to warm to room temperature and stir for 3.5 hours to form a pale yellow mixture with some unreacted Te (*ca.* 10%). The mixture was then re-frozen (-196°C) and a solution of MeI in thf added. The reaction was allowed to thaw and stirred at room temperature overnight to form a grey mixture, which was hydrolysed to form a yellow solution and a grey precipitate. To the mixture was added CH_2Cl_2 and the yellow organic layer separated and dried ($MgSO_4$) before filtering and removing the solvent *in vacuo* to give an orange oil. The ^1H and ^{13}C-{^1H} NMR spectra were both very complex, with no evidence for any $TeCH_3$ groups, while the ^{125}Te-{^1H} NMR spectrum showed a single resonance at δ 241 ppm (in contrast to *o*-$C_6H_4(CH_2TeMe)_2$ which has δ(^{125}Te) = 264 ppm). From these data

the identity of the tellurium-containing product of the reaction is unclear, although the desired product, *o*-$C_6H_4(CH_2TeMe)_2$ had not been formed. It may be possible that by changing the reaction conditions (for example the concentrations of the reagents, temperature, duration) however, that the desired reagent may be prepared.

5.8 Conclusions

The new ditelluroether ligands *m*- and *p*-$C_6H_4(CH_2TeMe)_2$ have been synthesised in good yield in a similar method previously used to prepare the analogous *o*-$C_6H_4(CH_2TeMe)_2$. The identity of the compounds have been confirmed by ^1H, $^{13}C\text{-}\{^1H\}$, $^{125}Te\text{-}\{^1H\}$ NMR spectroscopy and mass spectrometry, and the *m*- and *p*-$C_6H_4(CH_2TeMe)_2$ have been shown to form the white Te(IV) methiodide derivatives *m*- and *p*-$C_6H_4(CH_2TeMe_2I)_2$. The *o*-, *m*- and *p*-$C_6H_4(CH_2TeMe)_2$ all react with I_2 in thf solution to form the Te(IV) compounds *o*-, *m*- and *p*-$C_6H_4(CH_2TeI_2Me)_2$ respectively. The X-ray crystal structures of the *m*- and *p*-$C_6H_4(CH_2TeI_2Me)_2$ revealed extended structural motifs, with each Te(IV) atom in a very distorted octahedral environment comprising of two Te-C bonds, two primary Te-I bonds and two secondary Te···I contacts. Although the secondary Te···I contacts are at similar distances, the extended structures identified in the *m*- and *p*-$C_6H_4(CH_2TeI_2Me)_2$ are very different to the weakly associated dimer observed in *o*-$C_6H_4(CH_2TeMe_2I)_2$. This was almost certainly in part due to the different architectures of the units linking the Te atoms, which prevented simple dimer formation.

The *m*- and *p*-$C_6H_4(CH_2TeMe)_2$ reacted with $[Cu(MeCN)_4][BF_4]$ in CH_2Cl_2 solution to form white Cu(I) complexes, which were poorly soluble in common solvents apart from MeCN. The structures of the compounds are not clear, although the *m*- and *p*-substitution in the xylyl ditelluroethers, combined with the insolubility of the complexes in non-coordinating solvents suggests that they may adopt polymeric structures.

An attempt to synthesise the new compound 2,11-ditellura[3.3]orthocyclophane instead produced the previously known 1,3-dihydrobenzo[*c*]tellurophene, which was confirmed unambiguously from an X-ray crystal structure of 1,3-dihydrobenzo[*c*]tellurophenediiodide. Further investigations into this reaction chemistry would be needed to determine whether the 1,3-dihydrobenzo[*c*]tellurophene was formed directly from the reagents or whether it formed as a result of an elimination reaction from 2,11-ditellura[3.3]orthocyclophane. The formation of 2,11-ditellura[3.3]orthocyclophane may be favoured by changing the reaction conditions – for example changing the reaction temperature, duration or the volume of solvent. A similar attempt to prepare 2,11-ditellura[3.3]metacyclophane produced an unidentified tellurium-containing compound

as the major product. The limited data gathered for the compound support its identity as 2,11-ditellura[3.3]metacyclophane, however further work would be needed to conclusively establish this.

An attempt to prepare the di-Grignard reagent *o*-$C_6H_4(CH_2TeMgCl)_2$ and use it to form the previously prepared *o*-$C_6H_4(CH_2TeMe)_2$ was not successful, and instead formed an unidentified tellurium-containing species. The failure to produce *o*-$C_6H_4(CH_2TeMe)_2$ may have arisen before or after the production of the desired *in-situ* intermediate, however time constraints prevented an investigation of this. Further work would include performing the reaction under different conditions in order to try to prepare *o*-$C_6H_4(CH_2TeMe)_2$ and therefore confirm the production of the *in-situ* intermediate *o*-$C_6H_4(CH_2TeMgCl)_2$.

Table 5.4 - Crystallographic parameters

	***m*-$C_6H_4(CH_2TeI_2Me)_2$**	***p*-$C_6H_4(CH_2TeI_2Me)_2$**
Formula	$C_{10}H_{14}I_4Te_2$	$C_{10}H_{14}I_4Te_2$
M	897.01	897.01
Crystal system	monoclinic	monoclinic
Space group	$P2_1/c$	$P2_1/c$
a/Å	10.018(2)	10.8286(7)
b/Å	9.2154(18)	9.2821(3)
c/Å	20.264(4)	9.4672(6)
β/°	98.30(3)	104.816(2)
U/Å^3	1851.2(6)	919.93(9)
Z	4	2
μ(Mo-Kα)/mm^{-1}	98.02	98.62
Unique reflections	4146	2089
Obs. reflections [I>2σ(I)]	2674	1684
R_1	0.0786	0.0521
wR_2	0.1857	0.1283

$$R_1 = \Sigma \; | \; |F_o| - |F_c| \; |_i \; / \; \Sigma |F_o| \; ; \; wR_2 = [\Sigma_w (F_o^2 - F_c^2)^2 \; / \; \Sigma \; wF_{oi}^4]^{½}$$

5.9 Experimental

$[Cu(MeCN)_4][BF_4]$ was synthesised according to the literature method for $[Cu(MeCN)_4][PF_6]$[17] using HBF_4 instead of HPF_6.

o-$C_6H_4(CH_2TeMe)_2$[3]

Procedure as literature, using freshly ground tellurium powder (1.595g, 12.5 mmol), MeLi (8 cm^3) and *o*-$C_6H_4(CH_2Br)_2$ (1.650g, 6.25 mmol). Red oil. Yield 2.029g, 83%. ^1H NMR ($CDCl_3$): δ 7.0 – 7.03 (m, 4H, *o*-C_6H_4), 4.0 (s, 4H, CH_2), 1.79 (s, 6H, CH_3). ^{13}C-{^1H} NMR ($CDCl_3$): δ 138.3 (*ipso-C*, *o*-C_6H_4), 130.6, 126.9 (*o*-C_6H_4), 3.5 ($TeCH_2$), -18.9 ($TeCH_3$). ^{125}Te-{^1H} NMR (CH_2Cl_2): δ 264.

m-$C_6H_4(CH_2TeMe)_2$

Freshly ground tellurium powder (1.595g, 12.5 mmol) was frozen in thf (70 cm^3) and MeLi (8 cm^3, 12.5 mmol) added. The mixture was allowed to warm to room temperature and stirred for 30 minutes to form a clear yellow solution of MeTeLi. The mixture was then refrozen and a solution of *m*-$C_6H_4(CH_2Br)_2$ (1.650g, 6.25 mmol) in dry thf (30 cm^3) added. The mixture was then allowed to warm to room temperature and stirred for 20 hours, before hydrolysing (*ca.* 50 cm^3) and extracting with CH_2Cl_2 (2 × 50 cm^3). The combined organic extracts were dried ($MgSO_4$), filtered and the solvent removed to give a beige-yellow solid. Yield 1.675g, 69%. Mpt. 64°C. EIMS: found *m/z* = 390; calculated for $[m\text{-}C_6H_4(CH_2TeMe)_2]^+$ 390. ^1H NMR ($CDCl_3$): δ 7.0 – 7.2 (m, 4H, *m*-C_6H_4), 4.0 (s, 4H, CH_2), 1.95 (s, 6H, CH_3). ^{13}C-{^1H} NMR ($CDCl_3$): δ 141.4 (*ipso*-C, *m*-C_6H_4), 128.8 (1C, *m*-C_6H_4), 128.6 (1C, *m*-C_6H_4), 126.4 (2C, *m*-C_6H_4), 5.7 ($TeCH_2$), -20.1 ($TeCH_3$). ^{125}Te-{^1H} NMR (CH_2Cl_2): δ 311. IR ν/cm^{-1} (CsI disk): 3060w, 2920w, 1592w, 1584w, 1481m, 1435m, 1414m, 1263w, 1260m, 1246w, 1214m, 1150m, 1142m, 1116m, 1068m, 927w, 900w, 847m, 830m, 797m, 699m, 536m, 525w, 427w, 392w, 383w, 275w, 246w, 221w.

p-$C_6H_4(CH_2TeMe)_2$

Method and work-up as above, using freshly ground tellurium powder (1.595g, 12.5 mmol), MeLi (8 cm^3, 12.5 mmol) and p-$C_6H_4(CH_2Br)_2$ (1.650g, 6.25 mmol) to give a yellow solid. Yield 1.976g, 82%. Mpt. 85°C. EIMS: found m/z = 390; calculated for $[p\text{-}C_6H_4(CH_2TeMe)_2]^+$ 390. ^{1}H NMR ($CDCl_3$): δ 7.05 (s, 4H, p-C_6H_4), 3.9 (s, 4H, CH_2), 1.75 (s, 6H, CH_3). ^{13}C-{^{1}H} NMR ($CDCl_3$): δ 138.8 (*ipso*-C, p-C_6H_4), 129.0 (p-C_6H_4), 5.3 (TeCH_2), -20.1 (TeCH_3). ^{125}Te-{^{1}H} NMR (CH_2Cl_2): δ 311. IR ν/cm^{-1} (CsI disk): 3050w, 2925w, 2853w, 1600w, 1502m, 1457w, 1419m, 1364m, 1261m, 1214m, 1104m, 1018m, 861w, 830m, 614w, 586m, 523w, 462w, 315w, 246w, 222w.

o-$C_6H_4(CH_2TeI_2Me)_2$

To a solution of o-$C_6H_4(CH_2TeMe)_2$ (0.10g, 0.257 mmol) in dry thf (30 cm^3) was added a solution of I_2 (0.130g, 0.514 mmol) in dry thf (10 cm^3) and the solution stirred in a foil-wrapped vessel at room temperature for 2 hours. The solution volume was reduced (*ca.* 5 cm^3) and Et_2O (*ca.* 10 cm^3) added to form a precipitate that was filtered off, washed with Et_2O and dried *in vacuo* to give a brick-red solid. Yield 0.067g, 30%. Calc. for $[C_{10}H_{14}I_4Te_2]$: C, 13.4; H, 1.6%. Found: C, 13.8; H, 1.5%. ^{1}H NMR (d_6-dmso): δ 7.2 – 7.4 (m, 4H, o-C_6H_4), 4.30 (s, 4H, TeCH_2), 2.95 (s, 6H, TeCH_3). ^{125}Te-{^{1}H} NMR (thf-$CDCl_3$): see text. IR ν/cm^{-1} (CsI disk): 3020w, 2959w, 2925w, 2857w, 1595w, 1484m, 1446m, 1396w, 1359m, 1261w, 1220m, 1197w, 1128m, 1101sh, 1054m, 952w, 860w, 834sh, 797w, 761m, 615w, 555m, 523w, 325w, 300w, 247w, 223w.

m-$C_6H_4(CH_2TeI_2Me)_2$

Method as above using m-$C_6H_4(CH_2TeMe)_2$ (0.10g, 0.257 mmol) and I_2 (0.130g, 0.514 mmol). Brick-red solid. Yield 0.109g, 47%. Calc. for $[C_{10}H_{14}I_4Te_2].½Et_2O$: C, 15.4; H, 2.0%. Found: C, 15.6; H, 1.4%. ^{1}H NMR (d_6-dmso): δ 7.15 – 7.65 (m, 4H, m-C_6H_4), 4.6 (s, 4H, CH_2), 2.4 (s, 6H, CH_3). ^{13}C-{^{1}H} NMR (thf-$CDCl_3$): δ 133.2, 130.5, 130.3 (2C), 128.1 (m-C_6H_4), 41.3 (TeCH_2), 10.8 (TeCH_3). ^{125}Te-{^{1}H} NMR (thf-$CDCl_3$): δ 738. IR ν/cm^{-1} (CsI disk): 3017w, 2943w, 2858w, 1582w, 1482m, 1436w, 1406m, 1253w, 1213w, 1161m, 1150m, 1117w, 1100w, 1073m, 997w, 940w, 849m, 819w, 805m, 794m, 703m, 558w, 538sh, 531m, 394w, 348w, 324w, 300w, 224w.

p-$C_6H_4(CH_2TeI_2Me)_2$

Method as above using p-$C_6H_4(CH_2TeMe)_2$ (0.10g, 0.257 mmol) and I_2 (0.130g, 0.514 mmol). Brick-red solid. Yield 0.0921, 40%. Calc. for $[C_{10}H_{14}I_4Te_2]$: C, 13.4; H, 1.6%. Found: C, 13.9; H, 1.8%. ^{1}H NMR (d_6-dmso): δ 7.5 (s, 4H, p-C_6H_4), 4.65 (s, 4H, CH_2), 2.35 (s, 6H, CH_3). ^{13}C-{^{1}H} NMR (thf-$CDCl_3$): δ 133.6 (*ipso*-C, p-C_6H_4), 129.4 (p-C_6H_4), 41.4 (TeCH_2), 20.9 (TeCH_3). ^{125}Te-{^{1}H} NMR (thf-$CDCl_3$): δ 739. IR ν/cm^{-1} (CsI disk): 3020w, 2940w, 2863w, 1540w, 1501w, 1420m, 1396sh, 1358m, 1262w, 1216w, 1138m, 1107m, 1081m, 1020w, 995m, 829m, 792w, 759w, 626w, 573m, 434w, 415w, 312w, 247w, 222w.

m-$C_6H_4(CH_2TeMe_2I)_2$

MeI (*ca.* 1 cm^3, excess) was added to a solution of m-$C_6H_4(CH_2TeMe)_2$ (0.120g, 0.308 mmol) in CH_2Cl_2 (50 cm^3) and the mixture stirred at room temperature for two hours. The resulting cloudy yellow solution was concentrated (*ca.* 25 cm^3) and Et_2O (*ca.* 20 cm^3) added. The resultant precipitate was filtered off and washed with Et_2O to give a pale yellow powdered solid. Yield 0.149g, 72%. Calc. for $[C_{12}H_{20}I_2Te_2].½Et_2O$: C, 23.7; H, 3.5%. Found: C, 24.5; H, 3.5%. ESMS: found m/z = 547, 210; calculated for $[m$-$C_6H_4(CH_2TeMe_2)_2I]^+$ 547, calculated for $[m$-$C_6H_4(CH_2TeMe_2)_2]^+$ 210. ^{1}H NMR (d_6-dmso): δ 7.0 – 7.5 (m, 4H, m-C_6H_4), 4.1 (s, 4H, CH_2), 1.9 (s, 12H, CH_3). ^{13}C-{^{1}H} NMR (d_6-dmso): δ 134.7 (*ipso*-C, m-C_6H_4), 131.8 (1C, m-C_6H_4), 131.6, (1C, m-C_6H_4), 129.7 (2C, m-C_6H_4), 29.1 (TeCH_2), 7.1 (TeCH_3). ^{125}Te-{^{1}H} NMR (d_6-dmso): δ 531. IR ν/cm^{-1} (CsI disk): 3014w, 2977w, 2922w, 2861w, 1600w, 1584w, 1483m, 1441m, 1414m, 1360m, 1227m, 1155m, 1119m, 1075w, 934w, 893w, 856m, 803m, 741w, 708m, 617w, 541m, 431w, 340w, 244w, 222w.

p-$C_6H_4(CH_2TeMe_2I)_2$

MeI (*ca.* 1 cm^3, excess) was added to a solution of p-$C_6H_4(CH_2TeMe)_2$ (0.120g, 0.308 mmol) in CH_2Cl_2 (50 cm^3) and the mixture stirred at room temperature for 2 hours. The resultant precipitate was filtered off and washed with Et_2O to give a pale yellow powdered solid. Yield 0.150g, 72%. Calc. for $[C_{12}H_{20}I_2Te_2]$: C, 21.4; H, 3.0%. Found: C, 22.0; H, 3.2%. ESMS: found m/z = 405, 210; calculated for [p-

$C_6H_4(CH_2TeMe)(CH_2TeMe_2)]^+$ 405, calculated for $[p\text{-}C_6H_4(CH_2TeMe_2)_2]^+$ 210. ^1H NMR (d_6-dmso): δ 7.3 (s, 4H, *p*-C_6H_4), 4.05 (s, 4H, CH_2), 1.8 (s, 12H, CH_3). ^{13}C-{^1H} NMR: δ 133.4 (*ipso*-C, *p*-C_6H_4), 130.9 (*p*-C_6H_4), 28.2 ($TeCH_2$), 6.9 ($TeCH_3$). ^{125}Te-{^1H} NMR (d_6-dmso): δ 537. IR ν/cm^{-1} (CsI disk): 3017w, 2923w, 2858w, 1600w, 1506w, 1418m, 1358m, 1263w, 1227m, 1203w, 1128m, 1101m, 1018sh, 994m, 890w, 835m, 732w, 614w, 586m, 533w, 417w, 312w, 224w.

<u>*m*-$C_6H_4(CH_2TeMe)_2$ + $[Cu(MeCN)_4][BF_4]$</u>

A solution of *m*-$C_6H_4(CH_2TeMe)_2$ (0.15g, 0.385 mmol) and $[Cu(MeCN)_4][BF_4]$ (0.061g, 0.193 mmol) in CH_2Cl_2 (70 cm^3) was stirred at room temperature in a foil-wrapped vessel for 1.5 hours. The resulting precipitate was filtered off and washed with Et_2O to give a beige powdered solid. Yield 0.140g, 78%. Calc. for $[C_{20}H_{28}BCuF_4Te_4]$: C, 25.9; H, 3.0%. Found: C, 26.3; H, 2.73 %. ESMS: found *m/z* = 843, 559, 453, 186, 145; calculated for $[Cu(m\text{-}C_6H_4(CH_2Te)_2)_2]^+$ 843, calculated for $[Cu(m\text{-}C_6H_4(CH_2Te)_2)_2 - 2TeMe]^+$ 559, calculated for $[Cu(m\text{-}C_6H_4(CH_2Te)_2]^+$ 453, calculated for $[Cu(MeCN)_3]^+$ 186, calculated for $[Cu(MeCN)_2]^+$ 145. ^1H NMR (CD_3CN): δ 7.0 – 7.25 (m, 4H, *m*-C_6H_4), 3.95 (s, 4H, CH_2), 1.85 (s, 6H, CH_3). ^{125}Te-{^1H} NMR (CD_3CN): δ 292. IR ν/cm^{-1} (CsI disk): 3052w, 2929w, 2854w, 1600w, 1584w, 1486m, 1441m, 1419m, 1360m, 1283w, 1226m, 1053vs br, 997m, 933w, 849m, 801m, 735m, 702m, 614w, 543w, 521m. EDX (atom %): Te = 75.47, Cu = 24.53.

<u>*p*-$C_6H_4(CH_2TeMe)_2$ + $[Cu(MeCN)_4][BF_4]$</u>

Method as above using *p*-$C_6H_4(CH_2TeMe)_2$ (0.150g, 0.385 mmol) and $[Cu(MeCN)_4][BF_4]$ (0.061g, 0.193 mmol). Beige powdered solid. Yield 0.128g, 71%. Calc. for $[C_{15}H_{21}BCuF_4Te_3]$: C, 24.5; H, 2.9%. Found: C, 23.8; H, 2.8%. ESMS: found *m/z* = 559, 186, 145; calculated for $[Cu(m\text{-}C_6H_4(CH_2Te)_2)_2 - 2TeMe]^+$ 559, calculated for $[Cu(MeCN)_3]^+$ 186, calculated for $[Cu(MeCN)_2]^+$ 145. ^1H NMR (CD_3CN): δ 7.15 (s, 4H, *p*-C_6H_4), 3.95 (s, 4H, CH_2), 1.80 (s, 6H, CH_3). ^{125}Te-{^1H} NMR (CD_3CN): δ 292. IR ν/cm^{-1} (CsI disk): 3019w, 2924w, 2856w, 1507m, 1419m, 1362m, 1310w, 1280w, 1056vs br, 834m, 610m, 588m, 520w. EDX (atom %): Te = 73.42, Cu = 26.58.

Attempted preparation of 2,11-ditellura[3.3]orthocyclophane

Ammonia (600 cm^3) was condensed in a 1L flask at -78°C and freshly cut Na (0.348g, 15.16 mmol) added over the course of several minutes to give a deep blue solution. Freshly ground Te powder (0.967g, 7.58 mmol) was added and the mixture allowed to warm until a blue solution with a white precipitate of Na_2Te was observed. The mixture was re-cooled (-78°C) and a solution of α-α'-dibromo-*o*-xylene (2.0g, 7.58 mmol) in dry thf (150 cm^3) was added over the course of two hours. The mixture was allowed to warm to room temperature overnight, hydrolysed (100 cm^3) and extracted with Et_2O (*ca.* 150 cm^3). The organic extracts were dried ($MgSO_4$), filtered and the solvent removed *in vacuo* to give a waxy yellow solid that darkened to a green colour whilst under vacuum. Yield 1.00g, 57%. EIMS: found *m/z* = 464, 360, 234; calculated for $[C_{16}H_{16}Te_2]^+$ 464, calculated for $[C_8H_8Te_2]^+$ 360, calculated for $[C_8H_8Te]^+$ 234. ^{1}H NMR ($CDCl_3$): δ 6.9 – 7.2 (m, *o*-C_6H_4), 4.52 (s, TeCH_2) ($^1J_{H\text{-}Te}$ = 22.8 Hz). ^{13}C-{^{1}H} NMR ($CDCl_3$): δ 144.2 (*ipso-C*, *o*-C_6H_4), 128.1, 126.3 (*o*-C_6H_4), 9.73 (TeCH_2). ^{125}Te-{^{1}H} NMR (CH_2Cl_2): δ 277.

1-methyl-1-iodo-3,4-benzo-1-telluracyclopentane [22]

1,3-dihydrobenzo[*c*]tellurophene (0.053g, 0.230 mmol) and excess MeI (*ca.* 1 cm^3) were stirred in CH_2Cl_2 (40 cm^3) for two hours. The solution was concentrated (*ca.* 5 cm^3) and Et_2O added to form a precipitate that was filtered off, washed with Et_2O and dried *in vacuo* to give a pale cream solid. Yield 0.072g, 84%. Calc. for $[C_9H_{11}ITe]$: C, 28.9; H, 3.0%. Found: C, 29.6; H, 2.7%. ESMS: found *m/z* = 249; calculated for $[C_9H_{11}Te]^+$ 249. ^{1}H NMR ($CDCl_3$): δ 7.05 – 7.15 (m, 4H, *o*-C_6H_4), 4.90 (d, 2H, TeCH_2) ($^1J_{H\text{-}Te}$ = 14.7 Hz), 4.22 (d, 2H, TeC_{H2}) ($^1J_{H\text{-}Te}$ = 14.0 Hz), 1.50 (s, 3H, TeCH_3). ^{13}C-{^{1}H} NMR (CH_2Cl_2-$CDCl_3$): δ 138.7 (*ipso-C*, C_6H_4), 130.3, 128.0 (*o*-C_6H_4), 37.3 (TeCH_2), 7.69 (TeCH_3). ^{125}Te-{^{1}H} NMR (CH_2Cl_2-$CDCl_3$): δ 634. IR ν/cm^{-1} (CsI disk): 3068w, 3018w, 2995w, 2954w, 2917w, 1574m, 1486m, 1475m, 1451m, 1395m, 1359m, 1261w, 1227w, 1181w, 1086br m, 866m, 796m, 749m, 736m, 622w, 526w, 423m, 303w, 272w, 250w.

1,1-diiodo-3,4-benzo-1-telluracyclopentane[22]

1,3-dihydrobenzo[*c*]tellurophene (0.057g, 0.246 mmol) and I_2 (0.062g, 0.246 mmol) were stirred in thf (40 cm^3) in a foil-wrapped vessel for two hours. The solution was then concentrated (*ca.* 5 cm^3) and pentane added to form a precipitate that was filtered off, washed with pentane and dried *in vacuo* to give a brick-red solid. Yield 0.087g, 73%. Calc. for $[C_8H_8I_2Te].¼thf$: C, 20.8; H, 1.7%. Found: C, 21.1; H, 1.7%. ^1H NMR ($CDCl_3$): δ 7.15 – 7.25 (m, 4H, *o*-C_6H_4), 5.28 (s, 4H, TeCH_2) ($^1J_{H\text{-}Te}$ = 39.7 Hz). ^{13}C-{^1H} NMR (CH_2Cl_2-$CDCl_3$): δ 129.8, 128.6 (*o*-C_6H_4), 25.9 (TeCH_2). ^{125}Te-{^1H} NMR (CH_2Cl_2-$CDCl_3$): δ 699. IR ν/cm^{-1} (CsI disk): 3048w, 3020w, 2972w, 2920w, 1571m, 1489m, 1443m, 1381s, 1361m, 1283w, 1220w, 1182w, 1128w, 1098w, 1033w, 941w, 845w, 821w, 800s, 734s, 626w, 530w, 424m, 254m.

Attempted preparation of 2,11-ditellura[3.3]metacyclophane

Ammonia (600 cm^3) was condensed in a 1L flask at -78°C and freshly cut Na (0.523g, 22.7 mmol) added over the course of several minutes to give a deep blue solution. Freshly ground Te powder (1.450g, 11.4 mmol) was added and the mixture allowed to warm until a blue solution with a white precipitate of Na_2Te was observed. The mixture was re-cooled (-78°C) and a solution of α-α'-dibromo-*m*-xylene (3.0g, 11.4 mmol) in dry thf (150 cm^3) was added over the course of two hours. The mixture was allowed to warm to room temperature overnight. The resulting mixture was hydrolysed (100 cm^3) and Et_2O (50 cm^3) added. The organic layer was separated and the aqueous layer washed with Et_2O (50 cm^3). The combined organic extracts were dried ($MgSO_4$), filtered and the solvent removed to produce an orange solid, yield 1.476g. The crude material was recrystallised from CH_2Cl_2/hexane at -18°C to produce a poorly soluble yellow-beige solid that was filtered off and dried *in vacuo*, yield 0.309g. The mother liquor was concentrated and hexane added to produce a red gum that was separated and dried *in vacuo*, yield 0.892g. The remaining mother liquor was evaporated *in vacuo* to give a yellow wax, yield 0.272g. ^1H NMR ($CDCl_3$): δ 6.75 – 7.65 (m, *m*-C_6H_4), 3.75 – 4.1 (m, TeCH_2). ^{13}C-{^1H} NMR ($CDCl_3$): δ 125.1 – 142.7 (*m*-C_6H_4), 8.0, 7.7, 6.7, 5.8 (TeCH_2). ^{125}Te-{^1H} NMR (CH_2Cl_2-$CDCl_3$): δ 362, 341.

'2,11-ditellura[3.3]metacyclophane' + MeI

A solution of '2,11-ditellura[3.3]metacyclophane' (0.10g, 0.22 mmol) and MeI (1cm^3, excess) were stirred in CH_2Cl_2 at room temperature for 2 hours. The solution was then concentrated (*ca.* 10 cm^3) and Et_2O (*ca.* 5 cm^3) added to produce a pale cream coloured precipitate that was filtered off and dried *in vacuo*. Yield 0.126g, 78%. ESMS (MeCN): found *m/z* = 247, 175; calculated for $[C_{18}H_{22}Te_2]^{2+}$ 247, calculated for $[C_3H_9Te]^+$ 175. ^{1}H NMR (d_6-dmso): δ 7.0 – 7.5 (m, *m*-C_6H_4), 3.75 – 4.2 (m, TeCH_2), 1.85 (s, TeCH_3). ^{125}Te-{^{1}H} NMR (CH_2Cl_2-$CDCl_3$): δ 521.

Attempted preparation of *o*-$C_6H_4(CH_2TeMe)_2$ *via* Grignard route

Magnesium powder (1.143g, 47 mmol) and a few drops of 1,2-dibromoethane in dry thf (*ca.* 10 cm^3) were warmed gently until gentle fizzing was observed. A solution of *o*-$C_6H_4(CH_2Cl)_2$ in thf (250 cm^3) was added slowly to the mixture over the course of four hours and stirred for a further 18 hours at room temperature. The mixture was then transferred *via* a cannula onto a frozen suspension of freshly ground Te powder (3.00g, 23.5 mmol) in thf (*ca.* 100 cm^3) and allowed to warm to room temperature and stir for 3.5 hours. The resulting pale yellow mixture with some unreacted Te powder was then re-frozen and MeI (3.337g, 23.5 mmol) added in thf (20 cm^3). The reaction was allowed to thaw and stirred at room temperature overnight to form a grey mixture, which was hydrolysed (100 cm^3) to form a yellow solution and a grey precipitate. To the mixture was added CH_2Cl_2 (*ca.* 20 cm^3) and the yellow organic layer separated and dried ($MgSO_4$) before filtering and removing the solvent *in vacuo* to give an orange oil. Yield 4.87g. ^{125}Te-{^{1}H} NMR (CH_2Cl_2): δ 241.

X-ray crystallography

Details of the crystallographic data collection and refinement parameters are given in Table 5.4. Orange plate crystals of *m*- and *p*-$C_6H_4(CH_2TeI_2Me)_2$ were grown by slow evaporation from a solution of the appropriate compound in thf-$CDCl_3$. Data collection was performed by Melissa Matthews, Rina Patel and Lorna Nichols using a Nonius Kappa CCD diffractometer equipped with an Oxford Systems open-flow crysostat

operating at 120K, using graphite-monochromated Mo-K_α X-radiation (λ = 0.71073 Å). Structure solution and refinement were routine.[26,27]

5.10 References

1. E. G. Hope and W. Levason, *Coord. Chem. Rev.*, 1993, **122**, 109.
2. W. Levason, S. D. Orchard and G. Reid, *Coord. Chem. Rev.*, 2002, **225**, 159.
3. W. Levason, B. Patel, G. Reid and A. J. Ward, *J. Organomet. Chem.*, 2001, **619**, 218.
4. N. J. Hill, W. Levason, G. Reid and A. J. Ward, *J. Organomet. Chem.*, 2002, **642**, 186.
5. J. R. Black, N. R. Champness, W. Levason and G. Reid, *Inorg. Chem.*, 1996, **35**, 1820.
6. W. Levason, S. D. Orchard and G. Reid, *Organometallics*, 1999, **18**, 1275.
7. J. T. B. Ferreira and A. R. M. Oliveira, *Tetrahedron Lett.*, 1992, **33**, 915.
8. T. Okajima, Z.-H. Wang and Y. Fukazawa, *Tetrahedron Lett.*, 1989, **30**, 1551.
9. H. Higuchi, K. Tani, T. Otsubo, Y. Sakata and S. Misumi, *Bull. Chem. Soc. Jpn.*, 1987, **60**, 4027.
10. R. H. Mitchell and V. Boekelheide, *J. Am. Chem. Soc.*, 1974, **96**, 1547.
11. T. Kemmitt, Ph.D. thesis, University of Southampton, 1989.
12. C. Knobler and R. F. Ziolo, *J. Organomet. Chem.*, 1979, **178**, 423.
13. J. Emsley, in *The Elements*, 3rd Edn., Oxford University Press, 1998.
14. N. J. Hill, Ph.D. thesis, University of Southampton, 2002.
15. L. Y. Y. Chan and F. W. B. Einstein, *J. Chem. Soc., Dalton Trans.*, 1972, 316.
16. F. Einstein, J. Trotter and C. Williston, J. Chem. Soc., (A), 1967, 2018.
17. G. Kubas, *Inorg. Synth.*, 1990, **28**, 68.
18. J. R. Black, N. R. Champness, W. Levason and G. Reid, *Inorg. Chem.*, 1996, **35**, 4432.
19. J. R. Black, N. R. Champness, W. Levason and G. Reid, *J. Chem. Soc., Dalton Trans.*, 1995, 3439.
20. W. Levason, G. Reid and V-A. Tolhurst, *J. Chem. Soc., Dalton Trans.*, 1998, 3411.
21. H. Higuchi, T. Otsubo, F. Ogura, H. Yamaguchi, Y. Sahata and S. Misumi, *Bull. Chem. Soc. Jpn.*, 1982, **55**, 182.

22. A. Z. Al-Rubaie, W. R. McWhinnie, P. Granger and S. Chapelle, *J. Organomet. Chem.*, 1982, **234**, 287.
23. N. Yumbulyadis and H. J. Gysling, *J. Organomet. Chem.*, 1980, **192**, 183.
24. R. F. Ziolo and W. H. H. Günther, *J. Organomet. Chem.*, 1978, **146**, 245.
25. L. Engman and J. S. E. Hellberg, *J. Organomet. Chem.*, 1985, **296**, 357.
26. SHELXS-97, program for crystal structure solution, G. M. Sheldrick, University of Göttingen, 1997.
27. SHELXS-97, program for crystal structure refinement, G. M. Sheldrick, University of Göttingen, 1997.

5.11 Appendix

Infrared spectra were run as CsI disks, in solution using NaCl plates or as neat oils between CsI plates using a Perkin-Elmer 983 spectrometer over the range 180 – 4000 cm^{-1}.

Mass spectra were run either by positive ion electrospray (ESMS) in MeCN solution on a VG Biotech platform, or by low resolution electron impact (EI) on a VG 70-SE Normal Geometry Double Focusing Spectrometer, or by GC-EI on a ThermoQuest Trace MS Gas Chromatography Mass Spectrometer, or by fast atom bombardment (FAB) using 3-NOBA (3-nitrobenzyl alcohol) as a matrix on a VG analytical 70-250-SE Normal Geometry Double Focusing Mass Spectrometer.

^{1}H NMR spectra were recorded using a Bruker AC300 spectrometer operating at 300.13 MHz and are referenced to Me_4Si (δ = 0). ^{13}C-{^{1}H}, ^{55}Mn, ^{77}Se-{^{1}H}, ^{125}Te-{^{1}H}, ^{195}Pt and ^{63}Cu NMR spectra were recorded in 10mm diameter tubes using a Bruker DPX400 spectrometer operating at 100.6, 99.1, 76.3, 126.3, 85.7 or 106.1 MHz respectively and are referenced to external Me_4Si, saturated aqueous $KMnO_4$, external neat Me_2Se, external neat Me_2Te, aqueous 1 mol dm^{-3} $Na_2[PtCl_6]$ in D_2O or $[Cu(NCMe)_4]^+$ respectively (δ = 0). For the carbonyl compounds $[Cr(acac)_3]$ was added to the NMR solutions prior to recording ^{13}C-{^{1}H} NMR spectra and a pulse delay of two seconds was introduced to accommodate the long relaxation times.

EDX measurements were performed using an EDAX instrument with a Philips XL30 ESEM microscope.

Microanalyses were obtained from the University of Strathclyde microanalytical service. All preparations were conducted in degassed solvents under a dinitrogen atmosphere using standard Schlenk techniques.

Column chromatography was performed using a 2.5cm internal diameter glass column with a 25cm depth of silica gel 60 (Fluka). Chromatography of ligands was carried out on relatively small batches (*ca.* 1.5 – 2g) in order to avoid overloading the silica. The silica was made into a slurry with degassed CH_2Cl_2 and poured into the column, with extra degassed CH_2Cl_2 run thorough under a pressure of dinitrogen to thouroughly pack the silica and remove any trapped bubbles. The ligands were carefully

loaded onto the silica in the minimum volume of degassed CH_2Cl_2, and then eluted with degassed hexane : ethyl acetate 3 : 1 as eluent using a positive pressure of dinitrogen in order to elute the compounds as quickly as possible. The fractions were typically collected in conical flasks with an inlet of dinitrogen (through a needle) and the solvents were then removed *in vacuo* as soon as possible.